

UC Davis

UC Davis Electronic Theses and Dissertations

Title

Diastereoselective Reactions of Imines with Anhydrides and their Derivatives and Mechanistic Investigation of the Multicomponent Castagnoli-Cushman Reaction

Permalink

<https://escholarship.org/uc/item/47d3482f>

Author

Howard, Sara Yasmin

Publication Date

2021

Peer reviewed|Thesis/dissertation

Diastereoselective Reactions of Imines with Anhydrides and their Derivatives
and
Mechanistic Investigation of the Multicomponent Castagnoli-Cushman Reaction

By

SARA YASMIN HOWARD
DISSERTATION

Submitted in partial satisfaction of the requirements for the degree of

DOCTOR OF PHILOSOPHY

in

Chemistry

in the

OFFICE OF GRADUATE STUDIES

of the

UNIVERSITY OF CALIFORNIA

DAVIS

Approved:

Jared T. Shaw, Chair

Neil E. Schore

Dean J. Tantillo

Committee in Charge

2021

Copyright © 2021 Sara Yasmin Howard

All rights reserved.

DEDICATION

to my parents, Laleh and John Howard
for always believing I would make it this far
and
my fiancé, Joe Perryman
for standing beside me through it all

mom, this is for you

In the fields of observation, chance favors only the prepared mind.

—Louis Pasteur

Table of Contents

Chapter 1: Introduction	1
1.1 Background of the Castagnoli-Cushman Reaction	1
1.1.1 Reactivity of Cyclic Anhydrides in the Castagnoli-Cushman Reaction	2
1.1.2 Multicomponent Variants of the Castagnoli-Cushman Reaction.....	5
1.2 The Mechanism of the Castagnoli-Cushman Reaction	7
1.3 Development of the Base-Mediated Castagnoli-Cushman Reaction	11
1.4 Review of Catalytic and Enantioselective Castagnoli-Cushman Reactions	12
1.5 Conclusion.....	14
1.6 References	15
Chapter 2: Conjugate Addition Reactions of Anhydrides and α,β-Unsaturated <i>N</i>-Tosyl Ketimines¹	20
2.1 Introduction.....	20
2.1.1 Introduction to the Tamura Reaction.....	21
2.2 Results and Discussion	25
2.2.1 Unexpected Side Products in the Base-Mediated Castagnoli-Cushman Reaction	25
2.2.2 Synthesis of Chalcone Derived Imines	27
2.2.3 Failed Attempts at the Synthesis of Enolizable Ketimine 1m.....	29
2.2.4 Optimization and Diastereoselectivity of the Aza-Tamura Reaction	31
2.2.5 Effect of Imine Substituents on Diastereoselectivity	34
2.2.6 Conversion to Methyl Esters and Substrate Epimerization.....	35

2.3	Conclusion.....	37
2.4	Experimental Section	37
2.5	References	61
Chapter 3: Development of the Mukaiyama Castagnoli-Cushman Reaction¹.....		65
3.1	Introduction.....	65
3.1.1	Review of Acid-Catalyzed Mukaiyama Mannich Reactions	66
3.1.2	Anionic Counterion Directed Catalysis in Mukaiyama Mannich Type reactions	69
3.1.3	Synthesis and Reactivity of 2,5-(bistrimethyl)silyloxy furan and Related Nucleophiles	72
3.1.4	Intro to Computational NMR	76
3.2	Results and Discussion	79
3.2.1	Synthesis of N-Aryl and N-Alkyl Imines	80
3.2.2	Synthesis of 2,5-bis(trimethylsilyloxy) Furan.....	82
3.2.3	Optimization of Diastereoselective Acid-Catalyzed Mukaiyama Castagnoli-Cushman Reaction	83
3.2.4	Scope of the Mukaiyama Castagnoli-Cushman Reaction.....	85
3.2.5	Development of the Multicomponent Mukaiyama Castagnoli-Cushman Reaction	87
3.2.6	Further Optimization of the Double Mukaiyama Castagnoli-Cushman Reaction	88
3.2.7	Scope of the Double Mukaiyama Castagnoli-Cushman Reaction	90

3.2.8 Stereochemical Proof by Computational NMR	90
3.3 Conclusion.....	93
3.4 Experimental Section	94
3.5 References.....	127
Chapter 4: Progress Toward the Synthesis of Bisavenanthramide B-1.....	131
4.1 Introduction.....	131
4.1.1 Isolation of the Bisavenanthramides and Biosynthetic Hypothesis.....	132
4.1.2 Synthesis of Bisavenanthramide B-6 by Anionic Castagnoli-Cushman Reaction	134
4.1.3 Initial Route Toward the Synthesis of Bisavenanthramide B-1	136
4.2 Results and Discussion	137
4.2.1 Direct Synthesis of Bisavenanthramide B-1 Through 2-Cyanoaniline Derived Imine 137	
4.2.2 Attempted Synthesis of Bisavenanthramide B-1 Through Late-Stage Functionalization.....	138
4.2.3 New Retrosynthetic Analysis of Bisavenanthramide B-1	146
4.2.4 Reaction Optimization for Novel Electron Withdrawing Substrates	147
4.2.5 Additional Bromination Strategy.....	149
4.2.6 Synthesis of N-H Bis-Lactam Intermediate	150
4.2.7 Failure of the Buchwald Bis-Arylation	152
4.3 Conclusion and Future Work.....	153
4.4 Experimental Section	155

4.5	References	168
Chapter 5: Mechanistic Investigation of the Multicomponent Variants of the		
Castagnoli-Cushman Reaction		
		172
5.1	Introduction.....	172
5.1.1	Initial Development of the 3-Component Reaction and Proposed Mechanism	
	173	
5.1.2	Initial Mechanistic Hypothesis of the 4-Component Reaction.....	175
5.2	Results and Discussion	177
5.2.1	Mechanistic Investigation of the 4-Component Reaction.....	179
5.2.2	Mechanistic Investigation of the 3-Component Reaction.....	183
5.2.3	Development of Novel Reaction Conditions for the 3-Component Reaction	
	186	
5.3	Conclusion.....	187
5.4	Experimental Section	188
5.5	References	204
Appendix A: Relative Rates of the Castagnoli-Cushman Reaction		
		206
A.1	Introduction	206
A.1.1	Introduction to pK_E Calculations.....	206
A.1.2	Effect of Electron Withdrawing Anhydride Substituents on Reaction Time in	
	the Castagnoli Cushman Reaction	207
A.2	Results and Discussion.....	209

A.1.3	pKE Value Calculations of Anhydrides Commonly used in the Castagnoli Cushman Reaction	209
A.3	Conclusion	215
A.4	Experimental Section	215
A.5	References.....	234

ACKNOWLEDGEMENTS

I want to preface my acknowledgements by stating that I know that they will be *far* too long. But quite frankly, there are simply too many people that I feel compelled to thank for their support and presence throughout my graduate education. Five years is a long time to foster relationships, and this is likely the only time in my life that I'll be able to put into words how grateful I am for the people that I will be highlighting below. And as my mom has always said—I've never been good at summarizing. So here it goes:

First, I want to thank the person who pushed me to pursue my PhD—Dr. Leah Fung, my first mentor at NovoMedix. I am lucky to have worked with such an incredible mentor and friend, and I will always appreciate your kindness, patience, and support. At UC Davis, there are numerous faculty members I would like to acknowledge: Professor Sheila David, for always taking the time to chat in the hallway and write me letters of recommendation; Professor David Olson, for pulling me aside after my qualifying exam to encourage me to pursue academia; and Professor Jesús Velázquez, for always rooting for me, even though I wasn't officially part of his group. Professor Dean Tantillo, I want to thank you for your consistent mentorship and care throughout my graduate career. You've taught me to love physical organic chemistry and your teaching has had a profound impact on the way I view science. I would also like to thank Professor Neil Schore, for not only sitting on my dissertation committee and making my qualifying exam a truly enjoyable experience; but also, for co-writing the textbook that instilled my love for organic chemistry. Finally, I need to express my unending gratitude for Professor Jared Shaw, who I have been lucky enough to work with for the past five years. Thank you for always taking the time to talk to me when I barge into your office unsolicited, no matter how busy you are. Thank you, Jared, for believing in me, advocating for me, trusting me, and giving me the space to grow into the scientist that I am today. I am forever grateful for your encouragement and support.

They say it takes a village to raise a child, but I say it takes a village to get you through graduate school. Throughout my time in graduate school, the members of the Shaw lab have been my ever-growing village. It goes without saying that this group of individuals

are the most talented chemists I know, and I have learned so much from each and every one of them. But beyond the science is the humanity behind them: you can teach someone how to be a chemist, but you can't teach them how to be a friend. Thanks to Dr. Rich Squitieri for always brightening the mood and for taking me on as a rotator my first year. Dr. Stephen Laws and Noah Burlow were instrumental in helping me prepare for my qualifying exam and teaching me how to run projects. Dr. Mingchun Gao, I already miss our gossip time in lab. Jack Shiue, you are one of the kindest and most thoughtful people I know—thank you for never forgetting my birthday. Lucas Souza, thank you for accompanying me on our adventure to SFO; there is no one else I would have rather had that experience with. Jose Ruiz, you have been an incredible coworker and I'm glad we were able to work together for at least a little bit despite the pandemic. I wish the best of luck in grad school to the newer Shaw lab members, Garrett, Andy, and Matt. To the undergraduate researchers that I worked with, Nico Havenner and Kristin Shimabukuro, thank you for your hard work on our projects together. I am so excited to continue to watch you grow as scientists. Thank you to Dr. Lucas Moore for always being available to talk about life and science over a coffee in the breakroom, and for not minding too much when I was an overzealous TA. Dr. Christine Dimirjian is one of the hardest working, most generous people that I have the pleasure of calling a friend. Thank you for being a voice of reason and for keeping me sane throughout grad school. I don't know what I would have done without you. Ben Bergstrom, thank you for being my TA buddy and friend for all these years. I will miss our way-too-long conversations in 303 with Sarah over a dry ice bucket that David inevitably comes looking for. Sarah Dishman, thank you for all the surprise Reese's and pick-me-ups when times were tough. Your thoughtfulness means more than you know. David Gutierrez, thank you for being the *best* listener in 378. I appreciate our friendship so much, and I am so happy that I had the chance to work alongside you and get to know you the past three years. There are so many things that I could write about Dr. Leslie Nickerson. Thank you, Leslie, for letting me force you to be my mentor and for being there for me through my hardest times in grad school—from life struggles to research failures to my qualifying exam, you and Andrew were a constant support system for me. You are an amazing teacher, and you deserve so much credit for

all that you have accomplished in your life. Who would have known that my Shaw lab desk neighbor would become a lifelong best friend? And finally, Anna Lo. I have so much to thank you for, most of which you already know. Thank you for teaching me what it means to be a friend, for being there when things were dark and twisty, and for making me think more deeply about “why”. I’m excited to see where season six takes us.

It’s hard to believe that I’d have more people outside my family to thank here, but my friendships outside of the lab have reminded me that there is more to life than just research. Liz, Angela, Jessica, Savannah, Angel, Collin, Kaylee, Abby, Dave—thank you for all the great times we’ve had when I’ve needed a break from work. From pool days to wine nights to secret Santa, I couldn’t have done this without you.

To my family, thank you for your support leading up to this momentous occasion. Thank you, Aunt Katie, for being my home away from home in Davis. I am so grateful to have had you with me throughout the past five years. Thanks to the rest of CSG, Aunt Ceesa and Tess, for all our coloring and hilarious breaks from the day to day. Thank you to my brother James for always reminding me to be humble. Thank you, Mom, for showing me what it means to be dedicated to the quest for knowledge, and for pushing me to pursue research when I was young; it turns out you were right. Thank you, Dad, for the 9 AM study reminders, for being my cheerleader and my confidante, and for being the one person that will always make me laugh until I cry. Thank you to my grandma, Mom Pari, for everything you’ve done for me throughout my life and for always being so proud of me. And though you’re not here to see it, Grandma and Papa, I hope I’ve made you proud.

And finally, I don’t know if I can put into words how grateful I am for my fiancé Joe Perryman. Thank you for your constant support, for making dinner when I’ve been too overwhelmed to function, and for bringing light back into my world when it has felt so dark. Thank you for letting me fulfill my dream of having not just one, but two (!!) dogs and letting Dwayne and Johnson into our lives to sit next to me while I wrote this document. You are my inspiration, my role model, and my best friend. I love our life together and I am so excited for our future. You are my quantum entanglement.

Diastereoselective Reactions of Imines with Anhydrides and their Derivatives and Mechanistic Investigation of the Multicomponent Castagnoli-Cushman Reaction

ABSTRACT OF DISSERTATION

This dissertation describes four synthetic organic chemistry projects and two computational organic chemistry efforts centered on the Castagnoli-Cushman reaction (CCR) of imines with anhydrides and their derivatives. Chapter one includes a literature review and detailed background on the current state of the CCR, including mechanistic hypotheses and recent catalytic examples. Chapter two details the development of conjugate addition reactions of imines with cyclic enolizable anhydrides to afford β -enaminoketone products. Chapter three describes efforts toward an acid-catalyzed Mukaiyama-type CCR reaction of 2,5-bis(trimethylsilyloxy) furan, including a stereochemical proof by computational NMR. Chapter four describes progress toward the synthesis of the elusive bis- γ -lactam natural product bisavenanthramide B-1 by way of the Mukaiyama CCR. Finally, chapter five discusses the mechanistic investigation of the multicomponent variants of the CCR, leading to a new mechanistic proposal for reactions of these type.

Chapter 1: Introduction

1.1 Background of the Castagnoli-Cushman Reaction

The Castagnoli-Cushman reaction (CCR) and its related three- and four-component reactions (3CR, 4CR) are powerful methods for the synthesis of densely substituted lactams. Lactams are commonly found in natural products and other biologically relevant molecules, many of which have been synthesized using the CCR.¹⁻⁴ The CCR was first discovered in 1969 by Neal Castagnoli, wherein *N*-benzylidene methylamine and succinic anhydride were combined under refluxing conditions to form γ -lactam **3** as a mixture of diastereomers (Figure 1.1).⁵ In the following years, Castagnoli and his graduate student Mark Cushman expanded the scope of this reaction to a variety of *N*-alkyl and *N*-aryl imines for the synthesis of natural products.⁶⁻⁹ Cushman later independently discovered that the reaction of homophthalic anhydride with imines can occur at room temperature to afford *cis* dihydroisoquinolone products **5**.¹⁰ Shortly before Cushman's report, Haimova and coworkers developed a similar method, which included a basic workup, to afford exclusively *trans* dihydroisoquinolone products.¹¹ The general reaction of imines and cyclic enolizable anhydrides has aptly been named the Castagnoli-Cushman reaction to honor the initial discoverers.¹²

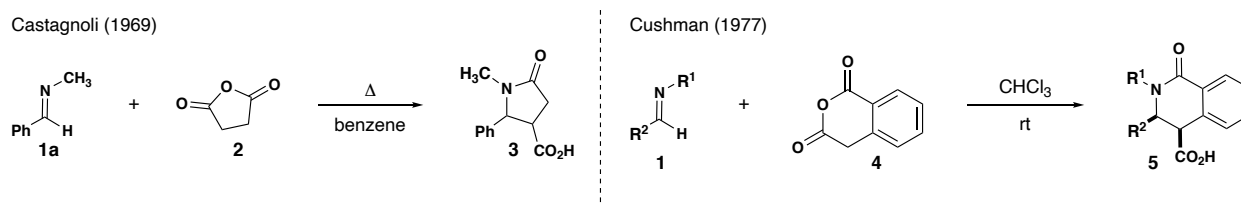


Figure 1.1 Initial development of the Castagnoli-Cushman reaction.

1.1.1 Reactivity of Cyclic Anhydrides in the Castagnoli-Cushman Reaction

A number of cyclic anhydrides have been used in the CCR since Castagnoli's initial discovery (Figure 1.2A). Reactions with unsubstituted succinic (**6**, R = H) and glutaric anhydrides (**7**, R = H) typically require refluxing conditions and proceed with modest yields and diastereoselectivities.^{6, 7, 13-16} On the other hand, reactions of homophthalic anhydride **4** can occur rapidly at or below room temperature, affording the kinetically favored cis diastereomer (Figure 1.2B). Reactions of homophthalic anhydride heated in xylenes affords exclusively the thermodynamically favored trans diastereomer.¹⁰ The kinetic cis products can be fully epimerized to the trans diastereomers under acidic, basic, or thermal conditions.^{10, 11} The substituents present on the anhydrides have been shown to have an influence on their reactivity. Specifically, in his study of the mechanism of the CCR, Cushman showed that phenylsuccinic anhydride had reactivity in between that of succinic and homophthalic anhydride (Figure 1.2C).¹⁷ Reactions of phenylsuccinic anhydride

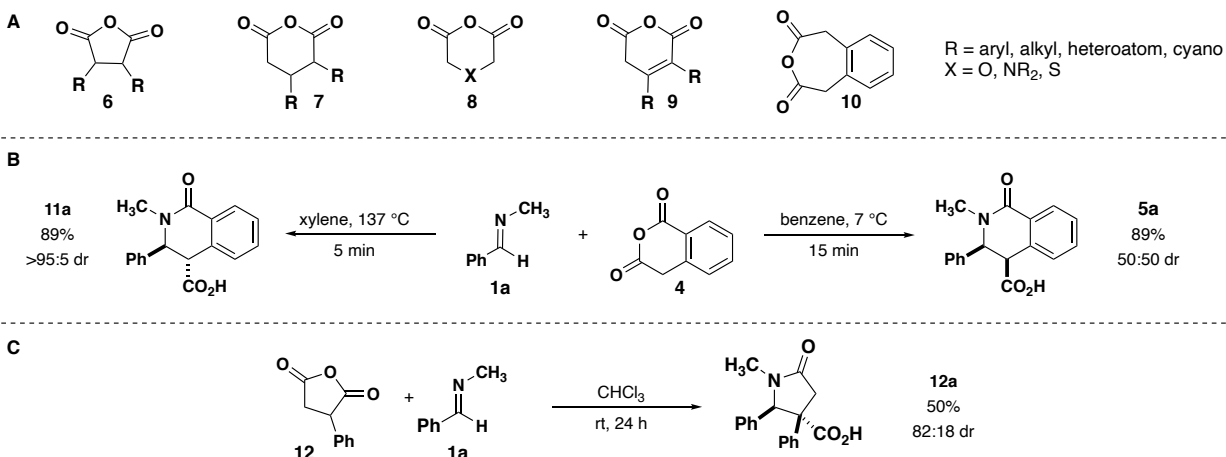


Figure 1.2 **A**. Anhydrides used in the CCR **B**. Results of the reaction of *N*-benzylidene methylamine with homophthalic anhydride at different temperatures. **C**. Reaction of phenylsuccinic anhydride with *N*-benzylidene methylamine.

performed in chloroform can be accelerated upon heating to 90 °C but can also proceed at room temperature for 24–36 hours. Moreover, when the phenyl substituent is replaced with a thioaryl group, similar reaction outcomes are observed.¹⁸

Additional advancements of the CCR involved newly synthesized and more reactive anhydrides. CCRs of cyano- and sulfonyl-substituted succinic (**14**, **22**) and glutaric anhydrides (**18**, **24**) react at room temperature to yield lactam products, demonstrating similar reactivity to homophthalic anhydride (Figure 1.3A, 1.3C, 1.3E, 1.3F).¹⁹ CCRs using chiral disubstituted cyano-succinic anhydrides **16** lead to densely substituted lactam products in high yields and proceed with high diastereoselectivity for a single, major diastereomer (Figure 1.3B).²⁰ Reactions with 3-cyanoglutaric anhydride (**18**) also proceed at room temperature in THF with modest to high diastereoselectivity, resulting in predominantly the *cis* diastereomer (Figure 1.3C).²¹ Higher diastereoselectivity is observed in reactions with cyano-substituted anhydrides bearing a substituent at the β -position (**20**), preferentially yielding one of four possible diastereomers (Figure 1.3D). Products of the CCR with sulfonyl-substituted anhydrides lead to lactam products **23** and **25**, which have the propensity for decarboxylation when subjected to magnesium in methanol or heat (Figure 1.3E, 1.3F).²²

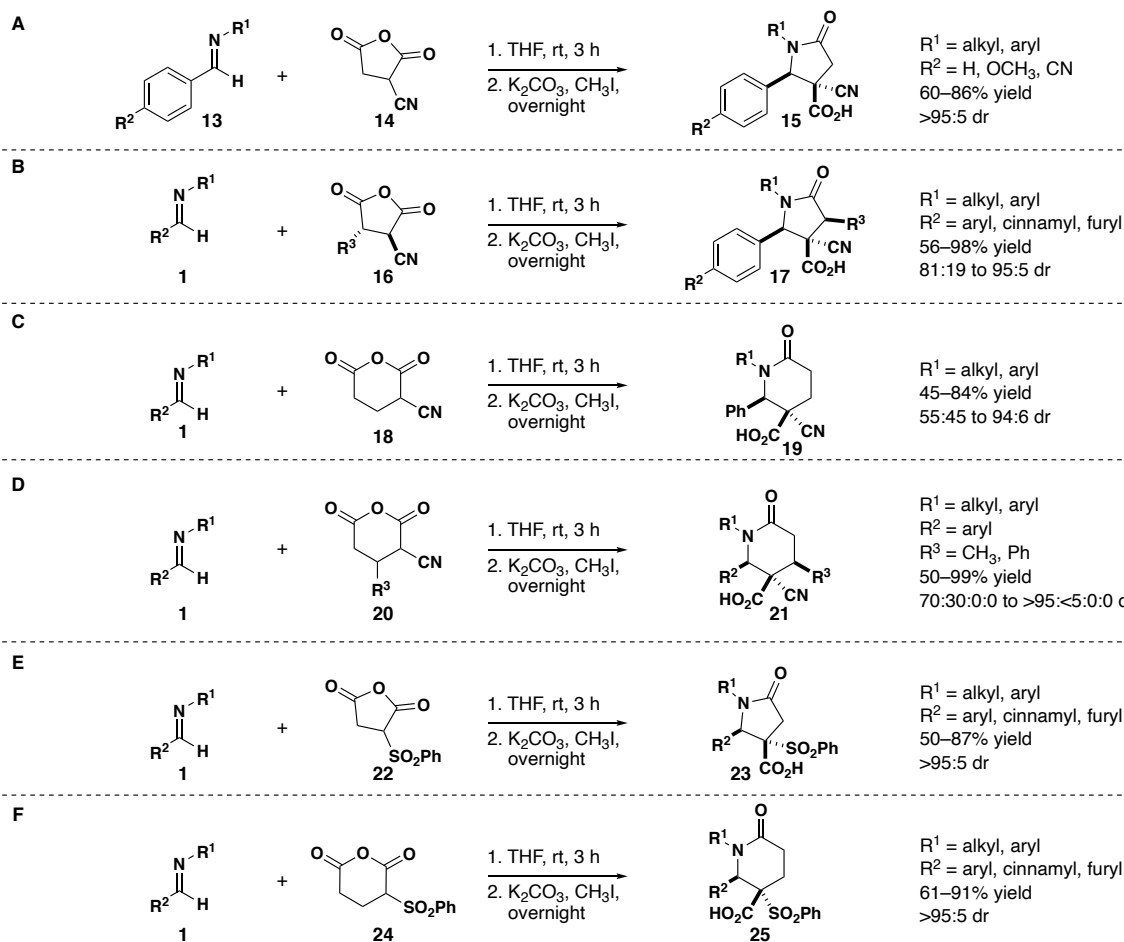


Figure 1.3 Reactions of cyano and sulfonyl-substituted succinic and glutaric anhydrides.

Mikael Krasavin at University of Saint Petersburg further advanced the CCR in 2015 by synthesizing cyclic anhydrides with heteroatoms embedded in the anhydride backbone.²³ Heteroglutaric anhydrides containing oxygen (**26**), nitrogen (**27**), and sulfur (**28**) were employed in the CCR.^{24–33} Reactions with heteroglutaric anhydrides are modestly diastereoselective and require mild heating to form the lactam products in modest yields (Figure 1.6). On the other hand, reactions of phenyl-substituted thiodiglycolic anhydrides, which are more similar to phenylglutaric anhydride, proceed at ambient temperature.^{12 24 27 33, 34}

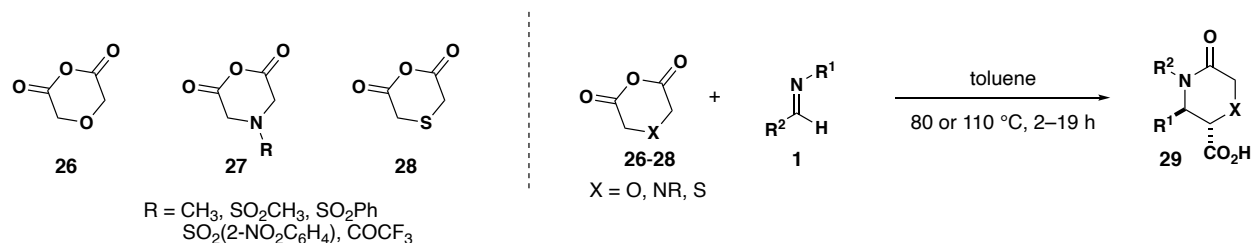


Figure 1.4 Heteroglutaric anhydrides **34–36** and their resulting product outcomes.

More recently, seven-membered ring analogues of homophthalic anhydride have been used in CCRs.³⁵⁻³⁸ The use of unsubstituted adipic anhydride was unsuccessful in the CCR, leading exclusively to its polymerized form **31**, amide-acid **32**, or diamide **33** (Figure 1.7A). In order to access ϵ -lactams, Grygorenko and Krasavin both utilize the more enolizable phenyl diacetic acid anhydride **34**. Reaction yields were modest, and all products were isolated as a single, trans, diastereomer **35** (Figure 1.7B). Interestingly, reactions with ketone derived imines led to byproducts **36**.

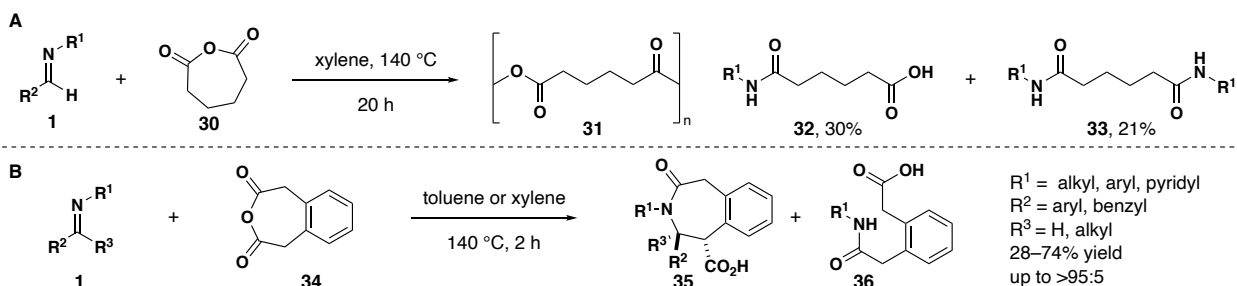


Figure 1.5 **A**. Unsuccessful reaction of adipic anhydride **B**. Successful reactions of phenyl diacetic acid anhydride **34** leading to ϵ -lactams.

1.1.2 Multicomponent Variants of the Castagnoli-Cushman Reaction

In the early 2000s, the first multicomponent variants of the CCR were discovered. The three-component CCR was first developed in 2003 using homophthalic anhydride with amines and aldehydes in the presence of ionic liquid $[\text{bmim}]\text{BF}_4$ and InCl_3 to afford cis dihydroisoquinolone products **5** (Figure 1.6).³⁹ Since this report, a variety of other

methods to form cis dihydroisoquinolones were developed, mediated by $\text{KAl}(\text{SO}_4)_2 \cdot \text{H}_2\text{O}$,^{40, 41} $\text{Yt}(\text{OTf})_3$,⁴² silica sulfuric acid,⁴³ iodine,⁴⁴ sulfonic acid functionalized silica,⁴⁵ $\text{ZnCl}_2/\text{AlCl}_3\text{-SiO}_2$,⁴⁶ L-proline,⁴⁷ or aspartic acid.⁴⁸ More recently, a new modified CCR was developed utilizing the diacid of homophthalic anhydride (**39**), amines, and aldehydes under dehydrating conditions.⁴⁹ In this case, it was hypothesized that both the anhydride and imine were being formed *in situ*, which then undergo the classic CCR reaction (Figure 1.6). Heating the reaction favors full epimerization to the trans diastereomer **11**.

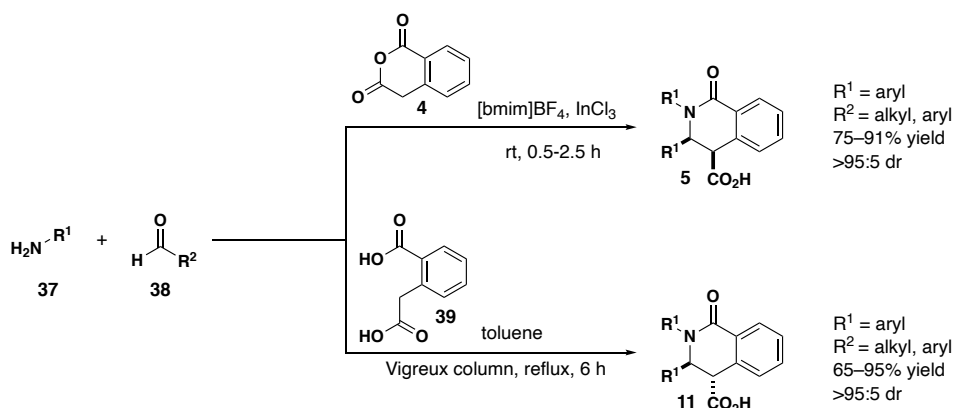


Figure 1.6 Three component reaction outcomes with either homophthalic anhydride **4** or its diacid precursor (**15**).

Our group's investigation of novel anhydrides in the CCR also led to the development of the 4CR.⁵⁰ In analogy to Cushman's use of phenylsuccinic anhydride,¹⁷ we sought to replace the phenyl ring with a substituent with similar electronics. Thioaryl succinic anhydride provided similar reactivity to phenyl succinic anhydride and could also undergo reductive cleavage of the thioaryl substituent, which allowed for the synthesis of the core of martinelllic acid.¹⁸ CCRs using thioaryl succinic anhydride afford tetra-substituted lactam products **40** in good diastereoselectivity (Figure 1.7).⁵⁰ This work helped to

establish the first 4CR using amines, aldehydes, thiols, and maleic anhydride. We observed that heating all four of the components (**37a**, **38a**, **40**, **41**) for 24 hours provided the lactam product in similar yield and diastereoselectivity, which obviated the need for pre-synthesizing imine or anhydride.

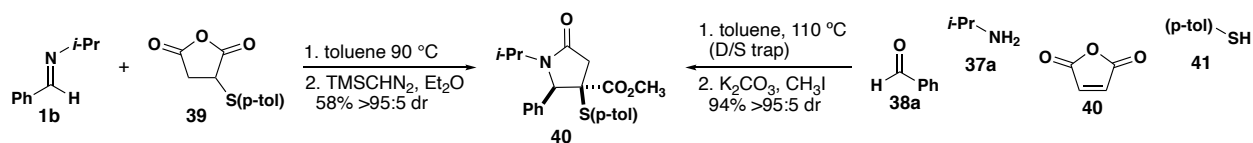


Figure 1.7 The reaction of thioaryl succinic anhydrides and the four-component reaction afford product **40** in comparable yields and diastereoselectivity.

1.2 The Mechanism of the Castagnoli-Cushman Reaction

The mechanism of the CCR has been under speculation since Cushman's 1987 mechanistic investigation.^{17, 51} Initial studies focused on the electronic and steric influences of the CCR with homophthalic anhydride, specifically analyzing the relationship between reactivity of the imine and diastereomeric outcomes.¹⁷ Cushman hypothesized that lactam formation in the CCR could follow several mechanistic pathways. For one, products of the CCR are reminiscent of products in the [4+2] cycloaddition, indicating an imino-Diels Alder mechanism through the enol tautomer of homophthalic anhydride **4a** could be operative (Figure 1.8A). Alternatively, it was hypothesized that the reaction proceeds through an iminolysis pathway, forming *N*-acyl iminium ion **44** through acylation of the imine nitrogen (Figure 1.8B). Subsequent intramolecular Mannich addition through the carboxylic acid enolate **44b** leads to **43**. Finally, the mechanism could also be analogous to that of the mechanism of the Perkin reaction. In this case, the reaction could

proceed through Mannich addition of the anhydride enolate **45**, followed by *N*-acylation of intermediate **47** to form lactam **43** (Figure 1.8C).

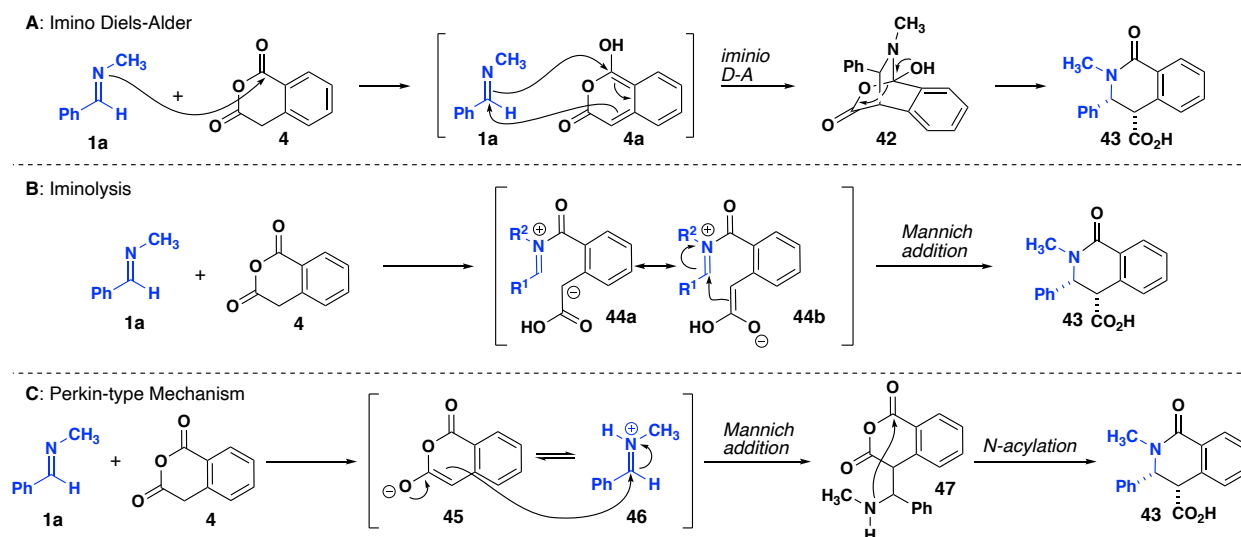


Figure 1.8 **A.** The imino Diels-Alder mechanism **B.** Cushman's proposed iminolysis pathway for the CCR. **C.** The Perkin-type mechanism beginning with Mannich addition, followed by intramolecular acylation.

Cushman's mechanistic investigation suggested that the mechanism for the CCR relied on the iminolysis pathway. He eliminated the possibility of the imino Diels-Alder mechanism due to inconsistencies with previously reported Diels-Alder reactions of homophthalic anhydride. Diels-Alder reactions of homophthalic anhydride typically require prolonged heating to afford Diels-Alder products with reactive dienophiles (Figure 1.9B), while the CCR of homophthalic anhydride proceeds rapidly at room temperature (Figure 1.9A).⁵² Furthermore, he suggested that the Perkin pathway was unlikely based on a competition experiment between benzaldehyde and *N*-benzylidene methylamine **1a** with triethylamine. The reaction resulted in exclusively dihydroisoquinolone product **46** with no lactone present. He suggested that the lactone should be favored based on the

reactivity of aldehydes versus imines, however he also noted that this argument hinged on the hypothesis that the neutral imine is reacting in the CCR. Based on these observations, Cushman concluded that the iminolysis mechanism was the most likely for the CCR.

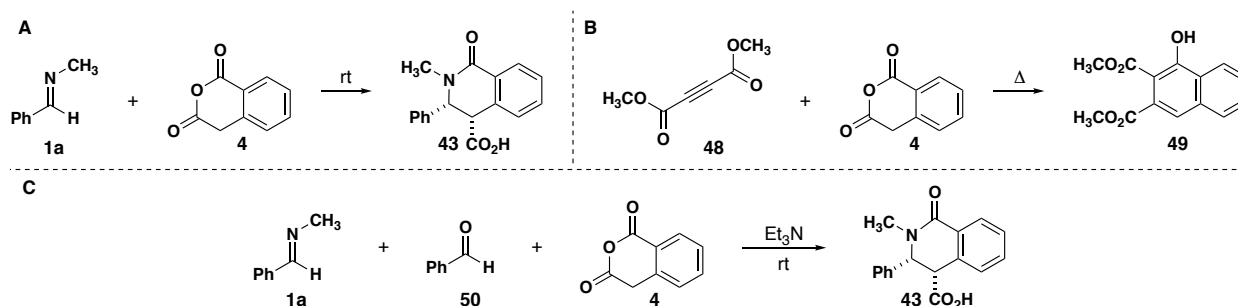


Figure 1.9 **A.** CCR reaction conditions leading to dihydroisoquinolone **46**. **B.** Forcing conditions required for Diels-Alder reaction of homophthalic anhydride with alkynes. **C.** Competition experiment of *N*-benzylidene methylamine and benzaldehyde with homophthalic anhydride, leading exclusively to dihydroisoquinolone product.

In 2013, our group, in collaboration with the Cheong group at Oregon State University, discovered that reactions of cyano-succinic anhydride with imines proceeds through a Mannich-like mechanism (Scheme 1.10A). In the case of cyanosuccinic anhydrides, computational studies indicate that enol-keto tautomerization of the anhydride (**14**, **14a**) reacts with the imine (**1**) through a Zimmerman-Traxler-like transition state (**53**) (Scheme 1.10A). It should be noted that *N,O*-acetal byproducts of the CCR (**58**, **61**), which are thought to proceed through zwitterionic intermediate **62**, have been isolated.^{3, 12, 26} However, **62** was computed to be unrealistically high in energy for the CCR of cyanosuccinic anhydrides.⁵¹ *N,O*-acetal byproducts have been found to form instantaneously in the case of cyclopentane fused maleic anhydride (**56**), and over the

course of three days with indolenines (**60**) and diglycolic anhydride (**59**), leading exclusively to the **61** and **64**, respectively with no evidence of the CCR product (Scheme 1.10B, Figure 1.10C).^{3, 26} It is possible that the zwitterionic intermediate **62** can be accessed with poor CCR substrates wherein Mannich addition is comparably high in energy. The Mannich-like mechanism for the reactions of cyano-succinic anhydride and imines and also explained the reaction outcomes of Castagnoli and Cushman. The stereochemical outcome of our original thiophenylsuccinic anhydride reaction and the reactions of cyano-glutaric anhydrides were also explained from the Mannich-like mechanism.^{18, 21} This mechanistic picture was also consistent with a proposal made by Connon for the lactone forming reaction of homophthalic anhydride and aldehydes.⁵³

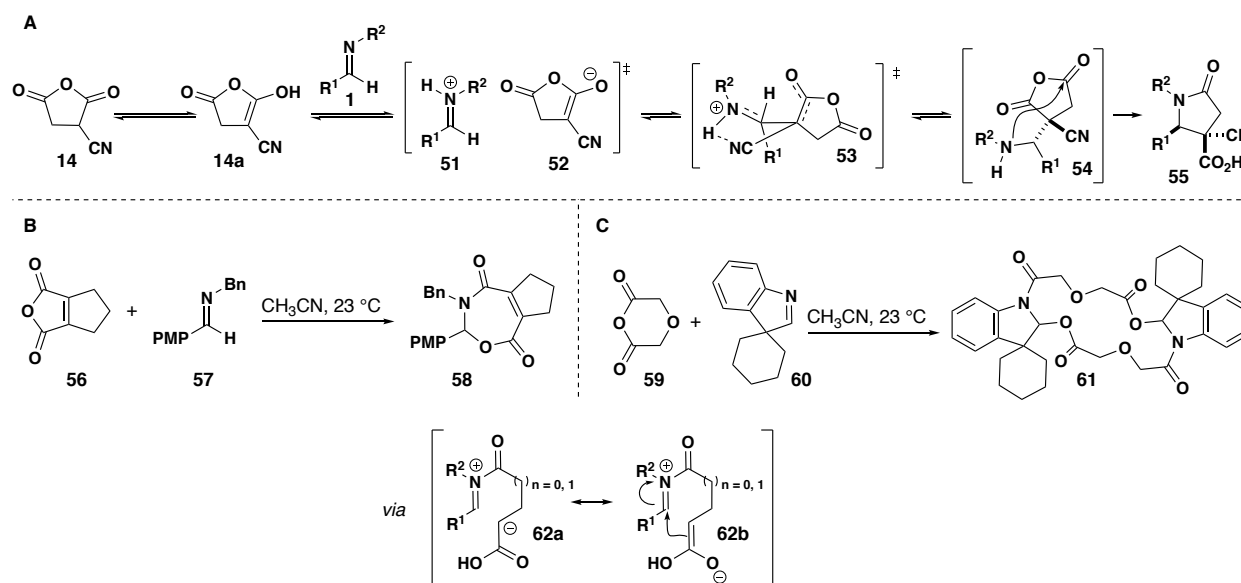


Figure 1.10 **A**. Mannich-like mechanism observed in computational studies. **B**. *N,O*-acetal product resulting from cyclopentane fused maleic anhydride **59**. **C**. *N,O*-acetal product observed in the reaction of glyoxylic anhydride with indolenines.

1.3 Development of the Base-Mediated Castagnoli-Cushman Reaction

Having determined that the mechanism of the CCR proceeds through Mannich addition, our group sought to use this mechanistic understanding to develop a base mediated CCR. Our group developed the first base-mediated variant of the CCR in 2016, which was applied to the synthesis of bisavenanthramide B-6 (see chapter 3).¹ Due to the high-reactivity of homophthalic anhydride, CCRs with *N*-alkyl or *N*-aryl imines typically proceeds with a high background rate. To enable a base catalyzed variant of the CCR, the less basic *N*-sulfonyl imines **66** were used, which simultaneously mimic the reactivity of an iminium ion and eliminate the background rate of the CCR (Figure 1.11A). We proposed that the mechanism of the reaction would begin with deprotonation of the anhydride to form the anhydride enolate (**48**) (Figure 1.11B). The enolate could then undergo a Mannich addition on the imine **66** leading to intermediate **69**. Subsequent intramolecular acylation affords lactam carboxylate **71**, which can be protonated to generate product **72** and regenerate the base catalyst. The scope of this work was expanded by our group in 2017 to reactions of a series of *N*-sulfonyl imines, as well as α -chiral *N*-sulfonyl imines (Scheme 1.11C).⁵⁴ In this reaction, either tetramethyl guanidine (TMG) in acetonitrile, or Hünig's base in dichloromethane afforded dihydroisoquinolone products **68** in good yields and excellent diastereoselectivity for the *trans* diastereomer. Notably, the reactions with α -chiral *N*-sulfonyl imines resulted in anti-Felkin products despite the absence of a chelatable Lewis acid.

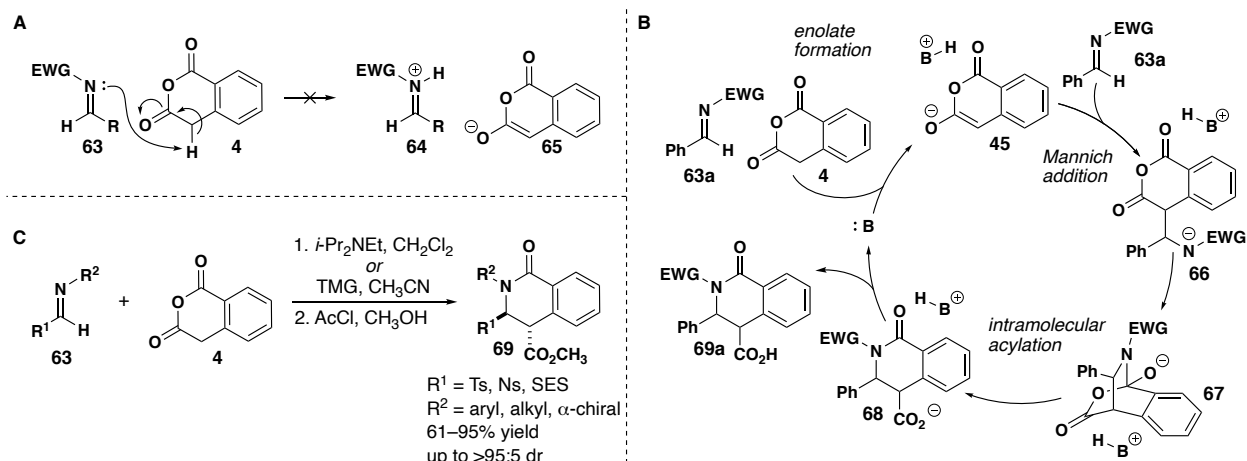


Figure 1.11 **A**. Imines bearing an electron withdrawing group eliminate the background rate of the CCR. **B**. Proposed mechanism for the base-mediated CCR. **C**. Optimized base-mediated CCR conditions and reaction outcomes.

1.4 Review of Catalytic and Enantioselective Castagnoli-Cushman Reactions

Prior to our group's development of the base-mediated CCR, the first catalytic, enantioselective variant of the CCR was reported in 2016 by the Connon group at University of Trinity Dublin.⁵⁵ Connon previously reported an enantio- and diastereoselective reaction of anhydrides with aldehydes to form lactones using squaramide based catalyst **72**.⁵⁶ They hypothesized that the catalyst facilitates the enolization of the anhydride and promotes the reaction between anhydride and aldehyde.^{55, 56} Connon sought to apply this to the CCR of homophthalic anhydride and a variety of imines. Initial results showed that the CCR of anhydrides with *N*-aryl and *N*-alkyl imines had a considerable background rate even at cryogenic temperatures. The proposed mechanism requires deprotonation of the anhydride by the base, and which led them to believe the imines were too basic to allow for catalysis. As a result, they screened

a series of less basic imines containing electron withdrawing *N*-substituents. Connon also utilized *N*-sulfonyl imines in the CCR and found that the suppressed basicity allowed for the addition of a squaramide base catalyst. However, they also found that larger *N*-substituents had a negative effect on enantioselectivity. To circumvent this, methane sulfonyl imines were employed. Additionally, a catalyst screen demonstrated that chiral quinine-derived catalysts improved enantioselectivity over the squaramide catalysts **72** used for the synthesis of lactones. Specifically, urea catalyst **73** showed the best enantioselectivity without eroding diastereoselectivity, albeit leading to variable enantiomer ratios (52:48 to 94:6) for a single diastereomer.

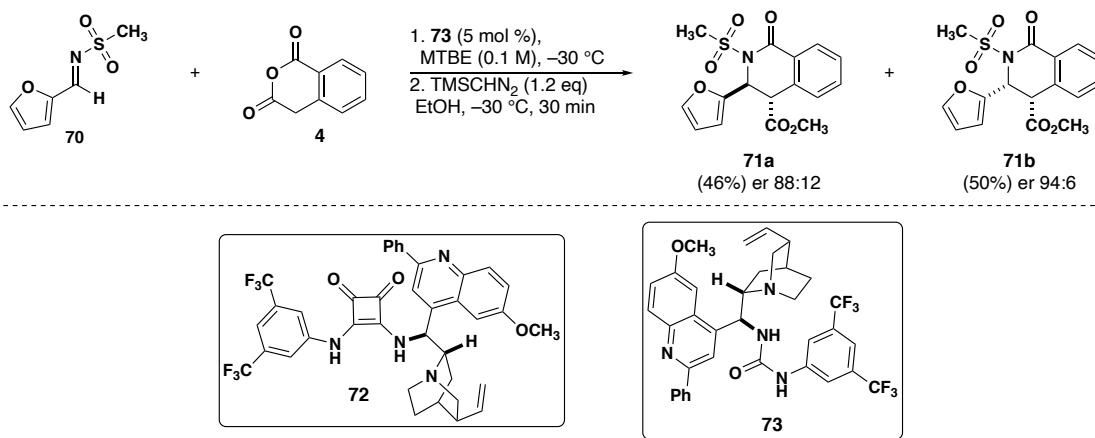


Figure 1.12 Selected example of Connon's the catalytic enantioselective CCR.

Later in 2017, a study performed by the Seidel group at University of Florida demonstrated that excellent enantioselectivity can be achieved by the use of a hydrogen-bonding chiral thiourea catalyst .⁵⁷ The Seidel group screened a series of catalysts and determined that the use of a dual functional anion binding/ion pairing catalyst **76** provided the best enantioselectivity for the reaction (Figure 1.13). In this case, it is proposed that the catalyst binds to homophthalic anhydride to increase its acidity, which allows for the

imine to deprotonate the anhydride to form an iminium ion that forms an ion pair with the catalyst-enolate complex. This dual functional catalyst allows for enantioselective synthesis of **75** ranging from 83:17 to 95:5 enantiomer ratios (Figure 1.13). *N*-alkyl, *N*-aryl, α,β -unsaturated and aliphatic aldehyde-derived imines were all tolerated in the reaction, expanding the substrate scope and obviating the need for *N*-sulfonyl substrates. The resulting product, **75**, was isolated as the kinetic *cis* isomer in good yields. The *cis* lactams are epimerized with diazobicycloundecane (DBU) to a single enantiomer of the thermodynamically stable *trans* product.

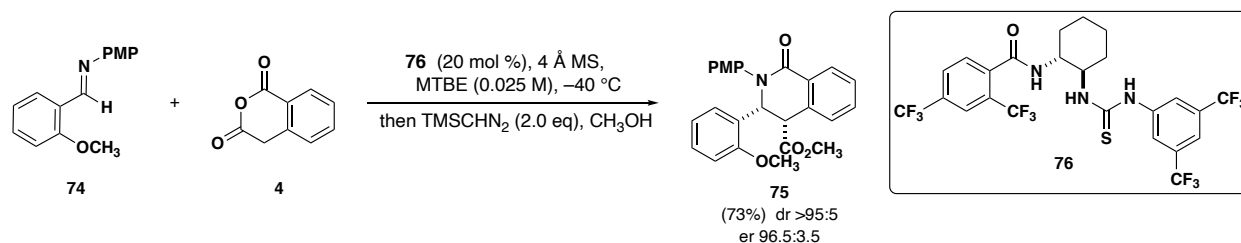


Figure 1.13 Selected example of Seidel's chiral thiourea catalyzed asymmetric CCR.

1.5 Conclusion

In summary, substantial advances in the CCR methodology have been observed over the past five decades. Several novel anhydrides have been synthesized and have been shown to have good reactivity in the CCR, expanding the scope of the reaction and facilitating the development of the first 4CR. A series of mechanistic investigations have led to the acceptance of the Mannich-like mechanism for lactam formation, which has enabled the development of catalytic CCR reactions. Finally, the most readily enolizable anhydride, homophthalic anhydride has been utilized for the development of the 3CR and the first asymmetric variants of the CCR.

1.6 References

1. Di Maso, M. J.; Nepomuceno, G. M.; St. Peter, M. A.; Gitre, H. H.; Martin, K. S.; Shaw, J. T., *Org. Lett.* **2016**, *18* (8), 1740-1743.
2. Younai, A.; Chin, G. F.; Shaw, J. T., *J. Org. Chem.* **2010**, *75* (23), 8333-8336.
3. Tang, Y.; Fettinger, J. C.; Shaw, J. T., *Org. Lett.* **2009**, *11* (17), 3802-3805.
4. Strumberg, D.; Pommier, Y.; Paull, K.; Jayaraman, M.; Nagafuji, P.; Cushman, M., *J. Med. Chem.* **1999**, *42* (3), 446-457.
5. Castagnoli, N., *J. Org. Chem.* **1969**, *34* (10), 3187-3189.
6. Cushman, M.; Castagnoli, N., Jr., *J. Org. Chem.* **1971**, *36* (22), 3404-3406.
7. Cushman, M.; Castagnoli, N., Jr., *J. Org. Chem.* **1972**, *37* (8), 1268-1271.
8. Cushman, M.; Castagnoli, N., Jr., *J. Org. Chem.* **1973**, *38* (3), 440-8.
9. Cushman, M.; Castagnoli, N., Jr., *J. Org. Chem.* **1974**, *39* (11), 1546-50.
10. Cushman, M.; Gentry, J.; Dekow, F. W., *J. Org. Chem.* **1977**, *42* (7), 1111-1116.
11. Haimova, M. A.; Mollov, N. M.; Ivanova, S. C.; Dimitrova, A. I.; Ognyanov, V. I., *Tetrahedron* **1977**, *33* (3), 331-336.
12. Dar'in, D.; Bakulina, O.; Chizhova, M.; Krasavin, M., *Org. Lett.* **2015**, *17* (15), 3930-3933.
13. Castagnoli, N., Jr., *J. Org. Chem.* **1969**, *34* (10), 3187-3189.
14. Robert, J.; Boucherle, A., *Ann. Pharm. Fr.* **1981**, *39* (4), 337-346.
15. Dallacker, F.; Jouck, W., *Chem.-Ztg.* **1985**, *109* (2), 82-4.
16. Baroudi, M.; Robert, J.; Luu-Duc, C., *Heterocycl. Commun.* **1996**, *2* (3), 255-260.
17. Cushman, M.; Madaj, E. J., *J. Org. Chem.* **1987**, *52* (5), 907-915.

18. Ng, P. Y.; Masse, C. E.; Shaw, J. T., *Org. Lett.* **2006**, *8* (18), 3999-4002.
19. Tan, D. Q.; Atherton, A. L.; Smith, A. J.; Soldi, C.; Hurley, K. A.; Fettinger, J. C.; Shaw, J. T., *ACS. Comb. Sci.* **2012**, *14* (3), 218-223.
20. Tan, D. Q.; Younai, A.; Pattawong, O.; Fettinger, J. C.; Cheong, P. H.-Y.; Shaw, J. T., *Org. Lett.* **2013**, *15* (19), 5126-5129.
21. Di Maso, M. J.; Snyder, K. M.; De Souza Fernandes, F.; Pattawong, O.; Tan, D. Q.; Fettinger, J. C.; Cheong, P. H.-Y.; Shaw, J. T., *Chem. Eur. J.* **2016**, *22* (14), 4794-4801.
22. Sorto, N. A.; Di Maso, M. J.; Muñoz, M. A.; Dougherty, R. J.; Fettinger, J. C.; Shaw, J. T., *J. Org. Chem.* **2014**, *79* (6), 2601-2610.
23. Dar'in, D.; Bakulina, O.; Chizhova, M.; Krasavin, M., *Org. Lett.* **2015**, *17* (15), 3930-3933.
24. Braunstein, H.; Langevin, S.; Khim, M.; Adamson, J.; Hovenkotter, K.; Kotlarz, L.; Mansker, B.; Beng, T. K., *Org. Biomol. Chem.* **2016**, *14* (37), 8864-8872.
25. Krasavin, M.; Dar'in, D., *Tetrahedron Lett.* **2016**, *57* (15), 1635-1640.
26. Chizhova, M.; Dar'in, D.; Krasavin, M., *Tetrahedron Lett.* **2017**, *58* (35), 3470-3473.
27. Usmanova, L.; Bakulina, O.; Dar'in, D.; Krasavin, M., *Chem. Heterocycl. Compd.* **2017**, *53* (4), 474-479.
28. Usmanova, L.; Dar'in, D.; Novikov, M. S.; Gureev, M.; Krasavin, M., *J. Org. Chem.* **2018**, *83* (10), 5859-5868.
29. Beng, T. K.; Moreno, A., *New J. Chem.* **2020**, *44* (11), 4257-4261.

30. Chizhova, M. E.; Dar'in, D. V.; Krasavin, M., *Mendeleev Commun.* **2020**, *30* (4), 496-497.
31. Moreno, A.; Beng, T. K., *Org. Biomol. Chem.* **2020**.
32. Pashev, A.; Burdzhiev, N.; Stanoeva, E., *Beilstein J. Org. Chem.* **2020**, *16*, 1456-1464.
33. Chizhova, M.; Bakulina, O.; Dar'in, D.; Krasavin, M., *ChemistrySelect* **2016**, *1* (17), 5487-5492.
34. Krasavin, M.; Gureyev, M. A.; Dar'in, D.; Bakulina, O.; Chizhova, M.; Lepikhina, A.; Novikova, D.; Grigoreva, T.; Ivanov, G.; Zhumagalieva, A.; Garabadzhiu, A. V.; Tribulovich, V. G., *Bioorg. Med. Chem.* **2018**, *26* (9), 2651-2673.
35. Adamovskiy, M. I.; Ryabukhin, S. V.; Sibgatulin, D. A.; Rusanov, E.; Grygorenko, O. O., *Org. Lett.* **2017**, *19* (1), 130-133.
36. Bakulina, O.; Dar'in, D.; Krasavin, M., *Synlett* **2017**, *28* (10), 1165-1169.
37. Bakulina, O.; Chizhova, M.; Dar'in, D.; Krasavin, M., *Eur. J. Org. Chem.* **2018**, *2018* (3), 362-371.
38. Adamovskiy, M. I.; Avramenko, M. M.; Volochnyuk, D. M.; Ryabukhin, S. V., *ACS Omega* **2020**, *5* (33), 20932-20942.
39. Yadav, J. S.; Reddy, B. V. S.; Saritha Raj, K.; Prasad, A. R., *Tetrahedron* **2003**, *59* (10), 1805-1809.
40. Azizian, J.; Mohammadi, A. A.; Karimi, A. R.; Mohammadzadeh, M. R.; Koohshari, M., *Heterocycles* **2004**, *63* (9), 2013-2017.

41. Azizian, J.; Mohammadi, A. A.; Karimi, A. R.; Mohammadizadeh, M. R., *J. Org. Chem.* **2005**, *70* (1), 350-352.
42. Wang, L.; Liu, J.; Tian, H.; Qian, C.; Sun, J., *Adv. Synth. Catal.* **2005**, *347* (5), 689-694.
43. Azizian, J.; Mohammadi, A. A.; Soleimani, E.; Karimi, A. R.; Mohammadizadeh, M. R., *J. Heterocycl. Chem.* **2006**, *43* (1), 187-190.
44. Yadav, J. S.; Reddy, B. V. S.; Reddy, A. R.; Narsaiah, A. V., *Synthesis* **2007**, (20), 3191-3194.
45. Karimi, A. R.; Pashazadeh, R., *Synthesis* **2010**, (3), 437-442.
46. Mohammadi, M. H.; Mohammadi, A. A., *Synth. Commun.* **2011**, *41* (4), 523-527.
47. Karimi, A. R.; Momeni, H. R.; Pashazadeh, R., *Tetrahedron Lett.* **2012**, *53* (27), 3440-3443.
48. Ghorbani-Choghamarani, A.; Hajjami, M.; Norouzi, M.; Abbasityula, Y.; Eigner, V.; Dušek, M., *Tetrahedron* **2013**, *69* (32), 6541-6544.
49. Chupakhin, E.; Dar'in, D.; Krasavin, M., *Tetrahedron Lett.* **2018**, *59* (26), 2595-2599.
50. Wei, J.; Shaw, J. T., *Org. Lett.* **2007**, *9* (20), 4077-4080.
51. Pattawong, O.; Tan, D. Q.; Fettinger, J. C.; Shaw, J. T.; Cheong, P. H.-Y., *Org. Lett.* **2013**, *15* (19), 5130-5133.
52. Tamura, Y.; Wada, A.; Sasho, M.; Kita, Y., *Tetrahedron Lett.* **1981**, *22* (43), 4283-4286.
53. Cornaggia, C.; Manoni, F.; Torrente, E.; Tallon, S.; Connon, S. J., *Org. Lett.* **2012**, *14* (7), 1850-1853.

54. Laws, S. W.; Moore, L. C.; Di Maso, M. J.; Nguyen, Q. N. N.; Tantillo, D. J.; Shaw, J. T., *Org. Lett.* **2017**, *19* (10), 2466-2469.
55. Cronin, S. A.; Gutierrez Collar, A.; Gundala, S.; Cornaggia, C.; Torrente, E.; Manoni, F.; Botte, A.; Twamley, B.; Connon, S. J., *Org. Biomol. Chem.* **2016**, *14* (29), 6955-6959.
56. Cornaggia, C.; Gundala, S.; Manoni, F.; Gopalasetty, N.; Connon, S. J., *Org. Biomol. Chem.* **2016**, *14* (11), 3040-3046.
57. Jarvis, C. L.; Hirschi, J. S.; Vetticatt, M. J.; Seidel, D., *Angew. Chem. Int. Ed.* **2017**, *56* (10), 2670-2674.

Chapter 2: Conjugate Addition Reactions of Anhydrides and α,β -Unsaturated *N*-Tosyl Ketimines¹

2.1 Introduction

The reaction of imines with cyclic enolizable anhydrides has been used extensively to form lactams through formal [4+2] cycloadditions.²⁻⁹ Recently our group has developed the first base-mediated variant of the CCR by utilizing *N*-sulfonyl imines, which eliminate the background rate of the CCR and allow for the addition of an exogenous base.^{7,9} Base-mediated CCR reactions proceed favorably with a variety of imines, however, a byproduct was observed in reactions with α,β -unsaturated imines. We hypothesized that this byproduct was the result of conjugate addition to form products similar to those formed in the Tamura reaction.¹⁰⁻¹³ To select for these conjugate addition products, we hypothesized that using ketone derived imines would afford products **3**. Thus, we developed a novel reaction of cyclic anhydrides with electron-deficient unsaturated imines which proceed to β -enamino ketone products **3** in high diastereoselectivity (Figure 2.1).

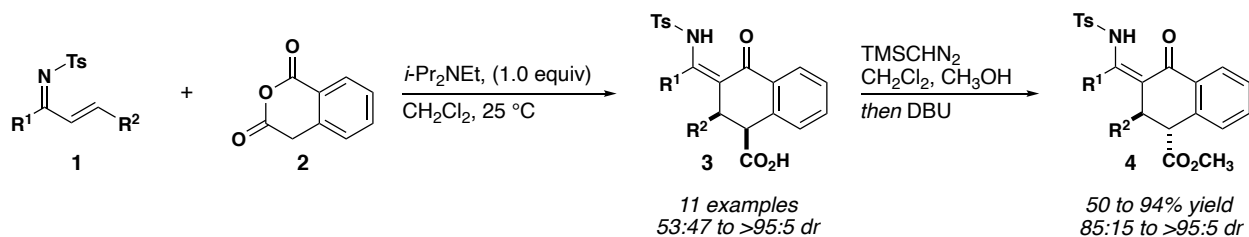


Figure 2.1 The aza-Tamura reaction leading to cis- β -enamino ketone products

2.1.1 Introduction to the Tamura Reaction

The Tamura reaction is known as the reaction of homophthalic anhydride with alkenes or alkynes to form highly substituted naphthalene products.^{10, 11} The reaction was first developed in 1981, when homophthalic anhydride was heated with a variety of activated alkynes or alkenes to afford a single regioisomer of products **5** or **9** after decarboxylation (Figure 2.2). Notably, alkenes or alkynes must be significantly activated in order to achieve optimal reaction outcomes.¹⁴ In 1984, Tamura and coworkers discovered that the addition of a strong base such as lithium diisopropylamide or sodium hydride improved reaction yields and lowered reaction temperatures.^{12, 13} This new method was also the basis for the synthesis of a series of anthracyclinone natural products **10–13**.^{12, 13}

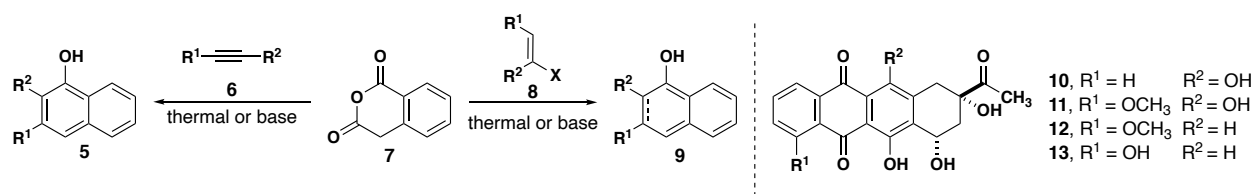


Figure 2.2: (Left) The Tamura reaction leading to substituted naphthalene products. (Right) Substituted anthracyclinone natural products synthesized using the Tamura reaction.

It was hypothesized that the Tamura reaction could proceed through three possible reaction mechanisms.¹¹ First, a Diels-Alder reaction resulting from the enol form of homophthalic anhydride could lead to intermediate **14a**, which after spontaneous decarboxylation affords shared intermediate **16** (Figure 2.3A, Mechanism i). Alternatively, Michael addition of the anhydride enol **14b** on the alkene could afford intermediate **17**, followed by decarboxylation to afford **16** (Figure 2.3A, Mechanism ii). Finally, spontaneous

decarboxylation to form benzocyclobuteneone **18** could open to form ortho-xylylene **19**. Compound **19** could then undergo a Diels-Alder reaction with the dienophile **13** to afford **16** (Figure 2.3A, Mechanism iii). Air mediated oxidation then yields Tamura products **5**. Several control experiments were performed that support either the first Diels-Alder mechanism through enol **14a** or the Michael addition mechanism. For one, heating homophthalic anhydride in dichlorobenzene for an extended period of time did not result in the formation of benzocyclobuteneone **18** (Figure 2.3B). Additionally, a double Diels-Alder reaction occurred to afford **21** when **2** was employed in the reaction with *N*-phenyl maleimide **20** (Figure 2.3C). These results suggest the mechanism proceeds through either the Diels-Alder mechanism or the Michael-type reaction, rather than the benzocyclobutene (Mechanism iii) Diels-Alder mechanism. The highly regioselective nature of this reaction can be attributed to the enolate attacking at the more electrophilic terminus of the dienophile carbon.

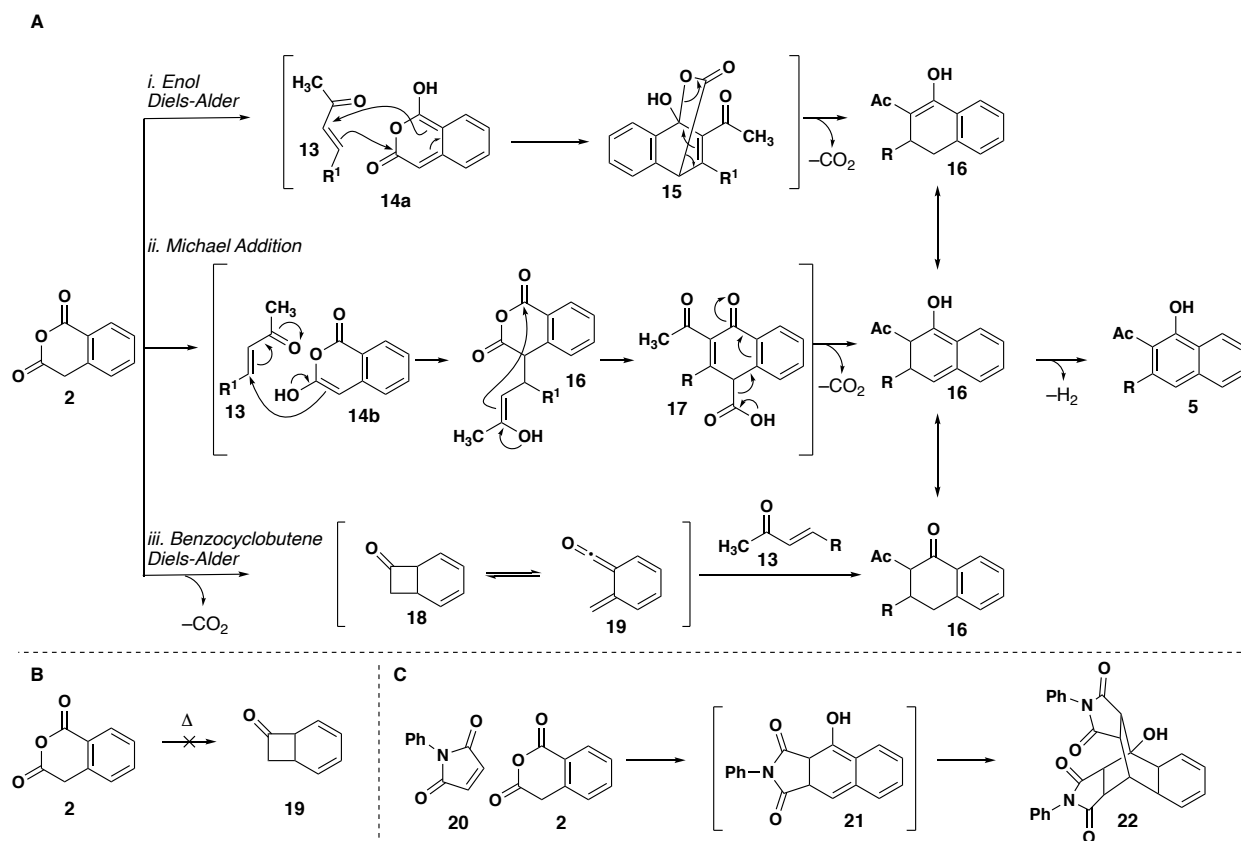


Figure 2.3 Possible mechanisms of the Tamura reaction. Experimental evidence supporting the enol-Diels-Alder mechanism.

In 1995, Haimova and coworkers developed a reaction that was both CCR- and Tamura-like by utilizing homophthalic anhydride and α,β -unsaturated aldimines at high temperatures.¹⁵ Interestingly, the reaction of *N*-isopropyl-substituted cinnamaldehyde derived imine **23** with homophthalic anhydride led to a mixture of five different products (Figure 2.4). The reaction outcomes are consistent with the Michael addition mechanism of the Tamura reaction, followed by either *C*- or *N*-acylation leading to products **24** or **25** and **27**, respectively. The predominant products were the *cis* **24** and *trans* **25** diastereomers of Tamura-like products in a 50:50 ratio, as well as the CCR product **26**. A small quantity of the *N*-acylation product **27** and Perkin condensation product **28** were

also observed in the reaction mixture. A solvent and temperature screen demonstrated that the *cis* isomer **24** converted to the *trans* isomer **25** at higher temperatures or over the course of longer reaction times.

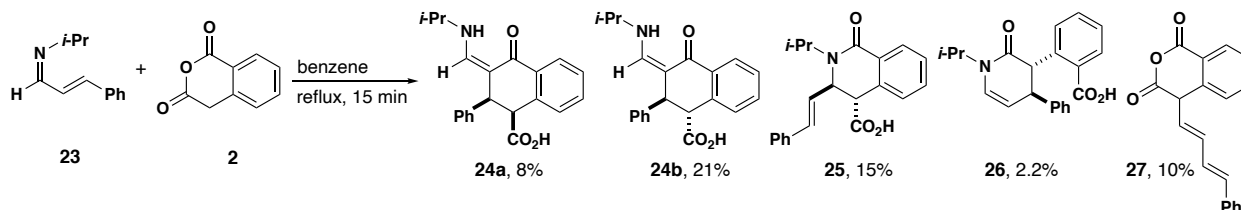


Figure 2.4 Product outcomes of Haimova's reaction of homophthalic anhydride with α,β -unsaturated imines

More recently, Connon developed the first asymmetric variants of the Tamura reaction utilizing alkylidene oxindoles and α -methyl nitrostyrenes with a variety of homophthalic anhydride derivatives.^{14, 16} The Tamura reaction typically forms highly aromatic systems, eliminating all possible stereogenic centers in products. However, Tamura reactions with **29** forgo aromatization to afford products **30**, rendering the reaction amenable to asymmetric catalysis (Figure 2.5A).¹⁴ Similar results were observed with alkylidene oxindoles **31** and α -methyl nitrostyrenes **34**. Using a bifunctional squaramide based catalyst similar to those tested in the asymmetric CCR reaction, Connon synthesized a series of spirooxindole products **32** in good yields, and the reactions proceeded with high enantioselectivity (Figure 2.5B). The enantio- and diastereoselectivity of the reaction were dependent on the temperature of the reaction, favoring **32a** at room temperature, and **32b** at -50 °C. Reactions with α -methyl nitrostyrenes afford products **35** in variable enantioselectivities (Figure 2.5C).

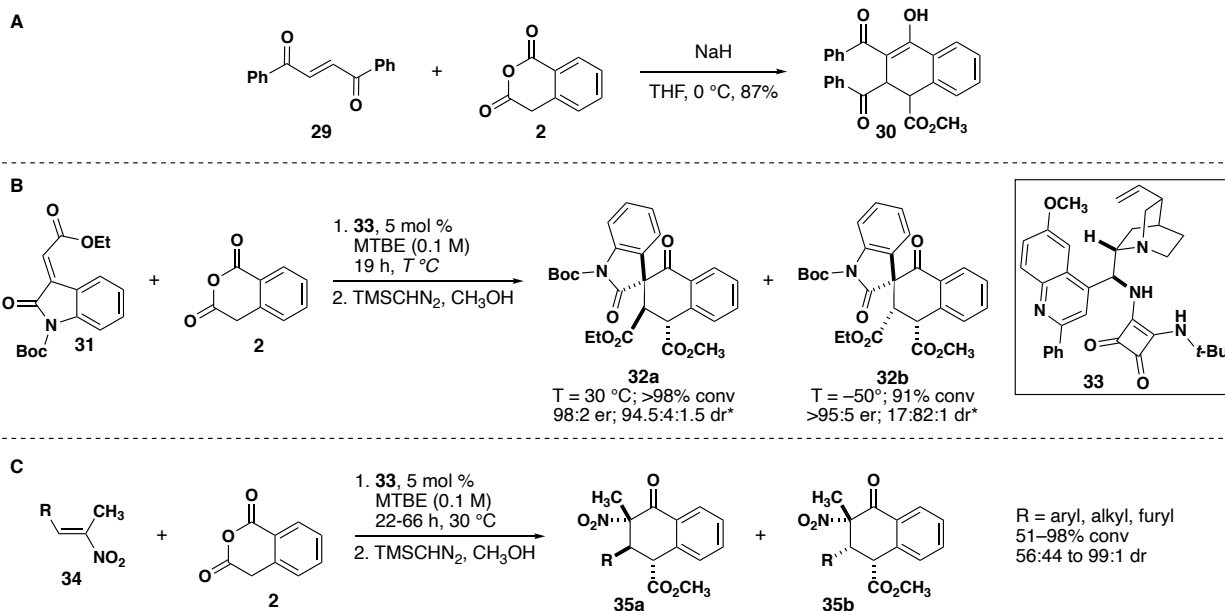


Figure 2.5 **A**. Reaction of dienone **29** leads to Tamura product with stereogenic centers. **B**. Connon's asymmetric Tamura reaction *The diastereomer ratio corresponds to **32a:32b:32c** wherein an additional diastereomer **32c** was detected in the reaction mixture in minute quantities. **C**. Tamura reactions of α -methyl nitrostyrenes with homophthalic anhydride

2.2 Results and Discussion

2.2.1 Unexpected Side Products in the Base-Mediated Castagnoli-Cushman Reaction

In 2017, our group developed a base-mediated variant of the CCR, leading to the synthesis of lactams **37**.⁹ This method proved useful for a variety of imines; however, an interesting result was observed with a certain subset of imines. Specifically, when cinnamaldehyde derived imines were employed in the reaction, the desired lactam product was formed, as well as a small quantity of a byproduct **38** (Figure 2.6). Based on Haimova's results, we hypothesized that the byproduct was the result of conjugate addition leading to β -enamino ketone **38**. While reactions of cyclic anhydrides and

aldimines have been well-studied, the reactions of enolizable anhydrides and α,β -unsaturated ketimines are relatively underexplored. As a result, we sought to develop a method to selectively form products **38** in a reaction that we refer to as the aza-Tamura reaction.

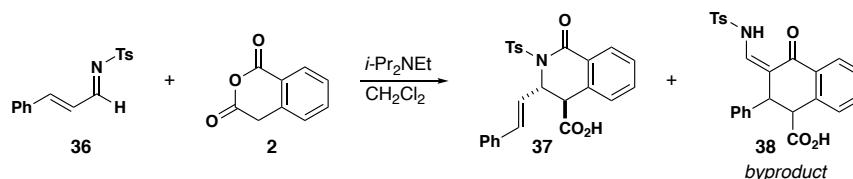


Figure 2.6 CCR reaction of cinnamaldehyde derived *N*-Tosyl imine to afford lactam **37** and byproduct **38**.

We believed that increasing steric bulk around the imine would select for conjugate addition products (Figure 2.7). In order to improve selectivity for the conjugate addition reaction, ketone derived imines were used in the reaction. Considering products **26** and **27** isolated in Haimova's reaction outcomes, we anticipated that after conjugate addition of the anhydride on the imine, intermediate **40** could lead to either the *C*-acylation product **3** or *N*-acylation product **41** (Figure 2.7).

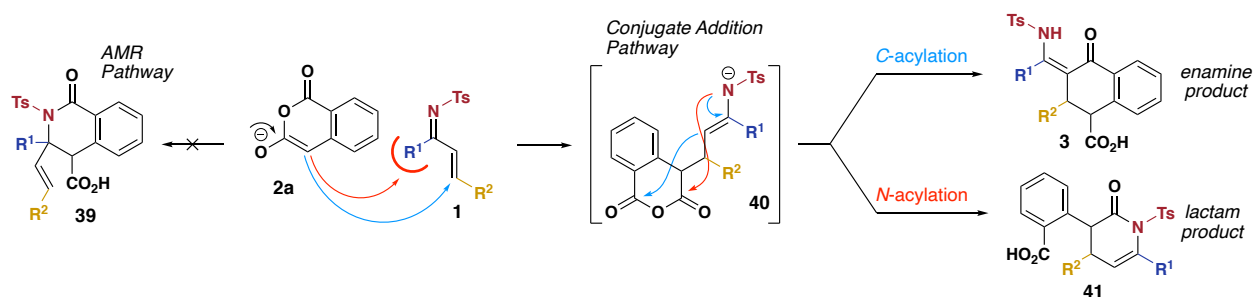


Figure 2.7 Possible mechanism for the formation of enamine and lactam products through the aza-Tamura reaction

2.2.2 Synthesis of Chalcone Derived Imines

Initial study of the aza-Tamura reaction began by synthesizing chalcone-derived imine substrates. Chalcone-derived substrates were chosen for their ease of synthesis and the breadth of commercially available reaction partners that allow for a broad substrate scope. Chalcones were either bought (**44a**, **44k**) or synthesized by aldol condensation using acetophenone and benzaldehyde derivatives with either NaOH or KOH (Figure 2.8). We were interested in investigating electronic effects of different *para*-substituents on either aryl group of the chalcone. *Para*-substituted chalcones would ultimately provide electronic influence on the imine without introducing the steric effect of an *ortho*-substituent. To test substitution on either ring, *para*-substituted benzaldehyde derivatives were condensed with acetophenone to yield **44b** and **44h**. Conversely, *para*-substituted acetophenone derivatives were condensed with benzaldehyde to yield **44c**, **44e**, and **44i**. To expand the scope of the reaction to heterocyclic substrates, similar reactions were performed to yield **44d**, **44e**, **44f**, and **44g** (Figure 2.8).

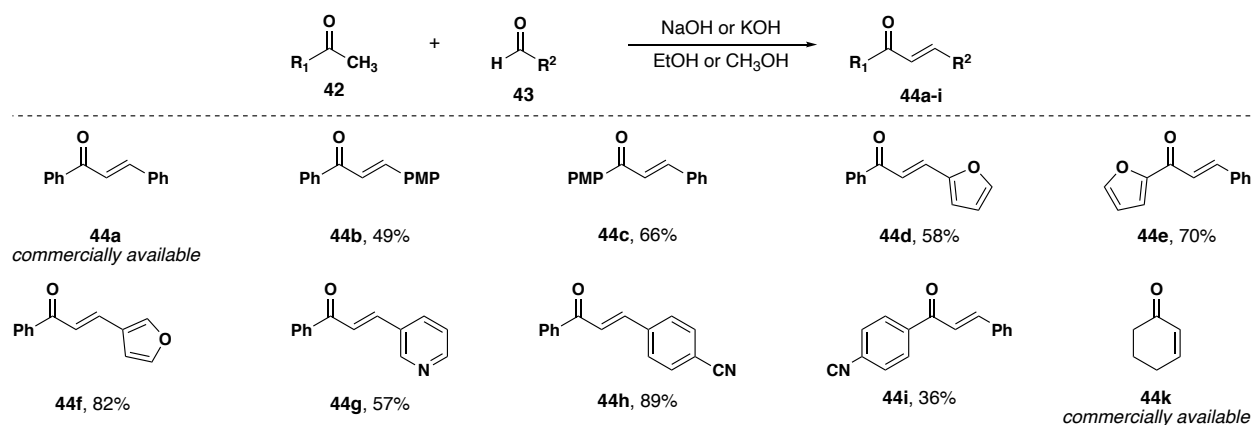


Figure 2.8 Scope of chalcones through aldol condensations.

After synthesizing chalcones and heterocyclic derivatives, enolizable α,β -unsaturated

ketones were investigated to ultimately afford enolizable imines. Initially, the synthesis of ketone **44j** was attempted using a Friedel-Crafts acylation of crotonoyl chloride (**46**) and benzene (Figure 2.9A). Crotonoyl chloride (**46**) was synthesized by chlorinating crotonic acid (**45**) with oxalyl chloride and was subsequently employed in the Friedel-Crafts acylation. Based on the ^1H NMR spectrum and mass spectrometry of the unpurified reaction mixture, the observed product was a Friedel-Crafts derivative of the desired acylation product.¹⁷ After the acylation, the product continued to react with the excess benzene to produce **47** (Figure 2.9A). A Pd-catalyzed rearrangement was also attempted to produce ketone **44j**.¹⁸ The starting material, **50**, was synthesized in one step¹⁸ and subjected to the Pd-catalyzed reaction—however no product was formed (Figure 2.9B). Due to the failure of the palladium catalyzed rearrangement, the synthesis of a different enolizable ketone, **44i**, was attempted. Acetophenone was employed in the aldol condensation with propionaldehyde, but the ^1H NMR of the unpurified reaction mixture revealed exclusively acetophenone (Figure 2.9C). Finally, Noah Burlow found an alternative procedure for the Friedel-Crafts reaction and successfully synthesized **44j**.

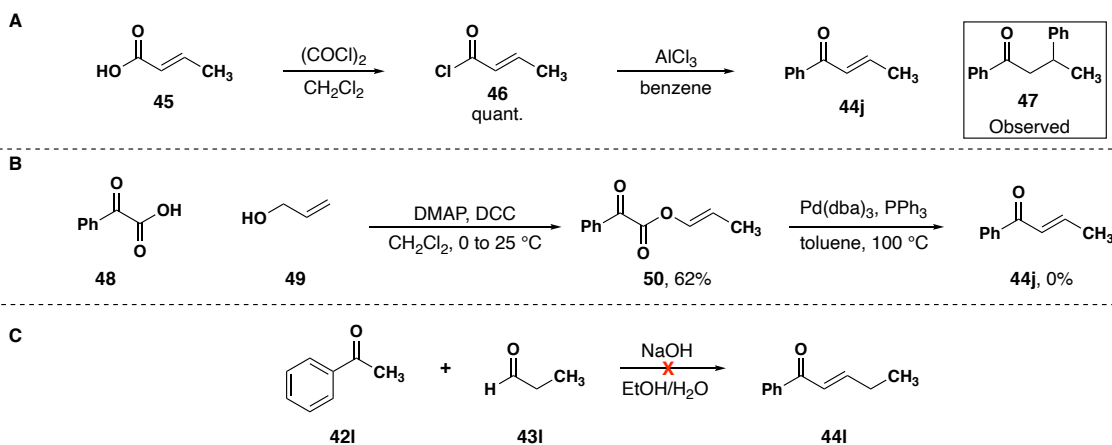


Figure 2.9 A. Friedel Crafts reaction used in the attempted synthesis of **44j**. B. Palladium catalyzed reaction toward the synthesis of **44j**. C. Attempt at aldol condensation to afford **44i**.

The synthesized α,β -unsaturated ketone products and *trans*-chalcone were then condensed with *p*-toluene sulfonamide in the presence of TiCl_4 to yield α,β -unsaturated imines **51** (Figure 2.10). Most reactions led to good, albeit incomplete conversion to imine products. As a result, the excess *p*-toluene sulfonamide present during flash column chromatography rendered the imine products difficult to isolate independently, leading to lower yields. To our delight, synthesis of enolizable imine product **1j** was successful. Finally, a cyclohexenone derived imine was synthesized from modified literature procedure involving both TiCl_4 and $\text{Ti}(\text{OEt})_4$, affording imine **1k** in modest yield (Scheme 2.10).¹⁹

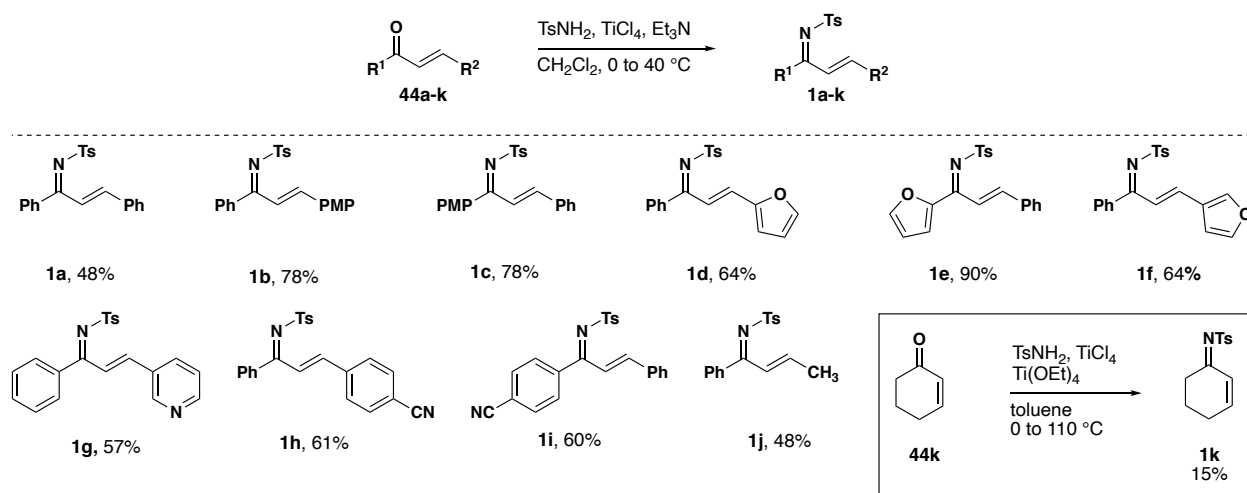


Figure 2.10 Synthesis of α,β -unsaturated ketimines to test in the aza-Tamura reaction.

2.2.3 Failed Attempts at the Synthesis of Enolizable Ketimine **1m**

In hopes of expanding our enolizable imine substrate scope, multiple syntheses of imine **1m** were attempted. First, typical condensation procedures were used on commercially available α,β -unsaturated ketone **44m**, however, due to the enolizable nature of the resulting imine, aldol addition product **51** was discovered by ^1H NMR

spectroscopy and mass spectrometry (Figure 2.11A). An additional condensation procedure from literature involving ketone **44m** and *p*-toluene sulfonamide with Ti(*Oi*-Pr)₄ and ZnCl₂ also failed, resulting exclusively in recovered starting material.²⁰ A new procedure was attempted by condensing *p*-toluene sulfinamide **53** with ketone **44m** using Ti(OEt)₄ in toluene, followed by oxidation with mCPBA (Figure 2.11B).²¹ Sulfinamide **53** was synthesized successfully, however condensation conversion was low. Despite the slow conversion, the unpurified material was subjected to mCPBA, yet no product was visible in the ¹H NMR spectrum. After searching through literature, a similar *N*-benzene sulfonyl imine was found to have been made from the rearrangement of an oxime with benzenesulfonyl chloride.²² Synthesis of the analogous *p*-toluene sulfonyl chloride **57** proved difficult due to rapid decomposition at room temperature, however, synthesis of **57** was successful after an additional attempt: condensation of ammonium hydroxide with ketone **44m** afforded **55** in 76% yield. Sulfonyl chloride **57** and oxime **55** were subjected to triethylamine in carbon tetrachloride in hopes of forming rearrangement product **1m**, however no conversion to product was observed.²² After numerous attempts at the synthesis of **1m**, a final publication was found that stated that due to the enolizable nature of imine **1m**, it could not be synthesized. As a result, substrate **1m** was discarded.²³

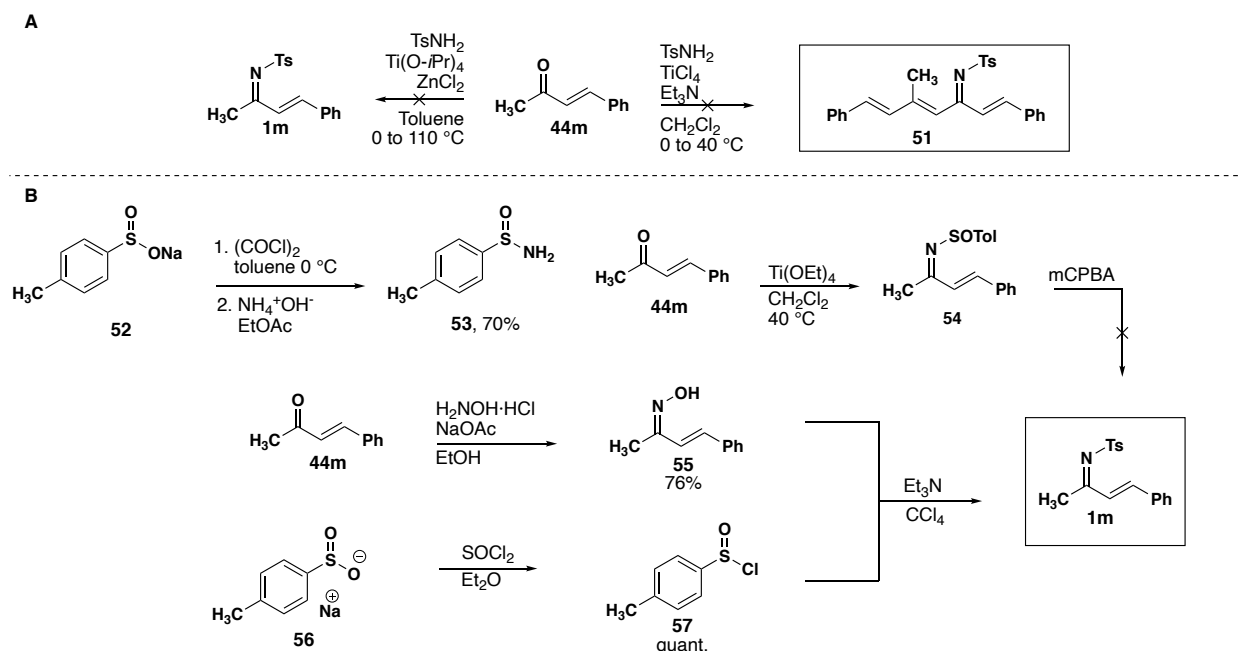


Figure 2.11 A. Attempted synthesis of **1m** through condensation of *p*-toluene sulfonamide. B. Two alternative routes toward the synthesis of **1m**.

2.2.4 Optimization and Diastereoselectivity of the Aza-Tamura Reaction

Satisfied with our substrate scope, Noah worked to optimize the aza-Tamura reaction for both diastereoselectivity and conversion to the *cis* β -enamino ketone product **3c**. Initial optimization reactions were performed with tetramethyl guanidine (TMG) in acetonitrile, the favored conditions for the base-mediated CCR (Table 2.1). Readily enolizable homophthalic anhydride and chalcone derived imine **1c** were utilized and subjected to various reaction conditions. Reactions with TMG resulted in effectively no diastereoselectivity, regardless of the equivalents of base or anhydride (Entries 1-5). Switching to Hünig's base in dichloromethane provided excellent diastereoselectivity and moderate conversion to the *cis* enamine product (Entry 8). Catalytic quantities of Hünig's base resulted in lower conversion to product (Entry 9), which we hypothesize this is due

to the acidity of the *N*-tosyl vinylogous amide proton, resulting in product inhibition. Conditions utilizing 1.2 equivalents of anhydride using stoichiometric Hünig's base provided excellent conversion and diastereoselectivity for product **3c**. Notably, the reaction proceeds to exclusively β -enamino ketone products, with no evidence of the CCR or Perkin-like products found in Haimova's studies.

Table 2.1 Optimization of the aza-Tamura reaction

entry	base (equiv)	equiv 2	solvent	dr (cis:trans) ^a	conv ^a
1	TMG (1.0)	1.0	CH ₃ CN	57:43	100%
2	TMG (0.2)	1.0	CH ₃ CN	54:46	82%
3	TMG (0.2)	1.2	CH ₃ CN	51:49	85%
4	TMG (1.0)	1.0	CH ₂ Cl ₂	29:71	97%
5	TMG (1.0)	1.0	THF	21:79	91%
6	<i>i</i> -Pr ₂ NEt (1.0)	1.0	CH ₃ CN	79:21	95%
7	<i>i</i> -Pr ₂ NEt (1.0)	1.0	THF	64:36	58%
8	<i>i</i> -Pr ₂ NEt (1.0)	1.0	CH ₂ Cl ₂	94:6	81%
9	<i>i</i> -Pr ₂ NEt (0.2)	1.0	CH ₂ Cl ₂	>95:5	20%
10	<i>i</i> -Pr ₂ NEt (1.2)	1.0	CH ₂ Cl ₂	79:21	89%
11	<i>i</i> -Pr ₂ NEt (1.0)	1.2	CH ₂ Cl ₂	93:7	97%

^aDetermined by the ¹H NMR spectrum of the unpurified reaction mixture

2.2.4.1 Temperature Dependent Reaction Outcomes

During optimization of the aza-Tamura reaction, Noah found that reaction outcomes were highly temperature dependent. Lactam **41c** is formed when the reaction is run overnight at -20 °C, albeit with poor conversion (Figure 2.12). On the other hand, the thermodynamically favored β -enamino ketone product **3c** is formed when the reaction is run at room temperature overnight. Resubjecting **41c** to reaction conditions at room temperature affords full conversion to product **3c** over 24 h. Analysis of the aza-Tamura reaction through ¹H NMR spectroscopy studies has shown that **41c** is formed first as the

kinetic product (Figure 2.13). Over the course of 24 hours, the lactam product converts to the imine product, which tautomerizes to the β -enamino ketone product **3c** as the reaction progresses. The structure of the kinetic product was assigned based on comparison of ^1H NMR signals with analogous molecules synthesized by Smith and coworkers.²⁴

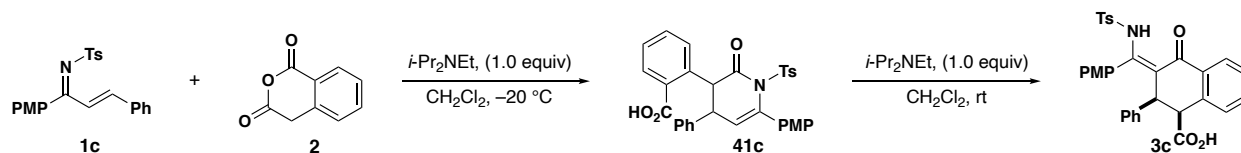


Figure 2.12 Lactam **41** converts back to enamine **3** over 24 hours at rt.

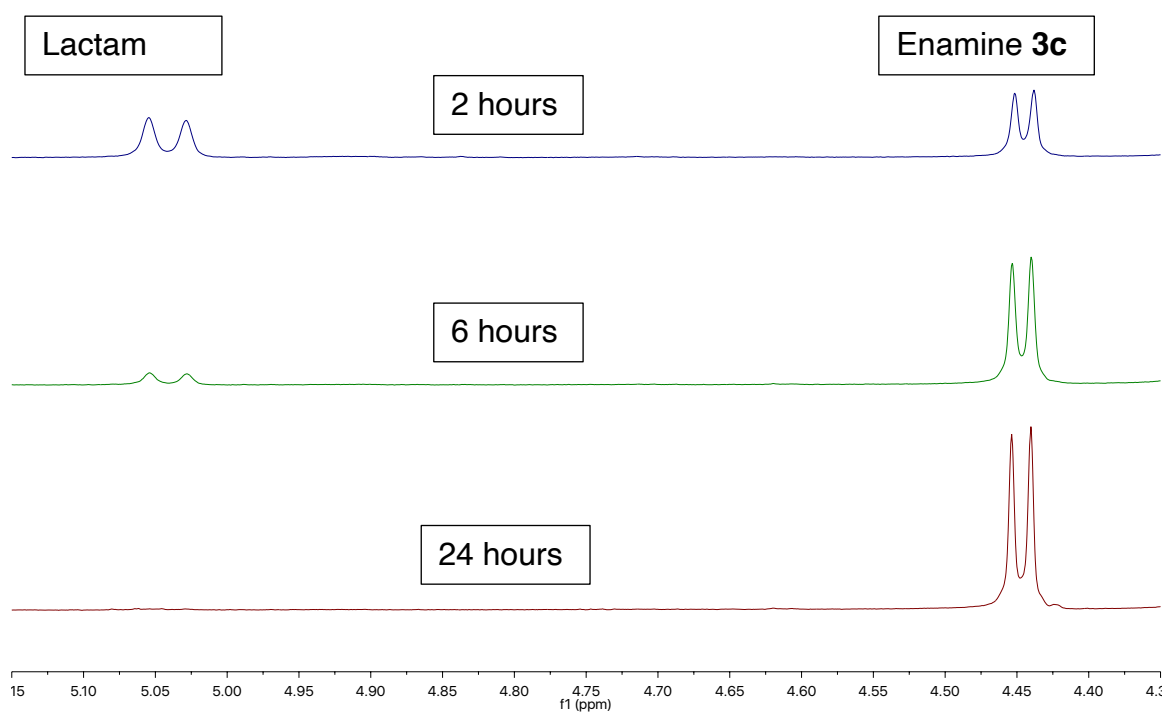


Figure 2.13 ^1H NMR experiment showing conversion from lactam to enamine product.

2.2.5 Effect of Imine Substituents on Diastereoselectivity

With optimized conditions in hand, *N*-sulfonyl ketimines **1** were subjected to the aza-Tamura reaction (Figure 2.14). Interestingly, the electronics of the substituent on the aryl ring of R¹ had a significant impact on diastereoselectivity. In particular, excellent diastereoselectivity for the *cis* enamine was observed for products containing electron donating groups on the aryl ring at R¹ (**3c**). On the other hand, electron withdrawing groups in the same position eroded selectivity (**3i**)—likely due to the faster rate of base-catalyzed epimerization to the *trans* diastereomer. The diastereomer ratio was less noticeably affected for products from imines with electron donating and withdrawing groups on the aryl ring at the R² position (**3b**, **3d**, **3f**, **3g**, **3h**). Enolizable imines (**1j** and **1k**) were also tolerated in the reaction yielding products **3j** and **3k** with moderate diastereoselectivity. The relative stereochemistry of the major product of **3k** was determined by computational NMR performed by Dr. Carla Saunders of the Tantillo group.

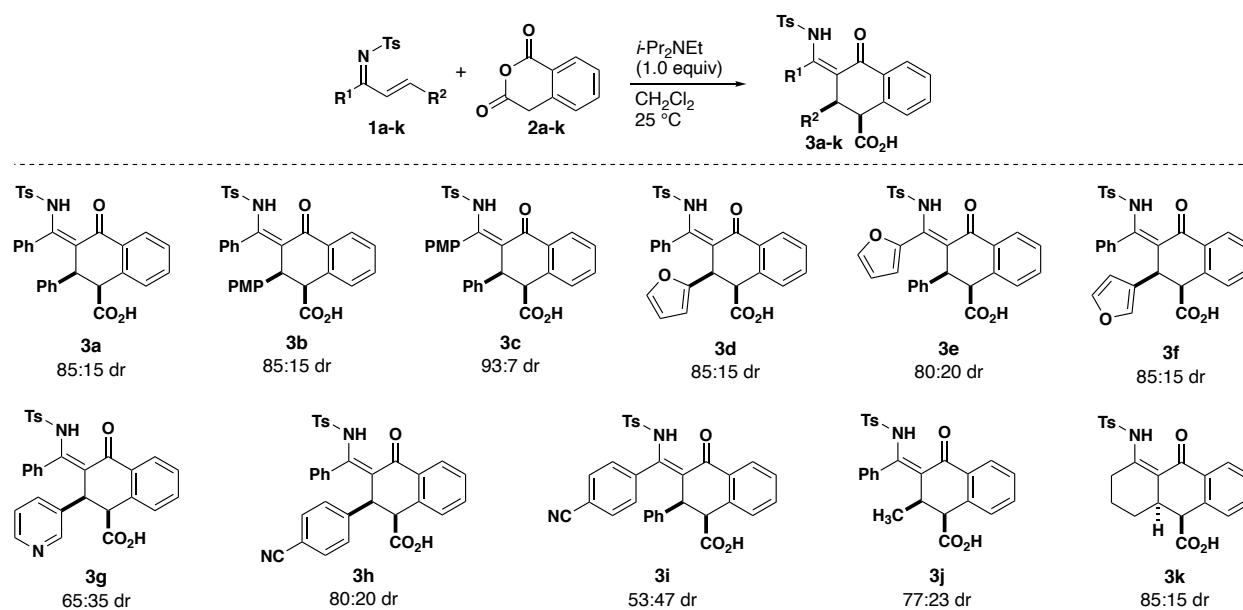


Figure 2.14 Substrate scope leading to *cis* β-enamino ketones

2.2.6 Conversion to Methyl Esters and Substrate Epimerization

β -enaminoketone products were then esterified to their corresponding methyl esters by treatment with TMS-diazomethane. Following conversion to the methyl ester, the *cis* products could be epimerized to the *trans* diastereomer using 1,8-diazobicyclo(5.4.0)undec-7-ene (DBU) in good yields over the two-step sequence (Figure 2.15). Though epimerization proved facile for majority of substrates, cyclohexenone derived product **4k** did not fully epimerize even after resubjecting to an additional equivalent of DBU. We hypothesized based on J_{H-H} values that the initial products of the chalcone derive substrates were the kinetic *cis* diastereomers **3**, and the epimerized

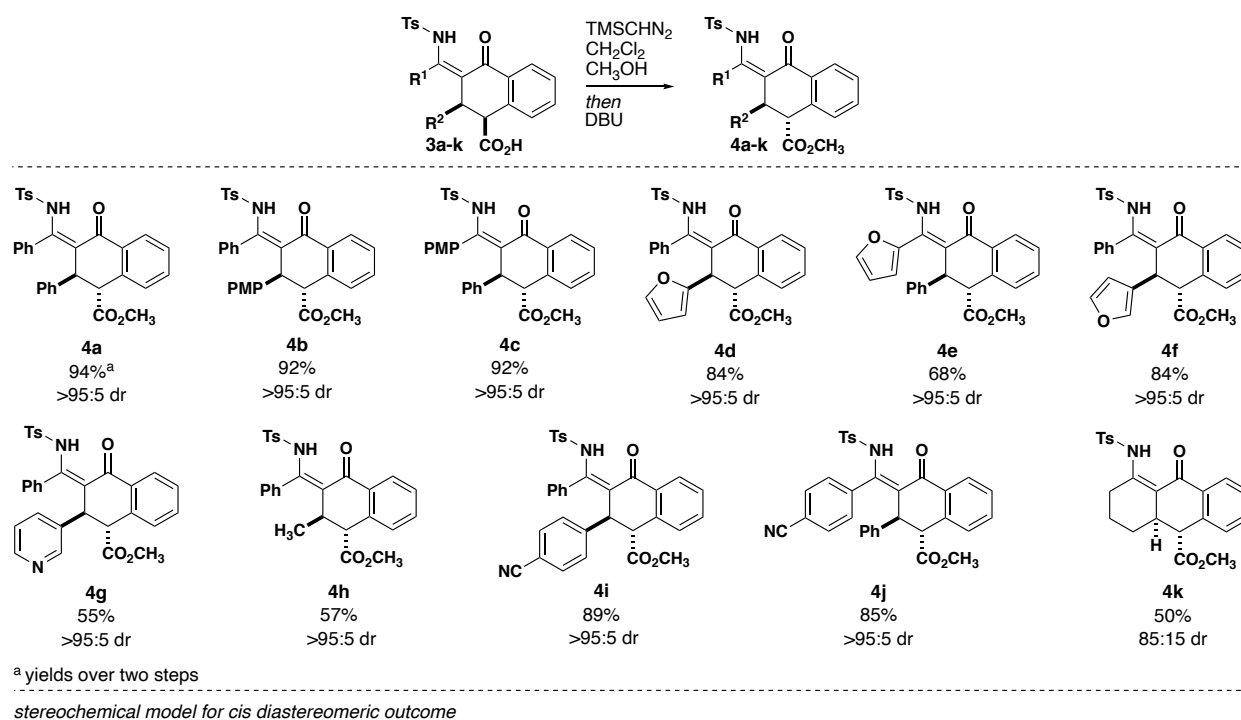


Figure 2.15 Esterification of aza-Tamura products **3a-k** yielding products **4a-k** in good yields and excellent diastereoselectivity. (Bottom) Transition state drawing leading to kinetic *cis* product through a syn-clinal transition state structure.

product was the thermodynamic trans diastereomers **4**. Additionally, transition state drawings suggest that the formation of the cis diastereomer would be preferred over formation of the trans diastereomer, consistent with the kinetic product (Figure 2.15 bottom). Though the trans diastereomer does contain two pseudo-axial substituents, due to the presence of four sp^2 hybridized centers in products **4c**, there are essentially no 1,3 diaxial interactions present which supports the assignment of the thermodynamic trans diastereomer.

To confirm the relative stereochemistry, Noah initially hydrolyzed the ester **4c** to acid using LiOH. Hydrolysis resulted in no changes to the J_{H-H} of the adjacent protons, indicating that no epimerization had occurred (Figure 2.16). He then attempted to perform an amidation reaction with $POCl_3$ and *p*-methoxybenzylamine. Interestingly, the resulting product was less polar than expected, and lacked protons corresponding to the amide in the 1H NMR spectrum.²⁵ We hypothesized the resulting product was the nitrile derivative **58**, which occurs through a von Braun-like mechanism proceeding through cleavage of the PMB amide.²⁶ An X-ray crystal structure was acquired which confirmed this hypothesis, and also confirmed relative stereochemistry to be trans.

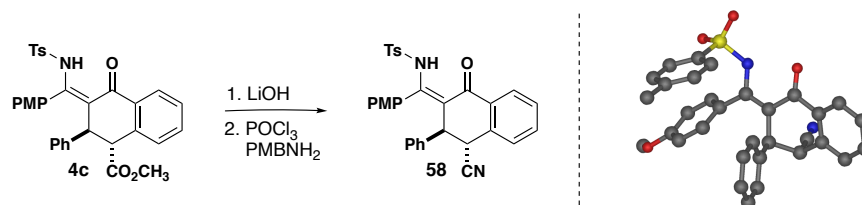


Figure 2.16 X-ray crystal structure of the nitrile derivative **58** confirms trans stereochemistry of aza-Tamura products.

2.3 Conclusion

We have developed a base-mediated reaction between α,β -unsaturated *N*-tosyl ketimines and cyclic enolizable anhydrides to form β -enamino ketone products. Reactions with TMG provided low diastereoselectivity, while stoichiometric Hünig's base afforded products in both higher yields and diastereoselectivity. β -enamino ketone products were converted to methyl esters for ease of purification. In all but one case, the resulting esters were then fully epimerized to the trans-diastereomer upon treatment with DBU.

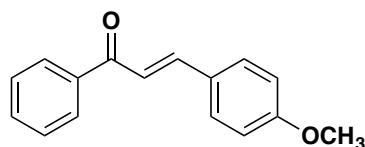
2.4 Experimental Section

I. Materials and Instrumentation:

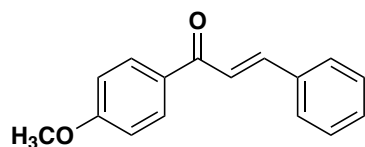
Unless otherwise specified, all commercially available reagents were used as received. All reactions using dried solvents were carried out under an atmosphere of argon in flame-dried glassware with magnetic stirring. Dry solvent was dispensed from a solvent purification system that passes solvent through two columns of dry neutral alumina. ^1H NMR spectra and proton decoupled ^{13}C NMR spectra were obtained on a 400 MHz Bruker or 600 MHz Varian NMR spectrometer. ^1H Chemical shifts (δ) are reported in parts per million (ppm) relative to TMS (s, δ 0). Multiplicities are given as: s (singlet), d (doublet), t (triplet), q (quartet), p (pentet), h (hexet), and m (multiplet). Complex splitting will be described by a combination of these abbreviations, i.e. dd (doublet of doublets). ^{13}C NMR chemical shifts are reported relative to CDCl_3 (t, δ 77.4) unless otherwise noted. Accurate mass measurements were recorded on positive ESI mode in methanol. Chromatographic

purifications were performed by flash chromatography with silica gel (Fisher, 40–63 μm) packed in glass columns.

II. Experimental Data:

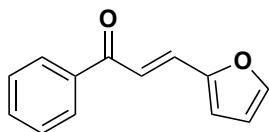


(E)-3-(4-methoxyphenyl)-1-phenylprop-2-en-1-one (44b): Following a literature procedure²⁷: to a solution of acetophenone (1.03 g, 8.56 mmol) in CH_3OH (8.6 mL), was added *p*-methoxybenzaldehyde (1.04 mL, 8.56 mmol) and 20% KOH solution (0.856 mL). The reaction mixture was stirred overnight at rt. After completion of reaction, reaction was added to 30 mL of water, acidified with 1 M HCl, filtered, and recrystallized in hot ethanol to yield **44b** as a white solid (0.99 g, 49%): $^1\text{H NMR}$ (400 MHz, CDCl_3) δ 8.04 – 7.99 (m, 2H), 7.79 (d, $J = 15.7$ Hz, 1H), 7.64 – 7.54 (m, 3H), 7.53 – 7.47 (m, 2H), 7.42 (d, $J = 15.6$ Hz, 1H), 6.97 – 6.91 (m, 2H), 3.86 (s, 3H). $^1\text{H NMR}$ shifts match literature values.²⁸

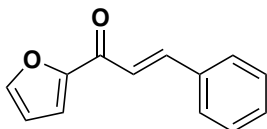


(E)-1-(4-methoxyphenyl)-3-phenylprop-2-en-1-one (44c): *p*-methoxyacetophenone (1.0 g, 6.65 mmol) was dissolved in CH_3OH (6.5 mL, 1 M). Benzaldehyde was added (0.68 mL, 6.65 mmol), followed by KOH (0.67 mL, 20% solution in H_2O) and the reaction was stirred overnight. The reaction was diluted with H_2O (15 mL) and acidified with 1M

HCl. The solid was filtered and recrystallized in ethanol to afford **44c** as a white solid (1.0 g, 66%). $^1\text{H NMR}$ (600 MHz, CDCl_3) δ 8.08 – 8.02 (m, 2H), 7.81 (d, $J = 15.7$ Hz, 1H), 7.65 (dd, $J = 7.1, 2.4$ Hz, 2H), 7.55 (dd, $J = 15.7, 1.4$ Hz, 1H), 7.47 – 7.39 (m, 3H), 7.02 – 6.96 (m, 2H), 3.90 (s, 3H).

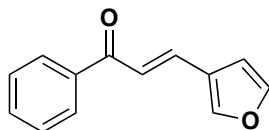


(E)-3-(furan-2-yl)-1-phenylprop-2-en-1-one (44d): Following a modified literature procedure²⁹: To a stirred solution of acetophenone (0.49 mL, 4.16 mmol) in CH_3OH (2.08 mL, 2M) was added dropwise a solution of NaOH (0.22 g, 5.14 mmol) in methanol (4.16 mL, 1.3 M) and stirred. After 15 minutes, 2-furaldehyde (0.35 mL, 4.16 mmol) was added, and the reaction mixture was stirred at rt overnight. Following completion of reaction, solvent was removed *in vacuo*. Resulting residue was treated with water (20 mL) and extracted with EtOAc (3x 30 mL), dried over Na_2SO_4 and concentrated *in vacuo*. Crude material was purified by flash column chromatography (70:30 hexanes/EtOAc) to yield **44d** as an orange oil (0.48 g, 58%): $^1\text{H NMR}$ (400 MHz, CDCl_3) δ 8.06 – 8.01 (m, 2H), 7.63 – 7.43 (m, 6H), 6.72 (d, $J = 3.4$ Hz, 1H), 6.52 (dd, $J = 3.4, 1.8$ Hz, 1H). $^1\text{H NMR}$ shifts match literature values.³⁰

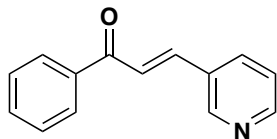


(E)-1-(furan-2-yl)-3-phenylprop-2-en-1-one (44e) Following a modified literature procedure:³¹ 2-acetyl furan (0.166 mL, 1.66 mmol) and benzaldehyde (0.15 mL, 1.5

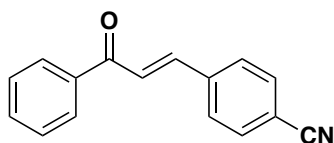
mmol) were dissolved in CH₃OH (8.0 mL, 0.18 M). A solution of NaOH (2.36 mL, 1M) was added and the reaction was stirred overnight. The product was acidified with HCl (1M). EtOAc was added, extracted 3x with EtOAc (10 mL), and dried over Na₂SO₄. The reaction mixture was purified by flash column chromatography (70:30 Hexanes/EtOAc) to yield **44c** (0.228 g, 70%). ¹H NMR (600 MHz, CDCl₃) δ 7.89 (d, *J* = 15.8 Hz, 1H), 7.66 (td, *J* = 5.9, 3.0 Hz, 3H), 7.49 – 7.41 (m, 4H), 7.34 (d, *J* = 3.6 Hz, 1H), 6.60 (dd, *J* = 3.6, 1.7 Hz, 1H).



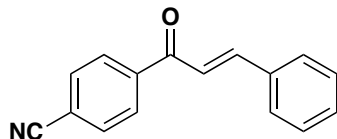
(E)-3-(furan-3-yl)-1-phenylprop-2-en-1-one (44f): Following a modified literature procedure³²: Acetophenone (0.36 mL, 4.16 mmol) was added to a solution of MeOH (10 mL) and water (2 mL) and finely ground KOH (0.467 g, 8.32 mmol). The solution was allowed to stir at rt for 10 min, then 3-furaldehyde (0.36 mL, 4.16 mmol) was added dropwise over 5 min. The dark brown solution was allowed to stir at rt. After 3 h, water (12 mL) and saturated NH₄Cl solution (8 mL) were added, and the mixture was extracted with ether (3x 30 mL), washed with brine, dried over Na₂SO₄ and concentrated *in vacuo*. The resulting solid was recrystallized in hot ethanol to yield **44f** as a light brown solid (0.68 g, 82%): ¹H NMR (400 MHz, CDCl₃) δ 8.03 – 7.96 (m, 2H), 7.76 – 7.69 (m, 2H), 7.61 – 7.54 (m, 1H), 7.53 – 7.46 (m, 3H), 7.25 (d, *J* = 15.5 Hz, 1H), 6.71 (d, *J* = 1.9 Hz, 1H). ¹H NMR shifts match literature values.³²



(E)-1-phenyl-3-(pyridin-3-yl)prop-2-en-1-one (44g): Following modified literature procedure³³, acetophenone (0.49 mL, 4.2 mmol,) was added dropwise under cooling (0 °C) to a stirred solution of 4-pyridinecarboxaldehyde (0.79 mL 8.4 mmol,) in methanol (1 mL) and 10% aq. NaOH (1.7 mL). After addition, the reaction mixture was stirred for 2h keeping temperature below 10 °C. The resulting suspension was diluted with water, filtered, washed with water, dried, and recrystallized in a hot ethanol/water mixture to yield **44g** as pale yellow crystals (0.50 g, 57%): ¹H NMR (400 MHz, CDCl₃) δ 8.87 (d, *J* = 2.2 Hz, 1H), 8.64 (dd, *J* = 4.8, 1.6 Hz, 1H), 8.07 – 8.00 (m, 2H), 7.96 (dt, *J* = 8.0, 2.0 Hz, 1H), 7.80 (d, *J* = 15.8 Hz, 1H), 7.64 – 7.58 (m, 2H), 7.53 (dd, *J* = 8.4, 6.9 Hz, 2H), 7.37 (dd, *J* = 8.0, 4.8 Hz, 1H). ¹H NMR shifts match literature values.³³



(E)-4-(3-oxo-3-phenylprop-1-en-1-yl)benzotrile (44h): Following a modified literature procedure²⁷: to a solution of acetophenone (1.03 g, 8.56 mmol) in MeOH (8.6 mL), was added 4-formylbenzotrile (1.04 mL, 8.56 mmol) and 20% KOH solution (0.86 mL). The reaction mixture was stirred overnight at rt. After completion of reaction, reaction was added to 30 mL of water, acidified with 1 M HCl, filtered, and recrystallized in hot ethanol to yield **44h** as a white solid (1.78 g, 89%): ¹H NMR (400 MHz, CDCl₃) δ 8.03 (d, *J* = 8.0 Hz, 2H), 7.81 – 7.69 (m, 5H), 7.66 – 7.58 (m, 2H), 7.53 (t, *J* = 7.5 Hz, 2H). ¹H NMR shifts match literature values.³⁴



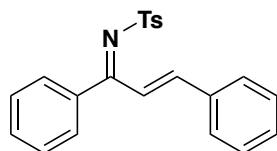
4-cinnamoylbenzonitrile (44i): Following a modified literature procedure³⁵: to a solution of EtOH (20 mL), water (20 mL), and NaOH (10 mmol) was added 4-acetylbenzonitrile (1.00 g, 6.9 mmol). After 15 minutes, benzaldehyde (0.7 mL, 6.9 mmol) was added. The reaction mixture was stirred overnight at rt. After completion of the reaction, reaction was filtered, and the solid recrystallized in hot ethanol to yield **44i** as a white solid (0.59 g, 36%): ¹H NMR (400 MHz, CDCl₃) δ 8.11 – 8.06 (m, 2H), 7.87 – 7.79 (m, 3H), 7.67 – 7.63 (m, 2H), 7.50 – 7.41 (m, 4H). ¹H NMR shifts match literature values.³⁶

General Procedure A for *N*-Tosyl Imines

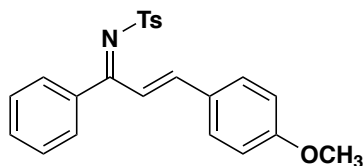
Following a modified literature procedure,²³ to a 0 °C solution of chalcone (1 equiv) and *p*-toluenesulfonamide (1 equiv) in CH₂Cl₂ (0.165 M) was added triethylamine (2 equiv). After 5 min, TiCl₄ (1 equiv, 1M in CH₂Cl₂) was added. The reaction was brought to reflux and stirred for 12 h, then quenched with 50 mL water. The aqueous layer was extracted CH₂Cl₂ (3x 30 mL). The combined organic layers were dried over Na₂SO₄, and solvent was concentrated *in vacuo*. The crude mixture was purified by flash column chromatography (70:30 hexanes/EtOAc) to yield the imine product as an amorphous solid.

General Procedure B for *N*-Tosyl Imines

Following a modified literature procedure,²³ to a 0 °C solution of chalcone (1 equiv) and *p*-toluenesulfonamide (1 equiv) in CH₂Cl₂ (0.08 M) was added triethylamine (2.2 equiv). After 5 min, TiCl₄ (1.1 equiv, 1M in CH₂Cl₂) was added. The reaction was brought to reflux and stirred for 12 h, then quenched with 50 mL water. The aqueous layer was extracted CH₂Cl₂ (3x 30 mL). The combined organic layers were dried over Na₂SO₄, and solvent was concentrated *in vacuo*. The crude mixture was purified by flash column chromatography (70:30 hexanes/EtOAc) to yield imine product as an amorphous solid.

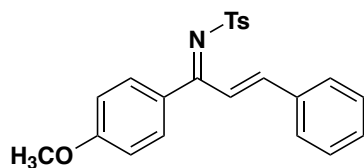


***N*-((1*E*,2*E*)-1,3-diphenylallylidene)-4-methylbenzenesulfonamide (1a):** The title compound was synthesized according to general procedure **A** with *trans*-chalcone, (2.88 mmol, 0.600 g) to yield **1a** as a yellow amorphous solid (0.422 mg, 48%). ¹H NMR (400 MHz, CDCl₃) δ 8.23 – 7.80 (m, 3H), 7.65 (s, 2H), 7.59 – 7.51 (m, 3H), 7.42 (tdd, *J* = 8.9, 6.1, 2.8 Hz, 5H), 7.31 (d, *J* = 8.1 Hz, 2H), 7.06 (d, *J* = 16.1 Hz, 1H), 2.42 (s, 3H). ¹H NMR spectrum is consistent with published data.²³



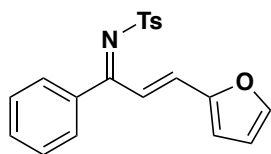
***N*-((1*E*,2*E*)-3-(4-methoxyphenyl)-1-phenylallylidene)-4-methylbenzenesulfonamide (1b):** The title compound was synthesized according to general procedure **A** with (*E*)-3-(4-methoxyphenyl)-1-phenylprop-2-en-1-one (2.1 mmol, 0.50 g) to yield **1b** as a yellow

amorphous solid (1.88 g, 89%). $^1\text{H NMR}$ (400 MHz, CDCl_3) δ 7.94 (d, $J = 8.2$ Hz, 3H), 7.64 (s, 2H), 7.55 (tq, $J = 5.6, 1.5$ Hz, 3H), 7.45 (dd, $J = 8.3, 6.9$ Hz, 2H), 7.33 (d, $J = 8.0$ Hz, 2H), 7.06 (d, $J = 16.0$ Hz, 1H), 6.98 – 6.91 (m, 2H), 3.88 (s, 3H), 2.44 (s, 3H). $^1\text{H NMR}$ spectrum is consistent with published data.²³



***N*-((1*E*,2*E*)-1-(4-methoxyphenyl)-3-phenylallylidene)-4-methylbenzenesulfonamide**

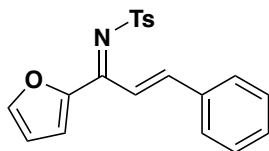
(1c): The title compound was synthesized according to general procedure A with (*E*)-1-(4-methoxyphenyl)-3-phenylprop-2-en-1-one (0.25 g, 1.05 mmol) to yield 1c as a yellow solid (0.295 g, 72%). $^1\text{H NMR}$ (600 MHz, CDCl_3) δ 8.01 – 7.87 (m, 3H), 7.70 (d, $J = 8.4$ Hz, 2H), 7.58 (d, $J = 5.9$ Hz, 2H), 7.44 – 7.40 (m, 3H), 7.30 (d, $J = 8.1$ Hz, 2H), 7.09 – 7.02 (m, 1H), 6.93 (t, $J = 6.0$ Hz, 2H), 3.87 (d, $J = 3.6$ Hz, 3H), 2.42 (s, 3H). $^1\text{H NMR}$ spectrum is consistent with published data.²³



***N*-((1*E*,2*E*)-3-(furan-2-yl)-1-phenylallylidene)-4-methylbenzenesulfonamide (1d):**

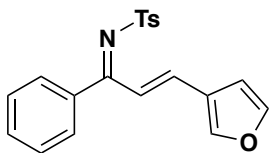
The title compound was synthesized according to general procedure B with (*E*)-3-(furan-2-yl)-1-phenylprop-2-en-1-one (1.01 mmol, 0.200 g), to yield crude 1d as a brown amorphous solid (0.230 g, 64%): $^1\text{H NMR}$ (400 MHz, CDCl_3) δ 7.92 (d, $J = 7.9$ Hz, 2H), 7.63 – 7.49 (m, 4H), 7.46 – 7.39 (m, 2H), 7.31 (dd, $J = 8.0, 4.7$ Hz, 3H), 6.83 (d, $J = 15.7$

Hz, 1H), 6.68 (d, $J = 3.5$ Hz, 1H), 6.51 (dd, $J = 3.5, 1.8$ Hz, 1H), 2.42 (s, 3H). ^1H NMR spectrum is consistent with published data.²³



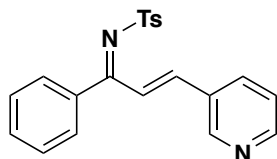
***N*-((1*E*,2*E*)-1-(furan-2-yl)-3-phenylallylidene)-4-methylbenzenesulfonamide (**1e**):**

The title compound was synthesized according to general procedure **B** with (*E*)-1-(furan-2-yl)-3-phenylprop-2-en-1-one (0.403 mmol, 0.080 mg), which produced crude **1e** as a brown amorphous solid (0.013 g, 90%) The crude product was recrystallized in EtOH for characterization. Spectroscopic data was acquired at 110 °C: mp: 170-173 °C. ^1H NMR (500 MHz, $\text{DMSO-}d_6$) δ 8.09 – 8.01 (m, 1H), 7.84 (d, $J = 8.0$ Hz, 2H), 7.72 – 7.59 (m, 3H), 7.59 – 7.44 (m, 5H), 7.40 (d, $J = 8.0$ Hz, 2H), 6.78 (d, $J = 3.7$ Hz, 1H), 2.40 (s, 3H). ^{13}C NMR (126 MHz, $\text{DMSO-}d_6$) δ 162.0, 149.5, 148.8, 144.1, 142.6, 138.6, 134.3, 130.1, 128.9, 128.4, 127.7, 125.9, 121.9, 120.7, 112.8, 20.3. AMM (ESI-TOF) m/z calcd for $\text{C}_{21}\text{H}_{18}\text{N}_2\text{O}_2\text{S}^+$ $[\text{M}+\text{H}]^+$ 352.1002, found 352.1010.



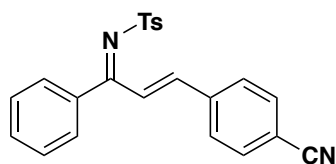
***N*-((1*E*,2*E*)-3-(furan-3-yl)-1-phenylallylidene)-4-methylbenzenesulfonamide (**1f**):** The title compound was synthesized according to general procedure **B** with (*E*)-3-(furan-3-yl)-1-phenylprop-2-en-1-one (2.02 mmol, 0.40 g), which produced **1f** as a brown amorphous

solid (0.450 g, 64%): ^1H NMR (400 MHz, CDCl_3) δ 7.91 (d, $J = 7.8$ Hz, 2H), 7.65 – 7.39 (m, 8H), 7.31 (d, $J = 7.9$ Hz, 2H), 6.98 (d, $J = 15.7$ Hz, 1H), 6.78 (s, 1H), 2.42 (d, $J = 3.1$ Hz, 3H). ^1H NMR spectrum is consistent with published data.²³



4-methyl-*N*-((1*E*,2*E*)-1-phenyl-3-(pyridin-3-yl)allylidene)benzenesulfonamide (1g):

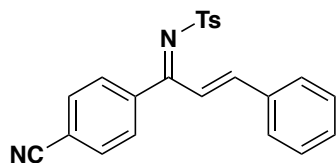
The title compound was synthesized according to general procedure **B** with (*E*)-1-phenyl-3-(pyridin-3-yl)prop-2-en-1-one (0.250 g, 1.19 mmol), which produced **1g** as a brown amorphous solid (0.182 g, 42%). The crude product was recrystallized in EtOH for characterization. Spectroscopic data was acquired at 108 °C. mp: 139.4 °C. ^1H NMR (500 MHz, $\text{DMSO-}d_6$) δ 8.78 (d, $J = 2.3$ Hz, 1H), 8.62 (d, $J = 4.7$ Hz, 1H), 8.07 (d, $J = 8.1$, 2.1 Hz, 1H), 7.87 – 7.77 (m, 3H), 7.70 (d, $J = 7.8$ Hz, 2H), 7.64 (t, $J = 7.4$ Hz, 1H), 7.53 (t, $J = 7.5$ Hz, 2H), 7.48 (dd, $J = 8.1$, 4.8 Hz, 1H), 7.41 (d, $J = 7.9$ Hz, 2H), 7.15 (d, $J = 16.3$ Hz, 1H), 2.40 (s, 3H). ^{13}C NMR (126 MHz, $\text{DMSO-}d_6$) δ 176.0, 150.5, 149.0, 142.8, 142.7, 138.1, 135.7, 133.9, 131.4, 129.8, 128.9, 128.9, 127.8, 126.0, 124.8, 123.2, 20.2. AMM (ESI-TOF) m/z calcd for $\text{C}_{21}\text{H}_{19}\text{N}_2\text{O}_2\text{S}^+$ $[\text{M}+\text{H}]^+$ 363.1162, found 363.1167.



***N*-((1*E*,2*E*)-3-(4-cyanophenyl)-1-phenylallylidene)-4-methylbenzenesulfonamide**

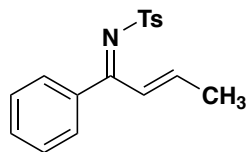
(1h): The title compound was synthesized according to general procedure **A** with (*E*)-4-

(3-oxo-3-phenylprop-1-en-1-yl)benzointrile (2.14 mmol, 0.50 g), to yield **1h** as a pale yellow amorphous solid (0.51 g, 61%): ¹H NMR (600 MHz, CDCl₃) δ 8.14 (d, *J* = 15.9 Hz, 1H), 7.97 – 7.87 (m, 2H), 7.75 – 7.62 (m, 6H), 7.60 – 7.54 (m, 1H), 7.49 – 7.43 (m, 2H), 7.33 (d, *J* = 7.9 Hz, 2H), 7.03 (d, *J* = 16.1 Hz, 1H), 2.43 (s, 3H).; ¹³C NMR (151 MHz, CDCl₃) δ 176.3, 144.8, 143.79, 138.8, 138.2, 136.7, 132.7, 132.5, 130.3, 129.5, 128.8, 128.6, 127.2, 125.7, 118.3, 113.8, 21.6.; AMM (ESI-TOF) *m/z* calcd for C₂₃H₁₉N₂O₂S⁺ [M+H]⁺ 387.1162, found 387.1166.



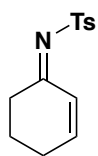
***N*-((1*E*,2*E*)-1-(4-cyanophenyl)-3-phenylallylidene)-4-methylbenzenesulfonamide**

(1i): The title compound was synthesized according to general procedure **A** with 4-cinnamoylbenzointrile (1.28 mmol, 0.30 g), to yield **1i** as a yellow amorphous solid (0.30 g, 60%): ¹H NMR (600 MHz, CDCl₃) δ 8.12 (d, *J* = 16.2 Hz, 1H), 7.98 – 7.85 (m, 2H), 7.81 – 7.69 (m, 4H), 7.66 – 7.52 (m, 2H), 7.50 – 7.39 (m, 3H), 7.34 (d, *J* = 7.9 Hz, 2H), 7.01 (d, *J* = 15.9 Hz, 1H), 2.44 (s, 3H).; ¹³C NMR (151 MHz, CDCl₃) δ 175.3, 149.6, 144.0, 141.4, 138.1, 134.0, 132.1, 131.7, 130.6, 129.6, 129.2, 128.9, 127.3, 121.8, 118.0, 115.2, 21.6.; IR: 1612, 2204, 2229, 2852, 2921, 3061 cm⁻¹; AMM (ESI-TOF) *m/z* calcd for C₂₃H₁₉N₂O₂S⁺ [M+H]⁺ 387.1162, found 387.1170.



4-methyl-*N*-((1*E*,2*E*)-1-phenylbut-2-en-1-ylidene)benzenesulfonamide (1j)

The title compound was synthesized according to general procedure **A** with (*E*)-1-phenylbut-2-en-1-one, (0.343 g, 2.34 mmol) to yield **1j** as a red oil (0.12 g, 17%): ¹H NMR (600 MHz, CDCl₃) δ 7.98 – 7.84 (m, 2H), 7.64 – 7.53 (m, 2H), 7.49 (t, *J* = 7.5 Hz, 1H), 7.39 (t, *J* = 7.9 Hz, 2H), 7.31 (d, *J* = 8.1 Hz, 2H), 6.43 (d, *J* = 13.8 Hz, 1H), 2.43 (s, 3H), 2.05 (d, *J* = 6.9 Hz, 3H). ¹H NMR spectrum is consistent with published data.²³

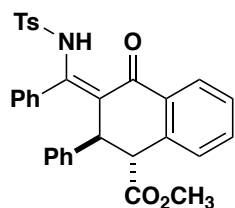


(*Z*)-*N*-(cyclohex-2-en-1-ylidene)-4-methylbenzenesulfonamide (1k): Following a modified literature procedure:¹⁹ To a solution of TiCl₄ and Ti(OEt)₄ in toluene was added NEt₃. The resulting mixture was stirred for 5 min at rt before TsNH₂ was added, and the reaction mixture was stirred for 15 min under reflux. A solution of cyclohexenone in toluene was added dropwise over 15 min to the refluxing solution and was stirred for 4 hours. The reaction mixture was poured into a stirred and precooled (0 °C) suspension of NaHCO₃ in acetone/water (200 mL 100:1), diluted with hexanes (100 mL), dried (MgSO₄), and filtered. The filtrate was concentrated under *in vacuo*, and the crude product was purified by flash chromatography (70:30 Hexanes/EtOAc) to yield **1k** as an off white solid (0.35 g, 15%): ¹H NMR (400 MHz, CDCl₃) δ 7.86 (dd, *J* = 8.4, 2.1 Hz, 2H),

7.35 – 7.28 (m, 2H), 6.94 (ddt, $J = 12.2, 9.9, 4.1$ Hz, 1H), 6.15 (dt, $J = 10.0, 2.0$ Hz, 1H), 3.22 – 3.13 (m, 1H), 2.57 – 2.51 (m, 1H), 2.43 (s, 3H), 2.36 (dddd, $J = 14.3, 6.2, 4.2, 2.1$ Hz, 2H), 1.96 (h, $J = 6.4$ Hz, 2H). ^1H NMR spectrum is consistent with published data.¹⁹

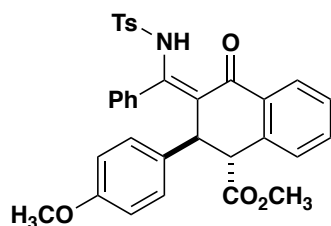
Imine Scope:

Due to restricted rotation of nearby aromatic rings, the aromatic region of the NMR of the aza-Tamura products does not have defined peaks in CDCl_3 at room temperature. A proton NMR experiment was run on product **4a** in DMSO at 80 °C, which gave defined product peaks. We expect that this example demonstrates the restricted rotation, and it can be extrapolated that the other products would provide the same result.



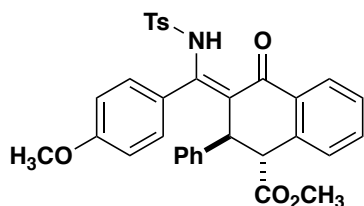
methyl (1R,2S,Z)-3-(((4-methylphenyl)sulfonamido)(phenyl)methylene)-4-oxo-2-phenyl-1,2,3,4-tetrahydronaphthalene-1-carboxylate (4a): To a solution of imine **1a** (0.05 g, 0.14 mmol) and homophthalic anhydride (28 mg, 0.17 mmol) in dry CH_2Cl_2 (1.4 mL, 0.1 M) was added $i\text{-Pr}_2\text{NEt}$ (0.024 mL, 0.14 mmol). The reaction mixture was stirred for 18 h at 25 °C and then quenched with 2 mL of 1 M HCl solution. The aqueous layer was extracted with CH_2Cl_2 (3 x 2 mL). The combined organic layers were dried over Na_2SO_4 and solvent was concentrated *in vacuo*. The resulting crude carboxylic acid was dissolved in dry CH_2Cl_2 (1.4 mL, 0.1 M) and CH_3OH (1 mL), and TMSCHN₂ solution (0.17

mL, 2M in hexanes) was added dropwise. The reaction was stirred at 25 °C for 1 h and then DBU solution (0.14 mL, 1M in CH₂Cl₂) was added. The reaction was stirred at 25 °C for 22 h and then quenched with 10 μL of AcOH. The volatiles were concentrated *in vacuo*, and the crude mixture was purified by flash chromatography (75:25 hexanes/EtOAc) to yield **4a** as a pale yellow amorphous solid (0.070 g, 94%): ¹H NMR (500 MHz, DMSO-*d*₆) δ 13.61 (s, 1H), 8.06 – 8.00 (m, 1H), 7.46 (dtd, *J* = 24.6, 7.5, 1.5 Hz, 2H), 7.40 – 7.27 (m, 5H), 7.23 – 7.15 (m, 3H), 7.10 – 7.00 (m, 3H), 6.79 – 6.73 (m, 2H), 6.70 (d, *J* = 7.5 Hz, 2H), 4.22 (s, 1H), 4.10 (d, *J* = 2.2 Hz, 1H), 3.58 (s, 3H), 2.38 (s, 3H). ¹³C NMR (151 MHz, CDCl₃) δ 189.3, 171.9, 155.2, 143.9, 142.7, 137.6, 136.0, 134.1, 133.7, 130.9, 130.0, 129.4, 129.4, 129.1, 128.6, 128.4, 127.8, 127.7, 127.6, 127.5, 126.7, 111.3, 52.6, 52.1, 43.8, 21.7. AMM (ESI-TOF) *m/z* calcd for C₃₂H₂₈NO₅S + [M+H]⁺ 538.1683, found 538.1670.



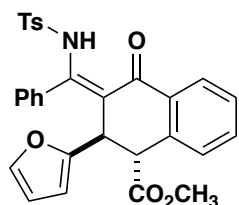
methyl (1*R*,2*S*,*Z*)-2-(4-methoxyphenyl)-3-(((4-methylphenyl)sulfonamido)(phenyl)methylene)-4-oxo-1,2,3,4-tetrahydronaphthalene-1-carboxylate (4b): To a solution of imine 1b (0.050 g, 0.128 mmol) and homophthalic anhydride (0.026 g, 0.154 mmol) in dry CH₂Cl₂ (1.28 mL, 0.1 M) was added *i*-Pr₂NEt (0.022 mL, 0.128 mmol). The reaction mixture was stirred for 18 h at 25 °C and then quenched with 2 mL of 1 M HCl solution. The aqueous layer was extracted with CH₂Cl₂ (3 x 2 mL). The combined organic layers

were dried over Na₂SO₄ and solvent was concentrated *in vacuo*. The resulting crude carboxylic acid was dissolved in dry CH₂Cl₂ (1.28 mL, 0.1 M) and CH₃OH (1 mL), and TMSCHN₂ solution (0.128 mL, 2M in hexanes) was added dropwise. The reaction was stirred at 25 °C for 1 h and then DBU solution (0.128 mL, 1M in CH₂Cl₂) was added. The reaction was stirred at 25 °C for 22 h and then quenched with 10 μL of AcOH. The volatiles were concentrated *in vacuo*, and the crude mixture was purified by flash chromatography (70:30 hexanes/EtOAc) to yield **4b** as a pale yellow amorphous solid (0.067 g, 92%): ¹H NMR (600 MHz, CDCl₃) δ 13.86 (s, 1H), 8.19 – 8.13 (m, 1H), 7.45 – 7.37 (m, 2H), 7.34 – 7.27 (m, 4H), 7.14 – 7.08 (m, 3H), 7.07 – 7.02 (m, 2H), 6.61 – 6.52 (m, 5H), 4.03 (d, *J* = 2.1 Hz, 1H), 3.82 (d, *J* = 2.2 Hz, 1H), 3.67 (s, 3H), 3.59 (s, 3H), 2.37 (s, 3H).; ¹³C NMR (151 MHz, CDCl₃) δ 189.2, 171.8, 158.0, 154.9, 143.7, 137.4, 136.0, 134.6, 134.0, 133.6, 130.8, 129.8, 129.3, 129.2, 128.9, 128.4, 128.3, 127.6, 127.6, 127.4, 113.5, 111.5, 55.0, 52.4, 52.1, 42.9, 21.6.; AMM (ESI-TOF) *m/z* calcd for C₃₃H₃₀NO₆S + [M+H]⁺ 568.1788, found 568.1782.



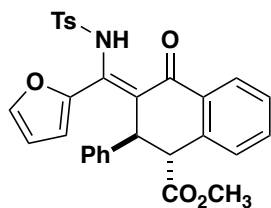
methyl (1*R*,2*S*,*Z*)-3-((4-methoxyphenyl)((4-methylphenyl)sulfonamido)methylene)-4-oxo-2-phenyl-1,2,3,4-tetrahydronaphthalene-1-carboxylate (4c): To a solution of imine 1c (0.05 g, 0.128 mmol) and homophthalic anhydride (0.025 g, 0.154 mmol) in dry CH₂Cl₂ (1.28 mL, 0.1 M) was added *i*-Pr₂NEt (0.022 mL, 0.128 mmol). The reaction

mixture was stirred for 18 h at 25 °C and then quenched with 2 mL of 1 M HCl solution. The aqueous layer was extracted with CH₂Cl₂ (3 x 2 mL). The combined organic layers were dried over Na₂SO₄ and solvent was concentrated *in vacuo*. The resulting crude carboxylic acid was dissolved in dry CH₂Cl₂ (1.28 mL, 0.1 M) and CH₃OH (1 mL), and TMSCHN₂ solution (0.128 mL, 2M in hexanes) was added dropwise. The reaction was stirred at 25 °C for 1 h and then DBU solution (0.128 mL, 1M in CH₂Cl₂) was added. The reaction was stirred at 25 °C for 22 h and then quenched with 10 μL of AcOH. The volatiles were concentrated *in vacuo*, and the crude mixture was purified by flash chromatography (75:25 hexanes/EtOAc) to yield **4c** as a pale yellow amorphous solid (0.067 g, 92%): ¹H NMR (600 MHz, CDCl₃) δ 13.80 (s, 1H), 8.18 – 8.11 (m, 1H), 7.42 – 7.36 (m, 2H), 7.34 (d, *J* = 8.0 Hz, 2H), 7.13 (d, *J* = 8.1 Hz, 2H), 7.06 – 6.98 (m, 4H), 6.73 – 6.50 (m, 6H), 4.17 (d, *J* = 2.1 Hz, 1H), 3.88 (d, *J* = 2.0 Hz, 1H), 3.79 (s, 3H), 3.59 (s, 3H), 2.37 (s, 3H).; ¹³C NMR (151 MHz, CDCl₃) δ 189.1, 171.7, 160.3, 155.1, 143.6, 142.6, 137.3, 135.8, 134.0, 133.5, 130.5, 129.7, 129.2, 128.4, 128.2, 127.6, 127.6, 127.3, 126.5, 123.1, 112.8, 111.6, 55.2, 52.4, 52.0, 43.6, 21.5. AMM (ESI-TOF) *m/z* calcd for C₃₃H₃₀NO₆S⁺ [M+H]⁺ 568.1788, found 568.1781.

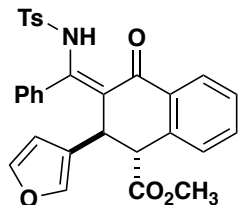


methyl (1*R,Z*)-2-(furan-2-yl)-3-(((4-methylphenyl)sulfonamido)(phenyl)methylene)-4-oxo-1,2,3,4-tetrahydronaphthalene-1-carboxylate (4d): To a solution of imine **1d**

(0.05 g, 0.142 mmol) and homophthalic anhydride (0.028 g, 0.171 mmol) in dry CH₂Cl₂ (1.42 mL, 0.1 M) was added *i*-Pr₂NEt (0.025 mL, 0.142 mmol). The reaction mixture was stirred for 18 h at 25 °C and then quenched with 2 mL of 1 M HCl solution. The aqueous layer was extracted with CH₂Cl₂ (3 x 2 mL). The combined organic layers were dried over Na₂SO₄ and solvent was concentrated *in vacuo*. The resulting crude carboxylic acid was dissolved in dry CH₂Cl₂ (1.42 mL, 0.1 M) and CH₃OH (1 mL), and TMSCHN₂ solution (0.142 mL, 2M in hexanes) was added dropwise. The reaction was stirred at 25 °C for 1 h and then DBU solution (0.142 mL, 1M in CH₂Cl₂) was added. The reaction was stirred at 25 °C for 22 h and then quenched with 10 μL of AcOH. The volatiles were concentrated *in vacuo*, and the crude mixture was purified by flash chromatography (80:20 hexanes/EtOAc) to yield **4d** as a pale yellow amorphous solid (0.062 g, 84%): ¹H NMR (600 MHz, CDCl₃) δ 13.71 (d, *J* = 2.2 Hz, 1H), 8.10 (d, *J* = 7.8 Hz, 1H), 7.42 (dt, *J* = 33.8, 7.5 Hz, 2H), 7.37 – 7.30 (m, 3H), 7.24 – 7.11 (m, 5H), 7.07 (s, 1H), 6.97 (d, *J* = 41.0 Hz, 2H), 6.02 (d, *J* = 2.6 Hz, 1H), 5.64 (d, *J* = 2.8 Hz, 1H), 4.17 (d, *J* = 2.4 Hz, 1H), 4.10 (s, 1H), 3.59 (d, *J* = 2.1 Hz, 3H), 2.39 (d, *J* = 2.0 Hz, 3H). ¹³C NMR (151 MHz, CDCl₃) δ 188.6, 171.1, 154.9, 154.5, 143.8, 141.6, 137.4, 136.1, 133.5, 133.4, 130.4, 129.6, 129.5, 129.3, 129.0, 128.4, 127.7, 127.6, 127.5, 110.0, 109.5, 107.7, 52.4, 48.2, 38.3, 21.6.; AMM (ESI-TOF) *m/z* calcd for C₃₀H₂₆NO₆S⁺ [M+H]⁺ 528.1475, found 528.1473.

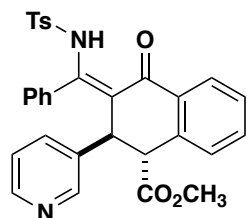


methyl (1*R*,2*S*,*Z*)-3-(furan-2-yl((4-methylphenyl)sulfonamido)methylene)-4-oxo-2-phenyl-1,2,3,4-tetrahydronaphthalene-1-carboxylate (4e): To a solution of imine **1e** (0.05 g, 0.142 mmol) and homophthalic anhydride (0.028 g, 0.171 mmol) in dry CH₂Cl₂ (1.42 mL, 0.1 M) was added *i*-Pr₂NEt (0.025 mL, 0.142 mmol). The reaction mixture was stirred for 18 h at 25 °C and then quenched with 2 mL of 1 M HCl solution. The aqueous layer was extracted with CH₂Cl₂ (3 x 2 mL). The combined organic layers were dried over Na₂SO₄ and solvent was concentrated *in vacuo*. The resulting crude carboxylic acid was dissolved in dry CH₂Cl₂ (1.42 mL, 0.1 M) and CH₃OH (1 mL), and TMSCHN₂ solution (0.142 mL, 2M in hexanes) was added dropwise. The reaction was stirred at 25 °C for 1 h and then DBU solution (0.142 mL, 1M in CH₂Cl₂) was added. The reaction was stirred at 25 °C for 22 h and then quenched with 10 μL of AcOH. The volatiles were concentrated *in vacuo*, and the crude mixture was purified by flash chromatography (80:20 hexanes/EtOAc) to yield **4e** as a pale yellow amorphous solid (0.058 mg, 68%): ¹H NMR (400 MHz, CDCl₃) δ 13.64 (s, 1H), 8.13 (dd, *J* = 7.5, 1.7 Hz, 1H), 7.51 – 7.39 (m, 2H), 7.39 – 7.29 (m, 3H), 7.25 – 6.99 (m, 7H), 6.62 (s, 1H), 5.72 (s, 1H), 3.99 (d, *J* = 2.2 Hz, 1H), 3.82 (d, *J* = 2.2 Hz, 1H), 3.59 (s, 3H), 2.38 (s, 3H).; ¹³C NMR (151 MHz, CD₃CN) δ 191.0, 172.6, 146.2, 145.6, 144.8, 143.3, 143.0, 137.5, 137.2, 135.0, 134.9, 130.7, 130.6, 129.5, 129.5, 128.2, 128.2, 128.1, 127.7, 117.1, 116.3, 112.4, 53.1, 52.0, 44.6, 21.6. AMM (ESI-TOF) *m/z* calcd for C₃₀H₂₆NO₆S⁺ [M+H]⁺ 528.1475, found 528.1481.



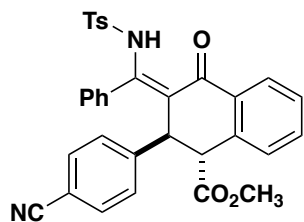
methyl (1R,2S,Z)-2-(furan-3-yl)-3-(((4-methylphenyl)sulfonamido)(phenyl)methylene)-4-oxo-1,2,3,4-tetrahydronaphthalene-1-carboxylate (4f): To a solution of imine 1f (0.05 g, 0.142 mmol) and homophthalic anhydride (0.028 g, 0.171 mmol) in dry CH₂Cl₂ (1.42 mL, 0.1 M) was added *i*-Pr₂NEt (0.025 mL, 0.142 mmol). The reaction mixture was stirred for 18 h at 25 °C and then quenched with 2 mL of 1 M HCl solution. The aqueous layer was extracted with CH₂Cl₂ (3 x 2 mL). The combined organic layers were dried over Na₂SO₄ and solvent was concentrated *in vacuo*. The resulting crude carboxylic acid was dissolved in dry CH₂Cl₂ (1.42 mL, 0.1 M) and CH₃OH (1 mL), and TMSCHN₂ solution (0.142 mL, 2M in hexanes) was added dropwise. The reaction was stirred at 25 °C for 1 h and then DBU solution (0.142 mL, 1M in CH₂Cl₂) was added. The reaction was stirred at 25 °C for 22 h and then quenched with 10 μL of AcOH. The volatiles were concentrated *in vacuo*, and the crude mixture was purified by flash chromatography (80:20 hexanes/EtOAc) to yield **4f** as a pale yellow amorphous solid (0.062 g, 84%): ¹H NMR (600 MHz, CDCl₃) δ 13.64 (d, *J* = 2.3 Hz, 1H), 8.13 (d, *J* = 7.8 Hz, 1H), 7.50 – 7.40 (m, 2H), 7.37 (t, *J* = 7.6 Hz, 1H), 7.32 (dd, *J* = 8.3, 2.2 Hz, 2H), 7.23 (d, *J* = 11.5 Hz, 4H), 7.07 (s, 1H), 7.00 – 6.72 (m, 2H), 6.62 (s, 1H), 5.72 (s, 1H), 3.99 (s, 1H), 3.83 (s, 1H), 3.59 (d, *J* = 2.2 Hz, 3H), 2.38 (d, *J* = 2.1 Hz, 3H).; ¹³C NMR (151 MHz, CDCl₃) δ 188.7, 171.3, 154.0, 143.8, 142.9, 139.8, 137.4, 136.4, 133.6, 133.6, 130.6, 129.8, 129.5, 129.3, 129.2,

128.5, 127.8, 127.6, 127.5, 126.8, 111.7, 109.3, 52.4, 50.5, 35.5, 21.6.; AMM (ESI-TOF)
m/z calcd for C₃₀H₂₆NO₆S⁺ [M+H]⁺ 528.1475, found 528.1464.



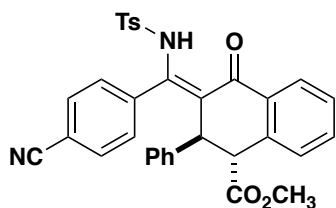
methyl (1R,2S,Z)-3-(((4-methylphenyl)sulfonamido)(phenyl)methylene)-4-oxo-2-(pyridin-3-yl)-1,2,3,4-tetrahydronaphthalene-1-carboxylate (4g): To a solution of imine 1g (0.05 g, 0.138 mmol) and homophthalic anhydride (0.027 g, 0.166 mmol) in dry CH₂Cl₂ (1.42 mL, 0.1 M) was added *i*-Pr₂NEt (0.025 mL, 0.142 mmol). The reaction mixture was stirred for 18 h at 25 °C and then quenched with 2 mL of 1 M HCl solution. The aqueous layer was extracted with CH₂Cl₂ (3 x 2 mL), followed by EtOAc (3x5 mL). The combined organic layers were dried over Na₂SO₄ and solvent was concentrated *in vacuo*. The resulting crude carboxylic acid was dissolved in dry CH₂Cl₂ (1.38 mL, 0.1 M) and CH₃OH (2 mL), and TMSCHN₂ solution (0.138 mL, 2M in hexanes) was added dropwise. The reaction was stirred at 25 °C for 1 h and then DBU solution (0.138 mL, 1M in CH₂Cl₂) was added. The reaction was stirred at 25 °C for 22 h and then quenched with 10 μL of AcOH. The volatiles were concentrated *in vacuo*, and the crude mixture was purified by flash chromatography (80:20 hexanes/EtOAc) to yield **4g** as a pale yellow amorphous solid (0.041 g, 55%): ¹H NMR (600 MHz, CDCl₃) δ 13.95 (s, 1H), 8.29 (t, *J* = 3.1 Hz, 1H), 8.20 – 8.15 (m, 1H), 7.90 (s, 1H), 7.48 – 7.41 (m, 2H), 7.33 (t, *J* = 7.4 Hz, 2H), 7.28 (d, *J* = 8.0 Hz, 2H), 7.13 – 7.05 (m, 4H), 6.95 (d, *J* = 3.4 Hz, 3H), 4.15 (s, 1H),

3.78 (s, 1H), 3.63 (s, 3H), 2.37 (s, 3H). ^{13}C NMR (151 MHz, CDCl_3) δ 188.7, 171.4, 156.1, 149.1, 148.2, 144.1, 138.2, 137.4, 135.3, 134.8, 134.0, 133.9, 130.5, 130.1, 129.7, 129.4, 129.0, 129.0, 128.0, 127.8, 127.7, 123.2, 109.9, 52.8, 51.7, 41.6, 21.7. AMM (ESI-TOF) m/z calcd for $\text{C}_{30}\text{H}_{26}\text{NO}_6\text{S}^+$ $[\text{M}+\text{H}]^+$ 539.1635, found 539.1626.



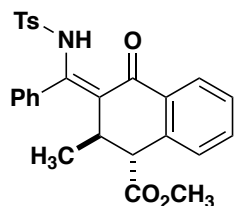
methyl (1*R*,2*S*,*Z*)-2-(4-cyanophenyl)-3-(((4-methylphenyl)sulfonamido)(phenyl) methyl-ene)-4-oxo-1,2,3,4-tetrahydronaphthalene-1-carboxylate (4h): To a solution of imine 1j (0.05 g, 0.129 mmol) and homophthalic anhydride (0.025 g, 0.155 mmol) in dry CH_2Cl_2 (1.29 mL, 0.1 M) was added *i*-Pr₂NEt (0.032 mL, 0.129 mmol). The reaction mixture was stirred for 18 h at 25 °C and then quenched with 2 mL of 1 M HCl solution. The aqueous layer was extracted with CH_2Cl_2 (3 x 2 mL). The combined organic layers were dried over Na_2SO_4 , and solvent was concentrated *in vacuo*. The resulting crude carboxylic acid was dissolved in dry CH_2Cl_2 (1.29 mL, 0.1 M) and CH_3OH (2 mL), and TMSCHN₂ solution (0.129 mL, 2M in hexanes) was added dropwise. The reaction was stirred at 25 °C for 1 h and then DBU solution (0.129 mL, 1M in CH_2Cl_2) was added. The reaction was stirred at 25 °C for 22 h and then quenched with 10 μL of AcOH. The volatiles were concentrated *in vacuo*, and the crude mixture was purified by flash chromatography (75:25 hexanes/EtOAc) to yield **4h** as a pale yellow amorphous solid (0.065 mg, 89%): ^1H NMR (600 MHz, CDCl_3) δ 13.77 (s, 1H), 8.19 – 8.11 (m, 1H), 7.49 – 7.37 (m, 3H), 7.36 – 7.25 (m, 3H), 7.17 (d, J = 8.0 Hz, 2H), 7.09 – 7.01 (m, 4H), 6.66 – 6.63 (m, 2H), 3.97

(d, $J = 1.8$ Hz, 1H), 3.85 (d, $J = 1.8$ Hz, 1H), 3.60 (d, $J = 1.1$ Hz, 3H), 2.40 (s, 3H).; ^{13}C NMR (151 MHz, CDCl_3) δ 189.1, 171.6, 152.2, 144.3, 142.0, 137.2, 135.7, 135.5, 134.0, 133.5, 131.2, 130.1, 129.9, 129.5, 128.7, 128.5, 127.7, 127.4, 127.2, 126.9, 118.2, 113.2, 111.8, 52.6, 51.8, 43.5, 21.6.; AMM (ESI-TOF) m/z calcd for $\text{C}_{33}\text{H}_{27}\text{N}_2\text{O}_5\text{S}^+$ $[\text{M}+\text{H}]^+$ 563.1633, found 563.1633.



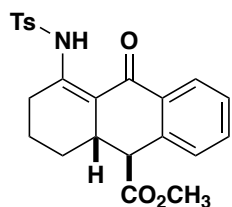
methyl (1R,2S,Z)-3-((4-cyanophenyl)((4-methylphenyl)sulfonamido)methylene)-4-oxo-2-phenyl-1,2,3,4-tetrahydronaphthalene-1-carboxylate (4i): To a solution of imine 1k (0.050 g, 0.129 mmol) and homophthalic anhydride (0.025 g, 0.155 mmol) in dry CH_2Cl_2 (1.29 mL, 0.1 M) was added $i\text{-Pr}_2\text{NEt}$ (0.032 mL, 0.129 mmol). The reaction mixture was stirred for 18 h at 25 °C and then quenched with 2 mL of 1 M HCl solution. The aqueous layer was extracted with CH_2Cl_2 (3 x 2 mL). The combined organic layers were dried over Na_2SO_4 and solvent was concentrated *in vacuo*. The resulting crude carboxylic acid was dissolved in dry CH_2Cl_2 (1.29 mL, 0.1 M) and CH_3OH (2 mL), and TMSCHN_2 solution (0.129 mL, 2M in hexanes) was added dropwise. The reaction was stirred at 25 °C for 1 h and then DBU solution (0.129 mL, 1M in CH_2Cl_2) was added. The reaction was stirred at 25 °C for 22 h and then quenched with 10 μL of AcOH. The volatiles were concentrated *in vacuo*, and the crude mixture was purified by flash chromatography (70:30 hexanes/EtOAc) to yield **4i** as a pale yellow amorphous solid (0.062 g, 85%): ^1H NMR (600 MHz, CDCl_3) δ 13.77 (s, 1H), 8.18 – 8.14 (m, 1H), 7.45 – 7.41 (m, 2H), 7.34

(d, $J = 7.9$ Hz, 2H), 7.17 (d, $J = 8.0$ Hz, 2H), 7.10 – 7.02 (m, 5H), 6.65 (d, $J = 7.3$ Hz, 2H), 3.97 (s, 1H), 3.85 (s, 1H), 3.60 (s, 3H), 2.40 (s, 3H).; ^{13}C NMR (151 MHz, CDCl_3) δ 189.1, 171.6, 152.2, 144.3, 141.9, 137.3, 135.7, 135.5, 134.0, 133.5, 131.2, 130.1, 129.9, 129.5, 128.7, 128.5, 127.7, 127.4, 127.2, 126.9, 118.2, 113.2, 111.8, 52.6, 51.8, 43.5, 21.6.; IR: 1576, 1611, 2228, 2852, 3061 cm^{-1} ; AMM (ESI-TOF) m/z calcd for $\text{C}_{33}\text{H}_{27}\text{N}_2\text{O}_5\text{S}^+$ $[\text{M}+\text{H}]^+$ 563.1635, found 563.1622.



methyl (1*R*,2*R*,*Z*)-2-methyl-3-(((4-methylphenyl)sulfonamido)(phenyl)methylene)-4-oxo-1,2,3,4-tetrahydronaphthalene-1-carboxylate (4j): To a solution of imine 1h (0.05 g, 0.167 mmol) and homophthalic anhydride (0.032 g, 0.200 mmol) in dry CH_2Cl_2 (1.67 mL, 0.1 M) was added *i*- Pr_2NEt (0.029 mL, 0.167 mmol). The reaction mixture was stirred for 18 h at 25 °C and then quenched with 2 mL of 1 M HCl solution. The aqueous layer was extracted with CH_2Cl_2 (3 x 2 mL). The combined organic layers were dried over Na_2SO_4 and solvent was concentrated *in vacuo*. The resulting crude carboxylic acid was dissolved in dry CH_2Cl_2 (1.67 mL, 0.1 M) and CH_3OH (1 mL), and TMSCHN_2 solution (0.167 mL, 2M in hexanes) was added dropwise. The reaction was stirred at 25 °C for 1 h and then DBU solution (0.167 mL, 1M in CH_2Cl_2) was added. The reaction was stirred at 25 °C for 22 h and then quenched with 10 μL of AcOH. The volatiles were concentrated *in vacuo*, and the crude mixture was purified by flash chromatography (85:15

hexanes/EtOAc) to yield **4j** as a pale yellow amorphous solid (0.045 mg, 57%): ^1H NMR (600 MHz, CDCl_3) δ 13.64 (s, 1H), 8.15 (dd, $J = 7.8, 1.5$ Hz, 1H), 7.52 (td, $J = 7.5, 1.5$ Hz, 1H), 7.45 (td, $J = 7.6, 1.3$ Hz, 1H), 7.41 – 7.36 (m, 1H), 7.32 – 7.29 (m, 2H), 7.28 – 7.26 (m, 1H), 7.24 – 7.22 (m, 1H), 7.13 (d, $J = 8.1$ Hz, 2H), 6.97 (s, 1H), 3.55 (s, 3H), 3.51 (d, $J = 2.1$ Hz, 1H), 2.99 (qd, $J = 7.1, 2.1$ Hz, 1H), 2.38 (s, 3H), 0.82 (d, $J = 7.1$ Hz, 3H).; ^{13}C NMR (151 MHz, CDCl_3) δ 188.7, 172.0, 152.6, 143.6, 137.6, 136.6, 133.5, 133.2, 130.9, 130.0, 129.2, 129.2, 129.2, 128.3, 128.0, 127.6, 127.5, 114.3, 52.2, 51.0, 33.2, 21.5, 21.3; AMM (ESI-TOF) m/z calcd for $\text{C}_{27}\text{H}_{26}\text{NO}_5\text{S}^+$ $[\text{M}+\text{H}]^+$ 476.1526, found 476.1547.



methyl 4-((4-methylphenyl)sulfonamido)-10-oxo-1,2,3,9,9a,10-hexahydroanthracene-9-carboxylate (4k): To a solution of imine **1i** (0.05 g, 0.201 mmol) and homophthalic anhydride (0.039 g, 0.241 mmol) in dry CH_2Cl_2 (2.01 mL, 0.1 M) was added $i\text{-Pr}_2\text{NEt}$ (0.035 mL, 0.142 mmol). The reaction mixture was stirred for 18 h at 25 °C and then quenched with 2 mL of 1 M HCl solution. The aqueous layer was extracted with CH_2Cl_2 (3 x 2 mL). The combined organic layers were dried over Na_2SO_4 and solvent was concentrated *in vacuo*. The resulting crude carboxylic acid was dissolved in dry CH_2Cl_2 (2.01 mL, 0.1 M) and CH_3OH (1 mL), and TMSCHN_2 solution (0.201 mL, 2M in hexanes) was added dropwise. The reaction was stirred at 25 °C for 1 h and then DBU solution (0.201 mL, 1M in CH_2Cl_2) was added. The reaction was stirred at 25 °C for 22 h and then

quenched with 10 μ L of AcOH. The volatiles were concentrated *in vacuo*, and the crude mixture was purified by flash chromatography (80:20 hexanes/EtOAc) to yield **4k** as a pale yellow amorphous solid (0.045 g, 55%). ^1H NMR (600 MHz, CDCl_3) δ 14.08 (s, 1H), 8.09 – 8.03 (m, 1H), 7.83 – 7.77 (m, 2H), 7.51 – 7.40 (m, 2H), 7.33 (d, J = 8.0 Hz, 2H), 6.99 (d, J = 7.7 Hz, 1H), 3.85 (s, 3H), 3.62 (d, J = 12.4 Hz, 1H), 3.07 – 2.96 (m, 1H), 2.80 (d, J = 19.7 Hz, 1H), 2.57 – 2.47 (m, 1H), 2.43 (s, 3H), 1.89 – 1.81 (m, 2H), 1.50 – 1.39 (m, 1H), 1.31 – 1.24 (m, 1H). ^{13}C NMR (151 MHz, CDCl_3) δ 188.0, 173.5, 154.7, 144.2, 139.0, 137.7, 133.4, 133.0, 130.0, 128.1, 128.0, 127.3, 125.6, 109.5, 52.2, 52.2, 37.3, 27.5, 26.7, 21.6, 20.0.; AMM (ESI-TOF) m/z calcd for $\text{C}_{23}\text{H}_{24}\text{NO}_5\text{S}^+$ $[\text{M}+\text{H}]^+$ 426.1370, found 426.1358.

2.5 References

1. Portions of this chapter are adapted with permission from Burlow, N. P. H., S. Y.; Saunders, C. M.; Fettinger J. C.; Tantillo D. J.; Shaw, J.T. , *Org. Lett.* **2019**, *21* (4), 1046-1049. Copyright 2019 American Chemical Society
2. Masse, C. E.; Ng, P. Y.; Fukase, Y.; Sánchez-Roselló, M.; Shaw, J. T., *J. Comb. Chem.* **2006**, *8* (3), 293-296.
3. Ng, P. Y.; Masse, C. E.; Shaw, J. T., *Org. Lett.* **2006**, *8* (18), 3999-4002.
4. Wei, J.; Shaw, J. T., *Org. Lett.* **2007**, *9* (20), 4077-4080.
5. Younai, A.; Chin, G. F.; Shaw, J. T., *J. Org. Chem.* **2010**, *75* (23), 8333-8336.
6. Biggs-Houck, J. E.; Davis, R. L.; Wei, J.; Mercado, B. Q.; Olmstead, M. M.; Tantillo, D. J.; Shaw, J. T., *J. Org. Chem.* **2012**, *77* (1), 160-172.

7. Di Maso, M. J.; Nepomuceno, G. M.; St. Peter, M. A.; Gitre, H. H.; Martin, K. S.; Shaw, J. T., *Org. Lett.* **2016**, *18* (8), 1740-1743.
8. Di Maso, M. J.; Snyder, K. M.; De Souza Fernandes, F.; Pattawong, O.; Tan, D. Q.; Fettinger, J. C.; Cheong, P. H.-Y.; Shaw, J. T., *Chem. Eur. J.* **2016**, *22* (14), 4794-4801.
9. Laws, S. W.; Moore, L. C.; Di Maso, M. J.; Nguyen, Q. N. N.; Tantillo, D. J.; Shaw, J. T., *Org. Lett.* **2017**, *19* (10), 2466-2469.
10. Tamura, Y.; Wada, A.; Sasho, M.; Kita, Y., *Tetrahedron Lett.* **1981**, *22* (43), 4283-4286.
11. Tamura, Y.; Wada, A.; Sasho, M.; Kita, Y., *Chem. Pharm. Bull* **1983**, *31* (8), 2691-2697.
12. Tamura, Y.; Sasho, M.; Akai, S.; Wada, A.; Kita, Y., *Tetrahedron* **1984**, *40* (22), 4539-4548.
13. Tamura, Y.; Sasho, M.; Nakagawa, K.; Tsugoshi, T.; Kita, Y., *J. Org. Chem.* **1984**, *49* (3), 473-478.
14. Manoni, F.; Connon, S. J., *Angew. Chem. Int. Ed.* **2014**, *53* (10), 2628-2632.
15. Georgieva, A.; Stanoeva, E.; Spassov, S.; Haimova, M.; De Kimpe, N.; Boelens, M.; Keppens, M.; Kemme, A.; Mishnev, A., *Tetrahedron* **1995**, *51* (21), 6099-6114.
16. Manoni, F.; Farid, U.; Trujillo, C.; Connon, S. J., *Org. Biomol. Chem.* **2017**, *15* (6), 1463-1474.
17. Breugst, M.; Detmar, E.; von der Heiden, D., *ACS Catal.* **2016**, *6* (5), 3203-3212.
18. Rodríguez, N.; Manjolinho, F.; Grünberg, M. F.; Gooßen, L. J., *Chem. Eur. J.* **2011**, *17* (49), 13688-13691.

19. Hirner, S.; Westmeier, J.; Gebhardt, S.; Müller, C. H.; von Zezschwitz, P., *Synlett* **2014**, 25 (12), 1697-1700.
20. Savile, C. K.; Kazlauskas, R. J., *Adv. Synth. Catal.* **2006**, 348 (10-11), 1183-1192.
21. García Ruano, J. L.; Alemán, J.; Belén Cid, M.; Parra, A., *Org. Lett.* **2005**, 7 (2), 179-182.
22. Boger, D. L.; Kasper, A. M., *J. Am. Chem. Soc.* **1989**, 111 (4), 1517-1519.
23. Espinosa, M.; Blay, G.; Cardona, L.; Pedro, J. R., *Chem. Eur. J.* **2013**, 19 (44), 14861-14866.
24. Carmen, S.; Tomas, L.; Z., S. A. M.; D., S. A., *Angew. Chem. Int. Ed.* **2012**, 51 (15), 3653-3657.
25. Wang, Z.; Barrows, R. D.; Emge, T. J.; Knapp, S., *Org. Process Res. Dev.* **2017**, 21 (3), 399-407.
26. V., B. J., *Berichte der deutschen chemischen Gesellschaft* **1904**, 37 (3), 3210-3213.
27. Asundaria, S.; Patel, K., *Pharm. Chem. J.* **2012**, 45 (12), 725-731.
28. Cabrera, M.; Simoens, M.; Falchi, G.; Lavaggi, M. L.; Piro, O. E.; Castellano, E. E.; Vidal, A.; Azqueta, A.; Monge, A.; de Ceráin, A. L.; Sagrera, G.; Seoane, G.; Cerecetto, H.; González, M., *Bioorg. Med. Chem.* **2007**, 15 (10), 3356-3367.
29. Zhang, X.; Kang, J.; Niu, P.; Wu, J.; Yu, W.; Chang, J., *J. Org. Chem.* **2014**, 79 (21), 10170-10178.
30. Liu, S.; Liebeskind, L. S., *J. Am. Chem. Soc.* **2008**, 130 (22), 6918-6919.
31. Nagano, M.; Doi, M.; Kurihara, M.; Suemune, H.; Tanaka, M., *Org. Lett.* **2010**, 12 (15), 3564-3566.

32. Armstrong, A.; Baxter, C. A.; Lamont, S. G.; Pape, A. R.; Wincewicz, R., *Org. Lett.* **2007**, *9* (2), 351-353.
33. Sheshenev, A. E.; Boltukhina, E. V.; White, A. J. P.; Hii, K. K., *Angew. Chem. Int. Ed.* **2013**, *52* (27), 6988-6991.
34. Batovska, D.; Parushev, S.; Slavova, A.; Bankova, V.; Tsvetkova, I.; Ninova, M.; Najdenski, H., *Eur. J. Med. Chem* **2007**, *42* (1), 87-92.
35. Xu, W.; Zhou, Y.; Wang, R.; Wu, G.; Chen, P., *Org. Biomol. Chem.* **2012**, *10* (2), 367-371.
36. Xin, B.; Zhang, Y.; Cheng, K., *Synthesis* **2007**, *2007* (13), 1970-1978.

Chapter 3: Development of the Mukaiyama Castagnoli-Cushman Reaction¹

3.1 Introduction

The Shaw group has been interested in the synthesis of δ - and γ -lactams through the Castagnoli-Cushman reaction (CCR) since our seminal publication on the 4-component variant in 2007.²⁻¹³ In 2013, we discovered that the mechanism of the CCR proceeds through a Mannich addition of an anhydride enolate on an iminium ion, or through a hydrogen bonding pair, followed by intramolecular acylation (for a detailed mechanistic discussion see chapter 1 and 4).^{7, 14} Based on our new mechanistic understanding, we recognized the possibility of developing catalytic variants of the CCR. To date, several catalytic examples of the CCR have been developed, however, catalytic reactions have exclusively used readily enolizable homophthalic anhydride (Figure 3.1, left).^{11, 15, 16} Our group was interested in developing an acid-catalyzed variant of the CCR using 2,5-bis(trimethylsilyloxy) furan as a synthon for succinic anhydride, which would enable the facile synthesis of γ -lactam structures (Figure 3.1, right).¹³

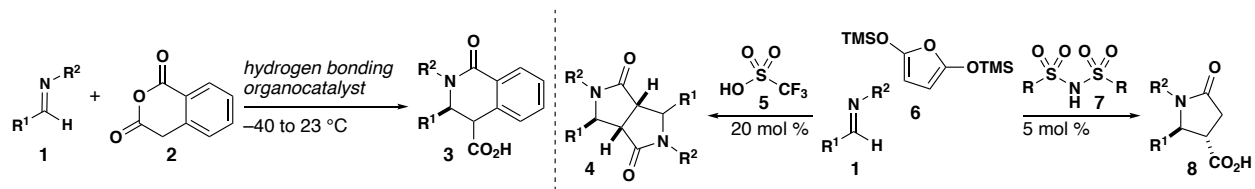


Figure 3.1 Previous catalytic examples of the CCR (left). Acid catalyzed Mukaiyama Mannich reaction (right).

3.1.1 Review of Acid-Catalyzed Mukaiyama Mannich Reactions

The first acid-mediated reaction of silyl ketene acetals with imines was reported by Ojima and coworkers in 1981.¹⁷ In association with the Mukaiyama aldol reaction of silyl enol ethers and ketene acetals with carbonyls, the reactions of silyl ketene acetals with imines have been referred to as the Mukaiyama Mannich reaction. Due to their prevalence in antibiotics like penicillin, Ojima and coworkers sought to synthesize β -lactams through Mannich reactions of silyl ketene acetals mediated by TiCl_4 (Figure 3.2). Nucleophilic addition and subsequent hydrolysis of the Lewis acid led to the β -amino esters **10**, which could be cyclized to β -lactams **11** with LDA.¹⁷ Although both β -amino esters **10** and β -lactams **11** were achieved in excellent yields, product inhibition necessitated the use of stoichiometric Lewis acid promoters.

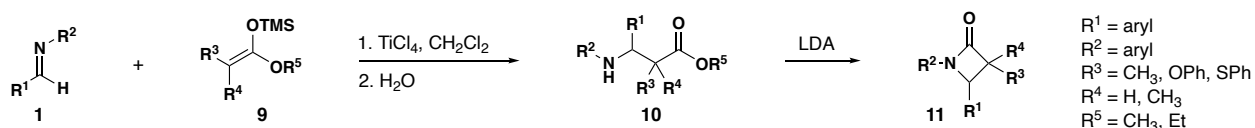


Figure 3.2 Ojima's synthesis of β -lactams through Mukaiyama Mannich-like reaction

In 1985, Morimoto and coworkers developed an α -formylation reaction of silyl ketene acetals **12** and *N-tert*-butylformimidoyl cyanide **13** catalyzed by trimethylsilyl triflate.¹⁸ Notably, the use of trimethyl silyl triflate allowed for the first catalytic variant of the Mukaiyama Mannich reaction. Compound **14** is formed after Mukaiyama Mannich addition, which after β -elimination of either trimethylsilyl cyanide or hydrogen cyanide provides imines **15**. Imine products **15** can then be hydrolyzed to the desired formylation products **16** (Figure 3.3).¹⁸ The success of this catalytic variant provided precedent for the development of catalytic enantioselective Mukaiyama Mannich reactions.

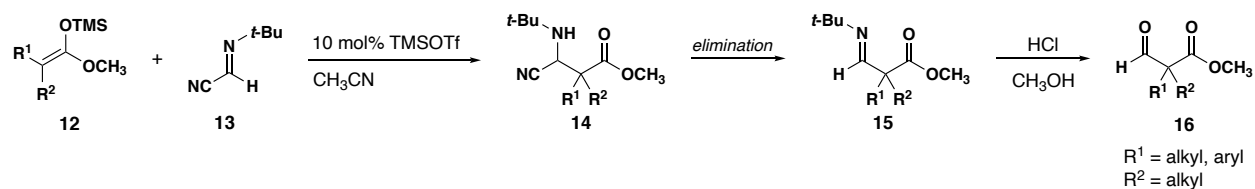


Figure 3.3 First catalytic Mukaiyama Mannich reaction leading to formylated products **16**.

Mukaiyama's initial work on the acid-catalyzed Mannich reaction involved a catalytic reaction of silyl ketene acetals with diphosphonium salt catalysts.¹⁹ In a previous report, Mukaiyama had shown diphosphonium salts could catalyze aldol-type reactions with aldehydes and silyl nucleophiles.²⁰ Later, similar reactions were reported with imines in a Mannich-like reaction promoted by the same catalysts.¹⁹ The reaction of *N*-benzylidene aniline with the silyl ketene acetal of methyl isobutyrate proceeds with excellent yields to the β -amino ester **10** (Figure 3.4).¹⁹ Mukaiyama notes that the reaction of trimethyl silyl ketene acetals were more reactive than *t*-butyldimethyl silyl (TBS) ketene acetals, which suggests that the silicon substituents have an impact on reactivity. He proposed that the mechanism involved initial coordination of the imine with the catalyst to form an iminium ion, which could then be attacked by the silyl ketene acetal to form products **10**.

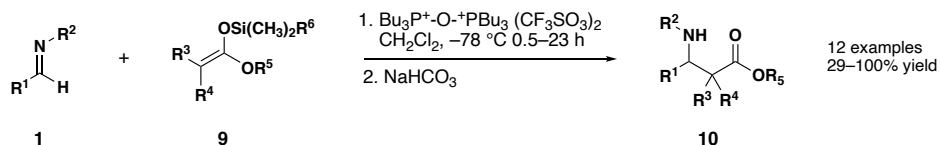


Figure 3.4 Mukaiyama Mannich reactions catalyzed by diphosphonium salts.

Yamamoto further expanded the scope of these types of reactions by developing an enantioselective Brønsted acid assisted chiral Lewis Acid Mukaiyama Mannich

reaction.²¹ The reaction of the trimethylsilyl ketene acetal (**18**) with a single enantiomer of imine **17** was shown to lead to Mannich products **19** with high diastereoselectivity. The reaction was then expanded to racemic imines to afford highly enantioenriched products **19** in modest yields and with increased enantioselectivity when bulky *N*-substituted imines were used (Figure 3.5). Notably, like Ojima's initial report, stoichiometric quantities of the Brønsted acid were required to induce asymmetry in this reaction.

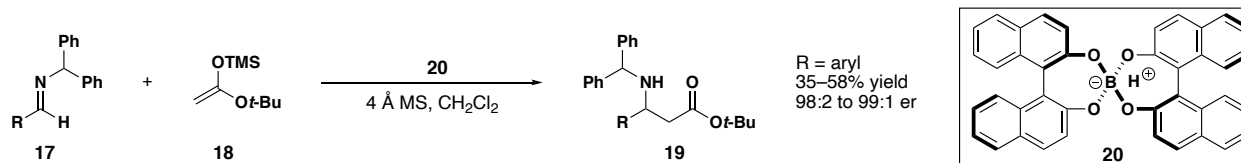


Figure 3.5 First enantioselective Mukaiyama Mannich type reaction to afford β -amino esters.

Kobayashi and coworkers reported the first catalytic enantioselective Mukaiyama Mannich reaction utilizing chiral zirconium complexes.²² In this work, substoichiometric quantities of a zirconium catalyst promoted reaction of silyl ketene acetal **22** and 2-aminophenol derived imines **21** to afford β -amino ketones **23** in good yields and moderate enantioselectivities (Figure 3.6). Modification of the catalyst backbone as well as addition of *N*-methyl imidazole ultimately improved enantioselectivity. They hypothesize that the mechanism of this reaction involves bidentate chelation which explains the requirement for an ortho phenol *N*-substituent on the imine substrates.

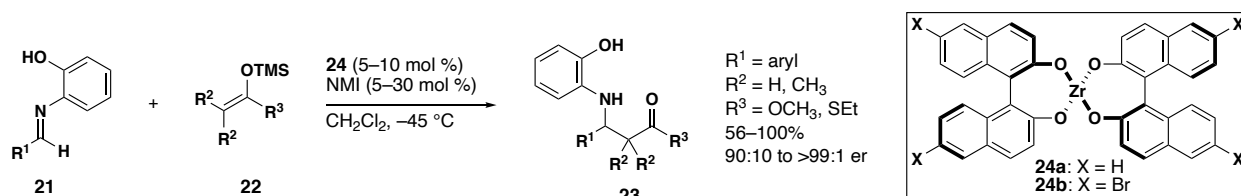


Figure 3.6 First catalytic enantioselective reaction of silyl ketene acetals and imines.

Akiyama also developed a chiral Brønsted acid catalyzed reaction using phosphoric acid catalysts derived from boronic acids.²³ Catalyst structure was modulated by using Suzuki coupling reactions to incorporate the aryl groups on the (*R*)-BINOL scaffold. The introduction of electron-withdrawing nitro groups on the catalyst improved enantioselectivity and accelerated the reaction rate. The reaction was optimized to afford high diastereo- and enantioselectivities and excellent yields for the *syn* products (**26a**) (Figure 3.7). In analogy to Kobayashi's method, the ortho hydroxyl group on the aniline portion of the imine was required to impart enantioselectivity.

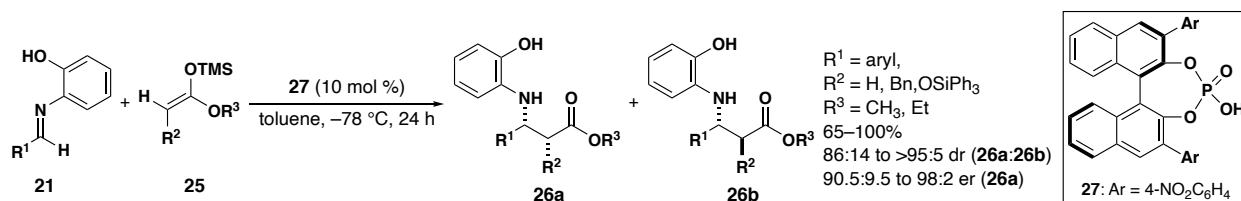


Figure 3.7 Improved enantioselective reaction of imines with silyl ketene acetals and a chiral phosphoric acid catalyst.

3.1.2 Anionic Counterion Directed Catalysis in Mukaiyama Mannich Type reactions

Anionic counterion directed catalysis (ACDC) is a catalytic method coined by Benjamin List at the Max Planck Institut für Kohlenforschung. The general premise centers around the idea that organic reactions typically proceed through polar transition states or charged intermediates, which can be influenced by counterions in solution.²⁴ ACDC involves the formation of a tight ion pair between a cationic substrate with an enantiomerically pure catalyst partner. In organic solvents, the low separation of charge encourages ion pair formation and can lead to enantioselective outcomes.²⁴ Asymmetric

counterions had previously been used in organic transformations to yield enantioselective reaction outcomes, albeit with only moderate success.²⁵⁻²⁸ List showed the initial utility of ACDC in 2006 by developing an asymmetric reduction of α,β -unsaturated aldehydes to their saturated counterparts.²⁴ In this report, he utilized a chiral phosphoric acid catalyst derived from BINOL to afford saturated aldehydes **31** (Figure 3.8).

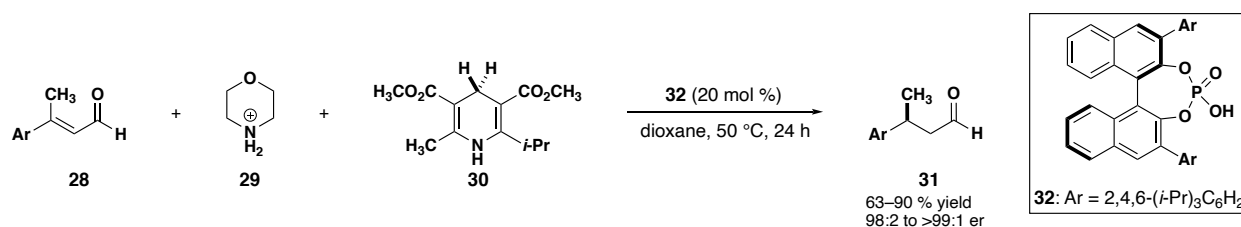


Figure 3.8 Enantioselective reduction of α,β -unsaturated aldehydes to show proof of concept for ACDC.

Subsequently, List published on advances in ACDC catalyst design and expansion to other reaction classes.²⁹ Notably, disulfonimide catalyst **36** was synthesized and shown to improve the Mukaiyama Aldol reaction. Previous literature reports of asymmetric Mukaiyama aldol reaction required chiral Lewis acid catalysts; however, limitations to the previously described method include the necessity of high catalyst loadings and highly activated starting materials. In order to improve this, List endeavored to synthesize a Brønsted acidic catalyst mimicking the acidity of triflic acid or triflimide, while maintaining the chiral BINOL backbone. While the Brønsted acidity of the catalyst was their initial consideration, it is important to note that under reaction conditions these catalysts may be silylated to form Lewis acid catalysts. An additional difference between the BINOL phosphoric acid catalysts and the disulfonimide catalysts is the difference in topology—the 3D structures of the phosphoric acid compared to the disulfonimide shows that the

acidic moiety is buried deeper in the pocket in the disulfonimide. This 3D conformation was hypothesized to be responsible for imparting a higher level of enantioselectivity. They discovered that disulfonimide **36** was an excellent catalyst for the Mukaiyama aldol reaction, leading to the synthesis of a variety of substrates in good yields and enantioselectivities (Figure 3.9).

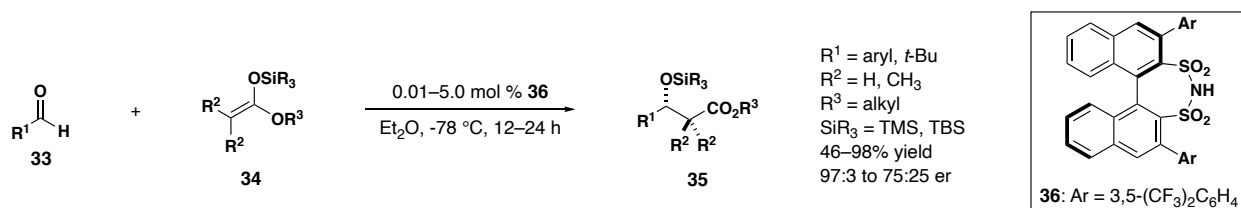


Figure 3.9 List's Mukaiyama aldol reaction catalyzed by sulfonimide catalyst **36**

List hypothesized that two different mechanistic pathways were possible for this enantioselective reaction.²⁹ First, the acid may be working as a Brønsted acid catalyst by protonating the aldehyde and forming an ion pair in analogy to the mechanism proposed by Akiyama.²³ Alternatively, the catalyst (**36**) may be silylated by a sacrificial quantity of silyl ketene acetal **37**, which would lead to a Lewis acid catalyzed reaction (Figure 3.10). An additional silyl transfer activates aldehyde **33** which forms a tight ion pair with the conjugate base of the catalyst (**36**), resulting in enantioselective induction for the subsequent Mannich addition. To probe the mechanism of the reaction, 2,6-ditertbutyl pyridine (2,6-DTBP), which functions as a proton scavenger, was employed as an additive. If the reaction were Brønsted acid catalyzed, the addition of 2,6-DTBP would halt reaction progress. Interestingly, the use of 2,6-DTBP had no impact on reaction outcomes, which supports the hypothesis the reaction is Lewis acid catalyzed.

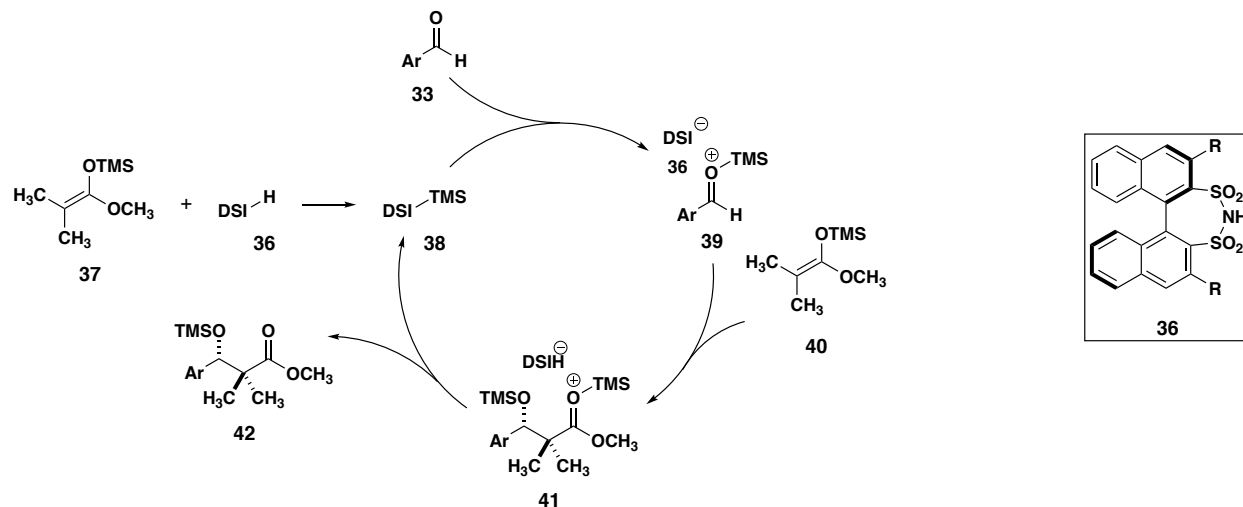


Figure 3.10 Proposed mechanism of the Mukaiyama Aldol reaction

3.1.3 Synthesis and Reactivity of 2,5-(bistrimethyl)silyloxy furan and Related Nucleophiles

A study of the synthesis and reactivity of 2,5-bis(trimethylsilyloxy) furan was reported in a series of three publications by Chan in 1980.³⁰⁻³² The first report describes the first synthesis of 2,5-bis(trimethylsilyloxy) furans **6a-e** through reaction of substituted succinic anhydrides **43** with triethylamine, zinc chloride, and chlorotrimethylsilane (Figure 3.11A).³⁰ The resulting products (**6a-e**) were found to be highly sensitive to water and air. When in contact with water, the furans are hydrolyzed to succinic acids **44**, whereas reactions with air lead to oxidation to bis(trimethyl) silyl maleates **45**. While the oxidation mechanism is unknown, it was proposed that the reaction occurs through a radical like mechanism based on how the relative rates of oxidation change depending on the substitution of the succinic anhydride precursor. These bis(trimethylsilyloxy)furan substrates (**6a-e**) were tested as dienes in Diels Alder reactions with DMAD to afford *p*-quinones **47** and hydroquinones **48** (Figure 3.11B). Finally, the novel bis(trimethylsilyloxy)

furans (**6a-e**) were shown to react with singly activated dienophile such as ethyl acrylate, rendering it more reactive than furan in Diels Alder reactions.

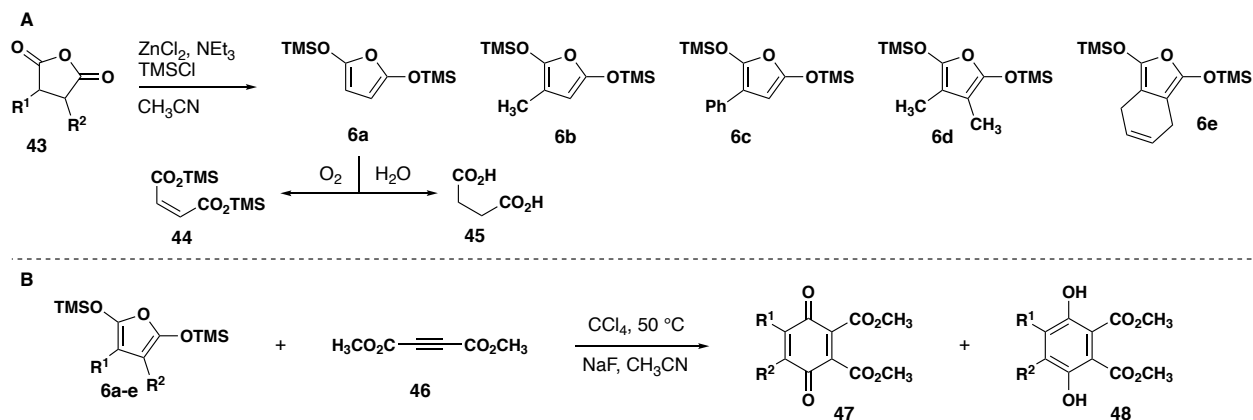


Figure 3.11 A. Synthesis of a series of 2,5-bis(trimethylsilyloxy) furan products. B. Synthesis of *p*-quinones and hydroquinones from **6**.

Simchen and coworkers also synthesized a variety of analogs of 2,5-bis(trimethylsilyloxy) furan **6** using trimethylsilyltriflate and triethylamine which obviated the use of zinc chloride in the reaction (Figure 3.12).³³ Using their novel method, a variety of anhydride derivatives (**6a-c**, **51**) were synthesized, as well as thiophenes derived from thioanhydrides **49a-b**. Additionally, it was found that purification by vacuum distillation afforded more consistently pure products.

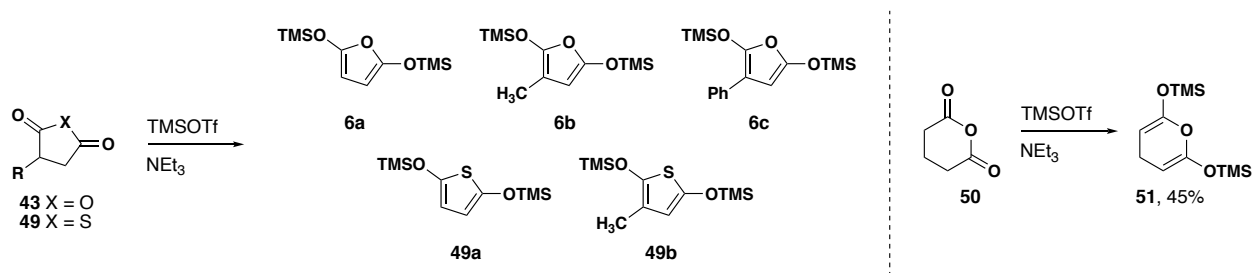


Figure 3.12 Novel reaction conditions for the synthesis of 2,5-bis(trimethylsilyloxy)furans, 2,5-bis(trimethylsilyloxy)thiophenes, and 2,6-bis(trimethylsilyloxy)pyran.

A follow-up paper by Chan and Brownbridge utilized these bis-(trimethylsilyloxy) furans in a novel synthesis of bis-lactones **54** from carbonyl compounds (Figure 3.13A).³¹ Although bis-lactone substrates **54** have previously been synthesized by performing an oxidative coupling of cinnamic acid,^{34, 35} Chan and Brownbridge developed a facile Lewis acid mediated synthesis using 2,5-bis(trimethylsilyloxy) furan **6a** and readily available carbonyl compounds (Figure 3.13A). **6a** was shown to react with two equivalents of acetone and two equivalents of titanium tetrachloride to afford all *cis*-bis-lactone **54**, the relative stereochemistry of which was assigned by J_{H-H} values. Interestingly, in the case of benzaldehyde, the moles of TiCl_4 used in the reaction influenced the ratio of diastereomers isolated in the reaction mixture. When two moles of TiCl_4 are used, the all *cis*-diastereomer **54a** is formed, whereas the use of one mole affords a mixture of **54a** and unsymmetrical diastereomer **54b** (Figure 3.13B). They hypothesized that the extra mole of titanium tetrachloride either impacts the structure of the intermediate formed, or perhaps the presence of excess TiCl_4 causes isomerization from the unsymmetrical diastereomer to the symmetrical diastereomer. A small series of bis-lactones **54** were synthesized using this methodology in modest yields.

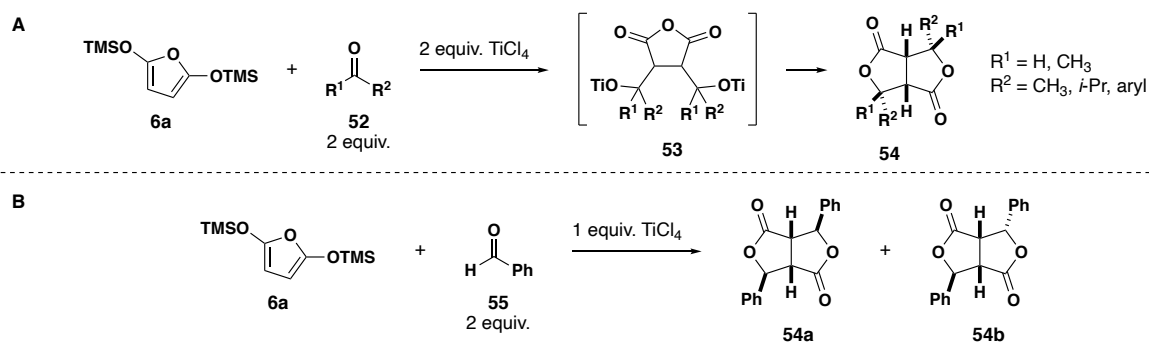


Figure 3.13 Chan and Brownbridge's synthesis of bis-lactones from 2,5-(bistrimethylsilyloxy) furan

Chan and Brownbridge's final report on the reactivity of 2,5-bis(trimethylsilyloxy) furans showed that more highly substituted silyloxy furans (**6b**, **6c**, **6e**) afford γ -hydroxybutenolides **57** (Figure 3.14A) when reacted with TiCl_4 and ketones or aldehydes.³² When 2,5-bis(trimethylsilyloxy) furan **6a** was reacted with methyl vinyl ketone and titanium tetrachloride at $-78\text{ }^\circ\text{C}$, product **59** is formed exclusively (Figure 3.14B). This result was surprising due to the fact that **6a** had been shown to undergo Diels Alder reactions with α,β -unsaturated esters (Scheme 3.11B). When more substituted silyloxy furans (**6b**, **6c**, **6e**) were reacted with methyl vinyl ketone, γ -hydroxybutenolides **60** resulting from Michael addition are observed (Figure 3.14C).³²

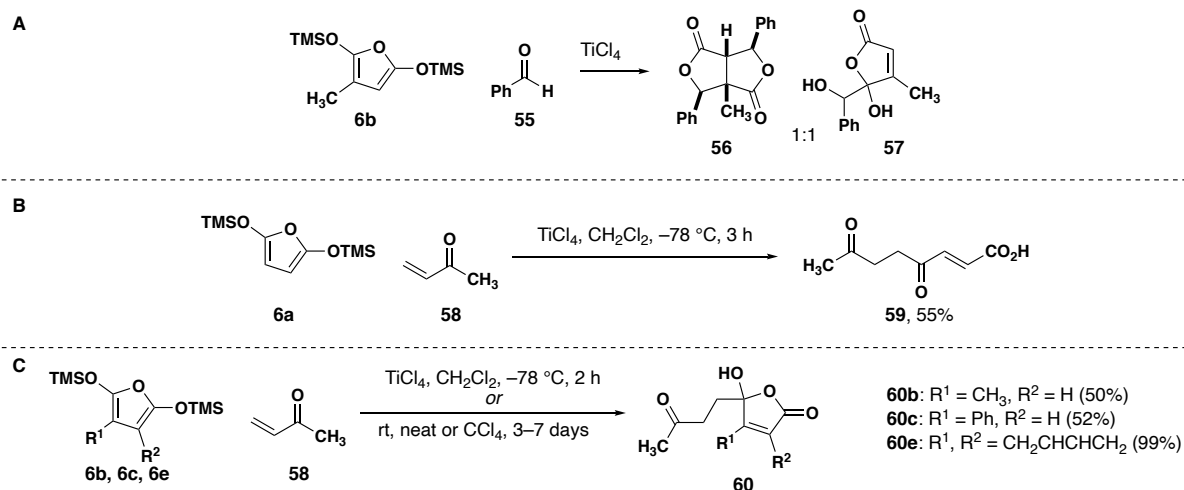


Figure 3.14 A. Reaction of **6b** with benzaldehyde to afford a mixture of bislactone and γ -hydroxybutenolides. B. **59** is formed exclusively when **6a** is reacted with methyl vinyl ketone, C. Reaction outcomes from more substituted silyl ketene acetals **6b**, **6c**, **6e**.

More recently in 2007, Pohmakotr showed that 2,5-bis(trimethylsilyloxy) furan **6a** can undergo Lewis acid-catalyzed Mukaiyama Mannich type reactions with *N*-phenyl and *N*-benzyl imines to afford lactams **8** with high diastereoselectivity (Figure 3.15).³⁶

Pohmakotr screened a variety of Lewis acids and found that $\text{Sc}(\text{OTf})_3$ provided the best diastereoselectivity and conversion to the trans lactam product. The diastereoselective outcome was hypothesized to arise from a staggered acyclic transition state, wherein $\text{Sc}(\text{OTf})_3$ coordinates to the nitrogen atom. This coordination forces **6a** to orient itself over the *N*-substituent and the imine hydrogen in order to generate the least sterically encumbered transition state, which leads to a high degree of trans diastereoselectivity (**61**). Notably, no alkyl-substituted imines were tested in the reaction.

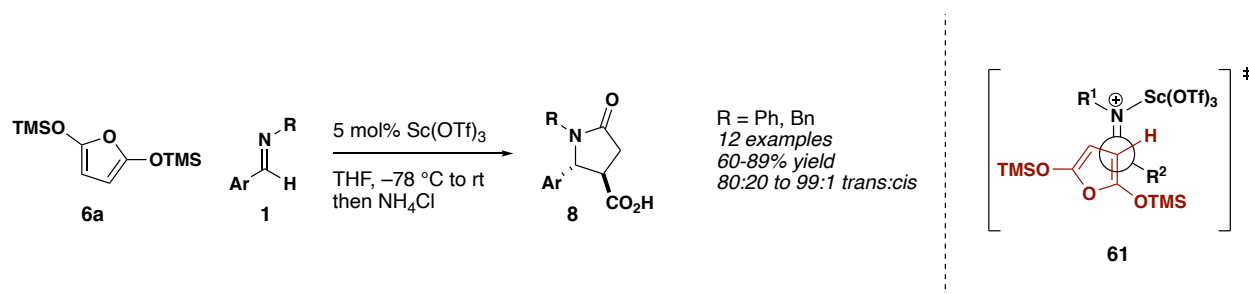


Figure 3.15 (Left) Lewis acid catalyzed Mukaiyama Manich reaction of 2,5-(bistrimethylsilyloxy) furan. (Right) Transition state drawing leading to diastereoselective outcome.

3.1.4 Intro to Computational NMR

Computational NMR has become an increasingly more accurate method for assigning chemical structures based on computed chemical shifts and $J_{\text{H-H}}$ values.³⁷ In particular, this technique has become widely used as a means to determine observed diastereomers from reaction outcomes. While classic multidimensional NMR experiments have been used to assign relative stereochemistry in molecules, these indirect methods can lead to incorrect structural assignments due to the vast structural similarities between diastereomers. On the other hand, NMR calculations can provide either calculated chemical shift values or $J_{\text{H-H}}$ values that can be directly compared to the experimentally

determined spectra. Tantillo and coworkers have even developed a chemical shift repository CHESHIRE CCAT (CHEmical SHift REpository with Coupling Constants Added Too) in order to make the calculation of NMR shifts and J_{H-H} values accessible to organic chemists who are unfamiliar with computational chemistry.³⁸

The general workflow for computing the chemical shift or J_{H-H} values of a particular compound begins with performing a conformer search to find the most reasonable conformer for the molecule of interest. (Figure 3.16).³⁷ Typically, conformer searches are performed using a program such as Spartan or Avogadro. Once the lowest energy conformer is found, a geometry optimization is performed to ensure the conformer has the correct geometry about each bond, including bond angles and bond lengths. The geometry optimized conformer is then employed in the NMR calculation. It is important to note that performing calculations on a single conformer can introduce error into the calculation, as experimental NMR spectroscopy occurs on a timescale that allows compounds conformational mobility.³⁷ NMR experiments correspond to multiple conformers, and the resulting NMR spectra are based on the Boltzmann weighted averages of conformations accessible at the experimental temperature.³⁷ It should be noted that all accessible conformations may not have a significant impact on the entire ^1H NMR spectrum, and reasonable results can be obtained without averaging results from different conformers.³⁷

Once the conformer of choice has been identified, NMR calculations can be performed using Gaussian. Typically, quantum chemical methods are used for such purposes, specifically density functional theory (DFT).^{37, 39} For chemical shift calculations,

NMR isotropic shielding constants are computed. When calculating these values, the isotropic shielding constants of related nuclei are typically averaged.³⁷ The computed isotropic shielding values can then be converted to chemical shift values analogous to how it is done in experimental NMR—isotropic shielding constants are subtracted from a reference compound, typically tetramethylsilane.³⁷

Larger basis sets are necessary for the calculation of J_{H-H} values, and special basis sets have been developed.⁴⁰ Bally and Rablen detailed the theoretical background and methods for the calculation of J_{H-H} values.³⁹ When calculating J_{H-H} values, the specific value computed are the Fermi contact (FC) terms, which are one of three terms that contribute to J_{H-H} values.³⁹ Bally and Rablen found that FC alone provide accurate predictions of J_{H-H} values. FC terms are then extracted and multiplied by calculated scaling factors to afford the true J_{H-H} values,

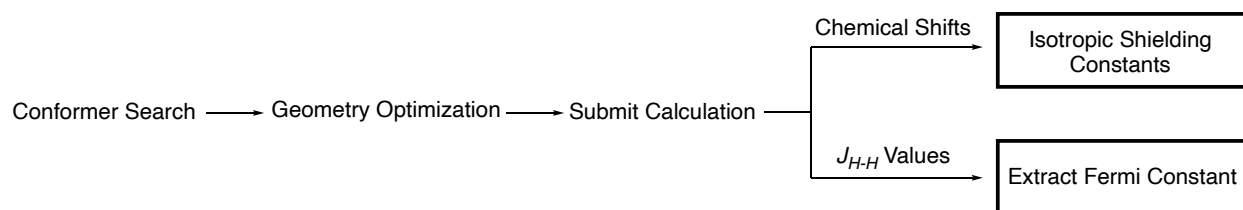


Figure 3.16 Workflow of computational NMR calculations.

The expansive resources for computational NMR allow for synthetic chemists to perform simple NMR calculations to assign relative stereochemistry of complex structures. Typical methods used by synthetic chemists for structural assignment involve Nuclear Overhauser Effect (NOE) experiments, which provide evidence that two nuclei are close in space. This technique can be applied to nuclei on stereogenic centers of

interest and provide evidence for relative stereochemistry. However, NOE experiments are typically only reliable in more rigid structures. For more definitive evidence for relative stereochemistry, X-Ray crystal structures may be acquired. This method relies on the ability of the molecule of interest to produce suitable crystals. Should this not be the case, synthetic chemists may attempt to perform computational NMR calculations to assign the relative stereochemistry of their molecule of interest.

3.2 Results and Discussion

A detailed description of the Mukaiyama CCR can be found in Dr. Stephen Law's dissertation.⁴¹ Specifically, Dr. Laws described his attempts at developing an enantioselective acid-catalyzed Mukaiyama CCR and delved deeper into the optimization of reaction outcomes in the Mukaiyama CCR. Here, I will summarize the development of the single and double addition reactions leading to mono and bis- γ -lactams, respectively, as well as my contribution to the scope of the Mukaiyama CCR.

With Pohmakotr's work as precedent,³⁶ we sought to develop a disulfonimide catalyzed synthesis of γ -lactams by a Mukaiyama Mannich-type reaction. We envisioned a strategy for catalyzing this reaction in analogy to the Mukaiyama aldol reaction using ACDC. Specifically, we were interested in developing an enantioselective acid-catalyzed Mukaiyama CCR reaction which would allow for non-readily enolizable anhydrides like succinic anhydrides to form CCR products under mild conditions. We hypothesized that the mechanism would be analogous to the mechanism described by List for the asymmetric Mukaiyama aldol reaction (Figure 3.17).²⁹ First the furan **6a** can undergo in situ silyl group exchange from a small quantity of substrate to form the active Lewis acid

catalyst (**62**) and activate the imine (**1**) to form iminium ion **63**. In theory, the conjugate base of the Brønsted acid catalyst (**5**, **65**, **66**, or **67**) can then form a tight ion pair to impart enantioselectivity in the following step. Then, the furan (**6a**) can undergo a Mukaiyama Mannich addition with the iminium ion pair (**63**) to form **64**. Upon acid work up, **64** reforms the anhydride, which undergoes an intramolecular *N*-acylation to form γ -lactam products (**8**).

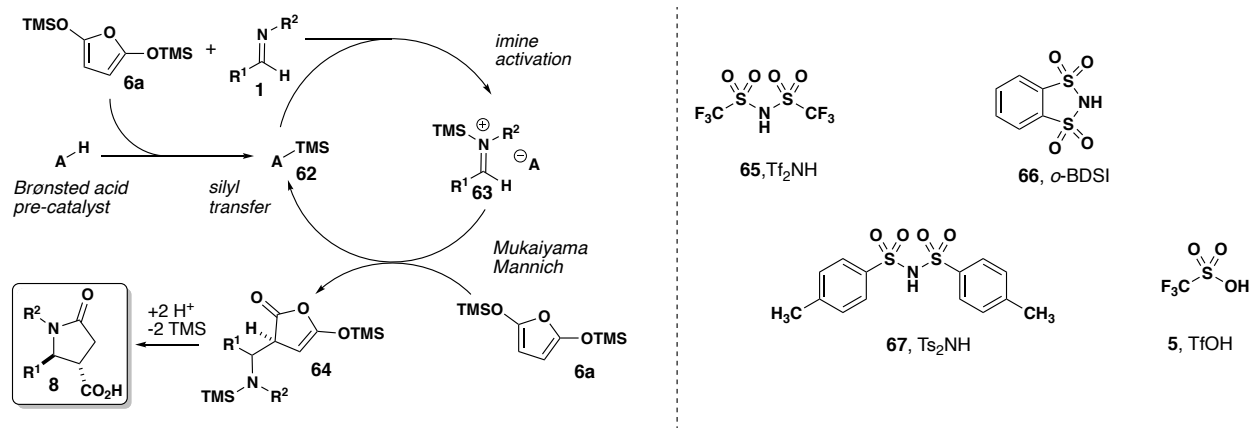


Figure 3.17 Proposed mechanism for the Mukaiyama CCR reaction, including possible acid catalysts

3.2.1 Synthesis of *N*-Aryl and *N*-Alkyl Imines

In order to test the limits of a Mukaiyama Mannich type CCR, we were required to synthesize a number of imine substrates. Dr. Stephen Laws endeavored to synthesize imines with cleavable *N*-substituents, such as Boc, CBz and *p*-methoxy phenyl groups, which would allow for further derivatization of our desired lactam products. While the *N*-Boc (**1a**)⁴² and *N*-CBz (**1b**)⁴³ imines had been synthesized previously, in our hands, reaction outcomes were low yielding and inconsistent (Figure 3.18). Instead, Dr. Laws was able to synthesize imine **1c** from the condensation of *p*-anisidine (**69**) with benzaldehyde (**54**).

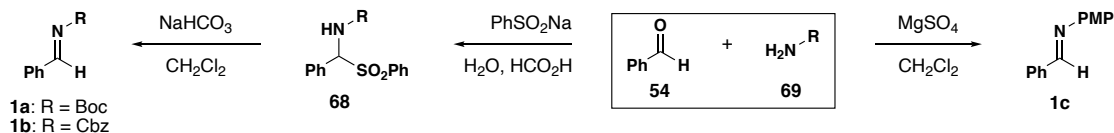


Figure 3.18 Initial synthesis of cleavable *N*-substituted aldimines.

A visiting undergraduate, Shuyu Meng, and then visiting graduate student Dr. Raquel Mato worked to synthesize a series of simple *N*-aryl imines **1d-r** through the condensation of a variety of primary amines **69** with various aromatic aldehydes **33** (Scheme 3.19). *N*-alkyl imines were synthesized similarly, providing products in good yields. Most imines were used without further purification, however some led to incomplete conversion to products, requiring purification. Recrystallization conditions proved effective and afforded pure imine products.

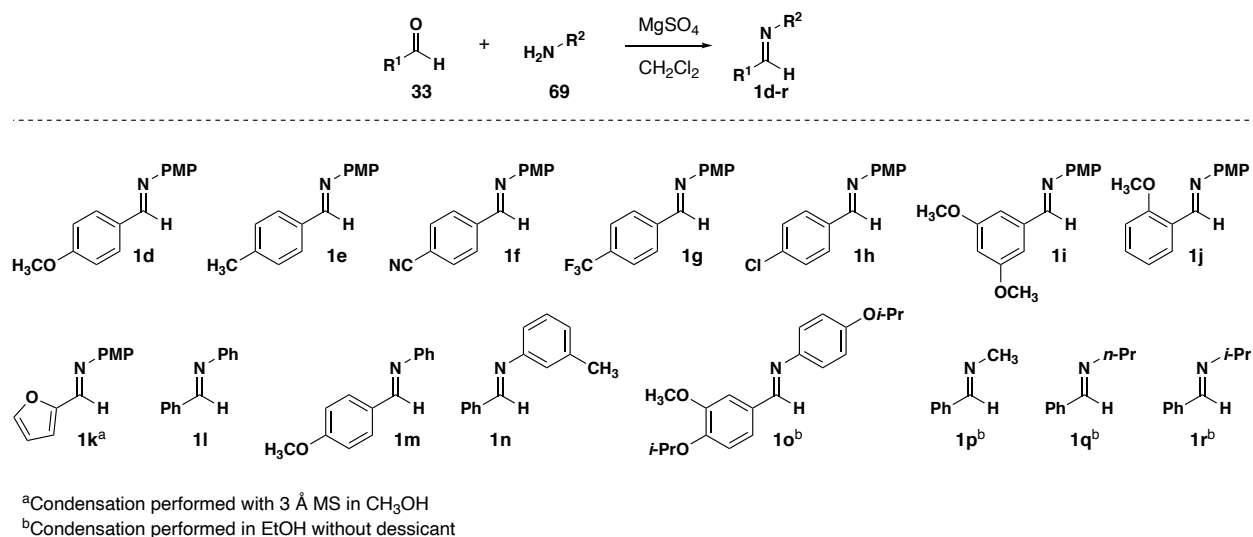


Figure 3.19 Imine scope used in the Mukaiyama CCR.

Similar reaction conditions were attempted in hopes of expanding the imine substrate scope to aliphatic aldehyde derived imines. While the synthesis of these substrates was also precededented,⁴⁴⁻⁴⁷ Dr. Laws found that the desired imine products

were inseparable from their enamine tautomer **70** and aldehyde precursor **33s** through either recrystallization or flash column chromatography (Figure 3.20). Ultimately, the synthesis of these types of imines was not optimized, but the development of a multicomponent variant of the Mukaiyama AMR allowed for the synthesis of the desired lactam substrates and will be discussed later in section 3.2.5.

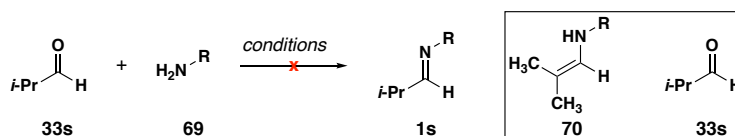


Figure 3.20 Attempted synthesis of isobutyraldehyde derived imine

3.2.2 Synthesis of 2,5-bis(trimethylsilyloxy) Furan

The synthesis of 2,5-bis(trimethylsilyloxy) furan **6a** had a significant impact on the development of the Mukaiyama CCR (Figure 3.21). Dr. Laws optimized the synthesis of this reaction by combining the reaction protocol of Chan and Brownbridge³⁰ and the vacuum distillation purification protocol reported by Simchen³³. As described previously, **6a** is highly air and water sensitive, and required rapid usage in order to generate consistent results. Fortunately, Dr. Laws found that **6a** remained viable for up to one week as a 0.4 M solution in THF at room temperature after purification. On the other hand, the unpurified reaction mixture reaction mixture could remain stirring under inert atmosphere indefinitely prior to purification. As a result, **6a** was synthesized on multi-gram scale and purified weekly for the duration of this project.

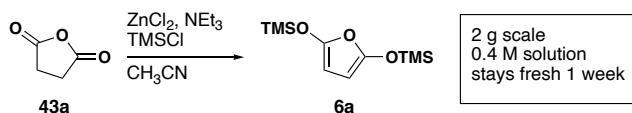


Figure 3.21 Optimized synthesis of 2,5-(bistrimethylsilyloxy) furan

3.2.3 Optimization of Diastereoselective Acid-Catalyzed Mukaiyama Castagnoli-Cushman Reaction

Considering Chan and Brownbridge's synthesis of bis-lactones and Pohmakotr's synthesis of mono-lactams, we imagined that eight product outcomes were possible in the Mukaiyama CCR. First, we envision two diastereomers of mono-lactam product are possible resulting from mono-addition (**71a-b**). Additionally, we hypothesized that a double addition reaction would be possible to form bis- γ -lactam products **72-77**. Based on the formation of four stereogenic centers and the highly symmetrical nature of the bis- γ -lactam, we determined that there are six possible diastereomers of bis- γ -lactams, four symmetrical and two unsymmetrical (**72-77**) (Figure 3.22).

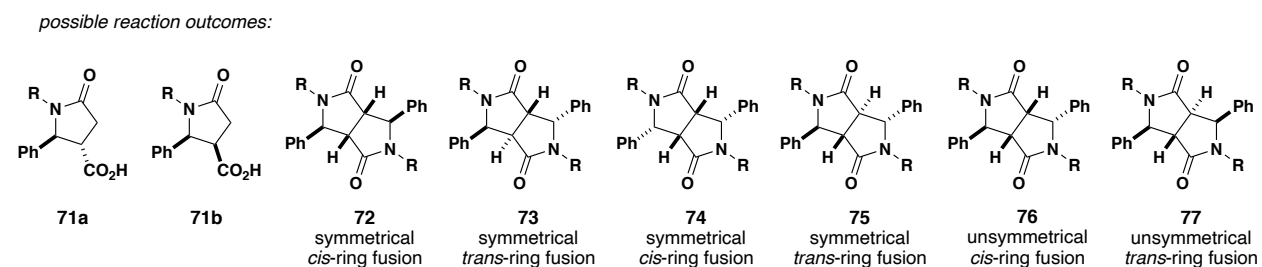
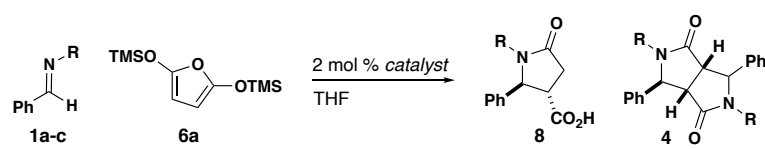


Figure 3.22 Possible reaction outcomes for the Mukaiyama CCR.

Optimization of the acid-catalyzed Mukaiyama CCR was performed by Dr. Laws. Initial screens of simple achiral acids with various *N*-substituted imines and **6a** were performed. Reactions were run between 24 and 48 hours to synthesize lactams **8a-c** (Table 3.1). Attempts at obtaining **8a** through reaction with *N*-Boc imine proved unsuccessful, marked by polymerization of the reaction solvent, THF. However, generation of imine **1a** *in situ* from its amidosulfone precursor catalyzed by *o*-benzenedisulfonimide (**66**, *o*-BDSI) afforded a single, *trans* diastereomer of lactam **8a** with good conversion (Table 3.1, entry

1). Analogous reactions of the *N*-Boc and *N*-Cbz amidosulfones catalyzed by triflimide (**65**) and *o*-BDSI provided lactams **8a** and **8b** with high conversion and diastereoselectivity (Table 3.1, entries 2-5). Unfortunately, the resulting products were challenging to isolate, and we turned our attention to *N*-aryl imines, which provided easily isolable products with slightly diminished conversion.

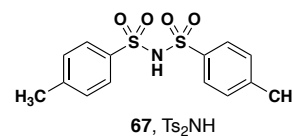
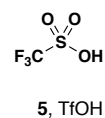
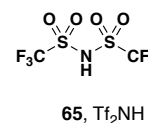
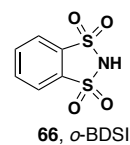
Table 3.1 Achiral Acid Screen for the Mukiyama CCR



entry	R	catalyst	time (h)	% conv. 8 ^a	trans:cis 8 ^a	% conv. 4 ^a
1	Boc	TfOH	24	<5	—	<5
2	Boc	Tf ₂ NH	24	<5	—	<5
3 ^b	Boc	<i>o</i> -BDSI	48	89	74:26	<5
4 ^b	Cbz	Tf ₂ NH	24	>95	>95:5	<5
5 ^b	Cbz	<i>o</i> -BDSI	48	>95	>95:5	<5
6	PMP	TfOH	24	7	n.d.	93
7	PMP	Tf ₂ NH	24	54	>95:5	46
8	PMP	Ts ₂ NH	24	62	90:10	7

^aAs determined by ¹H NMR spectroscopy of the unpurified reaction mixture

^bImine formed *in situ* from decomposition of corresponding amido-sulfone



Effect of Acid Catalyst on Product Outcome

Interestingly, the Brønsted acid used in the reaction had a significant impact on product outcomes. In particular, when triflic acid **5** used in the reaction of *N*-PMP imine **1c** with **6a**, the ¹H NMR spectrum of the unpurified reaction mixture showed consumption of starting materials but showed only 7% conversion to mono lactam **8c**. Instead, significant conversion to two diastereomers of bis- γ -lactam **4** were observed (Table 3.1, entry 6). The triflimide catalyzed reaction of **1c** and **6a** led to a 50:50 ratio of monolactam **8c** and two diastereomeric bis-lactams **4** (Table 3.1, entry 7). The use of ditoluenesulfonimide **67** selectively formed mono lactams with high conversion and diastereoselectivity (Table 3.1,

entry 8). These reaction outcomes led us to optimized mono-addition conditions using two equivalents of furan, increased catalyst loading of ditoluenesulfonimide, and 48-hour reaction times.

3.2.4 Scope of the Mukaiyama Castagnoli-Cushman Reaction

With optimized conditions in hand, Dr. Mato and I worked on expanding the scope of the mono addition products. A variety of *N*-aryl imines were screened in the reaction affording lactam products **8** with good yields and always isolated as the *trans* diastereomer (Figure 3.23). *N*-alkyl imines were also tolerated in the reaction, albeit with lower yields due to difficult purification conditions. While meta-substituted *N*-aryl imines led to the desired products, ortho-substituted *N*-aryl imines were not tolerated in the reaction, suggesting a steric influence on reaction outcomes. The resulting products were isolated as either the carboxylic acid or methyl ester, the latter of which allowed for more facile purification conditions. To prove relative stereochemistry a crystal structure was acquired of product **8h**.

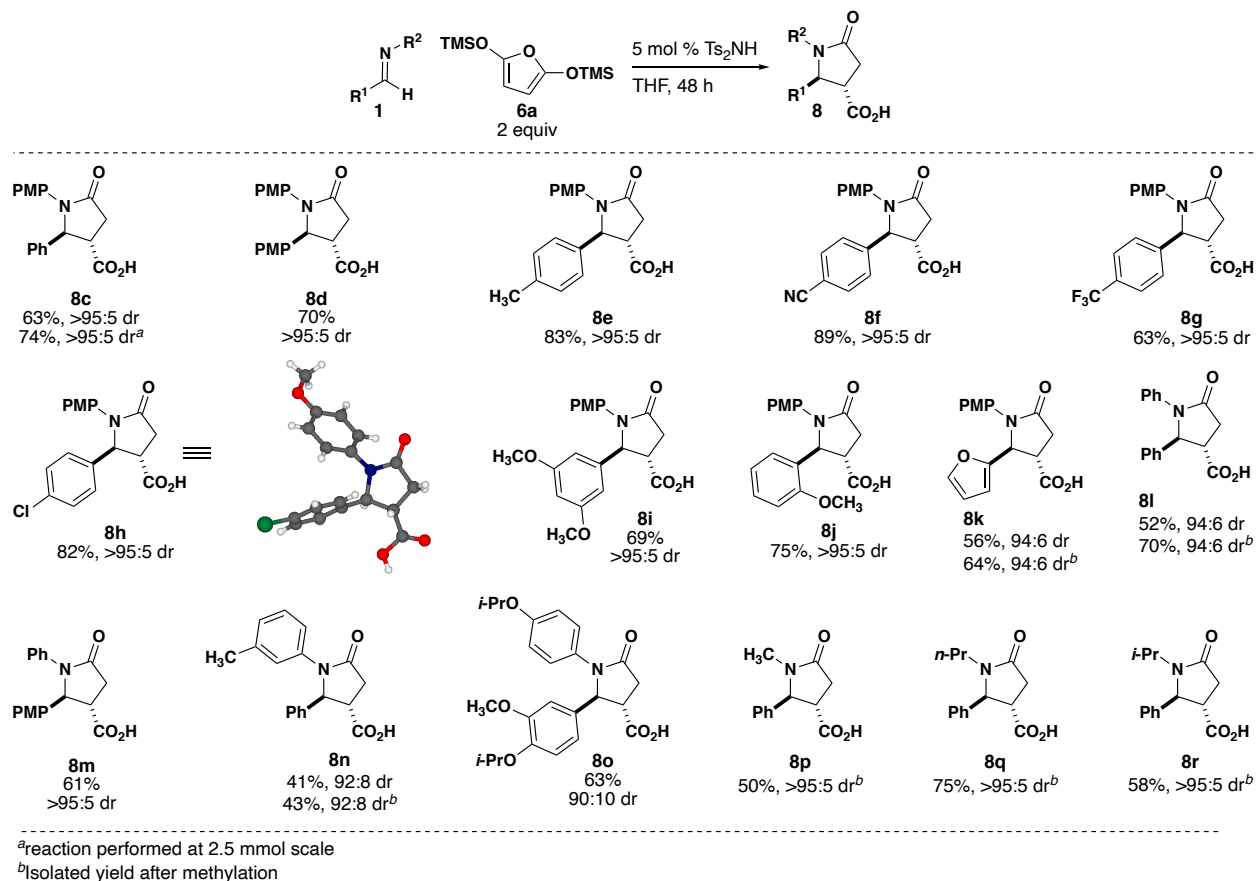


Figure 3.23 Reaction scope of the Mukaiyama CCR.

After expanding the scope of the Mukaiyama Mannich-type CCR, we sought to further functionalize lactam **8c** (Scheme 3.24). First, it was shown that lactam **8c** can be coupled to *p*-anisidine to afford amidated lactam **78**. Next, Dr. Mato showed that esterification of the carboxylic acid moiety can be achieved in high yield and CAN-mediated PMP-cleavage of esterified lactam **79a** provides *N*-H lactam **80** in good yield.

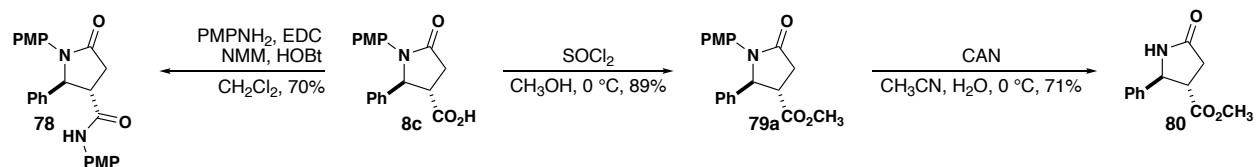


Figure 3.24 Derivatization of lactam **8c**.

3.2.5 Development of the Multicomponent Mukaiyama Castagnoli-Cushman Reaction

In hopes of expanding our reaction scope, we turned our attention to the synthesis of imines derived from aliphatic aldehydes. As discussed previously, the attempted synthesis of aliphatic aldehyde derived imines proved unsuccessful. To overcome this setback, we recognized that the Mukaiyama CCR was slow, necessitating 48-hour reaction times to afford good conversion. On the other hand, imine formation is typically quite fast. With that in mind, we began to screen the multicomponent assembly of γ -lactams by reaction of aldehydes, amines, and furan in the presence of desiccants. This allowed us to access the previously unobserved aliphatic aldehyde-derived lactams in fair to excellent yield as a single *trans* diastereomer (Figure 3.25). Additionally, the *N*-PMP lactam **79a** previously isolated in 74% was formed in the three-component reaction as a single diastereomer in 92% yield following esterification.

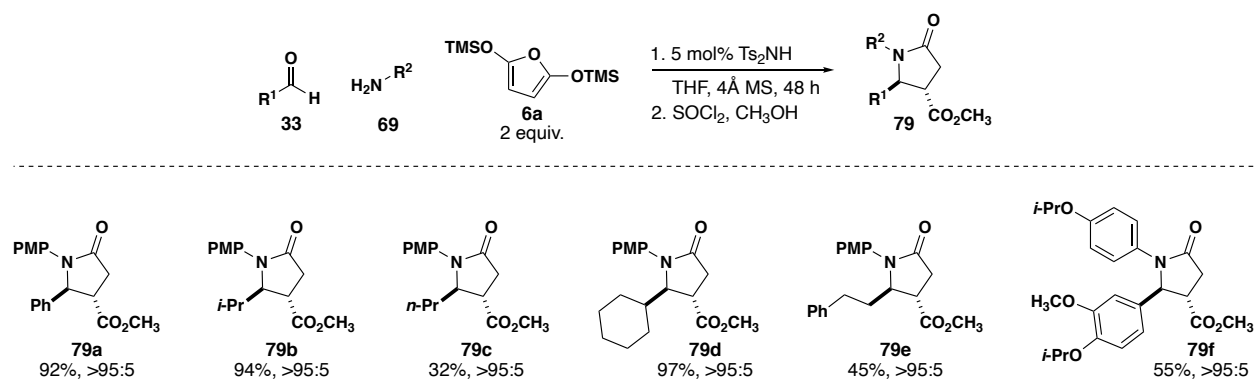


Figure 3.25 Scope of the multicomponent Mukaiyama Mannich CCR

3.2.6 Further Optimization of the Double Mukaiyama Castagnoli-Cushman Reaction

Next, we turned our attention to the scope of the double addition reaction. We hypothesize that these products (**4**) may be formed via two successive Mukaiyama Mannich reactions to afford intermediate **81**. Addition of ammonium chloride promotes protodesilylation followed by intramolecular acylation and amidation to yield **4**. We were pleased to observe only two of the six possible diastereomers in our reaction mixtures and were able to isolate two diastereomers by flash column chromatography (Figure 3.26). Based on the ^1H NMR of the unpurified reaction mixture, we determined that the reaction led to one symmetrical and one unsymmetrical diastereomer.

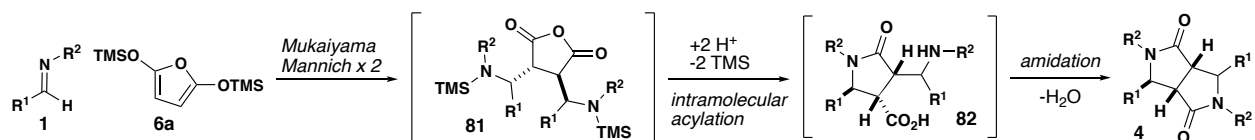
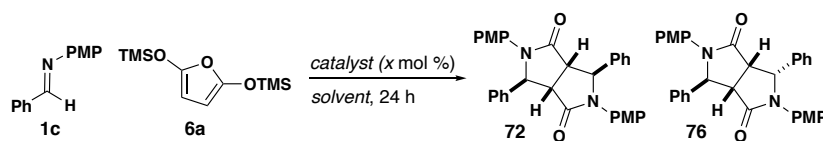


Figure 3.26 Proposed mechanism of the double Mukaiyama CCR

In an attempt to improve the diastereoselectivity and conversion of the bis- γ -lactam synthesis, a variety of different solvents, additives, and temperatures were screened in the reaction. Shuyu Meng and Dr. Laws performed a solvent screen and found that modifying the solvent exclusively led to decreased conversion (Table 3.2, entries 1-6). In order to determine if the acid was acting as a Brønsted acid activator or if trimethylsilyl triflate was forming *in situ* to act as a Lewis acid, a series of additives were also tested in the reaction. Addition of 2,6-DTBP, TMS triflate, pyridinium triflate, or DTBP triflate affected neither conversion nor diastereoselectivity, suggesting that Brønsted acid activation is not involved in the double addition reactions (Table 3.2, entries 7-11) These

reaction outcomes suggest that the catalytic activity of triflic acid in this reaction is the result of Lewis, not Brønsted, acid activity, similar to experimental observations in the Mukiyama aldol reaction. Though we imagined that triflic acid would react similarly to the disulfonimide catalysts, it became apparent that the Lewis acidity of TMS triflate must allow for two sequential Mannich additions (Table 3.2, entries 12-13). Finally, in an attempt to increase diastereoselectivity, the reaction temperature was lowered to $-20\text{ }^{\circ}\text{C}$ and $-78\text{ }^{\circ}\text{C}$ (Table .2, entries 14-15). These changes in temperature had minimal effect on diastereomer ratio and significantly lowered reaction conversion. Having completed our screens, we concluded that the stereochemical outcome of the reaction was unaffected by changes in reaction conditions, and we accepted the diastereoselectivity as a limitation to this method.

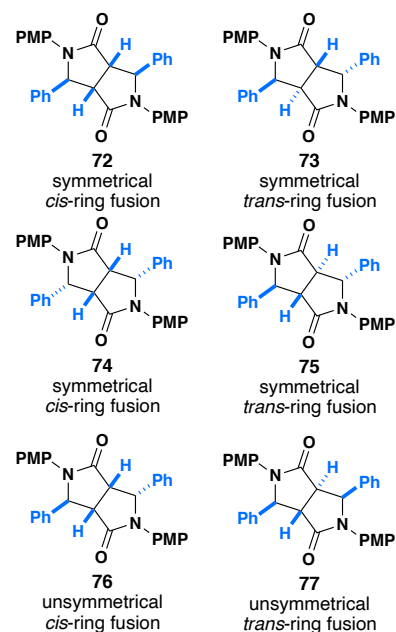
Table 3.2 Optimization of the Double Addition Reaction



entry	X mol %	catalyst	solvent	temp ($^{\circ}\text{C}$)	% conv. A ^a	% conv. B ^a
1	2 mol %	TfOH	THF	23	44	36
2	2 mol %	TfOH	Et ₂ O	23	14	31
3	2 mol %	TfOH	CH ₂ Cl ₂	23	31	38
4	2 mol %	TfOH	toluene	23	19	39
5	2 mol %	TfOH	<i>n</i> -hexane	23	<5	<5
6	2 mol %	TfOH	CH ₃ CN	23	38	24
7	20 mol %	TfOH	CH ₃ CN	23	41	40
8	20 mol %	TfOH, 2,6-(<i>t</i> -Bu) ₂ Py	CH ₃ CN	23	40	38
9	20 mol %	2,6-(<i>t</i> -Bu) ₂ Py·TfOH	CH ₃ CN	23	40	44
10	20 mol %	TMSOTf	CH ₃ CN	23	41	36
11	20 mol %	Py·TfOH	CH ₃ CN	23	41	44
12 ^b	20 mol %	TfOH	CH ₃ CN	23	40	48
13 ^b	20 mol %	TfOH	THF	23	35	58
14 ^b	20 mol %	TfOH	THF	-20	43	42
15 ^b	20 mol %	TfOH	THF	-78	28	18
16	20 mol %	Py·TfOH	THF	23	41	40
17 ^b	20 mol %	Py·TfOH	THF	23	39	26

^aAs determined by ¹H NMR spectroscopy of the unpurified reaction mixture

^bTwo equivalents of imine added.



3.2.7 Scope of the Double Mukaiyama Castagnoli-Cushman Reaction

After significant attempts at reaction optimization, Dr. Laws and I worked on the scope of the double addition reaction. Double addition reaction conditions were modified by utilizing two equivalents of imine, the addition of anhydrous sodium sulfate, as well as an increase in catalyst loading. With optimized conditions in hand, a small series of bis- γ -lactams were synthesized in modest yields and effectively 50:50:0:0:0 diastereoselectivity (Figure 3.27). Based on the ^1H NMR spectrum of the unpurified reaction mixture and the hypotheses of Chan and Brownbridge, we believed that the observed diastereomers were the symmetrical all-cis product (**72**) and the unsymmetrical product (**76**) (Table 3.2, right). X-ray crystallographic data confirmed the identity of the all-cis symmetrical diastereomer (**72**). However, the structure of the unsymmetrical diastereomer remained inconclusive, and as we were unable to grow suitable crystals to prove relative stereochemistry conclusively.

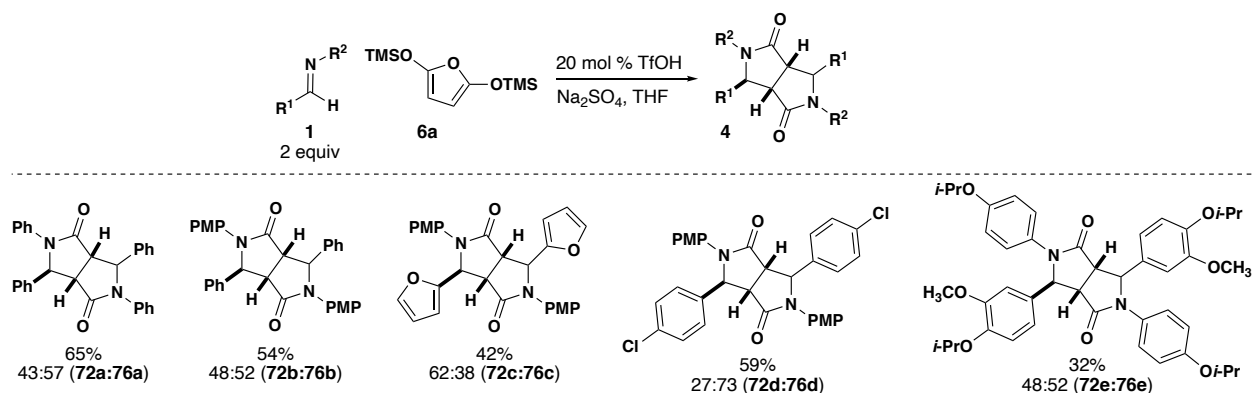


Figure 3.27 Scope of the double Mukaiyama Mannich CCR

3.2.8 Stereochemical Proof by Computational NMR

In order to determine the relative stereochemistry of the unsymmetrical diastereomer, we endeavored to calculate $J_{\text{H-H}}$ coupling values using computational

NMR. Although we were able to obtain a crystal structure that matched the stereochemistry of diastereomer **76**, this crystal structure was unsuitable for publication. As a result, with the help of Prof. Dean Tantillo, Dr. Carla Saunders, and Amy Bellinghiere, I used computational NMR to calculate the coupling constants of the two possible unsymmetrical diastereomers **76** and **77** to provide further evidence for the identity of the observed diastereomer.

Of the six diastereomers that could potentially form in the double addition reaction, only two were observed by ^1H NMR. One of these products clearly had no symmetry elements, indicating that it was one of the two possible unsymmetrical diastereomers. Computational ^1H NMR was then used to determine which of the two unsymmetrical diastereomers had formed. It seemed unlikely that a *trans* ring fusion would be present in the bis- γ -lactam, suggesting that the observed diastereomer was **76** (Figure 3.28). To assign the relative stereochemistry of the observed product, $J_{\text{H-H}}$ values between $\text{H}_1:\text{H}_2$, $\text{H}_2:\text{H}_3$, $\text{H}_3:\text{H}_4$ were computed and compared to the experimentally observed $J_{\text{H-H}}$ values

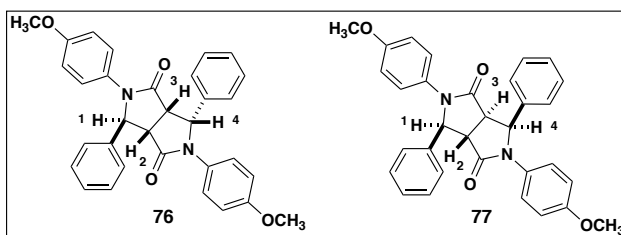


Figure 3.28 The $J_{\text{H-H}}$ coupling values of the two unsymmetrical diastereomers to be computed

The geometry of both diastereomers were optimized using Gaussian 16,⁴⁸ at the B3LYP/6-31G(d) level of theory in the gas phase. Then, two sets of GIAO NMR calculations were performed. First, the GIAO NMR calculation was performed at the B3LYP/6-31g(d,p) level of theory, following a literature procedure.⁴⁹ The final coupling

constants were determined by extracting the Fermi constant contribution to J_{H-H} (Hz) and scaling them by 0.9117 to produce coupling constants for each diastereomer (Table 3.3 and Table 3.4). As expected, the computed J_{H-H} values for **76** matched the experimental values much more consistently than diastereomer **77**.

Table 3.3 Computed J_{H-H} values for diastereomer **76** from calculation 1.

Diastereomer 76	Fermi Constant	Scaled (Hz)	Experimental J_{H-H} (Hz)	Deviation (Hz)
H1-H2	10.45	9.53	8.82	0.71
H2-H3	11.7	10.68	9.75	0.93
H3-H4	7.37	6.72	2.92	3.80

Table 3.4 Computed J_{H-H} values for diastereomer **77** from calculation 1.

Diastereomer 77	Fermi Constant	Scaled (Hz)	Experimental J (Hz)	Deviation (Hz)
H1-H2	6.36	5.80	8.82	3.02
H2-H3	17.62	16.06	9.75	6.31
H3-H4	10.36	9.45	2.92	6.53

Additionally, a second GIAO NMR calculation was run using B3LYP/631G (d,p) following the instructions on the cheshiremr.info website.^{37, 39, 50-52} The final coupling constants were determined by extracting the proton-proton Fermi constant contribution to the J_{H-H} (Hz) and scaling them by 0.9155 to produce coupling constants (Table 3.5 and Table 3.6). These results also support our hypothesis that **76** is in fact our observed diastereomer. In addition to the J_{H-H} coupling values, the computed energy of diastereomer **76** was lower than that of diastereomer **77**, further confirming the identity of the observed diastereomer.

Table 3.5 Computed J_{H-H} values for diastereomer **76** from calculation 2.

Diastereomer 76	Fermi Constant	Scaled (Hz)	Experimental J (Hz)	Deviation (Hz)
H1-H2	8.79	8.05	8.82	0.77
H2-H3	10.07	9.22	9.75	0.53
H3-H4	6.10	5.59	2.92	2.67

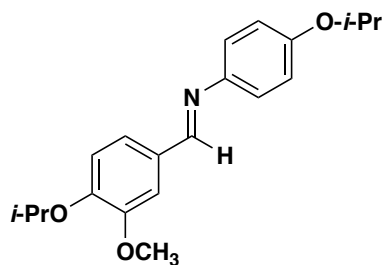
Table 3.6 Computed J_{H-H} values for diastereomer **77** from calculation 2.

Diastereomer 77	Fermi Constant	Scaled (Hz)	Experimental J_{H-H} (Hz)	Deviation (Hz)
H1-H2	5.39	4.94	8.82	3.88
H2-H3	15.09	13.81	9.75	4.06
H3-H4	8.61	7.88	2.92	4.96

3.3 Conclusion

In summary, an acid catalyzed Mukaiyama-CCR reaction has been developed. A series of γ -lactam products were synthesized in high yields and diastereoselectivity, allowing for the first synthesis of *N*-alkyl lactams in this type of reaction. Additionally, multicomponent assembly of aliphatic aldehyde derived lactam products allow access to previously elusive products. Finally, subtle changes in reaction stoichiometry as well as varying the catalyst had a significant impact on reaction outcomes, allowing for the selective synthesis of either mono- or bis- γ -lactams.

3.4 Experimental Section



(E)-1-(4-Isopropoxy-3-methoxyphenyl)-N-(4-isopropoxyphenyl)methanimine (1o).

Imine **2c** was synthesized by condensation of 4-isopropoxy-3-methoxybenzaldehyde (15.0 mmol) and 4-isopropoxyaniline (15.0 mmol) in EtOH (30 mL). After stirring at room temperature overnight, the reaction mixture was filtered, and solvent was removed *in vacuo* to yield the corresponding imine **1o** as a brown solid in 87% yield (3.36 g, 10 mmol). mp 112-113 °C. ¹H NMR (600 MHz, CDCl₃) δ 8.37 (s, 1H), 7.59 (d, *J* = 1.8 Hz, 1H), 7.30 – 7.23 (m, 1H), 7.21 – 7.16 (m, 2H), 6.96 – 6.85 (m, 3H), 4.63 (hept, *J* = 6.1 Hz, 1H), 4.54 (hept, *J* = 12.1, 6.0 Hz, 1H), 3.95 (s, 3H), 1.41 (d, *J* = 6.1 Hz, 6H), 1.35 (d, *J* = 6.1 Hz, 6H). ¹³C NMR (150 MHz, CDCl₃) δ 158.0, 156.2, 150.4, 150.1, 145.1, 129.7, 123.8, 122.1, 116.4, 113.9, 109.4, 71.2, 70.2, 56.0, 22.1, 22.0. IR 2972.8, 2923.2, 1596.6, 1572.0, 1466.8 cm⁻¹; AMM (ESI-TOF) *m/z* calcd for C₂₀H₂₆NO₃⁺ [M+H]⁺ 328.1907, found 328.1907.

General procedure A for the synthesis of lactam carboxylic acids:

Imine (1.0 equiv.) and NHTs₂ catalyst (0.05 equiv.) were placed in a flame-dried vial under argon atmosphere and a 0.4 M THF solution of 2,5-bis(trimethylsilyloxy)furan (2.0 equiv.) was added. The reaction mixture was allowed to stir at room temperature for 48 h, then 1.00 mL of sat. NH₄Cl aq. solution was added and the reaction mixture was stirred at

room temperature for 1 h. The biphasic mixture was extracted three times with EtOAc, the combined organic layers were dried over Na₂SO₄, and solvent was evaporated *in vacuo*.

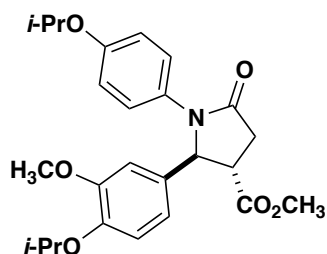
General procedure B for the synthesis of lactam methyl esters:

Imine (1.0 equiv.) and NHTs₂ catalyst (0.05 equiv.) were placed in a flame-dried vial under argon atmosphere and a 0.4 M THF solution of 2,5-bis(trimethylsilyloxy)furan (2.0 equiv.) was added. The reaction mixture was allowed to stir at room temperature for 48 h, then 1.00 mL of sat. NH₄Cl aq. solution was added and the reaction mixture was stirred at room temperature for 1 h. The biphasic mixture was extracted three times with EtOAc, the combined organic layers were dried over Na₂SO₄, and solvent was evaporated *in vacuo*. The unpurified reaction mixture was dissolved in CH₃OH (0.2 M), cooled to 0 °C and thionyl chloride (1.1 equiv.) was added dropwise. Reaction mixture was allowed to reach room temperature and stirred overnight. Solvent was removed *in vacuo* and the resulting concentrate was diluted in CH₂Cl₂ and water. The aqueous phase was extracted with CH₂Cl₂ (2 x 10 mL), and the combined organic layers were dried over Na₂SO₄, filtered, and concentrated *in vacuo*.

General procedure C for the synthesis of lactam methyl esters:

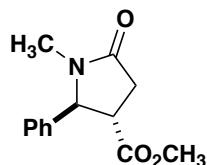
p-Anisidine (1 equiv.), 4 Å mol sieves (2 equiv.), NHTs₂ catalyst (0.05 equiv.) were placed in a flame-dried vial under argon atmosphere, then a 0.4 M THF solution of 2,5-bis(trimethylsilyloxy)furan (2 equiv.) was added. Benzaldehyde (1 equiv.) was then added, and reaction mixture was allowed to stir at room temperature for 48 h. Then, 1.00

mL of sat. NH_4Cl aq. solution was added, and the reaction mixture was stirred at room temperature for 1 h. The biphasic mixture was extracted three times with EtOAc, and the combined organic layers were dried over Na_2SO_4 , filtered, and concentrated *in vacuo*. The unpurified reaction mixture was dissolved in CH_3OH (3 mL), cooled to 0°C and thionyl chloride (1.1 equiv.) was added in a dropwise manner. The reaction mixture was allowed to reach room temperature and stirred overnight. Solvent was removed *in vacuo*, and the concentrated was diluted in CH_2Cl_2 and water. The aqueous phase was extracted three times with CH_2Cl_2 , then twice with EtOAc and the combined organic layers were dried over Na_2SO_4 , filtered, and concentrated *in vacuo*.

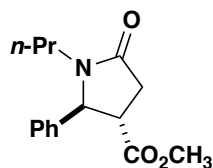


Methyl *trans*-2-(4-isopropoxy-3-methoxyphenyl)-1-(4-isopropoxyphenyl)-5-oxopyrrolidine-3-carboxylate (8o). Prepared according to general procedure B. The unpurified reaction mixture was purified by flash column chromatography (40-100% EtOAc/hexanes) to afford lactam **8o** (111.0 mg, 63%), a single diastereomer, as a yellow oil: ^1H NMR (400 MHz, CDCl_3) δ 7.24 – 7.18 (m, 2H), 6.81 – 6.72 (m, 4H), 6.69 (s, 1H), 5.36 (d, $J = 5.0$ Hz, 1H), 4.55 – 4.37 (m, 2H), 3.77 (t, $J = 1.5$ Hz, 6H), 3.19 – 3.10 (m, 1H), 3.06 – 2.85 (m, 2H), 1.33 (d, $J = 6.1$ Hz, 6H), 1.27 (d, $J = 6.1$ Hz, 6H); ^{13}C NMR (100 MHz, CDCl_3) δ 172.9, 171.9, 155.6, 150.6, 147.2, 132.2, 130.2, 124.8, 118.8, 115.9,

115.2, 109.8, 71.2, 70.0, 66.1, 56.0, 52.6, 46.4, 34.4, 22.1, 22.0; AMM (ESI-TOF) m/z calcd for $C_{25}H_{32}NO_6^+$ $[M+H]^+$: 442.2224, found: 442.2239.

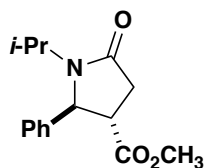


Methyl *trans*-1-methyl-5-oxo-2-phenylpyrrolidine-3-carboxylate (8p). Prepared according to general procedure B. The unpurified reaction mixture was purified by flash column chromatography (30-100% EtOAc/hexanes) to afford lactam **8p** (47.0 mg, 50%), a single diastereomer, as a yellow oil: 1H NMR (400 MHz, $CDCl_3$) δ 7.48 – 7.32 (m, 3H), 7.29 – 7.19 (m, 2H), 4.79 (d, $J = 5.8$ Hz, 1H), 3.73 (s, 3H), 3.06 (ddd, $J = 9.8, 7.7, 5.8$ Hz, 1H), 2.95 – 2.73 (m, 2H), 2.68 (s, 3H); ^{13}C NMR (100 MHz, $CDCl_3$) δ 172.9, 172.8, 139.4, 129.3, 128.7, 126.7, 66.5, 52.6, 46.2, 33.8, 28.4; AMM (ESI-TOF) m/z calcd for $C_{13}H_{16}NO_3^+$ $[M+H]^+$: 234.1125, found: 234.1131.

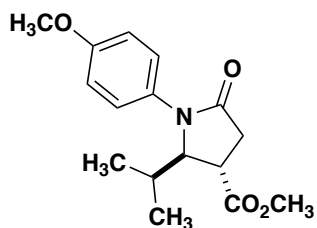


Methyl *trans*-5-oxo-2-phenyl-1-propylpyrrolidine-3-carboxylate (8q). Prepared according to general procedure B. The unpurified reaction mixture was purified by flash column chromatography (30-100% EtOAc/hexanes) to afford lactam **8q** (75.0 mg, 75%), a single diastereomer, as a yellow oil: 1H NMR (400 MHz, $CDCl_3$) δ 7.47 – 7.30 (m, 3H), 7.23 (d, $J = 7.3$ Hz, 2H), 4.90 (d, $J = 5.4$ Hz, 1H), 3.73 (d, $J = 1.5$ Hz, 2H), 3.72 – 3.58 (m,

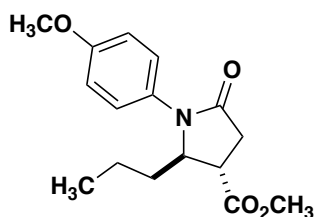
2H), 3.05 (ddd, $J = 14.0, 7.8, 3.9$ Hz, 1H), 2.93 – 2.72 (m, 2H), 2.64 – 2.48 (m, 1H), 1.52 – 1.38 (m, 2H), 0.82 (t, $J = 7.3$ Hz, 3H); ^{13}C NMR (100 MHz, CDCl_3) δ 173.0, 172.6, 139.4, 129.1, 128.5, 126.7, 64.1, 52.5, 46.1, 42.4, 33.7, 20.0, 11.2; AMM (ESI-TOF) m/z calcd for $\text{C}_{15}\text{H}_{20}\text{NO}_3^+$ $[\text{M}+\text{H}]^+$: 262.1438, found: 262.1444.



Methyl *trans*-1-isopropyl-5-oxo-2-phenylpyrrolidine-3-carboxylate (8r). Prepared according to general procedure B. The unpurified reaction mixture was purified by flash column chromatography (30-100% EtOAc/hexanes) to afford lactam **8r** (54.1 mg, 58%), a single diastereomer, as a yellow oil: ^1H NMR (400 MHz, CDCl_3) δ 7.42 – 7.30 (m, 3H), 7.29 (d, $J = 6.8$ Hz, 2H), 4.96 (d, $J = 3.8$ Hz, 1H), 4.06 (hept, $J = 7.1$ Hz, 1H), 3.73 (s, 3H), 3.04 – 2.83 (m, 2H), 2.79 – 2.62 (m, 1H), 1.23 (d, $J = 6.9$ Hz, 3H), 0.91 (d, $J = 6.9$ Hz, 3H); ^{13}C NMR (100 MHz, CDCl_3) δ 173.1, 172.8, 141.7, 129.0, 128.4, 126.5, 63.2, 52.5, 46.6, 45.3, 33.8, 20.6, 19.8; AMM (ESI-TOF) m/z calcd for $\text{C}_{15}\text{H}_{20}\text{NO}_3^+$ $[\text{M}+\text{H}]^+$: 262.1438, found: 262.1444.

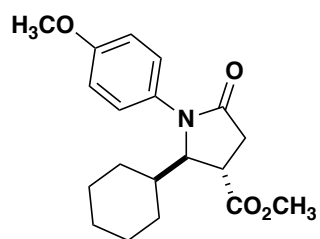


Methyl *trans*-2-isopropyl-1-(4-methoxyphenyl)-5-oxopyrrolidine-3-carboxylate (79b). Prepared according to general procedure C. The unpurified reaction mixture was purified by flash column chromatography (50-60% EtOAc/hexanes) to afford lactam **79b** (109.0 mg, 94%), a single diastereomer, as a yellow oil: ^1H NMR (400 MHz, CDCl_3) δ 7.26 (d, $J = 7.4$ Hz, 2H), 6.92 (d, $J = 7.5$ Hz, 2H), 4.37 (t, $J = 3.8$ Hz, 1H), 3.80 (s, 3H), 3.79 (s, 3H), 3.00 (td, $J = 7.7, 3.8$ Hz, 1H), 2.87 – 2.81 (m, 2H), 2.02 (qd, $J = 6.5, 3.1$ Hz, 1H), 0.91 (d, $J = 7.0$ Hz, 3H), 0.80 (d, $J = 6.8$ Hz, 3H); ^{13}C NMR (100 MHz, CDCl_3) δ 174.3, 171.8, 158.0, 129.9, 126.4, 114.5, 67.6, 55.5, 52.6, 36.2, 35.0, 28.7, 18.1, 14.8; AMM (ESI-TOF) m/z calcd for $\text{C}_{16}\text{H}_{22}\text{NO}_4^+$ $[\text{M}+\text{H}]^+$: 292.1543, found: 292.1552.

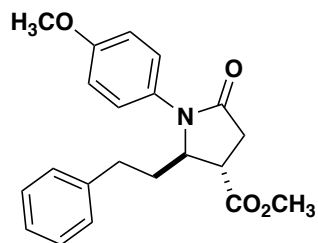


Methyl *trans*-1-(4-methoxyphenyl)-5-oxo-2-propylpyrrolidine-3-carboxylate (79c). Prepared according to general procedure C. The unpurified reaction mixture was purified by flash column chromatography (50-60% EtOAc/hexanes) to afford lactam **79c** (38.0 mg, 32%), a single diastereomer, as a yellow oil: ^1H NMR (600 MHz, CD_3CN) δ 7.25 (d, $J = 9.0$ Hz, 2H), 6.94 (d, $J = 9.0$ Hz, 2H), 4.31 (dt, $J = 7.9, 3.7$ Hz, 1H), 3.78 (s, 3H), 3.72 (s, 3H), 3.07 – 3.01 (m, 1H), 2.81 – 2.74 (m, 1H), 2.68 – 2.61 (m, 1H), 1.60 – 1.52 (m, 1H),

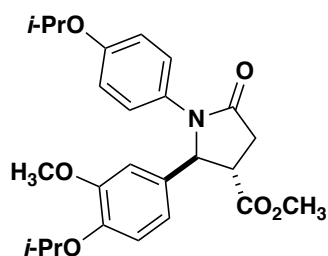
1.46 (dddd, $J = 13.5, 10.3, 8.3, 5.1$ Hz, 1H), 1.30 – 1.23 (m, 2H), 0.82 (t, $J = 7.3$ Hz, 3H); ^{13}C NMR (100 MHz, CDCl_3) δ 173.8, 171.7, 158.1, 130.0, 126.5, 114.6, 62.7, 55.6, 52.7, 41.7, 35.4, 34.7, 17.7, 14.0; AMM (ESI-TOF) m/z calcd for $\text{C}_{16}\text{H}_{22}\text{NO}_4^+$ $[\text{M}+\text{H}]^+$: 292.1543, found: 292.1552.



Methyl *trans*-2-cyclohexyl-1-(4-methoxyphenyl)-5-oxopyrrolidine-3-carboxylate (79d). Prepared according to general procedure C. The unpurified reaction mixture was purified by flash column chromatography (50-60% EtOAc/hexanes) to afford lactam **79d** (128.0 mg, 97%), a single diastereomer, as a yellow oil: ^1H NMR (400 MHz, CDCl_3) δ 7.25 (d, $J = 8.6$ Hz, 2H), 6.92 (d, $J = 8.8$ Hz, 2H), 4.32 (d, $J = 3.5$ Hz, 1H), 3.81 (d, $J = 1.4$ Hz, 3H), 3.78 (d, $J = 1.4$ Hz, 3H), 3.05 (td, $J = 7.6, 3.3$ Hz, 1H), 2.85 – 2.74 (m, 2H), 1.78 – 1.46 (m, 6H), 1.21 – 0.97 (m, 4H), 1.00 – 0.79 (m, 1H); ^{13}C NMR (100 MHz, CDCl_3) δ 174.4, 172.0, 158.1, 130.1, 126.5, 114.6, 67.6, 55.6, 52.7, 39.4, 37.5, 35.1, 29.0, 26.5, 26.2, 25.8, 25.8; AMM (ESI-TOF) m/z calcd for $\text{C}_{19}\text{H}_{26}\text{NO}_4^+$ $[\text{M}+\text{H}]^+$: 332.1856, found: 332.1869.

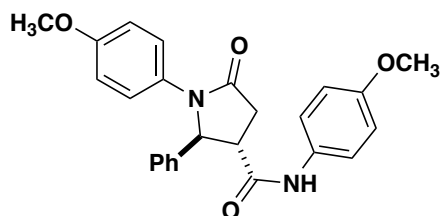


Methyl *trans*-1-(4-methoxyphenyl)-5-oxo-2-phenethylpyrrolidine-3-carboxylate (79e). Prepared according to general procedure C. The unpurified reaction mixture was purified by flash column chromatography (50-60% EtOAc/hexanes) to afford lactam **79e** (63.0 mg, 45%), a single diastereomer, as a yellow oil: $^1\text{H NMR}$ (400 MHz, CDCl_3) δ 7.25 – 7.15 (m, 5H), 7.03 (d, $J = 7.4$ Hz, 2H), 6.90 (d, $J = 8.3$ Hz, 2H), 4.41 (p, $J = 3.6$ Hz, 1H), 3.79 (d, $J = 3.1$ Hz, 6H), 3.12 – 3.03 (m, 1H), 2.91 – 2.83 (m, 2H), 2.67 – 2.47 (m, 2H), 2.09 – 1.95 (m, 1H), 1.81 (ddd, $J = 15.2, 9.9, 6.0$ Hz, 1H); $^{13}\text{C NMR}$ (150 MHz, CDCl_3) δ 173.6, 171.6, 158.1, 140.5, 129.7, 128.6, 128.3, 127.8, 126.3, 114.5, 62.1, 55.5, 52.7, 41.5, 34.7, 34.5, 30.6.; AMM (ESI-TOF) m/z calcd for $\text{C}_{21}\text{H}_{24}\text{NO}_4^+$ $[\text{M}+\text{H}]^+$: 354.1700, found: 354.1712.



Methyl *trans*-2-(4-isopropoxy-3-methoxyphenyl)-1-(4-isopropoxyphenyl)-5-oxopyrrolidine-3-carboxylate (79f). Prepared according to general procedure C. The unpurified reaction mixture was purified by flash column chromatography (40-100% EtOAc/hexanes) to afford lactam **79f** (97.0 mg, 55%), a single diastereomer, as a yellow

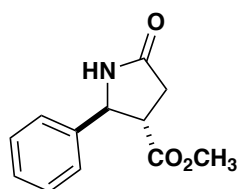
oil: ^1H NMR (400 MHz, CDCl_3) δ 7.24 – 7.18 (m, 2H), 6.81 – 6.72 (m, 4H), 6.69 (s, 1H), 5.36 (d, $J = 5.0$ Hz, 1H), 4.55 – 4.37 (m, 2H), 3.19 – 3.10 (m, 1H), 3.06 – 2.85 (m, 2H), 1.33 (d, $J = 6.1$ Hz, 6H), 1.27 (d, $J = 6.1$ Hz, 6H). ^{13}C NMR (100 MHz, CDCl_3) δ 172.9, 171.9, 155.6, 150.6, 147.2, 132.2, 130.2, 124.8, 118.8, 115.9, 115.2, 109.8, 71.2, 70.0, 66.1, 56.0, 52.6, 46.4, 34.4, 22.1, 22.0. AMM (ESI-TOF) m/z calcd for $\text{C}_{25}\text{H}_{32}\text{NO}_6^+$ $[\text{M}+\text{H}]^+$: 442.2224, found: 442.2239.



***trans*-N,1-Bis(4-methoxyphenyl)-5-oxo-2-phenylpyrrolidine-3-carboxamide (78).**

Lactam **10** was prepared according to modified literature procedure.⁵³ To a flame-dried flask under argon atmosphere at 0 °C was added acid **5c** (124.0 mg, 0.40 mmol) in CH_2Cl_2 (1 mL). HOBt (66.0 mg, 1.2 mmol), *p*-anisidine (148.0 mg, 1.2 mmol), *N*-methylmorpholine (0.017 mL, 1.6 mmol), and EDC (84.0 mg, 0.44 mmol) were added in succession. The reaction mixture was stirred at 0 °C for 2 h, then warmed to room temperature and stirred for 16 h. The reaction mixture was diluted with EtOAc, then washed with 3 x 20 mL of 1.2 N HCl, 3 x 20 mL of sat. NaHCO_3 , and 30 mL of brine. The combined organic layers were dried over Na_2SO_4 , filtered, and concentrated *in vacuo*. The unpurified reaction mixture residue was purified by flash chromatography (60-100% EtOAc/Hexanes) to afford lactam **10** (116.0 mg, 70%), a single, diastereomer, as a yellow oil. ^1H NMR (600 MHz, CDCl_3) δ 7.36 – 7.29 (m, 5H), 7.26 – 7.23 (m, 2H), 7.22 – 7.16 (m, 2H), 6.93 (s, 1H), 6.86 (dd, $J =$

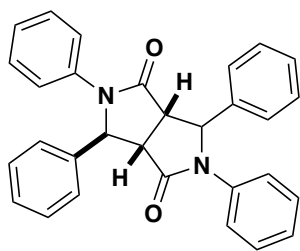
7.4, 4.8 Hz, 2H), 6.80 – 6.74 (m, 2H), 5.41 (d, $J = 7.3$ Hz, 1H), 3.79 (d, $J = 2.5$ Hz, 3H), 3.71 (s, 3H), 3.18 (dd, $J = 16.7, 9.0$ Hz, 1H), 3.06 – 2.98 (m, 1H), 2.95 (dd, $J = 16.7, 9.1$ Hz, 1H).; ^{13}C NMR (100 MHz, CDCl_3) δ 172.4, 168.8, 157.3, 156.9, 139.7, 130.2, 130.1, 129.2, 128.5, 126.8, 125.2, 121.9, 114.2, 114.1, 67.0, 55.5, 55.3, 50.1, 35.1.; AMM (ESI-TOF) m/z calcd for $\text{C}_{25}\text{H}_{25}\text{N}_2\text{O}_4^+$ $[\text{M}+\text{H}]^+$: 417.1809, found: 417.1827.



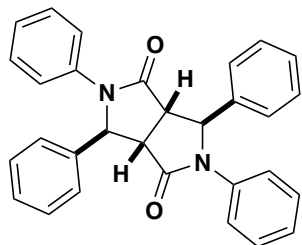
Methyl *trans*-5-oxo-2-phenylpyrrolidine-3-carboxylate (80). To a solution of methylated lactam **8a** (28.9 mg, 0.089 mmol) in $\text{CH}_3\text{CN}/\text{H}_2\text{O}$ (5:1, 3 mL) at 0 °C was added cerium ammonium nitrate (214.0 mg, 0.39 mmol) under argon atmosphere and the reaction was allowed to reach room temperature and stirred for 1 h. Reaction mixture was diluted in EtOAc and washed with NaHCO_3 , then with 1 M HCl, and extracted with EtOAc (3 x 10 mL). The combined organic layers were washed with brine, dried over Na_2SO_4 , and concentrated under vacuum. The unpurified reaction mixture was purified by flash column chromatography (50:50 EtOAc/hexanes + 0.25% AcOH) to yield lactam **9** (13.8 mg, 71%), a single diastereomer, as an amorphous yellow solid; ^1H NMR (400 MHz, CDCl_3) δ 7.43 – 7.31 (m, 5H), 6.24 (s, 1H), 5.00 (d, $J = 6.6$ Hz, 1H), 3.73 (s, 3H), 3.14 (td, $J = 9.1, 6.6$ Hz, 1H), 2.74 (d, $J = 9.1$ Hz, 2H); ^{13}C NMR (100 MHz, CDCl_3) δ 175.4, 172.6, 140.8, 129.2, 128.6, 126.1, 60.3, 52.6, 49.0, 33.8.; IR 3226, 2924, 1734, 1700 cm^{-1} ; AMM (ESI-TOF) m/z calcd for $\text{C}_{12}\text{H}_{14}\text{NO}_3^+$ $[\text{M}+\text{H}]^+$: 220.0968, found: 220.0959.

General procedure D for the synthesis of bis-lactams

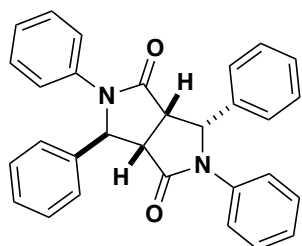
To a flame-dried vial under argon atmosphere was added imine (2.0 equiv.), Na₂SO₄, and a 0.4 M solution of 2,5-bis(trimethylsilyloxy)furan in THF (1.0 equiv.), followed by TfOH (0.2 equiv.). The reaction mixture was allowed to stir at room temperature for 24 h, then 1.00 mL of sat. NH₄Cl aq. solution was added, and the reaction mixture was stirred at room temperature for 1 h. The biphasic mixture was extracted three times with EtOAc, and the combined organic layers were washed with H₂O, then brine. The combined organics were dried over Na₂SO₄, filtered, and concentrated *in vacuo*. Due to the large number of aromatic carbon signals in the ¹³C NMR spectra of lactams **76**, some carbon signals were unresolved in spectra obtained with 400 and 600 MHz NMR spectrometer. As a representative example demonstrating the correct number of carbons, the ¹³C NMR spectrum of lactam **76c** was taken in CD₃CN on an 800 MHz spectrometer.



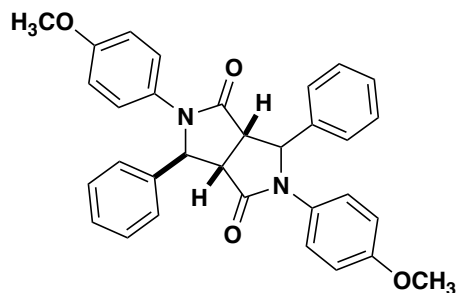
2,3,5,6-Tetraphenylhexahydropyrrolo[3,4-c]pyrrole-1,4-dione (72a, 76a). Prepared according to general procedure D. The unpurified reaction mixture was purified by recrystallization from EtOAc/hexanes and flash column chromatography (20-40% EtOAc/hexanes) to afford lactam **13b** and **14b** (115.1 mg, 65%), a 43:57 mixture of diastereomers, as an off-white solid.



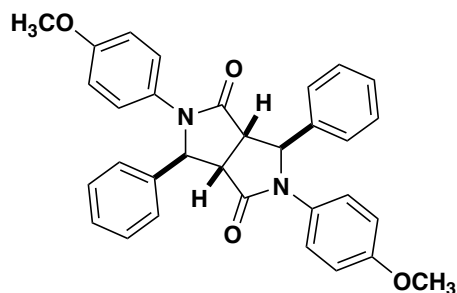
72a: mp 215-217 °C; ^1H NMR (400 MHz, CDCl_3) δ 7.57 (d, $J = 8.1$ Hz, 4H), 7.31 (dq, $J = 14.4, 7.5$ Hz, 14H), 7.17 – 7.07 (m, 2H), 5.75 (s, 2H), 3.38 (s, 2H); ^{13}C NMR (100 MHz, CDCl_3) δ 172.3, 139.6, 137.6, 129.3, 129.0, 128.3, 125.6, 125.6, 121.9, 65.1, 49.1; AMM (ESI-TOF) m/z calcd for $\text{C}_{30}\text{H}_{25}\text{N}_2\text{O}_2^+$ $[\text{M}+\text{H}]^+$: 445.1911, found: 445.1921.



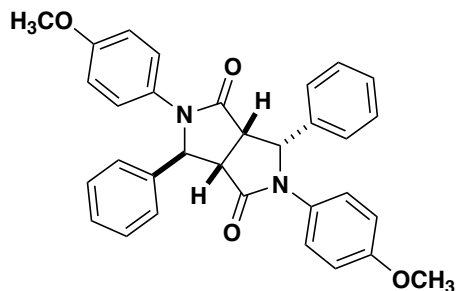
76a: mp 306-311 °C; ^1H NMR (400 MHz, CDCl_3) δ 7.41 (d, $J = 8.1$ Hz, 3H), 7.37 – 7.28 (m, 5H), 7.26 – 7.14 (m, 10H), 7.13 – 6.98 (m, 2H), 5.74 (d, $J = 8.8$ Hz, 1H), 5.68 – 5.60 (m, 1H), 3.99 – 3.85 (m, 1H), 3.41 (d, $J = 9.6$ Hz, 1H); ^{13}C NMR (100 MHz, CDCl_3) δ 172.7, 170.0, 140.8, 137.5, 137.2, 135.6, 129.3, 128.7, 128.4, 128.2, 127.5, 125.8, 125.7, 125.3, 122.9, 122.2, 64.9, 50.0, 44.7, 29.7; IR 3030.8, 2133.8, 1996.6, 1962.4, 1687.04 cm^{-1} ; AMM (ESI-TOF) m/z calcd for $\text{C}_{30}\text{H}_{25}\text{N}_2\text{O}_2^+$ $[\text{M}+\text{H}]^+$: 445.1911, found: 445.1922.



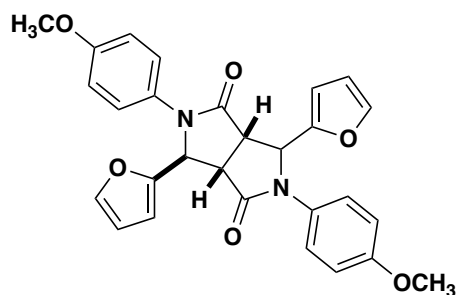
2,5-bis(4-Methoxyphenyl)-3,6-diphenylhexahydropyrrolo[3,4-c]pyrrole-1,4-dione (72b, 76b). Prepared according to general procedure D. The unpurified reaction mixture was purified by flash column chromatography (30-100% EtOAc/hexanes) to afford lactam **13a** and **14a** (110.0 mg, 54%), a 48:52 mixture of diastereomers, as an off-white solid.



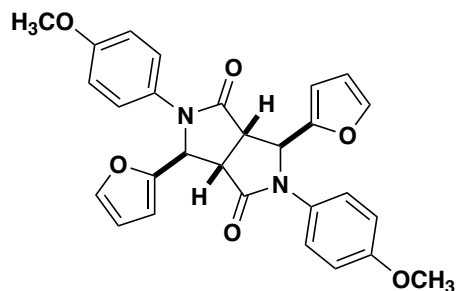
72b: mp 240-252 °C ^1H NMR (800 MHz, CDCl_3) δ 7.45 – 7.40 (m, 4H), 7.34 – 7.31 (m, 5H), 7.31 – 7.27 (m, 5H), 6.83 – 6.79 (m, 4H), 5.68 – 5.64 (m, 2H), 3.74 (s, 6H), 3.38 – 3.36 (m, 2H); ^{13}C NMR (150 MHz, CDCl_3) δ 172.1, 157.3, 139.7, 130.5, 129.3, 128.3, 125.7, 123.9, 114.1, 65.6, 55.4, 48.9.; AMM (ESI-TOF) m/z calcd for $\text{C}_{32}\text{H}_{29}\text{N}_2\text{O}_4^+$ $[\text{M}+\text{H}]^+$: 505.2122, found: 505.2138.



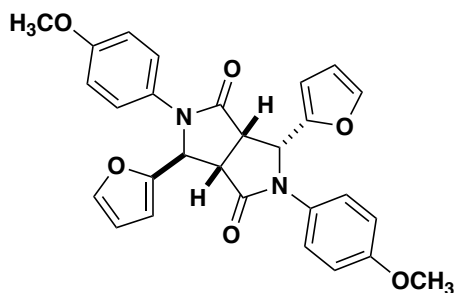
76b: mp 185-190 °C; ^1H NMR (400 MHz, CDCl_3) δ 7.36 – 7.27 (m, 7H), 7.23 (d, $J = 6.6$ Hz, 5H), 7.07 (d, $J = 8.6$ Hz, 2H), 6.78 (d, $J = 8.5$ Hz, 2H), 6.72 – 6.63 (m, 2H), 5.66 (d, $J = 8.8$ Hz, 1H), 5.53 (d, $J = 2.8$ Hz, 1H), 3.90 (s, 1H), 3.72 (s, 3H), 3.69 (s, 3H), 3.41 (dd, $J = 9.7, 2.7$ Hz, 1H); ^{13}C NMR (100 MHz, CDCl_3) δ 172.8, 170.1, 157.3, 157.2, 141.0, 135.9, 130.6, 130.4, 129.4, 128.5, 128.4, 127.7, 126.3, 124.6, 124.4, 114.1, 114.1, 65.8, 65.4, 55.5, 55.4, 50.0, 44.9.; AMM (ESI-TOF) m/z calcd for $\text{C}_{32}\text{H}_{29}\text{N}_2\text{O}_4^+$ $[\text{M}+\text{H}]^+$: 505.2122, found: 505.2141.



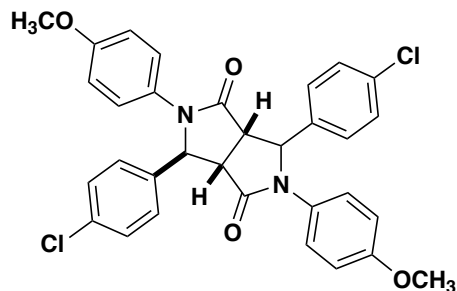
3,6-Di(furan-2-yl)-2,5-bis(4-methoxyphenyl)hexahydropyrrolo[3,4-c]pyrrole-1,4-dione (72c, 76c). Prepared according to general procedure D. The unpurified reaction mixture was purified by recrystallization from EtOAc/hexanes and flash column chromatography (30-90% EtOAc/hexanes) to afford lactam **13c** and **14c** (108.5 mg, 42%), a 62:38 mixture of diastereomers, as an off-white solid.



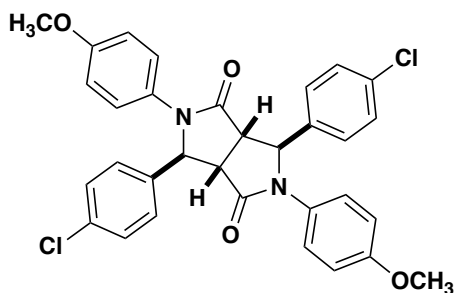
72c: mp 166-173 °C. ^1H NMR (400 MHz, CDCl_3) δ 7.37 (s, 2H), 7.21 (d, $J = 8.4$ Hz, 4H), 6.83 (d, $J = 8.4$ Hz, 4H), 6.31 – 6.20 (m, 4H), 5.53 (s, 2H), 3.75 (s, 6H), 3.72 (s, 2H); ^{13}C NMR (150 MHz, CDCl_3) δ 172.1, 158.2, 151.7, 143.1, 129.9, 125.7, 114.4, 110.6, 108.9, 60.1, 55.5, 46.6; IR 3116.0, 2948.6, 2838.62, 1679.0, 1609.5 cm^{-1} ; AMM (ESI-TOF) m/z calcd for $\text{C}_{28}\text{H}_{25}\text{N}_2\text{O}_6^+$ $[\text{M}+\text{H}]^+$: 485.1707, found: 485.1721.



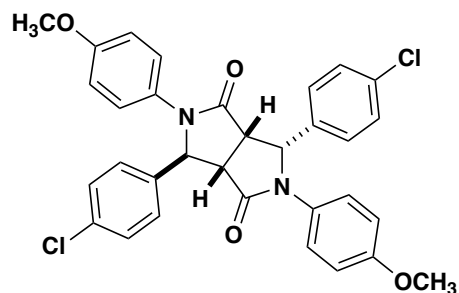
76c: mp 140-145 °C. ^1H NMR (800 MHz, CD_3CN) δ 7.51 – 7.47 (m, 1H), 7.41 – 7.36 (m, 1H), 7.22 (d, $J = 8.6$ Hz, 2H), 7.05 (d, $J = 8.5$ Hz, 2H), 6.87 (d, $J = 8.6$ Hz, 2H), 6.83 (d, $J = 8.6$ Hz, 2H), 6.39 – 6.33 (m, 2H), 6.30 (d, $J = 3.3$ Hz, 1H), 6.24 – 6.21 (m, 1H), 5.67 (d, $J = 9.7$ Hz, 1H), 5.55 (d, $J = 5.0$ Hz, 1H), 3.97 – 3.92 (m, 1H), 3.74 (s, 3H), 3.73 (s, 3H), 3.62 (dd, $J = 10.5, 5.0$ Hz, 1H); ^{13}C NMR (200 MHz, CD_3CN) δ 172.0, 170.2, 158.1, 158.1, 151.9, 149.8, 143.4, 142.9, 130.2, 130.1, 126.5, 126.4, 113.9, 113.9, 110.6, 110.5, 110.5, 109.7, 59.7, 59.1, 55.1, 55.1, 45.9, 43.2; AMM (ESI-TOF) m/z calcd for $\text{C}_{28}\text{H}_{25}\text{N}_2\text{O}_6^+$ $[\text{M}+\text{H}]^+$: 485.1707, found: 485.1725.



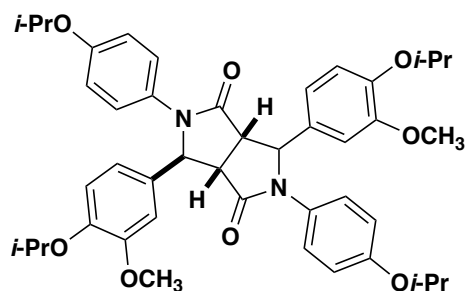
3,6-Bis(4-chlorophenyl)-2,5-bis(4-methoxyphenyl)hexahydropyrrolo[3,4-c]pyrrole-1,4-dione (72d, 76d). Prepared according to general procedure D. The unpurified reaction mixture was purified by recrystallization from EtOAc/hexanes and flash column chromatography (30-100% EtOAc/hexanes) to afford lactam **13d** and **14d** (135.6 mg, 59%), a 27:73 mixture of diastereomers, as an off-white solid.



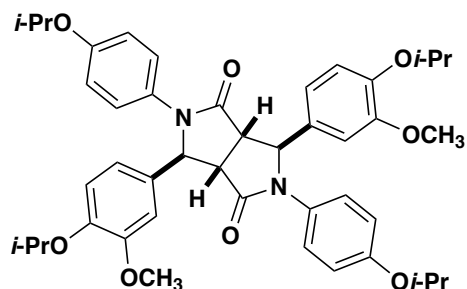
72d: mp 200-205 °C; ^1H NMR (400 MHz, CDCl_3) δ 7.39 (d, $J = 8.6$ Hz, 2H), 7.30 (d, $J = 8.1$ Hz, 2H), 7.22 (d, $J = 8.1$ Hz, 2H), 6.81 (d, $J = 8.5$ Hz, 2H), 5.72 – 5.60 (m, 1H), 3.74 (s, 3H), 3.39 – 3.20 (m, 1H); ^{13}C NMR (150 MHz, CDCl_3) δ 171.8, 157.6, 138.2, 134.3, 130.2, 129.6, 127.3, 124.0, 114.4, 65.1, 55.5, 48.7; AMM (ESI-TOF) m/z calcd for $\text{C}_{32}\text{H}_{27}\text{Cl}_2\text{N}_2\text{O}_4^+$ $[\text{M}+\text{H}]^+$: 573.1342, found: 573.1349.



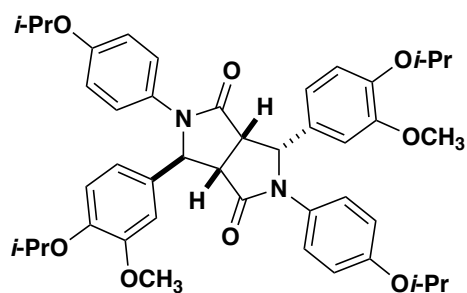
76d: mp 255-264 °C; ^1H NMR (400 MHz, CDCl_3) δ 7.34 – 7.29 (m, 2H), 7.22 (dd, $J = 13.1$, 5.9 Hz, 6H), 7.11 (d, $J = 8.5$ Hz, 4H), 6.84 – 6.70 (m, 4H), 5.64 (d, $J = 8.7$ Hz, 1H), 5.53 (d, $J = 2.4$ Hz, 1H), 3.88 (t, $J = 9.2$ Hz, 1H), 3.74 (s, 3H), 3.71 (s, 3H), 3.36 (dd, $J = 9.7$, 2.2 Hz, 1H); ^{13}C NMR (100 MHz, CDCl_3) δ 172.4, 169.6, 157.4, 157.3, 139.1, 134.2, 134.1, 131.5, 130.0, 129.7, 129.5, 129.0, 128.7, 127.4, 124.6, 124.2, 114.2, 114.1, 64.9, 64.6, 55.3, 55.3, 49.6, 44.3; AMM (ESI-TOF) m/z calcd for $\text{C}_{32}\text{H}_{27}\text{Cl}_2\text{N}_2\text{O}_4^+$ $[\text{M}+\text{H}]^+$: 573.1342, found: 573.1363.



3,6-Bis(4-isopropoxy-3-methoxyphenyl)-2,5-bis(4-isopropoxyphenyl)hexahydro-pyrrolo[3,4-c]pyrrole-1,4-dione (72e, 76e). Prepared according to general procedure D. The unpurified reaction mixture was purified by flash column chromatography (50-100% EtOAc/hexanes) to afford lactam **13e** and **14e** (568.0 mg, 32%), a 48:52 mixture of diastereomers, as an amorphous yellow solid.



72e: ^1H NMR (600 MHz, CDCl_3) δ 7.39 (d, $J = 9.0$ Hz, 4H), 6.81 – 6.75 (m, 10H), 5.56 (s, 2H), 4.49 – 4.42 (m, 4H), 3.81 (s, 6H), 3.36 (s, 2H), 1.33 (dd, $J = 6.1, 2.4$ Hz, 12H), 1.28 (dd, $J = 6.1, 1.9$ Hz, 12H); ^{13}C NMR (150 MHz, CDCl_3) δ 172.4, 155.8, 150.9, 147.3, 132.4, 130.5, 124.1, 117.6, 116.1, 115.5, 109.7, 71.4, 70.2, 65.6, 56.2, 49.2, 22.1; AMM (ESI-TOF) m/z calcd for $\text{C}_{44}\text{H}_{53}\text{N}_2\text{O}_8^+$ $[\text{M}+\text{H}]^+$: 737.3796, found: 737.3793



76e: ^1H NMR (400 MHz, CDCl_3) δ 7.32 – 7.22 (m, 2H), 7.01 (d, $J = 8.5$ Hz, 2H), 6.84 – 6.73 (m, 7H), 6.70 – 6.60 (m, 3H), 5.56 (d, $J = 9.0$ Hz, 1H), 5.39 (d, $J = 3.3$ Hz, 1H), 4.54 – 4.35 (m, 4H), 3.87 (t, $J = 9.4$ Hz, 1H), 3.80 (s, 3H), 3.65 (s, 3H), 3.40 (dd, $J = 10.1, 3.3$ Hz, 1H), 1.37 – 1.22 (m, 24H); ^{13}C NMR (100 MHz, CDCl_3) δ 172.7, 170.3, 155.6, 155.5, 150.9, 150.1, 147.4, 147.2, 133.7, 130.5, 130.2, 128.6, 124.6, 124.2, 120.1, 118.4, 115.9, 115.9, 115.7, 114.7, 111.7, 109.7, 71.4, 71.1, 70.1, 70.1, 65.8, 65.4, 56.1, 56.0, 50.0, 45.1, 22.2, 22.2, 22.1, 22.1, 22.1.; AMM (ESI-TOF) m/z calcd for $\text{C}_{44}\text{H}_{53}\text{N}_2\text{O}_8^+$ $[\text{M}+\text{H}]^+$: 737.3796, found: 737.3803.

Energies and Coordinates

Calculation 1: Diastereomer 76

HF = -1646.7190602 Hartrees (-1033316.2102755 kcal/mol)

Center Number	Atomic Number	Coordinates (Angstroms)		
		X	Y	Z

1	6	-1.610659	-0.397742	1.319582
2	6	-1.268792	-1.634832	0.489654
3	1	-2.271029	-0.703385	2.136972
4	6	-0.374524	0.355562	1.936120
5	7	-2.279697	0.658607	0.539109
6	6	-1.136470	-1.584532	-0.902849
7	6	-1.068320	-2.857827	1.144358
8	6	0.937748	-0.416290	1.913824
9	1	-0.609610	0.629099	2.967551
10	6	-0.153672	1.555263	1.029212
11	6	-1.438958	1.714375	0.226986
12	6	-3.636314	0.522101	0.119583

13	6	-0.802387	-2.731743	-1.625171
14	1	-1.319893	-0.653786	-1.431674
15	1	-1.151668	-2.907107	2.226627
16	6	-0.733792	-4.003124	0.423500
17	7	1.726011	0.093609	0.894163
18	8	1.225310	-1.323547	2.677844
19	6	1.108268	1.219713	0.168529
20	1	0.025045	2.483291	1.577330
21	8	-1.664955	2.635358	-0.544198
22	6	-4.323390	1.578367	-0.513122
23	6	-4.336322	-0.664219	0.373967
24	6	-0.599675	-3.943608	-0.965018
25	1	-0.708947	-2.676631	-2.706474
26	1	-0.576124	-4.941537	0.947962
27	6	2.925290	-0.524376	0.428307
28	1	0.786034	0.877011	-0.823405
29	6	2.012606	2.429693	-0.010885
30	1	-3.803329	2.499118	-0.732590
31	6	-5.657673	1.436858	-0.863932
32	6	-5.681123	-0.803503	0.020736
33	1	-3.843634	-1.511664	0.833671
34	1	-0.341342	-4.836472	-1.527828

35	6	3.322630	-0.375467	-0.904347
36	6	3.739056	-1.281854	1.291270
37	6	1.760215	3.307583	-1.072251
38	6	3.037556	2.730973	0.892946
39	1	-6.185710	2.251138	-1.350498
40	6	-6.354362	0.249447	-0.601762
41	1	-6.179870	-1.741709	0.234886
42	1	2.730966	0.214158	-1.594609
43	6	4.494688	-0.967774	-1.380240
44	6	4.899690	-1.876324	0.817169
45	1	3.445771	-1.417070	2.322409
46	1	0.945115	3.096588	-1.759649
47	6	2.523354	4.464593	-1.230651
48	6	3.804204	3.885675	0.730707
49	1	3.246439	2.054748	1.716502
50	8	-7.663613	0.222588	-0.991328
51	1	4.768075	-0.823459	-2.419088
52	6	5.291546	-1.727573	-0.520073
53	1	5.527652	-2.464333	1.479283
54	1	2.313795	5.138289	-2.057207
55	6	3.550729	4.755258	-0.331396
56	1	4.603120	4.102952	1.434778

57	6	-8.406601	-0.960501	-0.750623
58	8	6.454708	-2.350363	-0.876436
59	1	4.149541	5.653359	-0.457096
60	1	-8.465604	-1.190313	0.321889
61	1	-7.977497	-1.822506	-1.279119
62	1	-9.410780	-0.767657	-1.132823
63	6	6.891789	-2.229238	-2.219330
64	1	6.161321	-2.651624	-2.922622
65	1	7.085580	-1.182289	-2.489376
66	1	7.822770	-2.795613	-2.284568

Calculation 1: Diastereomer 77

HF = -1646.6992802 Hartrees (-1033303.7983255 kcal/mol)

Center Number	Atomic Number	Coordinates (Angstroms)		
		X	Y	Z
1	6	1.665058	-1.038586	-0.485679
2	1	2.134593	-1.586942	-1.308581

3	6	0.247091	-0.581950	-0.868092
4	1	0.310465	-0.229797	-1.911667
5	7	2.311272	0.307869	-0.399266
6	6	1.387438	1.340475	-0.179457
7	8	1.612385	2.537679	-0.140352
8	6	-1.341915	1.114717	-0.344386
9	7	-2.007267	-0.212286	-0.549305
10	6	-1.106085	-1.262351	-0.777269
11	8	-1.389145	-2.433275	-0.958906
12	6	3.711849	0.467716	-0.601363
13	6	4.284935	1.728174	-0.865795
14	1	3.656348	2.606391	-0.890216
15	6	5.649973	1.844673	-1.083603
16	1	6.091987	2.815047	-1.287719
17	6	6.487703	0.721488	-1.052230
18	8	7.813904	0.955171	-1.285613
19	6	5.928598	-0.530939	-0.789424
20	1	6.542184	-1.423565	-0.748911
21	6	4.554753	-0.650288	-0.563108
22	1	4.158340	-1.632636	-0.334955
23	6	8.700224	-0.150640	-1.258775
24	1	8.443968	-0.893825	-2.026057

25	1	8.708476	-0.639237	-0.274995
26	1	9.692315	0.254182	-1.467516
27	6	1.744995	-1.875184	0.788687
28	6	1.280621	-3.198615	0.748490
29	1	0.853096	-3.589562	-0.170366
30	6	1.326914	-3.998225	1.889090
31	1	0.959114	-5.019776	1.843714
32	6	1.839315	-3.489321	3.085194
33	1	1.876880	-4.114414	3.973348
34	6	2.301858	-2.174821	3.132125
35	1	2.704222	-1.769325	4.056612
36	6	2.255785	-1.371507	1.989832
37	1	2.633002	-0.354286	2.030866
38	6	-3.408779	-0.329251	-0.784824
39	6	-4.099750	-1.499600	-0.453303
40	1	-3.564649	-2.332533	-0.017730
41	6	-5.469163	-1.613553	-0.702248
42	1	-5.971073	-2.537599	-0.439089
43	6	-6.172547	-0.547988	-1.272821
44	8	-7.510519	-0.552408	-1.549992
45	6	-5.485573	0.630185	-1.594422
46	1	-6.039906	1.453521	-2.033544

47	6	-4.121840	0.735946	-1.358914
48	1	-3.615406	1.658879	-1.619322
49	6	-8.252179	-1.721265	-1.243147
50	1	-8.228593	-1.945092	-0.168115
51	1	-7.882201	-2.592963	-1.799434
52	1	-9.280310	-1.511786	-1.544421
53	1	-1.309247	1.665457	-1.296020
54	6	0.061541	0.627104	0.019567
55	1	0.027796	0.291320	1.066774
56	6	-1.980394	1.990615	0.716885
57	6	-1.876511	3.381116	0.596643
58	6	-2.596894	1.449056	1.850992
59	6	-2.383617	4.218338	1.590628
60	1	-1.376873	3.808584	-0.269152
61	6	-3.109278	2.286416	2.842083
62	1	-2.687924	0.371629	1.951968
63	6	-3.005091	3.672819	2.714889
64	1	-2.292755	5.295992	1.485058
65	1	-3.593122	1.853661	3.713677
66	1	-3.405979	4.323723	3.487220

Calculation 2: Diastereomer 76

HF = -1646.7190602 Hartrees (-1033316.2102755 kcal/mol)

Center Number	Atomic Number	Coordinates (Angstroms)		
		X	Y	Z

1	6	-1.610659	-0.397742	1.319582
2	6	-1.268792	-1.634832	0.489654
3	1	-2.271029	-0.703385	2.136972
4	6	-0.374524	0.355562	1.936120
5	7	-2.279697	0.658607	0.539109
6	6	-1.136470	-1.584532	-0.902849
7	6	-1.068320	-2.857827	1.144357
8	6	0.937748	-0.416290	1.913824
9	1	-0.609610	0.629099	2.967551
10	6	-0.153672	1.555263	1.029212
11	6	-1.438958	1.714375	0.226986
12	6	-3.636313	0.522101	0.119583
13	6	-0.802387	-2.731742	-1.625171
14	1	-1.319893	-0.653786	-1.431673
15	1	-1.151668	-2.907107	2.226627

16	6	-0.733792	-4.003123	0.423500
17	7	1.726011	0.093609	0.894163
18	8	1.225310	-1.323547	2.677844
19	6	1.108268	1.219713	0.168529
20	1	0.025045	2.483291	1.577330
21	8	-1.664955	2.635358	-0.544198
22	6	-4.323390	1.578367	-0.513122
23	6	-4.336322	-0.664219	0.373967
24	6	-0.599675	-3.943608	-0.965018
25	1	-0.708947	-2.676631	-2.706473
26	1	-0.576124	-4.941537	0.947962
27	6	2.925290	-0.524376	0.428307
28	1	0.786034	0.877011	-0.823405
29	6	2.012606	2.429693	-0.010885
30	1	-3.803329	2.499117	-0.732590
31	6	-5.657673	1.436858	-0.863932
32	6	-5.681122	-0.803503	0.020736
33	1	-3.843633	-1.511664	0.833671
34	1	-0.341342	-4.836472	-1.527828
35	6	3.322630	-0.375467	-0.904347
36	6	3.739055	-1.281854	1.291270
37	6	1.760215	3.307582	-1.072251

38	6	3.037556	2.730973	0.892946
39	1	-6.185710	2.251138	-1.350498
40	6	-6.354361	0.249447	-0.601762
41	1	-6.179869	-1.741709	0.234886
42	1	2.730966	0.214158	-1.594609
43	6	4.494687	-0.967774	-1.380240
44	6	4.899690	-1.876324	0.817169
45	1	3.445771	-1.417070	2.322409
46	1	0.945115	3.096588	-1.759649
47	6	2.523353	4.464593	-1.230651
48	6	3.804204	3.885674	0.730707
49	1	3.246439	2.054747	1.716502
50	8	-7.663612	0.222588	-0.991328
51	1	4.768074	-0.823459	-2.419088
52	6	5.291546	-1.727572	-0.520073
53	1	5.527652	-2.464333	1.479282
54	1	2.313795	5.138289	-2.057207
55	6	3.550728	4.755258	-0.331396
56	1	4.603120	4.102951	1.434778
57	6	-8.406600	-0.960501	-0.750623
58	8	6.454707	-2.350363	-0.876436
59	1	4.149541	5.653359	-0.457096

60	1	-8.465604	-1.190313	0.321889
61	1	-7.977496	-1.822506	-1.279119
62	1	-9.410780	-0.767657	-1.132822
63	6	6.891789	-2.229238	-2.219330
64	1	6.161320	-2.651623	-2.922622
65	1	7.085580	-1.182289	-2.489375
66	1	7.822769	-2.795613	-2.284568

Calculation 2: Diastereomer 77

HF = -1646.6992802 Hartrees (-1033303.7983255 kcal/mol)

Center	Atomic	Coordinates (Angstroms)		
Number	Number	X	Y	Z

1	6	1.665058	-1.038586	-0.485679
2	1	2.134592	-1.586941	-1.308581
3	6	0.247091	-0.581950	-0.868092
4	1	0.310465	-0.229797	-1.911667
5	7	2.311272	0.307869	-0.399266

6	6	1.387438	1.340475	-0.179457
7	8	1.612385	2.537679	-0.140352
8	6	-1.341915	1.114717	-0.344386
9	7	-2.007267	-0.212286	-0.549305
10	6	-1.106085	-1.262350	-0.777269
11	8	-1.389145	-2.433275	-0.958906
12	6	3.711849	0.467716	-0.601363
13	6	4.284935	1.728174	-0.865795
14	1	3.656348	2.606391	-0.890216
15	6	5.649973	1.844673	-1.083603
16	1	6.091987	2.815046	-1.287719
17	6	6.487702	0.721488	-1.052230
18	8	7.813903	0.955171	-1.285613
19	6	5.928598	-0.530939	-0.789423
20	1	6.542184	-1.423565	-0.748911
21	6	4.554753	-0.650288	-0.563108
22	1	4.158339	-1.632636	-0.334955
23	6	8.700224	-0.150640	-1.258775
24	1	8.443968	-0.893825	-2.026057
25	1	8.708476	-0.639237	-0.274995
26	1	9.692314	0.254182	-1.467516
27	6	1.744994	-1.875184	0.788687

28	6	1.280621	-3.198615	0.748490
29	1	0.853096	-3.589561	-0.170366
30	6	1.326914	-3.998225	1.889089
31	1	0.959114	-5.019776	1.843714
32	6	1.839315	-3.489320	3.085194
33	1	1.876880	-4.114414	3.973348
34	6	2.301858	-2.174821	3.132125
35	1	2.704222	-1.769325	4.056612
36	6	2.255785	-1.371507	1.989832
37	1	2.633002	-0.354286	2.030866
38	6	-3.408779	-0.329251	-0.784824
39	6	-4.099749	-1.499600	-0.453303
40	1	-3.564649	-2.332533	-0.017730
41	6	-5.469163	-1.613553	-0.702248
42	1	-5.971072	-2.537599	-0.439089
43	6	-6.172546	-0.547988	-1.272821
44	8	-7.510519	-0.552408	-1.549992
45	6	-5.485572	0.630185	-1.594422
46	1	-6.039905	1.453521	-2.033544
47	6	-4.121840	0.735946	-1.358914
48	1	-3.615406	1.658879	-1.619322
49	6	-8.252178	-1.721265	-1.243147

50	1	-8.228592	-1.945092	-0.168115
51	1	-7.882201	-2.592962	-1.799433
52	1	-9.280310	-1.511786	-1.544421
53	1	-1.309247	1.665456	-1.296020
54	6	0.061541	0.627104	0.019567
55	1	0.027796	0.291320	1.066774
56	6	-1.980394	1.990615	0.716885
57	6	-1.876511	3.381116	0.596643
58	6	-2.596894	1.449056	1.850992
59	6	-2.383617	4.218337	1.590627
60	1	-1.376873	3.808583	-0.269152
61	6	-3.109277	2.286416	2.842083
62	1	-2.687924	0.371629	1.951968
63	6	-3.005091	3.672819	2.714889
64	1	-2.292755	5.295992	1.485058
65	1	-3.593121	1.853660	3.713677
66	1	-3.405979	4.323723	3.487220

Full G16 Citation

Gaussian 16, Revision A.03, M. J. Frisch, G. W. Trucks, H. B. Schlegel, G. E. Scuseria, M. A. Robb, J. R. Cheeseman, G. Scalmani, V. Barone, G. A. Petersson, H. Nakatsuji, X. Li, M. Caricato, A. V. Marenich, J. Bloino, B. G. Janesko, R. Gomperts, B. Mennucci,

H. P. Hratchian, J. V. Ortiz, A. F. Izmaylov, J. L. Sonnenberg, D. Williams-Young, F. Ding, F. Lipparini, F. Egidi, J. Goings, B. Peng, A. Petrone, T. Henderson, D. Ranasinghe, V. G. Zakrzewski, J. Gao, N. Rega, G. Zheng, W. Liang, M. Hada, M. Ehara, K. Toyota, R. Fukuda, J. Hasegawa, M. Ishida, T. Nakajima, Y. Honda, O. Kitao, H. Nakai, T. Vreven, K. Throssell, J. A. Montgomery, Jr., J. E. Peralta, F. Ogliaro, M. J. Bearpark, J. J. Heyd, E. N. Brothers, K. N. Kudin, V. N. Staroverov, T. A. Keith, R. Kobayashi, J. Normand, K. Raghavachari, A. P. Rendell, J. C. Burant, S. S. Iyengar, J. Tomasi, M. Cossi, J. M. Millam, M. Klene, C. Adamo, R. Cammi, J. W. Ochterski, R. L. Martin, K. Morokuma, O. Farkas, J. B. Foresman, and D. J. Fox, Gaussian, Inc., Wallingford CT, 2016.

3.5 References

1. Portions of this chapter are adapted with permission from Laws, S. W. H., S. Y.; Mato, R.; Meng, S.; Fettinger J. C.; Shaw, J.T. , *Org. Lett.* **2019**, *21* (13). Copyright 2019 American Chemical Society
2. Ng, P. Y.; Masse, C. E.; Shaw, J. T., *Org. Lett.* **2006**, *8* (18), 3999-4002.
3. Wei, J.; Shaw, J. T., *Org. Lett.* **2007**, *9* (20), 4077-4080.
4. González-López, M.; Shaw, J. T., *Chem. Rev.* **2009**, *109* (1), 164-189.
5. Tang, Y.; Fettinger, J. C.; Shaw, J. T., *Org. Lett.* **2009**, *11* (17), 3802-3805.
6. Younai, A.; Chin, G. F.; Shaw, J. T., *J. Org. Chem.* **2010**, *75* (23), 8333-8336.
7. Tan, D. Q.; Younai, A.; Pattawong, O.; Fettinger, J. C.; Cheong, P. H.-Y.; Shaw, J. T., *Org. Lett.* **2013**, *15* (19), 5126-5129.
8. Sorto, N. A.; Di Maso, M. J.; Muñoz, M. A.; Dougherty, R. J.; Fettinger, J. C.; Shaw, J. T., *J. Org. Chem.* **2014**, *79* (6), 2601-2610.
9. Di Maso, M. J.; Nepomuceno, G. M.; St. Peter, M. A.; Gitre, H. H.; Martin, K. S.; Shaw, J. T., *Org. Lett.* **2016**, *18* (8), 1740-1743.
10. Di Maso, M. J.; Snyder, K. M.; De Souza Fernandes, F.; Pattawong, O.; Tan, D. Q.; Fettinger, J. C.; Cheong, P. H.-Y.; Shaw, J. T., *Chem. Eur. J.* **2016**, *22* (14), 4794-4801.
11. Laws, S. W.; Moore, L. C.; Di Maso, M. J.; Nguyen, Q. N. N.; Tantillo, D. J.; Shaw, J. T., *Org. Lett.* **2017**, *19* (10), 2466-2469.
12. Burlow, N. P.; Howard, S. Y.; Saunders, C. M.; Fettinger, J. C.; Tantillo, D. J.; Shaw, J. T., *Org. Lett.* **2019**, *21* (4), 1046-1049.

13. Laws, S. W.; Howard, S. Y.; Mato, R.; Meng, S.; Fettinger, J. C.; Shaw, J. T., *Org. Lett.* **2019**, *21* (13), 5073-5077.
14. Pattawong, O.; Tan, D. Q.; Fettinger, J. C.; Shaw, J. T.; Cheong, P. H.-Y., *Org. Lett.* **2013**, *15* (19), 5130-5133.
15. Cronin, S. A.; Gutierrez Collar, A.; Gundala, S.; Cornaggia, C.; Torrente, E.; Manoni, F.; Botte, A.; Twamley, B.; Connon, S. J., *Org. Biomol. Chem.* **2016**, *14* (29), 6955-6959.
16. Jarvis, C. L.; Hirschi, J. S.; Veticatt, M. J.; Seidel, D., *Angew. Chem. Int. Ed.* **2017**, *56* (10), 2670-2674.
17. Ojima, I.; Inaba, S.; Nagai, M., *Synthesis* **1981**, (7), 545.
18. Okano, K.; Morimoto, T.; Sekiya, M., *Chem. Commun.* **1985**, (3), 119-120.
19. Mukaiyama, T.; Kashiwagi, K.; Matsui, S., *Chem. Lett.* **1989**, *18* (8), 1397-1400.
20. Mukaiyama, T.; Matsui, S.; Kashiwagi, K., *Chem. Lett.* **1989**, *18* (6), 993-996.
21. Ishihara, K.; Miyata, M.; Hattori, K.; Tada, T.; Yamamoto, H., *J. Am. Chem. Soc.* **1994**, *116* (23), 10520-10524.
22. Ishitani, H.; Ueno, M.; Kobayashi, S., *J. Am. Chem. Soc.* **1997**, *119* (30), 7153-7154.
23. Akiyama, T.; Itoh, J.; Yokota, K.; Fuchibe, K., *Angew. Chem. Int. Ed.* **2004**, *43* (12), 1566-1568.
24. Mayer, S.; List, B., *Angew. Chem. Int. Ed.* **2006**, *45* (25), 4193-4195.
25. Carter, C.; Fletcher, S.; Nelson, A., *Tetrahedron: Asymmetry* **2003**, *14* (14), 1995-2004.
26. Lacour, J.; Hebbe-Viton, V., *Chem. Soc. Rev.* **2003**, *32* (6), 373-382.

27. Dorta, R.; Shimon, L.; Milstein, D., *J. Organomet. Chem* **2004**, 689 (4), 751-758.
28. Llewellyn, D. B.; Arndtsen, B. A., *Tetrahedron: Asymmetry* **2005**, 16 (10), 1789-1799.
29. García-García, P.; Lay, F.; García-García, P.; Rabalakos, C.; List, B., *Angew. Chem. Int. Ed.* **2009**, 48 (24), 4363-4366.
30. Brownbridge, P.; Chan, T.-H., *Tetrahedron Lett.* **1980**, 21 (36), 3423-3426.
31. Brownbridge, P.; Chan, T.-H., *Tetrahedron Lett.* **1980**, 21 (36), 3427-3430.
32. Brownbridge, P.; Chan, T.-H., *Tetrahedron Lett.* **1980**, 21 (36), 3431-3434.
33. Frick, U.; Simchen, G., *Liebigs Annalen der Chemie* **1987**, 1987 (10), 839-845.
34. Taylor, E. C.; Andrade, J. G.; Rall, G. J. H.; McKillop, A., *Tetrahedron Lett.* **1978**, 19 (38), 3623-3626.
35. Pelter, A.; Ward, R. S.; Watson, D. J.; Collins, P.; Kay, I. T., *Tetrahedron Lett.* **1979**, 20 (24), 2275-2278.
36. Pohmakotr, M.; Yotapan, N.; Tuchinda, P.; Kuhakarn, C.; Reutrakul, V., *J. Org. Chem.* **2007**, 72 (13), 5016-5019.
37. Lodewyk, M. W.; Siebert, M. R.; Tantillo, D. J., *Chem. Rev.* **2012**, 112 (3), 1839-1862.
38. Tantillo, D. J. CHESHIRE. CHEmical SHift REpository with Coupling Constants Added Too <http://cheshirenmr.info>.
39. Bally, T.; Rablen, P. R., *J. Org. Chem.* **2011**, 76 (12), 4818-4830.
40. Jensen, F., *J. Chem. Theory Comput.* **2006**, 2 (5), 1360-1369.
41. Laws, S. W., **2019**.
42. Wenzel, A. G.; Jacobsen, E. N., *J. Am. Chem. Soc.* **2002**, 124 (44), 12964-12965.

43. Tillman, A. L.; Ye, J.; Dixon, D. J., *Chem. Commun.* **2006**, (11), 1191-1193.
44. Denmark, S. E.; Nakajima, N.; Stiff, C. M.; Nicaise, O. J.; Kranz, M., *Adv Synth Catal* **2008**, *350* (7-8), 1023-1045.
45. Han, R.-G.; Wang, Y.; Li, Y.-Y.; Xu, P.-F., *Adv. Synth. Catal.* **2008**, *350* (10), 1474-1478.
46. Grote, R. E.; Jarvo, E. R., *Org. Lett.* **2009**, *11* (2), 485-488.
47. Piens, N.; Goossens, H.; Hertsen, D.; Deketelaere, S.; Crul, L.; Demeurisse, L.; De Moor, J.; Van den Broeck, E.; Mollet, K.; Van Hecke, K.; Van Speybroeck, V.; D'Hooghe, M., *Chem. Eur. J.* **2017**, *23* (71), 18002-18009.
48. *Gaussian 16 Rev. A.03*, Wallingford, CT, 2016.
49. Lodewyk, M. W.; Soldi, C.; Jones, P. B.; Olmstead, M. M.; Rita, J.; Shaw, J. T.; Tantillo, D. J., *J. Am. Chem. Soc.* **2012**, *134* (45), 18550-18553.
50. Jain, R.; Bally, T.; Rablen, P. R., *J. Org. Chem.* **2009**, *74* (11), 4017-4023.
51. Rablen, P. R.; Pearlman, S. A.; Finkbiner, J., *J. Phys. Chem. A* **1999**, *103* (36), 7357-7363.
52. Tantillo, D. J. CHESHIRE. CHEmical SHift REpository with Coupling Constants Added Too. <http://cheshirenmr.info>.
53. Tan, D. Q.; Atherton, A. L.; Smith, A. J.; Soldi, C.; Hurley, K. A.; Fettinger, J. C.; Shaw, J. T., *ACS. Comb. Sci.* **2012**, *14* (3), 218-223.

Chapter 4: Progress Toward the Synthesis of Bisavenanthramide B-1

4.1 Introduction

Plants secrete defensive molecules at sites of pathogenic infection and stress.¹⁻⁷ These compounds are typically low molecular weight antimicrobial compounds referred to as phytoalexins.⁵ In oats, avenanthramide B and its dimers have been identified as a family of phytoalexins that are bioavailable in mammals and possess antifungal, antimicrobial, and antibiotic properties.^{2-5, 7} One such dimer, bisavenanthramide B-1 (**1**), contains a fused bis- γ -lactam core, which can be synthesized using the Mukaiyama-type CCR reactions discussed in the previous chapter (Figure 4.1). This method highlights the divergent reactivity of 2,5-bis(trimethylsilyloxy)furan (**5**), which forms both mono (**7**) and bis- γ -lactam (**2**) products in either a single or double Mukaiyama CCR-type reaction.⁸ Our group was interested in demonstrating the utility of our methodology by developing the first synthesis of a novel bis- γ -lactam natural product bisavenanthramide B-1.

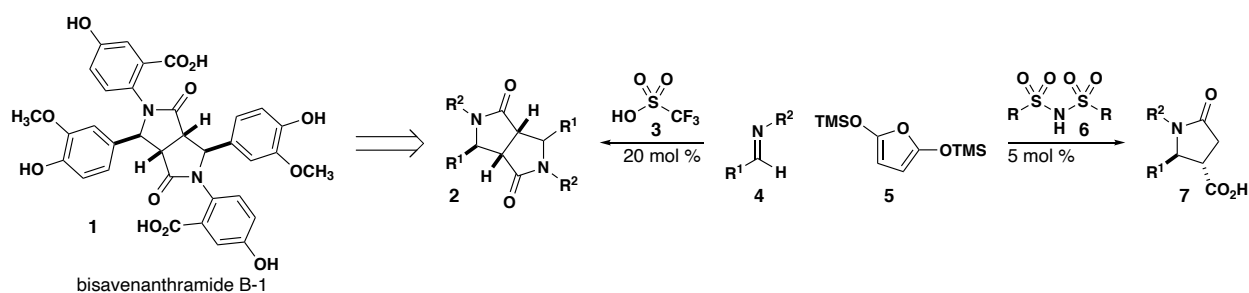


Figure 4.1 Synthesis of bisavenanthramide B-1 exploiting divergent reactivity of 2,5-bis(trimethylsilyloxy) furan

4.1.1 Isolation of the Bisavenanthramides and Biosynthetic Hypothesis

In oats (*Avena sativa* L.), the avenanthramides have been identified as a family of phytoalexins that inhibit the accumulation of toxic pathogens.⁹⁻¹¹ The avenanthramides are conjugated amides derived from anthranilic acids with hydroxycinnamic acids (Figure 4.2).³ Avenanthramides are secreted when oats are exposed elicitors, which are described as foreign molecules that provoke a defensive response in plants. Elicitors known to promote the production of avenanthramides include phytopathogenic fungi such as the crown rust fungus (*Puccinia coronata* f. sp. *avenae*),⁹ as well as leaves of oligo-*N*-acetylchitooligosaccharides,² a host specific toxin victorin C,¹⁰ and heavy metal ions¹².² Similar structures have been found to be secreted as a stress response in other plants.²

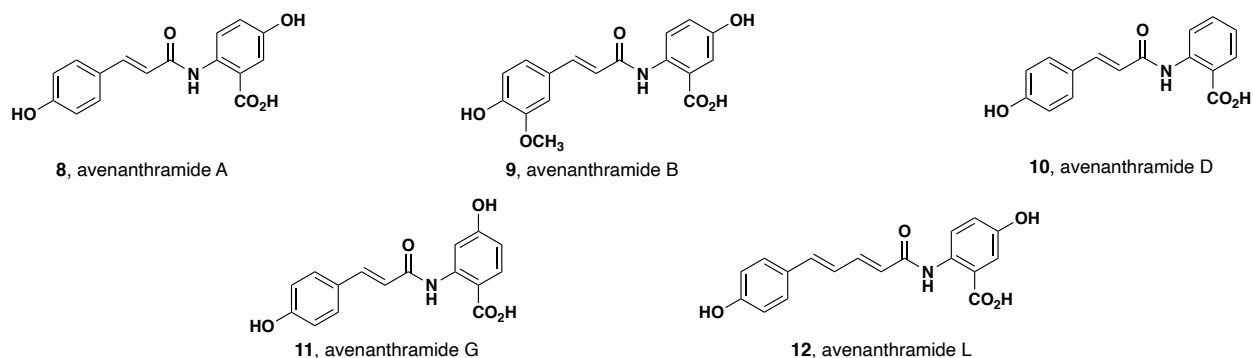


Figure 4.2 Avenanthramides are substituted hydroxycinnamic acid amides made from anthranilic acid.

Feeding experiments and enzyme activity measurements have led to an understanding of the biosynthetic pathway of the avenanthramides.³ Ishira and coworkers at University of Kyoto found compelling evidence from deuterium labeling experiments that suggest the avenanthramides are biosynthesized from anthranilic acid and coumaric acid derived from L-phenylalanine.⁴ In the case of avenanthramide B (**9**), 4-coumarate CoA ligase (4CL) can convert ferulic acid (**14**) to its hydroxycinnamoyl-CoA thioester (**15**).

Exposure to elicitors induces hydroxyanthranilate hydroxycinnamoyl-CoA *N*-hydroxycinnamoyl transferase (HHT) activity, which is said to facilitate the condensation of hydroxyanthranilates and hydroxycinnamoyl-CoA thioesters to form the avenanthramides (Figure 4.3).²⁻⁴

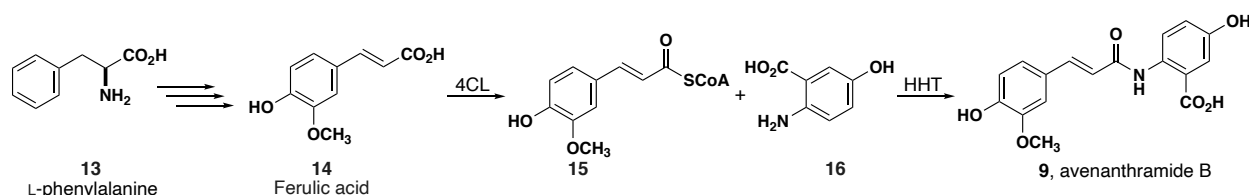


Figure 4.3 Biosynthetic hypothesis for the biosynthesis of avenanthramide B.

Bisavenanthramide B-6 (**20**), a dimer of avenanthramide B, was first isolated in by the Ishira group in 2004 (Figure 4.4).⁵ When oat leaves were treated separately with chitin and penta-*N*-acetylchitopentaose, **20** was isolated by reverse phase HPLC and identified as the dehydrodimer of avenanthramide B using ion spray LCMS.⁵ **20** was also found to be synthesized from peroxidase extracted from oat leaves in the presence of hydrogen peroxide, suggesting a radical mechanism for its biosynthesis (Figure 4.4).⁵

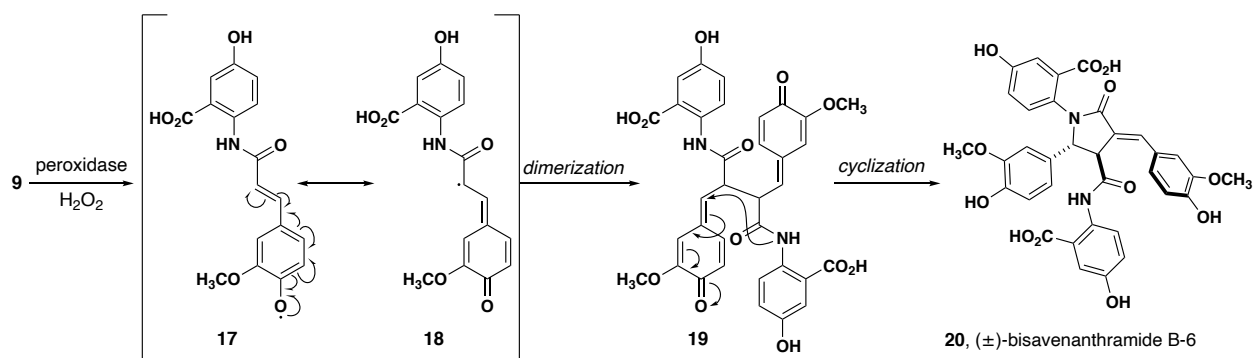


Figure 4.4 Biosynthetic hypothesis leading to bisavenanthramide B-6

Further studies of the metabolism of the avenanthramides showed that avenanthramide B is metabolized to its hydrated- and dehydrodimers. In particular, this

metabolic study led to the identification of five additional dimers called the bisavenanthramides (Figure 4.5).^{6, 7} Due to the presence of the two amide groups and having been derived from hydroxycinnamic acid, the bisavenanthramides are classified as lignanamides.⁷ Interestingly, bisavenanthramide B-1 (**1**) contains a fused bis- γ -lactam core which has not previously been observed in natural products.⁷

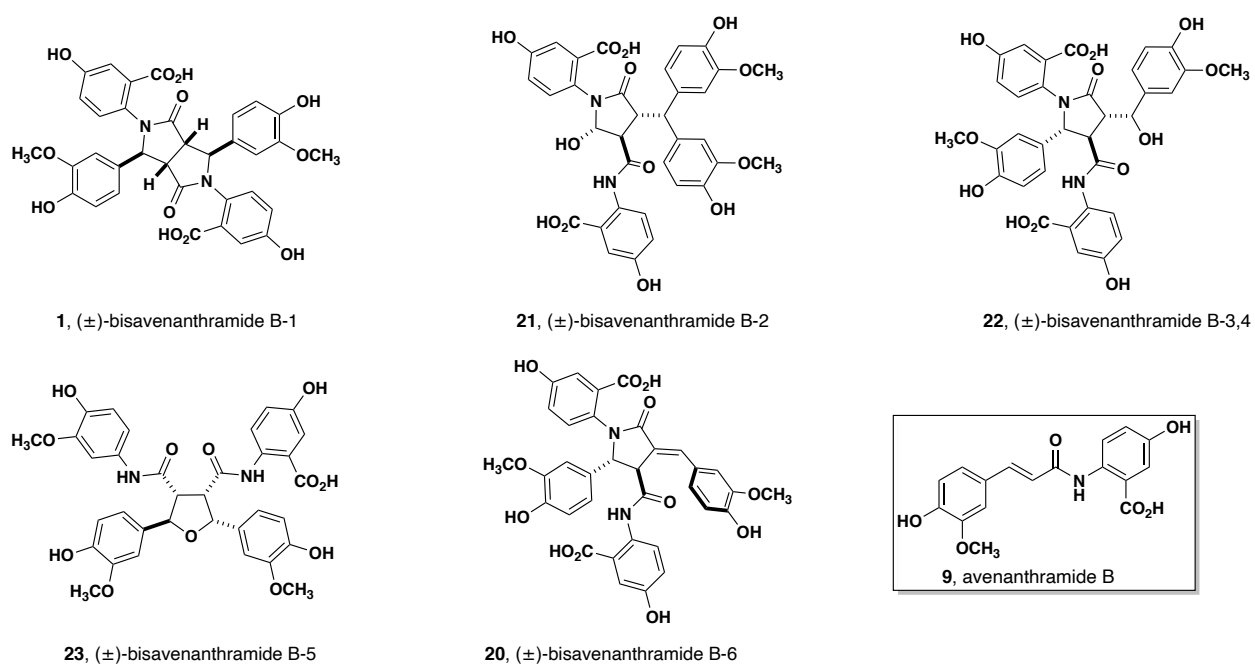


Figure 4.5 Six dimers of avenanthramide B were identified through studying the metabolism of avenanthramide-B.

4.1.2 Synthesis of Bisavenanthramide B-6 by Anionic Castagnoli-Cushman Reaction

The Shaw group has had a longstanding interest in the reactions of imines with cyclic enolizable anhydrides to form densely substituted lactam products in what is known as the Castagnoli-Cushman reaction (CCR). The CCR has been used for the synthesis of a variety of natural products containing lactam cores including the benzophenanthridine

alkaloids,¹³⁻²¹ protoberberine alkaloids,²²⁻²⁶ and oxopyrrolidine natural products.^{27, 28} In our group, we have developed methods allowing for the synthesis of two structurally similar oxopyrrolidine natural products heliotropamide²⁷ and bisavenanthramide B-6²⁸. The synthesis of bisavenanthramide B-6 highlighted the development of the first anionic CCR which utilizes an electron withdrawing *N*-sulfonyl imine to form the γ -lactam core in a single step (Figure 4.6). The *N*-sulfonyl imine electrophile served two purposes—for one, the resulting CCR product could be deprotected to afford the free *N*-H lactam allowing for further functionalization. Furthermore, the use of an electron withdrawing group maintains similar electrophilicity to an iminium ion and also allows for the addition of an exogenous base. To begin the synthesis, a novel anhydride (**25**) was synthesized from a modified Stobbe condensation with vanillin and diethylmaleate (Figure 4.6). The anionic CCR reaction of *N*-(2-(trimethylsilyl)ethanesulfonyl) (SES) imine (**24**) and **25** with LDA afforded the complete core of bisavenanthramide B-6 with correct *trans* stereochemistry and *E*-alkene geometry. After deprotection of the SES group using TBAF, a late-stage double Buchwald *N*-arylation allowed for the installation of the two amide functionalities. Global deprotection ultimately afforded bisavenanthramide B-6 in 43% yield with a longest linear sequence of 9 steps.

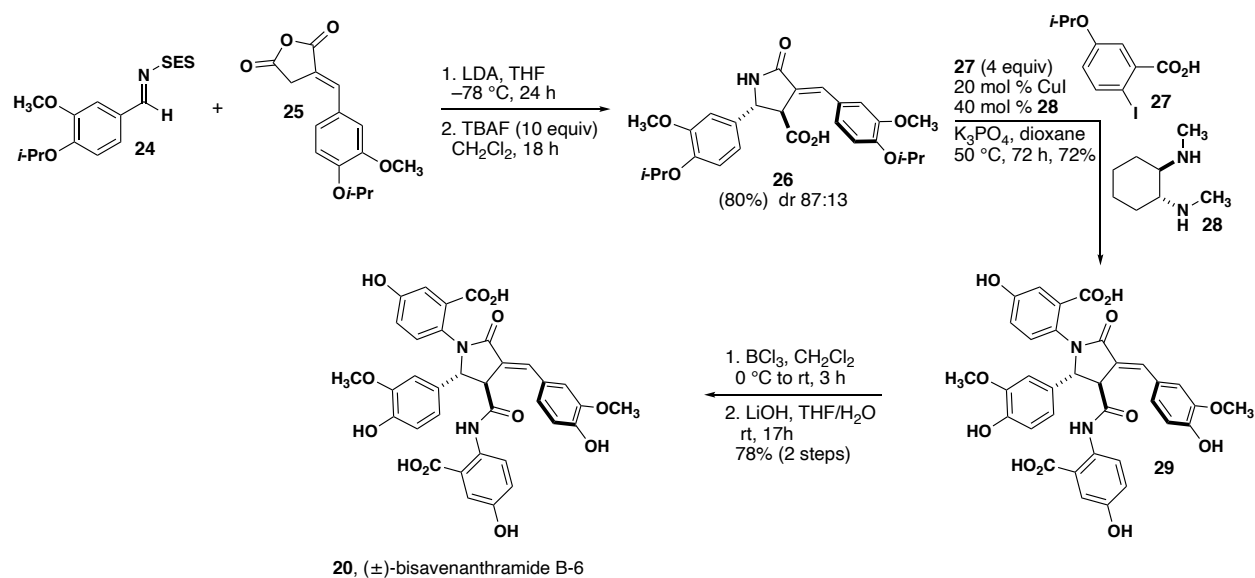


Figure 4.6 Nine step synthesis of bisavenanthramide B-6

4.1.3 Initial Route Toward the Synthesis of Bisavenanthramide B-1

A detailed discussion of the initial route toward bisavenanthramide B-1 can be found in the dissertation of Dr. Stephen Laws.²⁹ Having developed the only known method for the synthesis of bis- γ -lactams through the double Mukaiyama CCR,⁸ we sought to develop a synthesis for bisavenanthramide B-1. Using our methodology and the inherent symmetry of our target molecule, we initially envisioned synthesizing bisavenanthramide B-1 in as few as three steps from the isopropyl-protected vanillin derived imine **30** (Figure 4.7). However, after further development of the double Mukaiyama CCR, we recognized several limitations to our method. One critical drawback is that the double Mukaiyama Mannich reaction typically proceeds with a 50:50:0:0:0 ratio of C_2 -symmetric to C_1 -symmetric diastereomer, irrespective of changes to temperature and solvent. While this diastereoselectivity is exceptionally high considering the formation of four stereogenic centers and the six possible diastereomers, the observed 50:50 ratio limits the yield of

the desired symmetrical diastereomer needed to synthesize **1**. Additionally, the 2,5-bis(trimethylsilyloxy) furan (**5**) starting material is highly water and air sensitive and requires purification by vacuum distillation in low yields (20-70%). The distilled product remains viable for up to one week stored as a 0.4 M solution in THF with diminishing returns the longer it remains unused. The highly sensitive nature of the furan starting material ultimately leads to inconsistent results. Finally, we discovered that *ortho*-substituted aniline derived imines were not tolerated in the reaction,⁸ and our proposed three step route to bisavenanthramide B-1 was not feasible. For the duration of this chapter, I will describe my attempts at synthesizing bisavenanthramide B-1.

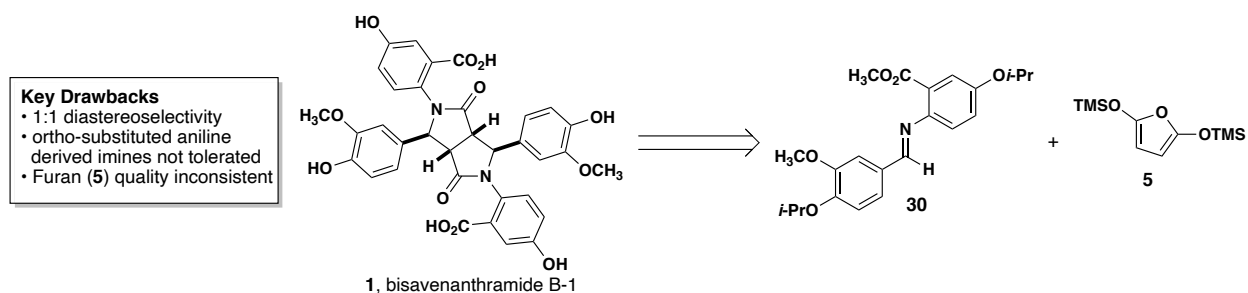


Figure 4.7 Initial retrosynthetic analysis of bisavenanthramide B-1

4.2 Results and Discussion

4.2.1 Direct Synthesis of Bisavenanthramide B-1 Through 2-Cyanoaniline Derived

Imine

Having failed at developing a route using an imine with the carboxylic acid or ester substituent *ortho* to the aniline, we hypothesized that the steric bulk of the acid or ester moiety was preventing reaction progress. To circumvent this issue, a smaller nitrile substituent was used in hopes of minimizing steric interactions. The nitrile substituent would also allow for a later hydrolysis to form the desired carboxylic acid. To begin this

route, 2-cyanoaniline (**32**) and benzaldehyde (**31**) were condensed to form imine **33** in 70% yield (Figure 4.8). As a model system, imine **33** was subjected to the mono-addition reaction conditions, with no conversion to the desired product **34**. Although it was unlikely that the double addition reaction would be successful based on the failure of the mono-addition, **33** was subjected to double addition reaction conditions. Unfortunately, the THF polymerized, which has been identified as the result of an unreactive imine in double addition reactions.

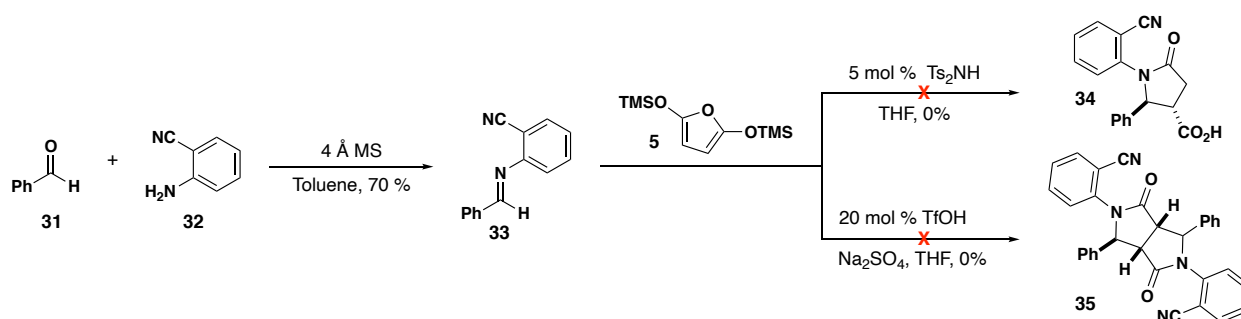


Figure 4.8 Unsuccessful synthesis of 2-cyanoaniline containing lactam products.

4.2.2 Attempted Synthesis of Bisavenanthramide B-1 Through Late-Stage Functionalization

Due to the observation that ortho-substituted aniline derived imines were not tolerated in the reaction, we were required to rethink our retrosynthetic analysis. We hypothesized that we could perform a late-stage functionalization to install a functional handle such as a bromine, or directly install the carboxylic acid moiety using palladium catalyzed carboxylation conditions (Figure 4.9).³⁰ To do this, bis- γ -lactam **36** would need to be synthesized through the double Mukaiyama CCR of **5** and **37**, which forms the core of bisavenanthramide B-1 in a single step.

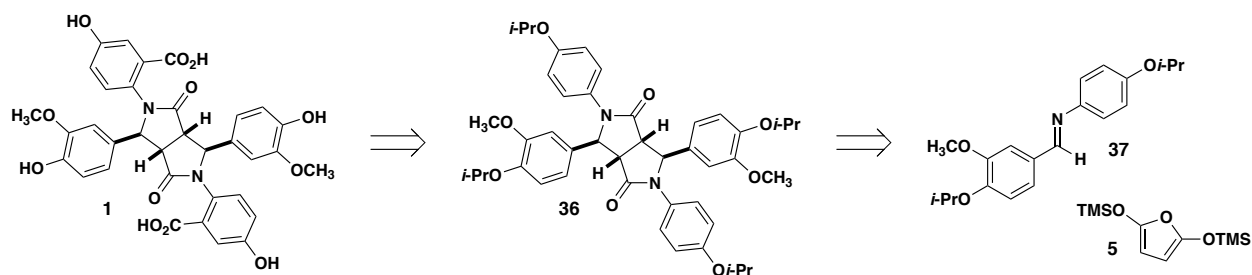


Figure 4.9 Retrosynthetic analysis for the late-stage functionalization strategy.

4.2.2.1 Attempts at Palladium Catalyzed C–H Functionalization Reaction

The palladium directed C–H carboxylation reaction to form *N*-acyl anthranilic acids was developed in the Yu group in 2010.³⁰ This work relies on the presence of an acylated aniline to direct the insertion of CO *ortho* to the aniline. The Yu group showed that *N*-aryl lactam substrates could also be carboxylated with good yields. We hoped that we would be able to modify the reaction conditions to perform a late-stage *double* carboxylation reaction on bis-γ-lactam **36** to afford the penultimate intermediate (**42b**) to bisavenanthramide B-1. To begin this new route, a precedented reaction was repeated to ensure that the results could be replicated in my hands utilizing a carbon monoxide balloon. First, aniline **39** was synthesized from *p*-toluidine in 38% yield (Figure 4.10). **39** was then subjected to the palladium directed carboxylation conditions, which afforded full conversion to carboxylated aniline **40** based on the ¹H NMR spectrum of the unpurified reaction mixture.

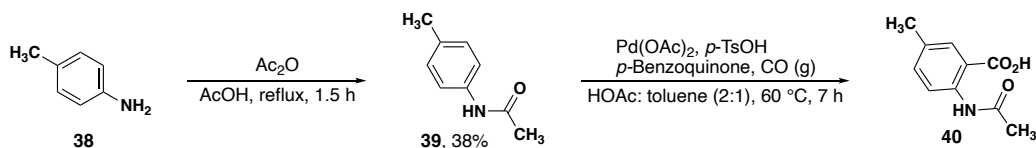


Figure 4.10 Proof of concept for the use of carbon monoxide balloon.

Satisfied with the modified reaction conditions, the carboxylation reaction was tested in the bis- γ -lactam system. Initially, the carboxylation reaction was attempted on phenyl substituted bis- γ -lactam **41** as a model system. (Figure 4.11). After running the reaction overnight, the ^1H NMR spectrum of the unpurified reaction mixture of **42a** was inconclusive. Thus, **42a** was subjected to TMSCHN_2 for ease of isolation and to our delight, the resulting ^1H NMR spectrum appeared to be consistent with the carboxylated product **43a**! Next, the reaction was performed on the requisite bis- γ -lactam **36**, which was synthesized as discussed in the previous chapter in 15% yield.³¹ However, upon subjecting to the carboxylation conditions used for the synthesis of **42a**, there was no conversion to product based on analysis of the ^1H NMR spectrum of the unpurified reaction mixture.

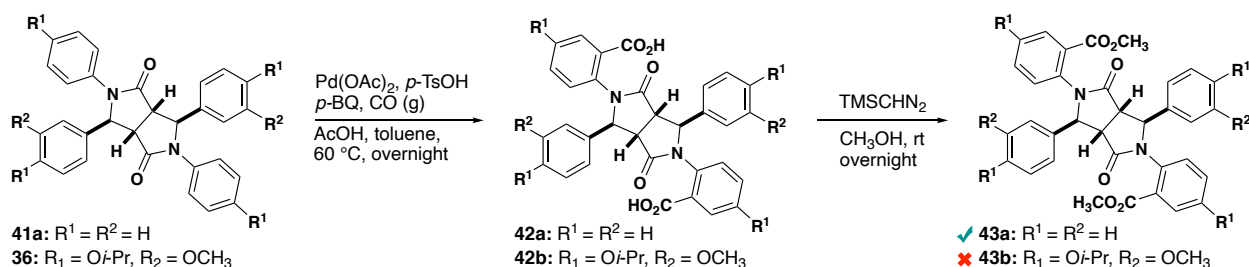
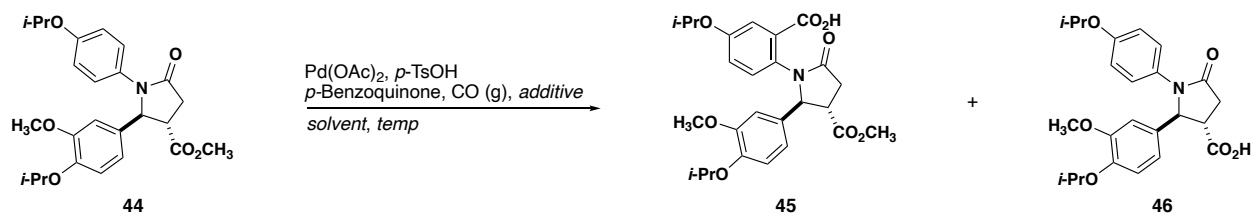


Figure 4.11 Attempt on unsubstituted bis- γ -lactam **43b**

Due to the consistently poor yields of the double-addition reaction, esterified mono-addition product **44** was used as a model system for reaction optimization.³¹ Using **44**, a series of reaction conditions were screened, varying the solvent mixture, additive, and reaction temperature based on conditions described by the Yu group (Table 4.1).³⁰ Based on the ^1H NMR spectra of the unpurified reaction mixtures, the resulting products were either the hydrolyzed ester (**46**) or recovered starting material (**44**). After consulting with

Prof. Yu, he suggested that the bulky aryl ring adjacent to the lactam nitrogen might not allow for the amide to position itself in a way that to direct the palladium. To circumvent this, he suggested increasing the temperature of the reaction. Additionally, he commented that the hydrolysis of the ester might be limiting and suggested a bulkier group to protect the ester. Because the esterified monolactam was being used as a model system, we endeavored to apply Prof. Yu's advice on the double-addition product **36**.

Table 4.1 Reaction screen of the palladium catalyzed carbonylation reaction



entry	solvent	temp (°C)	additive	products recovered
1	HOAc : dioxane	60	NaOAc	44
2	HOAc : dioxane	60	—	44
3	HOAc : toluene	60	NaOAc	44 and 46
4	HOAc : toluene	60	—	46
5	dioxane	60	NaOAc	44
6	dioxane	60	—	44
7	HOAc : dioxane	80	NaOAc	46
8	HOAc : dioxane	80	—	44
9	HOAc : toluene	80	NaOAc	44
10	HOAc : toluene	80	—	44 and 46
11	dioxane	80	NaOAc	44
12	dioxane	80	—	46

To test the reaction with Prof. Yu's advice, **36** was subjected to modified reaction conditions at 120 °C (Figure 4.12). The reaction was stirred at this temperature for 5 days, but the TLC and ¹H NMR spectrum remained inconclusive. For ease of isolation, the unpurified reaction mixture was esterified using TMSCHN₂ in analogy to **43a**. After isolating the resulting product, ¹H NMR spectroscopy and mass spectrometry analysis suggested that a Saegusa-like oxidation followed by an oxidative aryl cleavage had occurred to afford **47**. When subjected to TMSCHN₂, the free *N*-H lactam was esterified

to the putative product **48**. Due to the unsuccessful attempts at carboxylation, this late-stage functionalization route was abandoned.

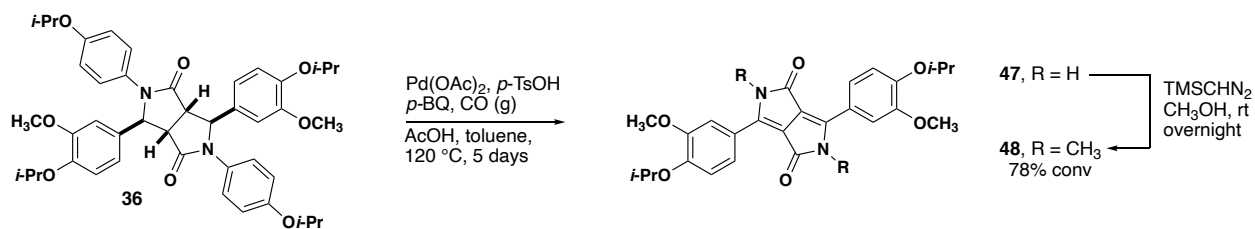


Figure 4.12 Attempted carbonylation resulted in Saegusa-like oxidation followed by oxidative aryl cleavage.

4.2.2.2 Initial Attempt at Directed Ortho Bromination

Next, we considered the possibility of a late-stage bromination reaction. In this route, the *ortho* bromide could be installed which would allow for a subsequent lithium halogen exchange and carboxylation with CO_2 .³² In analogy to the carboxylation reaction, the monolactam was used as a model system and subjected to two bromination conditions. First, monolactam **44** was subjected to NBS, which undergoes an electrophilic aromatic substitution reaction in DMF at 60°C (Figure 4.13).³³ The ^1H NMR spectrum of the unpurified reaction mixture indicated that there was 82% conversion to two brominated products, the structures of which were assigned to be **49** and **50**. Next, conditions utilizing Br_2 as the bromine source were employed.³³ In this case, the ^1H NMR spectrum of the unpurified reaction mixture indicated that an undesired double bromination had occurred wherein the product was brominated on both aryl rings (**51**). Having screened conditions with the monolactam product, I turned my attention to optimizing the double addition bromination reaction.

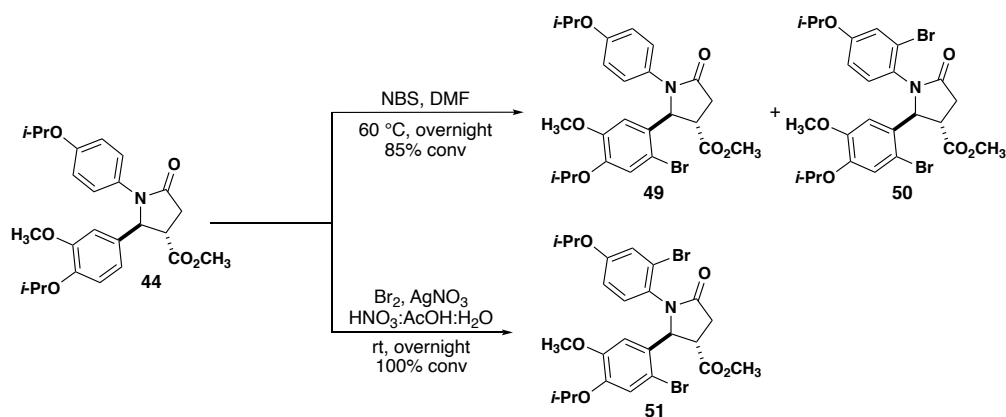


Figure 4.13 Attempts at an *ortho*-bromination on the monolactam model system

Considering the apparent success of the NBS bromination on the monolactam substrate, bis- γ -lactam **36** was employed in the double-bromination reaction (Figure 4.14). Interestingly, the products of these reaction conditions were a combination of a regioisomer, **52**, wherein the bromine was installed on the incorrect aryl rings, as well as the undesired product **53** wherein the bromide was installed on both of the incorrect aryl rings *as well as* the two desired aryl rings. While the structures of these products were not fully characterized, we were confident that the isolated products were not the desired product by comparing the J_{H-H} values to that of bisavenanthramide B-1. It is possible that products **52** and **53** were favored due to the more highly activated aryl ring alpha to the amide.

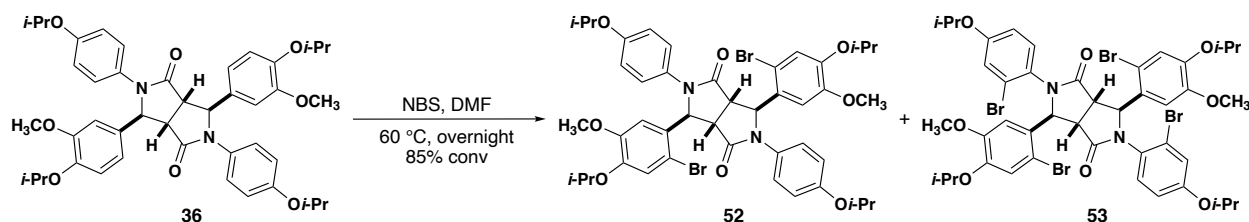


Figure 4.14 Attempts at performing a double bromination on the bis- γ -lactam **36**

4.2.2.3 Initial Attempt at the Double CAN Deprotection

Having failed at a late-stage functionalization reaction, it was necessary to restructure our synthetic route. We hypothesized that we could use our method to form a bis- γ -lactam precursor (**55**) which could be doubly deprotected to afford *N*-H bis- γ -lactam (**54**). **54** could then undergo a copper-mediated Buchwald bis-arylation to afford the penultimate intermediate, analogous to the synthesis of bisavenanthramide B-6 that our group reported in 2016 (Figure 4.15).²⁸

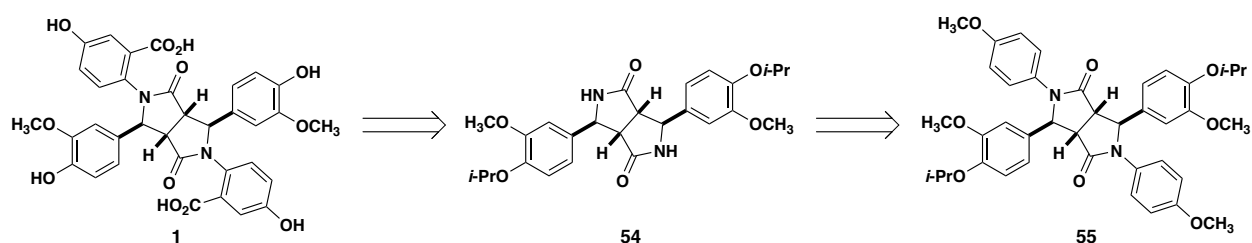


Figure 4.15 New retrosynthetic analysis involving a double deprotection to form lactam **51**

While working on derivatization of the monolactam products in the Mukaiyama CCR project, Dr. Raquel Mato showed that the *N*-PMP lactam **56** underwent oxidative cleavage with cerium ammonium nitrate (CAN) (Figure 4.16). We wanted to apply this deprotection to bis- γ -lactam **55** which contains the functionalized vanillin derived aryl ring for the synthesis of bisavenanthramide B-1. As a model system, **58** was synthesized and subjected to CAN deprotection conditions. *To our delight, 100% conversion to the doubly deprotected product was observed* (Figure 4.15)!

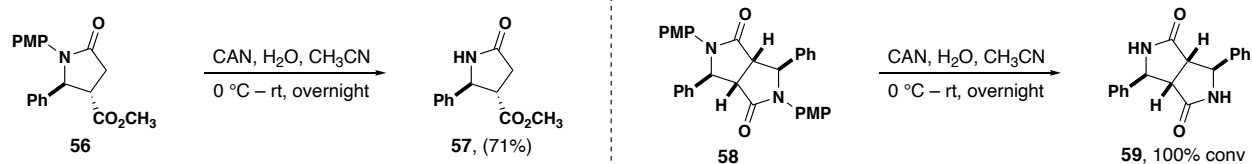


Figure 4.16 (Left) Derivatization of monolactam substrate **56**. (Right) Application of CAN deprotection to bis- γ -lactam

Next, we endeavored to apply the CAN deprotection conditions to the desired system. Nico Havenner, an undergraduate in the lab, synthesized the requisite imine **60** for the desired bis- γ -lactam **55** in 52% yield (Figure 4.17) The imine was employed in the double Mukaiyama CCR which afforded symmetrical bis- γ -lactam **55** in 7% yield. **55** was subjected to CAN deprotection conditions, and after 24 hours there was no conversion to product. Adding another portion of CAN to the reaction mixture and stirring for an additional day proved futile, and ultimately the reaction failed. Based on the success of the electron neutral lactam (**57**) and the failure of the reaction to form **54** from the activated lactam **55**, we hypothesize that the discrepancy might be attributed to the highly electron donating aryl ring derived from vanillin. Although it is unclear why an electron donating group adjacent to the amide would have an impact on the CAN deprotection, the only discernible difference between lactam **59** and **55** is the electronics of the aldehyde derived aryl group, supporting this hypothesis.

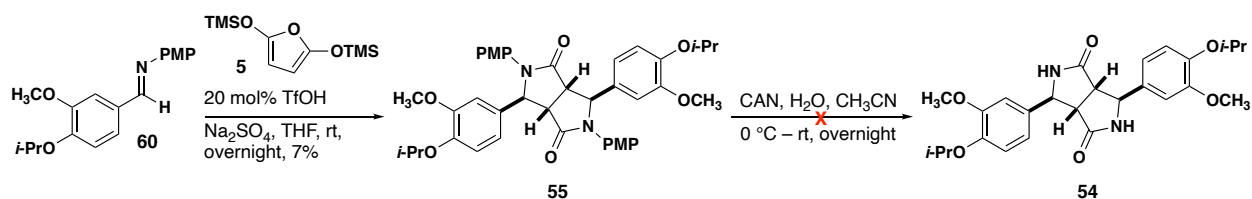


Figure 4.17 CAN deprotection attempt from imine **60**

4.2.3 New Retrosynthetic Analysis of Bisavenanthramide B-1

The limitations of our methods as well as our previous routes drove us to reconsider our synthetic strategy once more. While perusing the literature, we found precedent for an oxidative phenol deprotection using (bis(trifluoroacetoxy)iodo) benzene, PIFA, which would allow for the synthesis of the *N*-H bis- γ -lactam. In order to utilize this deprotection, it was necessary to find orthogonal protecting groups for the *para*-phenol substituents on both the aniline and aldehyde-derived aryl rings of the imine precursor (**62**) (Figure 4.18). In addition, the highly-electron donating nature of the benzylic aryl ring

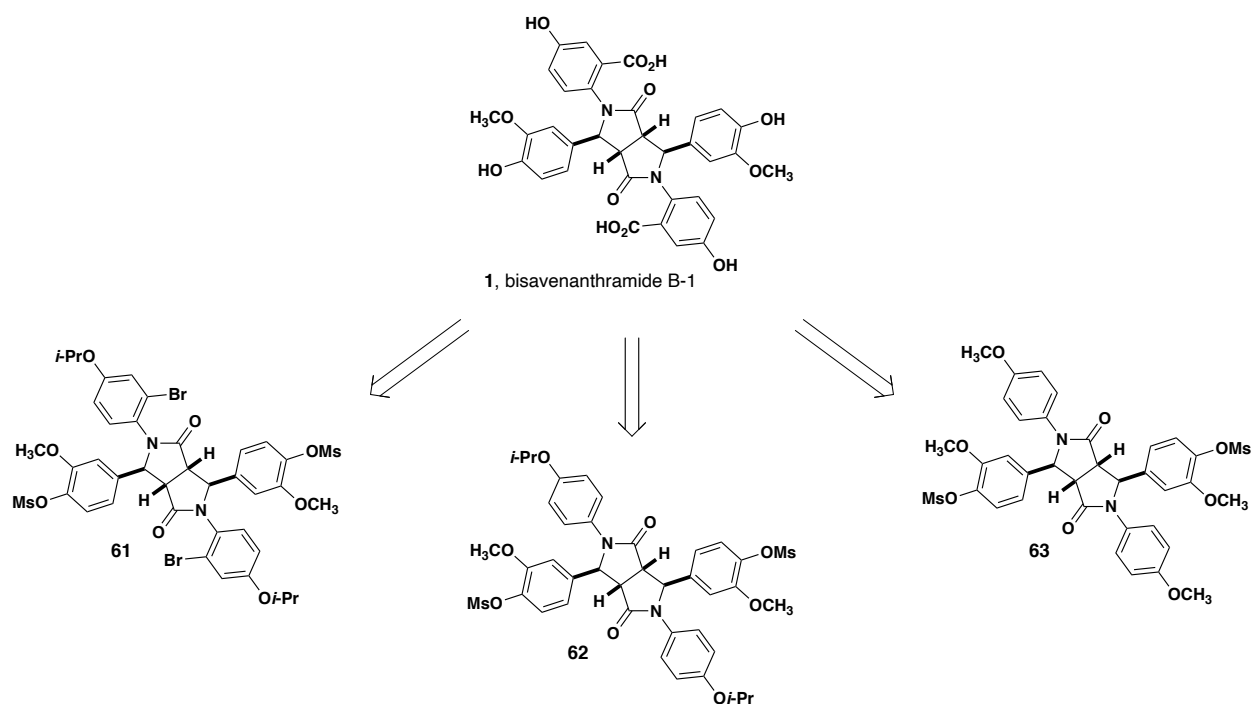


Figure 4.18 Retrosynthetic analysis using a mesylate protecting group on the aryl aldehyde derived portion of the bis- γ -lactam. Using an electron withdrawing protecting group, the failed CAN deprotection (precursor **63**) and bromination (**62**) reactions might be successful. Additionally, the use of orthogonal protecting groups (*i*-Pr and Ms) allows for the use of PIFA deprotection conditions from **62**.

had proven to have an effect on both the bromination and the CAN deprotection reaction. I hypothesized that it might be possible to remedy these failed results by utilizing a protecting group that would mediate the electron donating nature of the aryl aldehyde derived portion of the molecule (**61**, **63**).

4.2.4 Reaction Optimization for Novel Electron Withdrawing Substrates

To attempt this new route, orthogonal protecting groups on the phenolic oxygen atoms were required. Nico Havenner and I began by synthesizing a series of imines to be tested in the reaction (Figure 4.19). First, the protecting groups were modified on the vanillin portion of the imine to form mesylated vanillin **65** and *tert*-butyldiphenylsilyl (TBDPS)

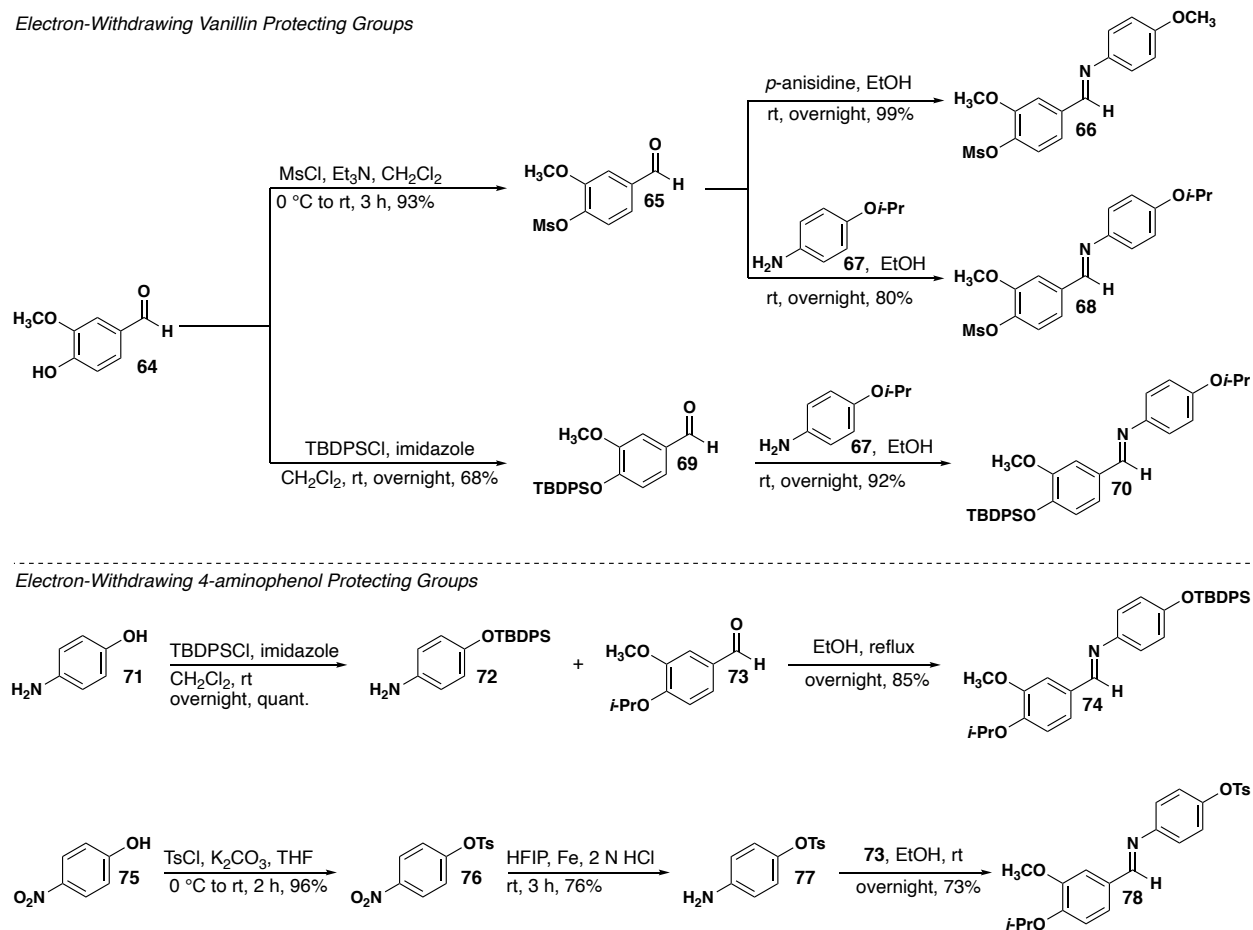


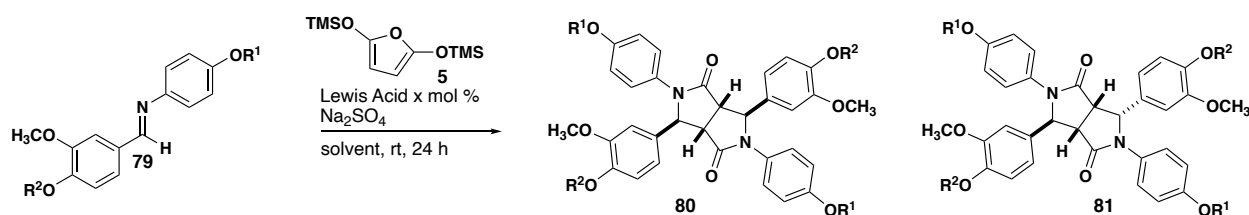
Figure 4.19 Synthesis of novel imines for the synthesis of bisavenanthramide B-1

protected vanillin **69** in 93 and 80% yield, respectively. **65** was then condensed with *p*-anisidine to afford **66** in 99% yield. **65** was also condensed with isopropyl protected 4-amino phenol **67** which provided **68** in 80% yield. Next, we worked to modify the protecting groups on 4-aminophenol. TBDPS protected imine **74** was formed in 2 steps and isolated in 85% yield. Finally, 4-nitrophenol was tosylated and subsequently reduced to the tosyl-protected 4-aminophenol **77**, which led to imine **78** in 73% yield.

The novel imines were then subjected to the original optimized reaction conditions (Table 4.2). Interestingly, the electronics of the *N*-substituent significantly influenced the reactivity of the imine precursor—specifically, electron withdrawing groups *para* to the aniline resulted in 0% conversion to product (Table 4.2, entry 1, 2). We hypothesize this is due to the influence of the *para* substituents on the aniline on the basicity and electrophilicity of the imine. As a result, we turned our attention to modifying the protecting group from the vanillin component, specifically by using TBDPS and methane sulfonyl protecting groups (Table 4.2). Formation of the bis- γ -lactam product proved unproductive with TBDPS (entries 10 and 11), and the use of the methane sulfonyl protecting group significantly decreased the overall conversion to product, resulting in a yield of 8% of our desired diastereomer. This initiated my attempt at re-optimizing conditions to increase the yield of the symmetrical diastereomer. A variety of conditions were screened, modifying the solvent, protecting group, and Lewis acid (Table 4.2). The use of 0.4 equivalents of triflic acid in dichloromethane provided 90% conversion and a 25% isolated yield of our desired diastereomer (Table 4.2 entry 12). With optimized conditions in hand, we

endeavored to use these new bis- γ -lactams toward the synthesis of bisavenanthramide B-1.

Table 4.2 Reaction Optimization for Imine Substrates Bearing Electron Withdrawing Groups



entry	R ¹	R ²	Lewis Acid	eq.	solvent	conv ^{a,b}	dr ^a (sym : unsym)
1	TBDPS	<i>i</i> -Pr	TfOH	0.2	THF	<5	—
2	Ts	<i>i</i> -Pr	TfOH	0.2	THF	<5	—
3	<i>i</i> -Pr	Ms	TfOH	0.2	THF	32	48:52
4	<i>i</i> -Pr	Ms	TMSOTf	0.2	THF	35	32:68
5	<i>i</i> -Pr	Ms	TfOH	0.2	toluene	<5	—
6	<i>i</i> -Pr	Ms	TfOH	0.2	CH ₂ Cl ₂	50	36:64
7	<i>i</i> -Pr	Ms	TfOH	0.2	Et ₂ O	<5	—
8	<i>i</i> -Pr	Ms	TfOH	2.0	THF	20	20:80
9	<i>i</i> -Pr	Ms	TMSOTf	2.0	THF	<5	—
10	<i>i</i> -Pr	TBDPS	TfOH	0.2	THF	<5	—
11	<i>i</i> -Pr	TBDPS	TfOH	0.2	CH ₂ Cl ₂	<5	—
12	<i>i</i> -Pr	Ms	TfOH	0.4	CH ₂ Cl ₂	90	50:50
13	<i>i</i> -Pr	Ms	TfOH	1.0	CH ₂ Cl ₂	82	40:60
14	<i>i</i> -Pr	Ms	Sc(OTf) ₃	0.2	CH ₂ Cl ₂	<5	—
15	<i>i</i> -Pr	Ms	TiCl ₄	0.2	CH ₂ Cl ₂	<5	—
16	<i>i</i> -Pr	Ms	BF ₃ ·OEt ₂	0.2	CH ₂ Cl ₂	<5	—
17	<i>i</i> -Pr	Ms	AlCl ₃	0.2	CH ₂ Cl ₂	<5	—
18	<i>i</i> -Pr	Ms	ZnBr ₂	0.2	CH ₂ Cl ₂	<5	—
19	CH ₃	Ms	TfOH	0.2	CH ₂ Cl ₂	61	42:58
20	CH ₃	Ms	TfOH	0.4	CH ₂ Cl ₂	45	26:74
21	CH ₃	Ms	TfOH	0.4	THF	45	42:58

^a Determined by the ¹H NMR spectrum of the unpurified reaction mixture

^b Conversion to both diastereomers

4.2.5 Additional Bromination Strategy

Using bis- γ -lactam **59**, I sought to reconsider the late-stage functionalization strategy. Since the previous bromination attempts resulted in the incorrect regioisomer of product, we hypothesized that changing the electronics of the aldehyde-derived aryl ring would allow for the preferential bromination of our desired aniline-derived aryl ring. Mesylated imine **68** was subjected to optimized reaction conditions to afford bis- γ -lactam **62** (Figure 4.20). **62** was subjected to a cobalt-directed method in an attempt to afford the singly

bromination product.³⁴ Interestingly, the reaction yielded a 50:50 mixture of the putative doubly brominated product (**61**) and starting material! Unfortunately, due to the simultaneous studies that are discussed in the next two sections and the difficulty in obtaining an appreciable quantity of bis- γ -lactam product **62**, these bromination conditions were not attempted further.

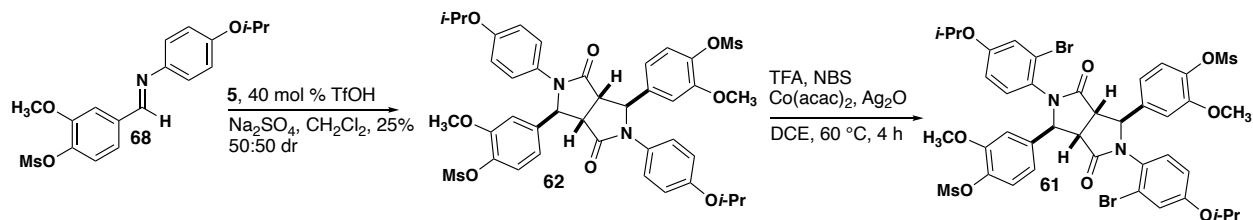


Figure 4.20 Final attempt at ortho-directed bromination conditions

4.2.6 Synthesis of N-H Bis-Lactam Intermediate

4.2.6.1 CAN Deprotection to N-H Bis- γ -lactam

In the previous attempts to synthesize bisavenanthramide B-1, we found that the CAN deprotection was successful on an electronically neutral aryl ring on the aldehyde portion of the imine but could not be repeated when the adjacent aryl ring was highly electron donating. We hypothesized that these novel electron withdrawing imine substrates might circumvent the issue observed in our previous attempt. Thus, the symmetrical bis- γ -lactam diastereomer **60** was isolated in modest yield and subjected to cerium ammonium nitrate (CAN) deprotection conditions. The reaction resulted in 90% conversion to the desired N-H bis- γ -lactam **82** (Figure 4.21)! However, subsequent attempts to scale up the CAN double-deprotection reaction resulted in poor yields in comparison to our final

route, which will be discussed in the next section and this route was subsequently abandoned.

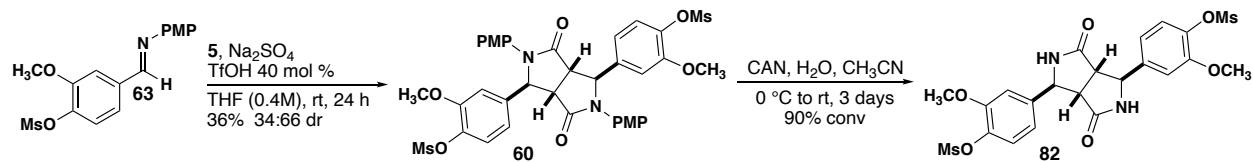


Figure 4.21 Successful synthesis of *N*-H bis-lactam through CAN deprotection

4.2.6.2 PIFA Deprotection of *N*-Phenol Lactam to *N*-H Bis- γ -lactam

Finally, the PIFA oxidation reaction was attempted in order to yield the *N*-H bis- γ -lactam product. To begin this route, bis- γ -lactam **59** was synthesized from **65** using optimized conditions affording a 40:60 ratio of symmetrical to unsymmetrical diastereomers and 25% yield of **62**. Deprotection of **59** to yield *N*-phenol intermediate (**83**) proceeded in excellent yield using BCl_3 conditions. Next, **83** was deprotected using PIFA deprotection conditions and the desired *N*-H bis-lactam **82** was obtained in 92% yield (Figure 4.22).

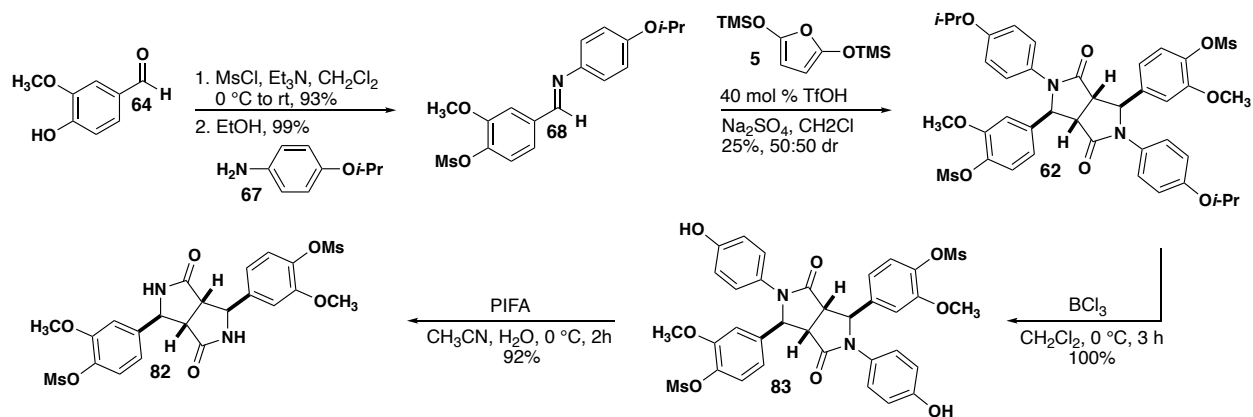


Figure 4.22 Optimized route to *N*-H bis- γ -lactam **82**.

4.2.7 Failure of the Buchwald Bis-Arylation

With the *N*-H lactam finally in hand, my goal was to optimize conditions for a copper-mediated Buchwald bis-arylation which would install the aryl groups containing ester precursors to the necessary *ortho*-carboxylic acid substituents. Nico Havenner worked to synthesize the aryl-iodide (**27**) coupling agent used in the synthesis of bisavenanthramide B-6. To do this, he first performed a Sandmeyer reaction on 2-amino-5-hydroxybenzoic acid to afford iodide (**85**) in modest yield. He then esterified the carboxylic acid moiety using acetyl chloride and methanol, yielding phenol **86** in 88% yield (Figure 4.23). **86** was then used to synthesize both **27** and the methane sulfonyl protected aryl iodide (**87**). Performing the Buchwald bis-arylation with **87** would allow for a global deprotection of both aryl rings, while **27** would be the most comparable to the successful synthesis of bisavenanthramide B-6. He was able to obtain the Buchwald coupling agents **86** and **87** in 24% and 97% yield, respectively

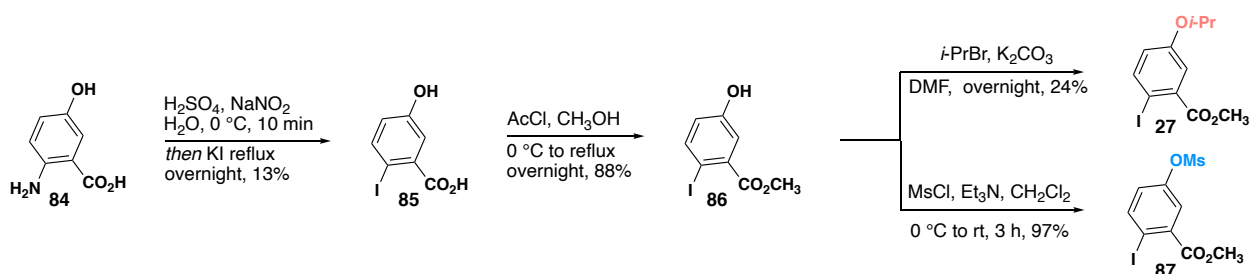


Figure 4.23 Synthesis of aryl iodides **27** and **87** for the Buchwald bis-arylation

As described previously, one major drawback of the double Mukaiyama CCR is the poor yield for the desired symmetrical diastereomer. To compound this, the two deprotection steps to afford **82** result in a decrease in mass of the product. Even running the double-addition reactions on large scale only provides a few hundred milligrams of

material to move forward in the synthesis. In order to obtain an appreciable amount of starting material, multiple reactions were performed in parallel and subsequently combined to afford bis- γ -lactam **62**. As a result, after significant optimization of the previous five steps, only two attempts were made to perform the double Buchwald arylation—one with aryl iodide **27**, and one with **87**, both of which resulted in 0% conversion to the desired product (Figure 4.24).

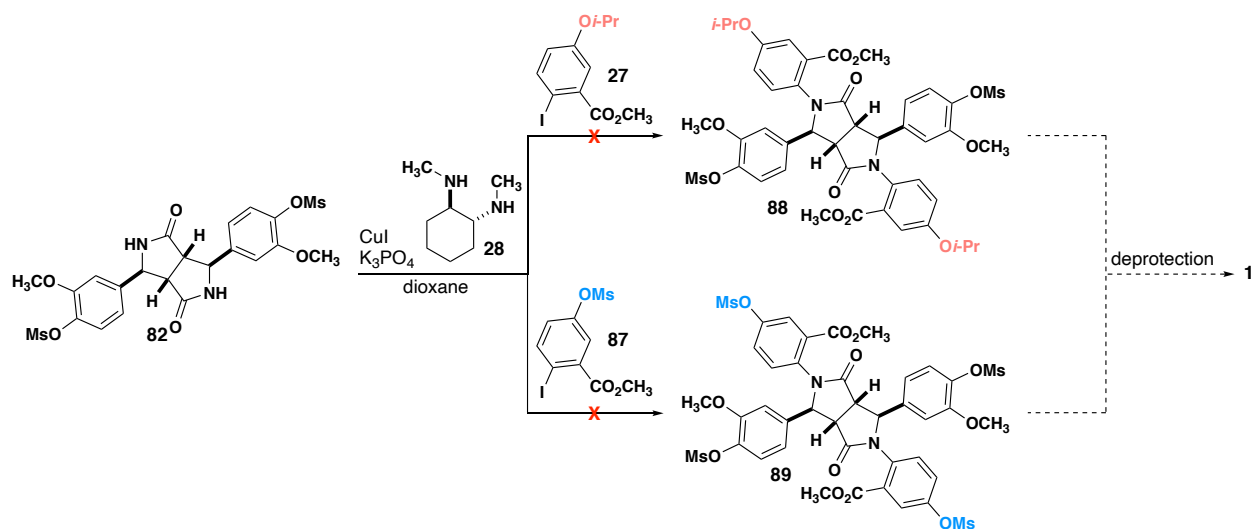


Figure 4.24 Final attempts at synthesizing bisavenanthramide B-1 through the Buchwald bis-arylation.

4.3 Conclusion and Future Work

Using the Mukaiyama-like CCR, I have made significant progress toward the synthesis of bisavenanthramide B-1. The current limitations to this synthesis include the poor yield and diastereoselectivity of the key Mukaiyama Mannich reaction. While better yields have been observed for the substrates described in chapter 2, the new electron withdrawing substrates used in the final route were consistently below 50% yield with a 50:50 mixture of diastereomers. Additionally, the electronics of the aryl aldehyde derived portion of the molecule has had a significant impact on the reactivity of the bis- γ -lactam

product, namely with respect to the CAN deprotection and directed bromination. With this in mind, it might be possible that the failure of the Buchwald bis-arylation results from changing the electronics of the aryl aldehyde-derived ring compared to bisavenanthramide B-6.

Future work will require significant optimization of the Buchwald bis-arylation. Additionally, utilizing a different protecting group on the aryl aldehyde derived portion of the molecule could improve both the yield and reactivity in the bis-arylation reaction. Our modified route relied on the orthogonality of the protecting groups on the bis- γ -lactam, however it is possible that the PIFA oxidation could occur even on the deprotected intermediate **90** (Figure 4.25). Using bis- γ -lactam **36**, it is possible that a double BCl_3 deprotection followed by double PIFA deprotection could produce bis- γ -lactam **91**. This new intermediate can then be isopropylated to afford intermediate **92**, which is more electronically similar to the lactam used in the synthesis of bisavenanthramide B-6. Optimization of the Buchwald bis-arylation followed by global deprotection could then afford bisavenanthramide B-1.

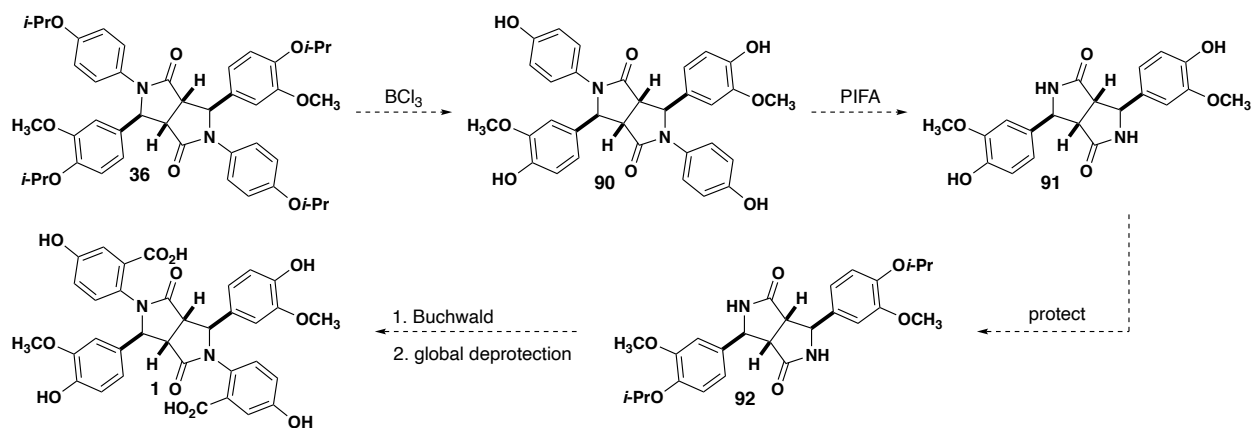


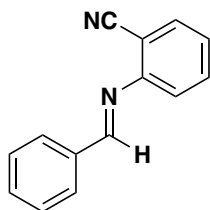
Figure 4.25 Possible route toward the synthesis of bisavenanthramide B-1

Additionally, a more thorough optimization of the directed bromination reaction might be worth pursuing. Changing the electronics of the aldehyde derived portion of the aryl ring resulted in a 50:50 mixture of the doubly brominated product and starting material **62** (Figure 4.26). Optimizing the reaction conditions to improve conversion to the desired brominated product could ultimately lead to the synthesis of bisavenanthramide B-1.

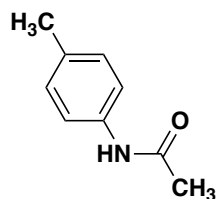


Figure 4.26 Possible optimization of bromination reaction

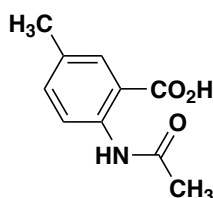
4.4 Experimental Section



(2-(benzylideneamino)benzonitrile (33)): Following a modified literature procedure,³⁵ to a flame dried round bottom flask was added 2-aminobenzonitrile (0.5 g, 4.23 mmol) and dissolved in toluene (9.3 mL, 0.5M). 4 Å mol sieves (2.5 g) were added to the reaction flask. Benzaldehyde (0.47 mL, 4.65 mmol) was added, and the reaction was heated to reflux overnight. The reaction was then cooled, filtered through celite, and concentrated in vacuo. The unpurified reaction was recrystallized in EtOH to afford **33** (0.658, 70%). ¹H NMR (400 MHz, CDCl₃) δ 8.48 (s, 1H), 8.00 – 7.94 (m, 2H), 7.68 (dd, *J* = 7.7, 1.5 Hz, 1H), 7.59 (td, *J* = 7.8, 1.5 Hz, 1H), 7.56 – 7.45 (m, 3H), 7.31 – 7.24 (m, 1H), 7.18 (dd, *J* = 8.1, 1.1 Hz, 1H). ¹H NMR spectrum matches literature values.³⁵

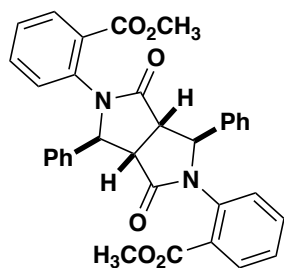


***N*-(*p*-tolyl)acetamide (39):** Following a modified literature procedure,³⁶ to a flame dried round bottom flask under argon was added 4-methylaniline (0.160 g, 1.5 mmol). Acetic anhydride (0.142 mL, 1.5 mmol) and glacial acetic acid (0.15 mL, 2.63 mmol) were added, and the reaction was heated to reflux for one hour. The reaction was cooled to room temperature and poured into 20 mL ice cold H₂O and filtered. The unpurified reaction mixture was recrystallized in 2:1 H₂O:AcOH to afford **39** as a white solid (0.85 mg, 38%). ¹H NMR (400 MHz, CDCl₃) δ 7.37 (d, *J* = 8.2 Hz, 2H), 7.12 (d, *J* = 8.0 Hz, 2H), 2.31 (s, 3H), 2.16 (s, 3H).



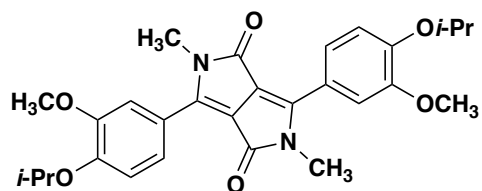
2-acetamido-5-methylbenzoic acid (40): Following a modified literature procedure,³⁰ to a flame dried round bottom flask under argon was added **39** (0.075 g, 0.5 mmol), Pd(OAc)₂ (0.011 g, 0.05 mmol), *p*-TsOH (0.048 g, 0.25 mmol), and *p*-benzoquinone (0.054 g, 0.5 mmol). AcOH:toluene (2:1, 1.0 mL) was added, the reaction was sparged with a balloon of CO for 10 minutes. An additional balloon of CO was added to the reaction and heated to 60 °C. After 7 hours, the reaction was cooled to room temperature and concentrated in vacuo. The unpurified reaction mixture was dissolved in NaHCO₃ and washed 3x with CH₂Cl₂ (5 mL). The aqueous layer was acidified with 6 N HCl at 0 °C and

extracted 5x with EtOAc (2 mL). The organic layer was washed with H₂O, dried over Na₂SO₄ and concentrated in vacuo. ¹H NMR (400 MHz, CDCl₃) δ 10.77 (s, 1H), 8.61 (d, *J* = 8.7 Hz, 1H), 7.91 (d, *J* = 1.8 Hz, 1H), 7.41 (d, *J* = 8.8 Hz, 1H), 6.72 (s, 1H), 2.35 (s, 3H), 2.24 (s, 3H).



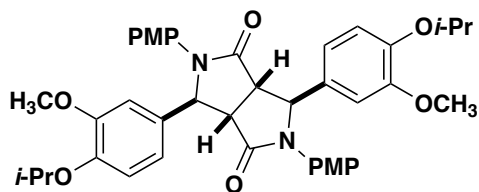
dimethyl 2,2'-(1,4-dioxo-3,6-diphenyltetrahydropyrrolo[3,4-c]pyrrole-2,5(1H,3H)-diyl)dibenzoate (43a) Following a modified literature procedure,³⁰ to a flame dried round bottom flask under argon was added **41a** (0.050 g, 0.112 mmol), Pd(OAc)₂ (0.005 g, 0.022 mmol), *p*-TsOH (0.021 g, 0.112 mmol), and *p*-benzoquinone (0.024 g, 0.224 mmol). AcOH:toluene (2:1, 1.0 mL) was added, the reaction was sparged with a balloon of CO for 10 minutes. An additional balloon of CO was added to the reaction and heated to 60 °C overnight. The reaction was then cooled to room temperature and concentrated in vacuo. The unpurified reaction mixture was dissolved in NaHCO₃ and washed 3x with CH₂Cl₂ (5 mL). The aqueous layer was acidified with 6 N HCl at 0 °C and extracted 5x with EtOAc (2 mL). The organic layer was washed with H₂O and dried over Na₂SO₄ and concentrated in vacuo. The unpurified reaction mixture was dissolved in CH₃OH (2 mL) and TMSCHN₂ (0.280 mL, 2M in hexane) was added, and the reaction was stirred at room temperature overnight. The reaction was quenched with AcOH (0.050 mL) and concentrated in vacuo. The unpurified reaction mixture was purified by flash column chromatography (70:30 hexanes:EtOAc) to afford the putative product **41a**. ¹H NMR (400

MHz, CDCl₃) δ 7.84 – 7.76 (m, 4H), 7.57 (t, *J* = 6.5 Hz, 4H), 7.45 (q, *J* = 7.4 Hz, 6H), 7.33 (d, *J* = 4.3 Hz, 4H), 5.12 (s, 2H), 4.61 (s, 2H), 3.35 (s, 6H).



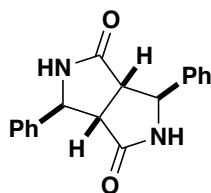
3,6-bis(4-isopropoxy-3-methoxyphenyl)-2,5-dimethyl-2,5-dihydropyrrolo[3,4-c]pyrrole-1,4-dione (48) Following a modified literature procedure,³⁰ to a flame dried round bottom flask under argon was added **36** (0.064 g, 0.087mmol), Pd(OAc)₂ (0.004 g, 0.017 mmol), *p*-TsOH (0.017 g, 0.087 mmol), and *p*-benzoquinone (0.019 g, 0.174 mmol). AcOH:toluene (2:1, 2.0 mL) was added, the reaction was sparged with a balloon of CO for 10 minutes. An additional balloon of CO was added to the reaction and heated to 60 °C overnight. The reaction was then cooled to room temperature. **Note:** The unpurified reaction mixture was not concentrated in vacuo. Instead, NaHCO₃ was added to the reaction mixture, which reacted violently, then washed 3x with CH₂Cl₂ (5 mL). The aqueous layer was acidified with 6 N HCl at 0 °C and extracted 5x with EtOAc (2 mL). The organic layer was washed with H₂O and dried over Na₂SO₄ and concentrated in vacuo. The unpurified reaction mixture was dissolved in CH₃OH (2 mL) and TMSCHN₂ (0.280 mL, 2M in hexane) was added, and the reaction was stirred at room temperature overnight. The reaction was quenched with AcOH (0.2 mL) and concentrated in vacuo. The unpurified reaction mixture was purified by flash column chromatography (70:30 hexanes:EtOAc) to afford the putative product **48**. ¹H NMR (400 MHz, CDCl₃) δ 7.64 (d,

$J = 8.4$ Hz, 2H), 7.55 (s, 2H), 6.89 (d, $J = 8.5$ Hz, 2H), 4.65 (p, $J = 6.3$ Hz, 2H), 3.91 (s, 6H), 3.89 (d, $J = 1.5$ Hz, 6H), 1.41 (dd, $J = 6.1, 1.4$ Hz, 12H).



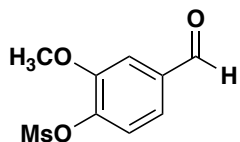
3,6-bis(4-isopropoxy-3-methoxyphenyl)-2,5-bis(4-methoxyphenyl)hexa-

hydropyrrolo[3,4-c]pyrrole-1,4-dione (55): Na_2SO_4 (0.474, 3.34 mmol) was flame dried in a round bottom flask under argon. Imine **60** (1.0 g, 3.34 mmol) was added followed by 2,5-bis(trimethylsilyloxy)furan (4.2 mL, 0.4 Min THF). An additional portion of THF was added (8.36 mL, 0.2 M). TfOH (0.029 mL, 0.334 mmol) was added, and the reaction was sealed with parafilm. After 24 hours at room temperature, NH_4Cl was added to the reaction using air-free technique. The reaction was then extracted 3x with EtOAc (15 mL) dried over Na_2SO_4 and concentrated in vacuo. The product was purified by flash column chromatography 30-100% EtOAc in hexanes to afford **55** 31:79 dr (sym:unsym) (0.071 g, 6%). ^1H NMR (600 MHz, CDCl_3) δ 7.42 (d, $J = 9.1$ Hz, 4H), 6.83 – 6.75 (m, 10H), 5.57 (s, 2H), 4.46 (hept, $J = 5.4$ Hz, 2H), 3.81 (s, 6H), 3.75 (s, 6H), 3.37 (d, $J = 2.1$ Hz, 2H), 1.33 (d, 12H).

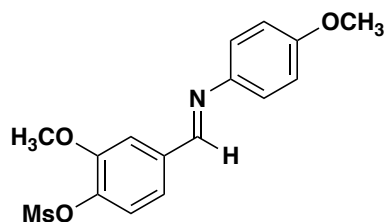


3,6-diphenylhexahydropyrrolo[3,4-c]pyrrole-1,4-dione (59). **58** (0.012 g, 0.024 mmol) was dissolved in CH_3CN at 0 °C. Cerium ammonium nitrate (0.104 mg, 0.190 mmol) was

dissolved in H₂O at 0 °C and added to the solution and warmed up to room temperature. After 18 h, the reaction was cooled to 0 °C and another portion of cerium ammonium nitrate was added to the reaction and stirred for another 6 h. NaHCO₃ was then added, and the reaction was extracted 3x with EtOAc (5 mL). The reaction was acidified, and extracted with 3x EtOAc (5 mL), dried over Na₂SO₄ and concentrated in vacuo. The desired product **59** was isolated from the first organic extract. ¹H NMR (400 MHz, CDCl₃) δ 7.38 – 7.28 (m, 10H), 6.85 (s, 2H), 5.09 (s, 2H), 3.16 (s, 2H).

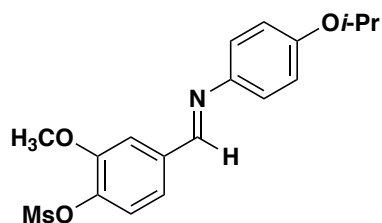


4-formyl-2-methoxyphenyl methanesulfonate (64) Following a modified literature procedure:³⁷ To a flame dried round bottom flask was added vanillin (3.0 g, 20 mmol) and dissolved in CH₂Cl₂ (10 mL). Methanesulfonyl chloride (1.5 mL, 20 mmol) was added, and the reaction was cooled to 0 °C. Et₃N was added and the reaction was stirred at RT for 3 h. The reaction was then quenched with H₂O (10 mL), extracted 3x with CH₂Cl₂ (15 mL), dried over Na₂SO₄ and concentrated in vacuo. The unpurified reaction mixture was purified by recrystallization in EtOH to afford **64** (4.28 g, 93%) as a white crystalline solid. ¹H NMR (400 MHz, CDCl₃) δ 9.97 (d, *J* = 1.4 Hz, 1H), 7.54 (d, *J* = 1.6 Hz, 1H), 7.51 – 7.46 (m, 2H), 3.98 (s, 4H), 3.25 (s, 3H).



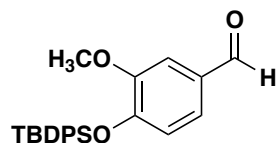
(E)-2-methoxy-4-(((4-methoxyphenyl)imino)methyl)phenyl methanesulfonate (66)

p-anisidine (2.5 g, 20 mmol) and aldehyde **65** (4.6 g, 20 mmol) were dissolved in EtOH (10 mL, 0.5 M) and stirred overnight. The reaction was filtered and recrystallized in EtOH to afford **66** (5.4 g, 91%) as a grey solid. ¹H NMR (300 MHz, CDCl₃) δ 8.44 (s, 1H), 7.73 (s, 1H), 7.45 – 7.31 (m, 2H), 7.25 (d, *J* = 9.4 Hz, 3H), 6.94 (d, *J* = 8.2 Hz, 1H), 4.00 (s, 3H), 3.84 (s, 3H), 3.22 (s, 3H).

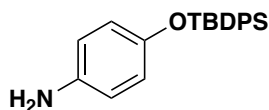


4-(((4-isopropoxyphenyl)imino)methyl)-2-methoxyphenyl methanesulfonate (68)

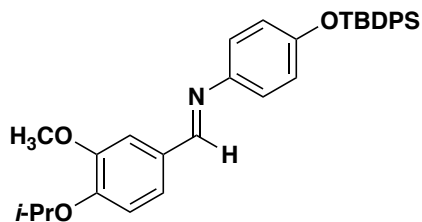
Aniline **67** (0.5 g, 3.3 mmol) and aldehyde **65** (0.759 g, 3.3 mmol) were dissolved in EtOH and stirred overnight. The reaction was filtered and recrystallized in EtOH to afford **68** (0.787 g, 66%). ¹H NMR (400 MHz, CDCl₃) δ 8.44 (s, 1H), 7.73 (s, 1H), 7.43 – 7.30 (m, 2H), 7.22 (d, *J* = 8.4 Hz, 2H), 6.92 (d, *J* = 8.3 Hz, 2H), 4.56 (p, *J* = 6.1 Hz, 1H), 4.00 (s, 3H), 3.22 (s, 3H), 1.36 (d, *J* = 6.0 Hz, 6H).



4-((*tert*-butyldiphenylsilyloxy)-3-methoxybenzaldehyde (69) To a flame dried round bottom flask was added vanillin (1.945 g, 12.8 mmol) and dissolved in CH₂Cl₂ (42 mL, 0.3 M). Imidazole (1.742 g, 25.6 mmol) was added, and the reaction was stirred for 15 min before TBDPSCI (3.3 mL, 12.8 mmol) was added. After 24 h, H₂O was added. The unpurified reaction was extracted 3x with CH₂Cl₂ (15 mL), dried over Na₂SO₄ and concentrated in vacuo. The unpurified reaction mixture was purified by gradient flash column chromatography 2-40% EtOAc in hexanes to afford **69** (3.4 g, 68%) as a clear oil. ¹H NMR (400 MHz, CDCl₃) δ 9.76 (d, *J* = 1.3 Hz, 1H), 7.79 – 7.64 (m, 4H), 7.51 – 7.24 (m, 8H), 6.79 (dd, *J* = 8.2, 1.3 Hz, 1H), 3.63 (d, *J* = 1.3 Hz, 3H), 1.12 (d, *J* = 1.3 Hz, 9H).

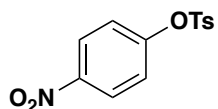


4-((*tert*-butyldiphenylsilyloxy)aniline (72) Following a modified literature procedure:³⁸ 4-aminophenol was added to a flame dried flask under argon. CH₂Cl₂ (167 mL, 0.09 M) was added to the flask using a cannula. Imidazole (1.7 mL, 30.42 mmol) was added, followed by TBDPSCI (2.2 mL, 8.4 mmol). **Note:** an excess of imidazole and 4-aminophenol were used erroneously. After 24 h, the reaction was concentrated in vacuo. The unpurified product was purified by flash column chromatography in CH₂Cl₂ to afford product **72** in quantitative yield (2.9 g, 100%). ¹H NMR (600 MHz, CDCl₃) δ 7.71 (d, *J* = 7.3 Hz, 4H), 7.41 – 7.37 (m, 2H), 7.34 (d, *J* = 15.0 Hz, 4H), 6.58 (d, *J* = 8.7 Hz, 2H), 6.42 (d, *J* = 8.7 Hz, 2H), 3.28 (s, 2H), 1.08 (s, 9H). ¹H NMR matches literature values.³⁸



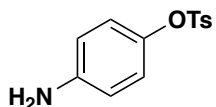
(*N*-(4-((*tert*-butyldiphenylsilyl)oxy)phenyl)-1-(4-isopropoxy-3-

methoxyphenyl)methanimine (74). Following a modified literature procedure:³⁹ To a flame dried round bottom flask was added aniline **72** (1.3 g, 4.0 mmol) and **73** (0.776 g, 4 mmol) and dissolved in EtOH (20 mL, 0.2 M). The reaction was stirred to reflux and stirred overnight. After 24 h, the reaction was cooled and concentrated to afford **74** (1.78 g, 85%) as a yellow oil. ¹H NMR (600 MHz, CDCl₃) δ 8.30 (s, 1H), 7.73 (d, *J* = 7.3 Hz, 4H), 7.54 (s, 1H), 7.45 – 7.30 (m, 6H), 7.21 (d, *J* = 6.2 Hz, 1H), 6.99 (d, *J* = 8.7 Hz, 2H), 6.91 (d, *J* = 8.3 Hz, 1H), 6.77 (d, *J* = 8.7 Hz, 2H), 4.62 (p, *J* = 6.1 Hz, 1H), 3.93 (s, 3H), 1.40 (d, *J* = 6.1 Hz, 6H), 1.11 (d, *J* = 5.3 Hz, 9H).

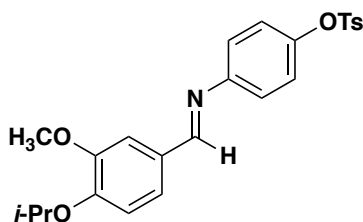


4-nitrophenyl 4-methylbenzenesulfonate (75) Following a modified literature procedure:⁴⁰ To a round bottom flask was added 4-nitrophenol (0.948 g, 6.8 mmol) and dissolved in THF (4.3 mL, 1.6 M w.r.t 4-nitrophenol). 10% K₂CO₃ aqueous solution (17 mL) was added, and the reaction was cooled to 0 °C. *p*-toluenesulfonyl chloride (1.3 g, 6.9 mmol) was added to the reaction as a solution in THF (9.54 mL, 0.72 M w.r.t. TsCl) over 5 minutes. The reaction was stirred at room temperature and monitored by TLC until the reaction was complete. EtOAc (15 mL) was added, and the reaction was washed with H₂O (15 mL), dried over Na₂SO₄, concentrated in vacuo and used without further

purification (1.92 g, 96%). $^1\text{H NMR}$ (400 MHz, CDCl_3) δ 8.19 (d, $J = 8.7$ Hz, 2H), 7.73 (d, $J = 8.0$ Hz, 2H), 7.36 (d, $J = 7.9$ Hz, 2H), 7.19 (d, $J = 8.7$ Hz, 2H), 2.47 (s, 3H).

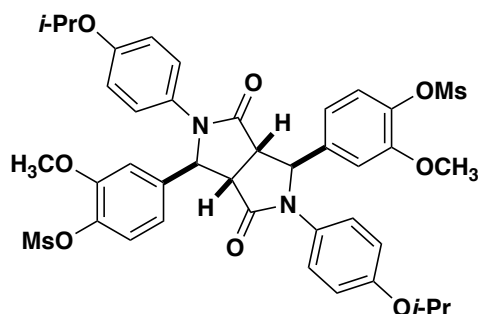


4-aminophenyl 4-methylbenzenesulfonate (76). Following a modified literature procedure:⁴¹ To a flame dried round bottom flask was added **75** (1.9 g, 6.5 mmol), HFIP (6.8 mL, 65 mmol), and Fe (powder) (1.8 g, 32.5 mmol). 2N HCl was added (65 mL) and stirred at rt for 30 min. The reaction was neutralized with saturated NaHCO_3 , extracted 3x with EtOAc (15 mL), and washed with brine. The unpurified reaction mixture was dried over Na_2SO_4 and concentrated. The product was purified by gradient flash column chromatography 20-100% EtOAc in hexanes to afford **76** (1.31 g, 76%). $^1\text{H NMR}$ (400 MHz, CDCl_3) δ 7.68 (d, $J = 7.9$ Hz, 2H), 7.29 (d, $J = 7.9$ Hz, 2H), 6.73 (d, $J = 9.1$ Hz, 2H), 6.52 (d, $J = 8.7$ Hz, 2H), 3.66 (s, 2H), 2.44 (s, 3H).

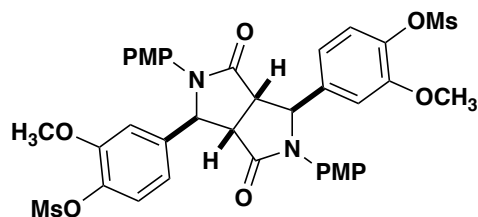


4-((4-isopropoxy-3-methoxybenzylidene)amino)phenyl 4-methylbenzenesulfonate (78) Following a modified literature procedure:⁴² Aniline **76** (0.40 g, 1.5 mmol) and aldehyde **64** (0.291 g, 1.5 mmol) were dissolved in EtOH and stirred overnight. The reaction was filtered and used without further purification to afford **78** (0.480 g, 73%). $^1\text{H NMR}$ (400 MHz, CDCl_3) δ 8.28 (s, 1H), 7.70 (d, $J = 8.1$ Hz, 3H), 7.55 (s, 1H), 7.31 (s, 2H),

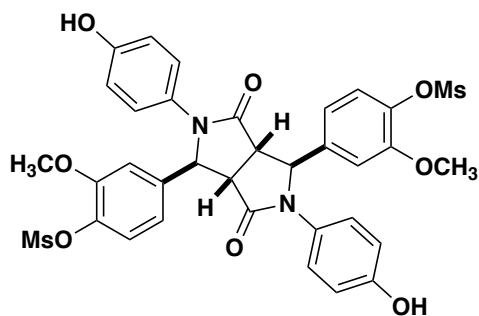
7.08 (d, $J = 8.2$ Hz, 2H), 6.95 (dd, $J = 15.1, 8.3$ Hz, 3H), 4.64 (p, $J = 6.1$ Hz, 1H), 3.92 (s, 3H), 2.43 (s, 3H), 1.41 (d, $J = 6.1$ Hz, 6H).



((1S,3aS,4S,6aS)-2,5-bis(4-isopropoxyphenyl)-3,6-dioxooctahydropyrrolo[3,4-c]pyrrole-1,4-diyl)bis(2-methoxy-4,1-phenylene) dimethanesulfonate (62) Na₂SO₄ (0.057, 0.4 mmol) was flame dried in a round bottom flask under argon. Imine **68** (0.132 g, 0.4 mmol) was dissolved in CH₂Cl₂ (1.0 mL, 0.2 M). added followed by 2,5-bis(trimethylsilyloxy)furan (0.050 mL 0.2 mmol). TfOH (0.007 mL, 0.08 mmol) was added, and the reaction was sealed with parafilm. After 24 hours at rt, NH₄Cl was added to the reaction using air-free technique. The reaction was then extracted 3x with EtOAc (15 mL) dried over Na₂SO₄ and concentrated. The product was purified by flash column chromatography 30-100% EtOAc in hexanes to afford **62** (0.040 g, 25%) a yellow foam, as a 50:50 (sym:unsym) mixture of diastereomers. ¹H NMR (400 MHz, CDCl₃) δ 7.38 (d, $J = 8.6$ Hz, 4H), 7.25 (s, 2H), 6.94 – 6.79 (m, 8H), 5.64 (s, 2H), 4.55 – 4.42 (m, 2H), 3.87 (s, 6H), 3.31 (s, 2H), 3.17 (d, $J = 1.4$ Hz, 6H), 1.29 (dd, $J = 6.1, 1.5$ Hz, 12H).

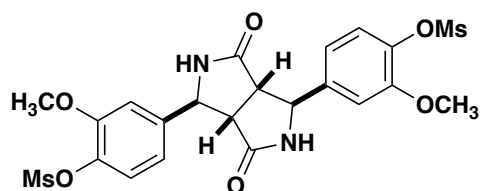


(2,5-bis(4-methoxyphenyl)-3,6-dioxooctahydropyrrolo[3,4-c]pyrrole-1,4-diyl)bis(2-methoxy-4,1-phenylene) dimethanesulfonate (63) Na₂SO₄ (0.113 g, 0.8 mmol) was flame dried in a round bottom flask under argon. Imine **66** (0.240 g, 0.8 mmol) was added followed by 2,5-bis(trimethylsilyloxy)furan (1 mL, 0.4M in THF). An additional portion of THF was added (1 mL). TfOH (0.010 mL, 0.16mmol) was added, and the reaction was sealed with parafilm. After 24 hours at rt, NH₄Cl was added to the reaction using air-free technique. The reaction was then extracted 3x with EtOAc (15 mL) dried over Na₂SO₄ and concentrated. The product was purified by flash column chromatography 30-100% EtOAc in hexanes to afford **63** (0.174 g, 36%) as a 34:66 (sym:unsym) mixture of diastereomers. ¹H NMR (600 MHz, CDCl₃) δ 7.44 – 7.37 (m, 4H), 7.24 (s, 2H), 6.94 (d, *J* = 2.1 Hz, 2H), 6.88 – 6.80 (m, 6H), 5.65 (d, *J* = 1.8 Hz, 2H), 3.85 (s, 6H), 3.75 (s, 6H), 3.34 (d, *J* = 2.3 Hz, 2H), 3.15 (s, 6H).



(2,5-bis(4-hydroxyphenyl)-3,6-dioxooctahydropyrrolo[3,4-c]pyrrole-1,4-diyl)bis(2-methoxy-4,1-phenylene) dimethanesulfonate (83). Following a modified literature procedure:²⁸ To a flame dried round bottom flask was added **62** (0.150 g, 0.186 mmol) and dissolved in CH₂Cl₂ (1.55 mL, 0.12 M). The solution was cooled to 0 °C and BCl₃ (2.22 mL, 1M in CH₂Cl₂) was added dropwise. The reaction was stirred at 0 °C for 1h, after which the reaction was warmed to rt and stirred for an additional 2 h. The reaction

was quenched with H₂O, extracted 3x with EtOAc (5 mL), dried over Na₂SO₄ and concentrated in vacuo. The unpurified reaction mixture was purified by flash column chromatography 70-100% EtOAc in hexanes to afford **83** in (0.134 g, 100%). ¹H NMR (600 MHz, CD₃OD) δ 7.26 – 7.21 (m, 6H), 7.11 (s, 2H), 6.96 (d, *J* = 8.3 Hz, 2H), 6.75 – 6.70 (m, 4H), 5.56 (s, 2H), 3.86 (d, *J* = 1.8 Hz, 6H), 3.67 (s, 2H), 3.16 (d, *J* = 1.8 Hz, 6H).



(3,6-dioxooctahydropyrrolo[3,4-c]pyrrole-1,4-diyl)bis(2-methoxy-4,1-phenylene)

dimethanesulfonate (82) Following a modified literature procedure:⁴³ To a vial was added **83** (0.157 g, 0.216 mmol) and dissolved in a 9:1 CH₃CN:H₂O (2 mL) mixture. The solution was cooled to 0 °C and PIFA (0.204 g, 0.476 mmol) was added. The reaction was stirred for 2 h and then concentrated. The unpurified reaction mixture was purified by flash column chromatography 99:1 CH₂Cl₂:CH₃OH to afford **82** (0.107 g, 92%). ¹H NMR (600 MHz, CDCl₃) δ 7.30 (d, *J* = 8.2 Hz, 2H), 6.91 (d, *J* = 14.2 Hz, 4H), 6.12 (s, 2H), 5.08 (s, 2H), 3.90 (s, 6H), 3.19 (s, 6H), 3.15 (s, 2H).

4.5 References

1. Miyagawa, H.; Ishihara, A.; Nishimoto, T.; Ueno, T.; Mayama, S., *Biosci. Biotechnol. Biochem.* **1995**, *59* (12), 2305-2306.
2. Ishihara, A.; Miyagawa, H.; Matsukawa, T.; Ueno, T.; Mayama, S.; Iwamura, H., *Phytochemistry* **1998**, *47* (6), 969-974.
3. Ishihara, A.; Ohtsu, Y.; Iwamura, H., *Planta* **1999**, *208* (4), 512-518.
4. Ishihara, A.; Ohtsu, Y.; Iwamura, H., *Phytochemistry* **1999**, *50* (2), 237-242.
5. Okazaki, Y.; Ishihara, A.; Nishioka, T.; Iwamura, H., *Tetrahedron* **2004**, *60* (22), 4765-4771.
6. Okazaki, Y.; Isobe, T.; Iwata, Y.; Matsukawa, T.; Matsuda, F.; Miyagawa, H.; Ishihara, A.; Nishioka, T.; Iwamura, H., *Plant. J.* **2004**, *39* (4), 560-572.
7. Okazaki, Y.; Ishizuka, A.; Ishihara, A.; Nishioka, T.; Iwamura, H., *J. Org. Chem.* **2007**, *72* (10), 3830-3839.
8. Laws, S. W.; Howard, S. Y.; Mato, R.; Meng, S.; Fettingner, J. C.; Shaw, J. T., *Org. Lett.* **2019**, *21* (13), 5073-5077.
9. Mayama, S.; Tani, T., *Physiol. Plant Pathol.* **1982**, *21* (2), 141-149.
10. Mayama, S.; Tani, T.; Ueno, T.; Midland, S. L.; Sims, J. J.; Keen, N. T., *Physiol. Mol. Plant. Path.* **1986**, *29* (1), 1-18.
11. Collins, F. W., *J. Agric. Food Chem.* **1989**, *37* (1), 60-66.
12. Fink, W.; Liefland, M.; Mendgen, K., *Physiol. Mol. Plant. Path.* **1990**, *37* (4), 309-321.

13. Cushman, M.; Cheng, L., *J. Org. Chem.* **1978**, *43* (2), 286-288.
14. Cushman, M.; Dekow, F. W., *Tetrahedron* **1978**, *34* (10), 1435-1439.
15. Cushman, M.; Choong, T.-C.; Valko, J. T.; Koleck, M. P., *J. Org. Chem.* **1980**, *45* (25), 5067-73.
16. Cushman, M.; Choong, T. C.; Valko, J. T.; Koleck, M. P., *Tetrahedron Lett.* **1980**, *21* (40), 3845-3848.
17. Cushman, M.; Abbaspour, A.; Gupta, Y. P., *Heterocycles* **1982**, *19* (9), 1587-1590.
18. Cushman, M.; Gupta, Y. P., *Heterocycles* **1982**, *19* (8), 1431-1433.
19. Cushman, M.; Mohan, P.; Smith, E. C. R., *J. Med. Chem.* **1984**, *27* (4), 544-547.
20. Smidrkal, J., *Collect. Czechoslov. Chem. Commun.* **1984**, *49* (6), 1412-1420.
21. Cushman, M.; Chen, J. K., *J. Org. Chem.* **1987**, *52* (8), 1517-1521.
22. Cushman, M.; Dekow, F. W., *J. Org. Chem.* **1979**, *44* (3), 407-409.
23. Iwasa, K.; Gupta, Y. P.; Cushman, M., *Tetrahedron Lett.* **1981**, *22* (25), 2333-2336.
24. Iwasa, K.; Gupta, Y. P.; Cushman, M., *J. Org. Chem.* **1981**, *46* (23), 4744-4750.
25. Cushman, M.; Abbaspour, A.; Gupta, Y. P., *J. Am. Chem. Soc.* **1983**, *105* (9), 2873-2879.
26. Cushman, M.; Wong, W. C., *J. Org. Chem.* **1984**, *49* (7), 1278-1280.
27. Younai, A.; Chin, G. F.; Shaw, J. T., *J. Org. Chem.* **2010**, *75* (23), 8333-8336.
28. Di Maso, M. J.; Nepomuceno, G. M.; St. Peter, M. A.; Gitre, H. H.; Martin, K. S.; Shaw, J. T., *Org. Lett.* **2016**, *18* (8), 1740-1743.
29. Laws, S. W., **2019**.
30. Giri, R.; Lam, J. K.; Yu, J.-Q., *J. Am. Chem. Soc.* **2010**, *132* (2), 686-693.

31. See chapter 3 for a detailed discussion.
32. Lockman, J. W.; Murphy, B. R.; Zigar, D. F.; Judd, W. R.; Slattum, P. M.; Gao, Z.-H.; Ostanin, K.; Green, J.; McKinnon, R.; Terry-Lorenzo, R. T.; Fleischer, T. C.; Boniface, J. J.; Shenderovich, M.; Willardsen, J. A., *J. Med. Chem.* **2010**, *53* (24), 8734-8746.
33. Guyonnet, M.; Baudoin, O., *Org. Lett.* **2012**, *14* (1), 398-401.
34. Li, Z.-I.; Sun, K.-k.; Cai, C., *Org. Biomol. Chem.* **2018**, *16* (30), 5433-5440.
35. Leijendekker, L. H.; Weweler, J.; Leuther, T. M.; Streuff, J., *Angew. Chem. Int. Ed.* **2017**, *56* (22), 6103-6106.
36. Govender, H.; Mocktar, C.; Koorbanally, N. A., *J. Heterocycl. Chem.* **2018**, *55* (4), 1002-1009.
37. Kazancıoğlu, E. A.; Güney, M.; Şentürk, M.; Supuran, C. T., *J. Enzyme Inhib. Med. Chem.* **2012**, *27* (6), 880-885.
38. Handayani, M.; Gohda, S.; Tanaka, D.; Ogawa, T., *Chem. Eur. J.* **2014**, *20* (25), 7655-7664.
39. O'Boyle, N. M.; Pollock, J. K.; Carr, M.; Knox, A. J. S.; Nathwani, S. M.; Wang, S.; Caboni, L.; Zisterer, D. M.; Meegan, M. J., *J. Med. Chem.* **2014**, *57* (22), 9370-9382.
40. Lei, X.; Jalla, A.; Shama, M. A. A.; Stafford, J. M.; Cao, B., *Synthesis* **2015**, *47*, 2578-2585.
41. Chen, X.-L.; Ai, B.-R.; Dong, Y.; Zhang, X.-M.; Wang, J.-Y., *Tetrahedron Lett.* **2017**, *58* (37), 3646-3649.
42. Kağıt, R.; Dayan, O.; Özdemir, N., *Polyhedron* **2016**, *117*, 504-512.

43. Southgate, E. H.; Holycross, D. R.; Sarlah, D., *Angew. Chem. Int. Ed.* **2017**, *56* (47), 15049-15052.

Chapter 5: Mechanistic Investigation of the Multicomponent Variants of the Castagnoli-Cushman Reaction

5.1 Introduction

Several decades after the first CCR was performed, the first 3- and 4-component variants of the CCR were developed with amines, aldehydes, anhydrides (3CR) and thiols (4CR) were developed. It was originally hypothesized that the mechanism was analogous to Cushman's initial proposal for the CCR involving an *N*-acyl iminium ion (see chapter 1), however insights into the Mannich-like mechanism caused our group to reconsider this mechanism. Our group was interested in using this information to probe the mechanism of the multicomponent variants of the CCR. At the time of our initial publication, it was found that when the 4CR is performed at room temperature, equimolar quantities of amide acids **6a** and **6b** are formed, which form a single regioisomer and diastereomer of lactam product upon heating with aldehyde **1a** (Figure 5.1).¹ Similar amide-acid isomers have been observed in the 3CRs of homophthalic anhydride, amines, and aldehydes **9**. The formation of amide-acid in the 3- and 4CR prompted our group to explore how these intermediates played a role in the overall mechanism of the multicomponent CCRs leading to lactam products **5** and **8**.

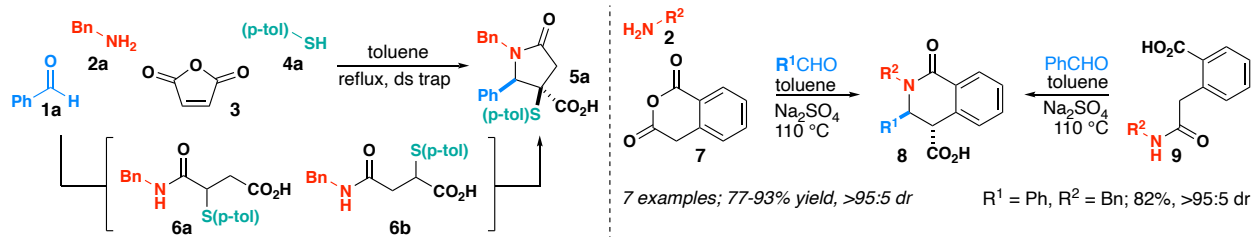


Figure 5.1 Known amide-acid intermediates **6** leading to tetrasubstituted lactam **5** (left). 3CR of homophthalic anhydride, amines and aldehydes leading to dihydroisoquinolone **8** (right).

5.1.1 Initial Development of the 3-Component Reaction and Proposed Mechanism

In 2003, the first 3CR using amines, aldehydes and homophthalic anhydride was developed by Yadav and coworkers using ionic liquids and $InCl_3$ as a catalyst.² Soon after, a variety of modified 3CRs of homophthalic anhydride, amines, and aldehydes were developed with either Lewis acid catalysts or additives.²⁻¹² In 2005, Azizian and coworkers described a 3CR using an aluminum based catalyst to afford cis lactams **12** (Figure 5.2). In this report, a mechanism was proposed for the formation of the dihydroisoquinolone products that was consistent with Cushman's original zwitterionic proposal. Azizian performed 1H NMR spectroscopy experiments which indicated that the initial reaction outcome was amide-acid **10**, which after four hours led to dihydroisoquinolones **12**. It was hypothesized that the initial acylation of amine (**2**) by homophthalic anhydride **7** forms amide-acid **10**. It was suggested that **10** would then condense with aldehyde **1**, which can undergo a Mannich addition to form **12**.⁴ Although *N*-acyl iminium ions (**11**) have been observed as intermediates in other reactions, there is little precedent for their formation by the condensation of substituted amides with aldehydes.⁴ Furthermore, amide acid **10** is indistinguishable from its regioisomer **9** based on 1H NMR spectroscopy alone.

Azizian, 2005

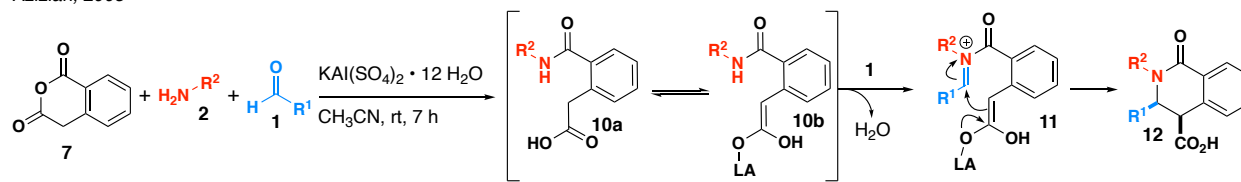


Figure 5.2 Azizian's proposed mechanism for the 3CR

In 2018 Mikael Krasavin described a new 3CR utilizing the diacid of homophthalic anhydride with amines and aldehydes (Figure 5.3A).¹³ Krasavin suggested that the actual outcome of the 3CR was amide acid **14b**, due to the higher electrophilicity of the phenyl acetyl carbonyl. To support this hypothesis, Krasavin repeated Azizian's reaction conditions to synthesize the amide-acid intermediate in the 3CR for further characterization. The outcome of this reaction was consistent with the ¹H NMR spectroscopy data provided by Azizian, and X-ray crystallographic analysis showed that the amide-acid intermediate was actually **14b** (Figure 5.3B).¹³ Based on this outcome, it was suggested that a 3CR wherein amine, aldehyde, and homophthalic anhydride are simultaneously combined without additives was not possible, as amide-acid **14b** would be unproductive for lactam formation by the previously described mechanism. As a result, Krasavin utilized the diacid of homophthalic anhydride (**13**) with amines and aldehydes. He suggested that the use of diacid allowed for slow formation of anhydride and imine *in situ* under dehydrating conditions. The slow formation of the anhydride is hypothesized to preclude amide-acid formation and allows the reaction to proceed through the classic CCR mechanism. However, Krasavin and Azizian's opposing results made it unclear how the previously discovered 3CRs proceed to product if amide-acid **14a** is not formed.

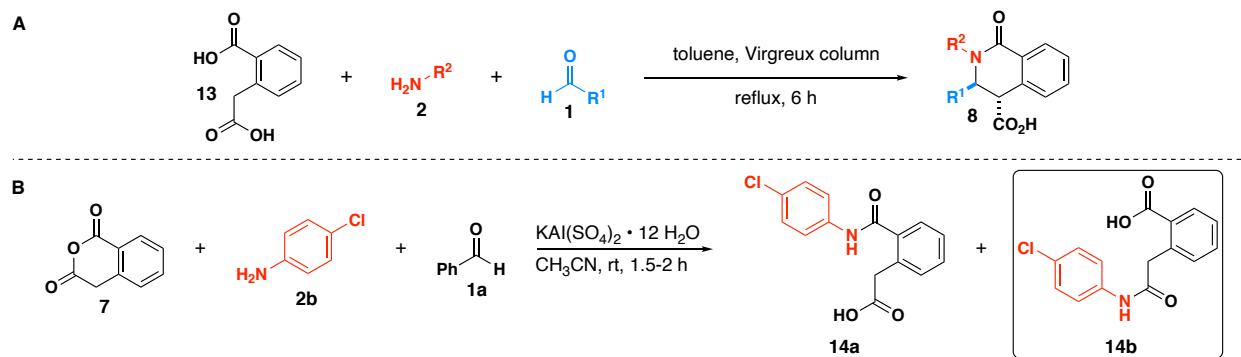


Figure 5.3 **A**. Krasavin's novel 3CR using the diacid of homophthalic anhydride. **B**. Azizian's original reaction outcome was consistent with product **14b**, which was confirmed by X-ray crystallography.

5.1.2 Initial Mechanistic Hypothesis of the 4-Component Reaction

The four-component variant of the CCR was first developed in our group in 2007. At the time of discovery, we assumed that the mechanism proceeded *via* the same zwitterionic intermediate originally proposed by Cushman and Azizian based on the isolation of similar amide-acid intermediates (Figure 5.4A). Experimental observations in our lab showed that the imine, anhydride, and thiol lead to the room temperature formation of amide-acid regioisomer mixture **6a** and **6b** (Figure 5.4B). Heating this mixture with aldehyde (**1**) leads to a single regioisomer and diastereomer of product **5**. Additionally, taking a single regioisomer **6b** leads to a mixture of amide acid regioisomers **6a** and **6b**. Furthermore, if benzaldehyde was added to **6b** under refluxing conditions, a mixture of **6a** and **6b** was observed, as well as the desired lactam **5a**. To rationalize these results, we hypothesized that both zwitterionic intermediates were being formed through condensation of amide-acids **6** with aldehyde (**1**), but only one regioisomer of *N*-acyl iminium ion (**15b**) was productive for lactam formation (Figure 5.4A). As a result, a kinetic

resolution involving equilibration of the incorrect regioisomer **15a** with free imine (**17**) and anhydride (**16**) leads to a single regioisomer and diastereomer of product **5**.

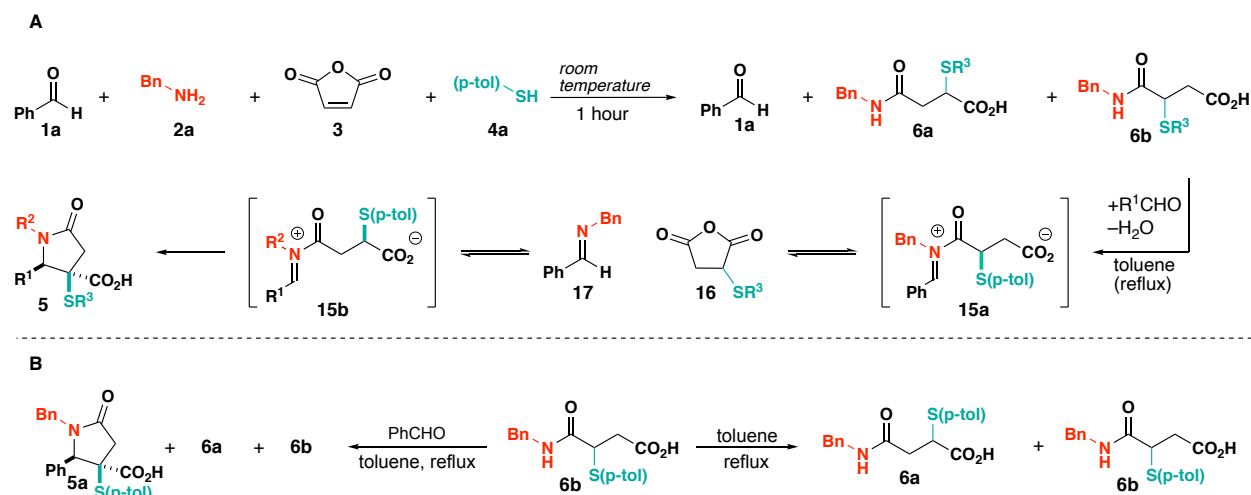


Figure 5.4 **A.** Initially Proposed Mechanism of the 4CR. **B.** Initial mechanistic investigation of the 4CR.

Mechanistic evidence leading to the acceptance of a Mannich-like mechanism (Figure 5.5) for cyanosuccinic anhydrides caused us to reconsider the mechanism of the 3- and 4CR. While this mechanism explains the reactions of cyclic anhydrides with pre-formed imines, it does not explain how amide-acids **6a** and **6b** proceed to the lactam product. Furthermore, in the study of the mechanism of cyano-succinic anhydride, Cheong discovered that the zwitterionic intermediates such as **15** are unrealistically high in energy to afford CCR products. We endeavored to perform a detailed mechanistic investigation in order to understand how the known amide-acid intermediates in the 3- and 4CR ultimately lead to CCR products.

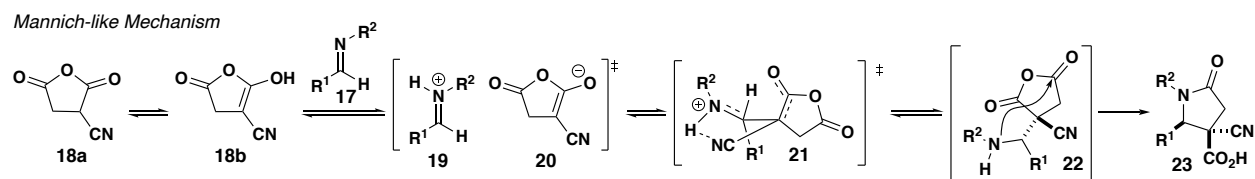


Figure 5.5 Proposed Mannich-like mechanism for the CCR of cyanosuccinic anhydrides

5.2 Results and Discussion

Initial efforts to determine the mechanism of the 4CR are detailed in Dr. Mike Di Maso's dissertation. Our computational collaborator, Prof. Paul Cheong at University of Oregon, found evidence that the 4CR proceeds through a Mannich-like mechanism, wherein the anhydride and imine are formed *in situ* from amide-acid intermediates **6**. To support this computed mechanism, kinetic isotope effect (KIE) experiments were performed to determine the rate-determining step in the 4CR; however, due to the reversible nature of the reactions studied, Dr. Di Maso found that the proposed KIE experiments would not be able to support the proposed mechanism. Instead, Dr. Di Maso designed experiments that would shed light on how the amide-acid **6a** and **6b** ultimately lead to the imine and anhydride precursors in the reaction (Figure 5.6A). Specifically, he performed an amide-exchange experiment with amide-acid **6b** and *p*-chlorobenzylamine, as well as a thiol exchange experiment with *p*-methoxybenzylamine and the same amide-acid **6b**. The unpurified reaction mixtures of these two exchange experiments were analyzed by mass spectroscopy and led to the determination that while amide exchange was observed, while thiol exchange was not observed (Figure 5.6A). The reaction outcomes from the exchange experiments, coupled with the computational evidence contributed by the Cheong lab, led us to conclude that amide acid **6b** was in equilibrium with the thioarylsuccinic anhydride, which, under refluxing conditions in the presence of aldehyde, would lead to irreversible formation of lactam **5** (Figure 5.6B).

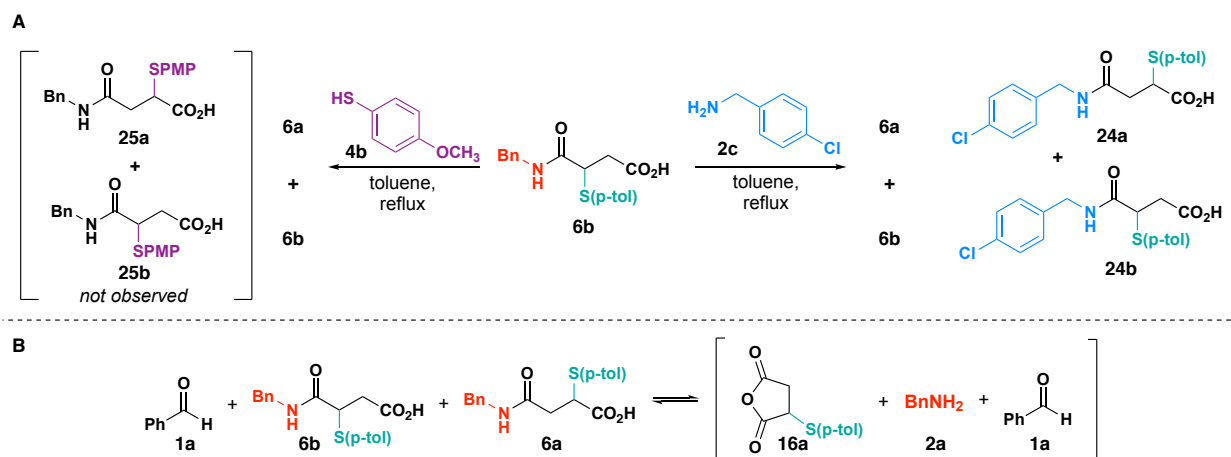


Figure 5.6 A. Amide and thiol-exchange experiments designed to test the reversibility of amine addition and thiol addition. B. Proposed intermediates for the 4CR.

Due to unforeseen circumstances, the collaboration which led to the calculated proposed mechanism was terminated in 2019. As a result, we were tasked with designing a series of synthetic experiments that would support the proposed 4CR mechanism. First, Noah Burlow worked to replicate Dr. Di Maso's reaction outcomes from the amide- and thiol-exchange experiments. Interestingly, it was found that imide products resulting from dehydration of the amide-acid were observed, rather than a mixture of amide-acids (*vide infra*). After several attempts, Noah consistently found that the imide product was the major product of the amide exchange experiments. I then endeavored to probe the mechanism of both the 3CR and the 4CR, which I will describe for the duration of this chapter.

5.2.1 Mechanistic Investigation of the 4-Component Reaction

5.2.1.1 Crossover Experiments of the 4-Component Reaction

After consulting the results of both Dr. Di Maso and Noah, I sought to replicate the same amide- and thiol-exchange experiments. In order to adequately analyze the reaction outcomes, the possible products from the exchange reactions were synthesized and isolated. First, amide-acids **6a** and **6b** were synthesized by reaction of thioarylsuccinic anhydride **16a** with benzylamine, followed by esterification *in situ* to afford two regioisomeric amide esters **26a** and **26b** (Figure 5.7A). *p*-Methoxybenzyl esters **26a** and **26b** were then deprotected with trifluoroacetic acid to afford amide-acids **6a** and **6b**, respectively (Figure 5.7B). Additionally, the two *p*-chlorobenzylamine derived amide-acid products **28a** and **28b**, the expected amide-exchange products, were also synthesized in the same manner (Figure 5.7A, Figure 5.7B). Finally, the amide-acid regioisomers that would result from thiol exchange were also attempted, however under reaction conditions, the *p*-methoxybenzenethiol products spontaneously cyclized to the corresponding imide product (**29**) (Figure 5.7C).

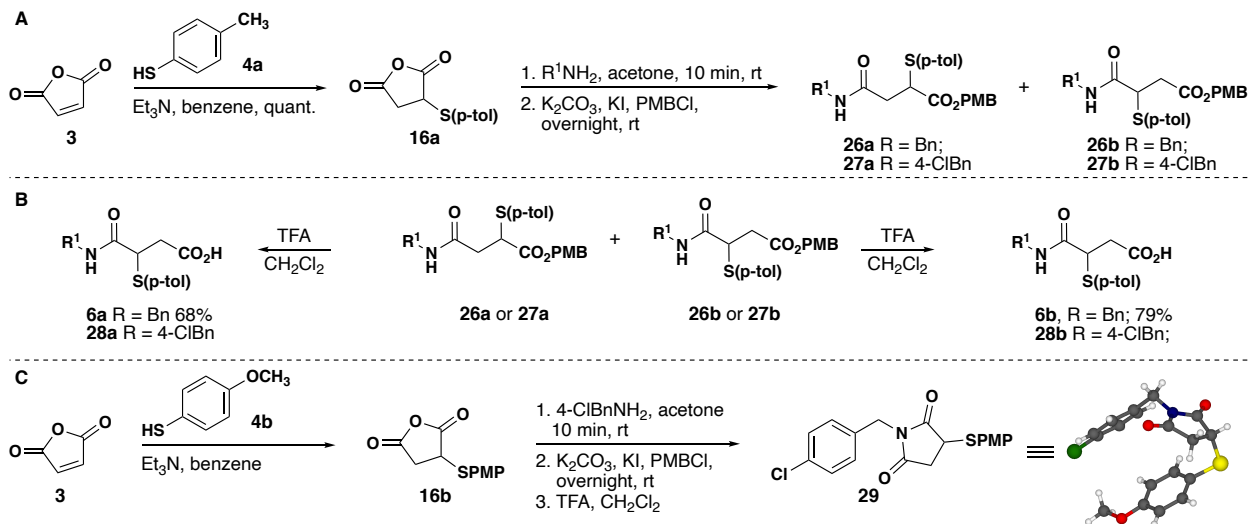
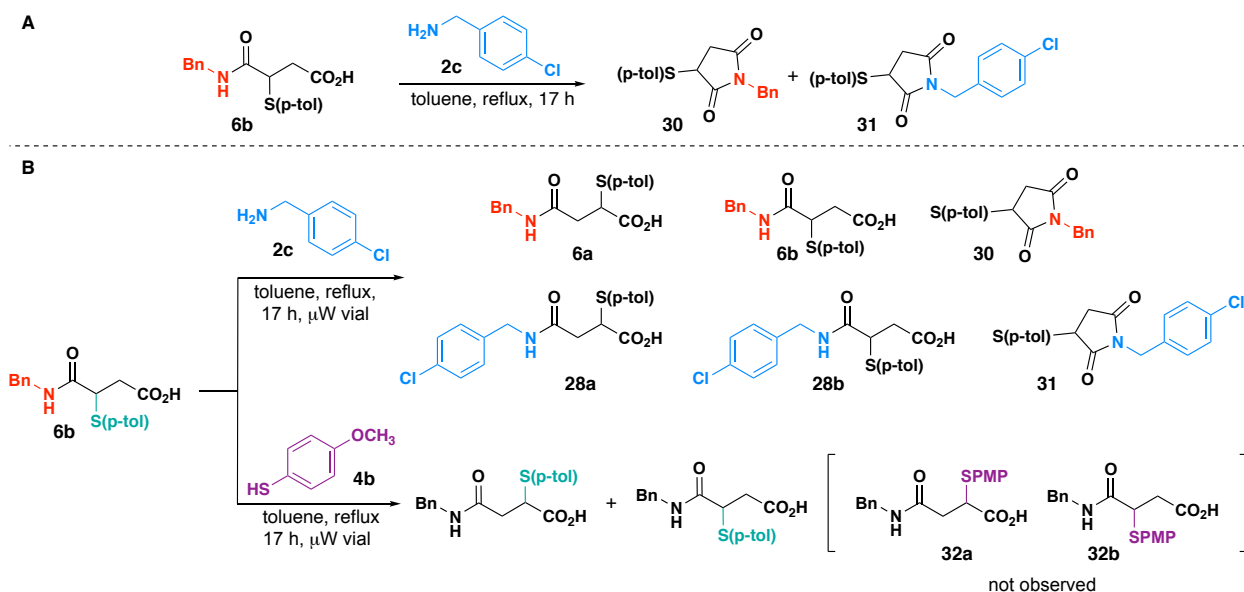


Figure 5.7 A. Synthesis of regioisomeric amide-esters. B. Deprotection amide-esters to afford amide-acid products. C. Attempted synthesis of imide **29**.

To begin the mechanistic investigation of the 4CR, the amide-exchange experiment originally performed by Dr. Di Maso was attempted. First, amide-acid **6b** was heated in toluene in the presence of *p*-chlorobenzylamine for 17 hours (Figure 5.8A). The resulting products were difficult to interpret by ^1H NMR spectroscopy, so the unpurified reaction mixture was subjected to esterification conditions in hopes of isolating the amide-ester products **26** and **27**. Purification by flash column chromatography showed that the predominant products were imides **30** and **31**—similar to Noah's findings. It was hypothesized that the imide formed as a result of the escape of water through the reflux condenser, and as a result, subsequent reactions were performed in sealed microwave tubes. ^1H NMR spectroscopy and LCMS analysis of the reaction run in a sealed microwave tube showed the presence of **6a** and **6b**, the exchange products **28a** and **28b**, as well as imides **30** and **31** (Figure 5.8B). The thiol-exchange experiment was then attempted in a similar manner. When **6b** was heated in the presence of a second



thiophenol (*p*-methoxythiophenol), **6a** and **6b** were observed as expected while negligible quantities of the products of thiol exchange (**32a** and **32b**) were observed by ^1H NMR spectroscopy and LCMS.

Figure 5.8 **A**. Results of amide-exchange reactions using a reflux condenser. **B**. Results of amide-exchange and thiol-exchange experiments

5.2.1.2 React IR Analysis of 4-Component Reaction Intermediates

To further investigate the mechanism of the 4CR, we collaborated with Jason Hein's group at University of British Columbia, Vancouver. The group's specialization in developing novel reaction monitoring technology provided us an opportunity to directly inspect the mechanistic course of the 4CR. Then graduate student, Dr. Thomas Malig, monitored the relative rates of the proposed first steps of the 4CR leading to **6a** and **6b** using infrared spectroscopy in situ (React-IRTM) (Figure 5.9). It was found that the acylation of benzylamine with maleic anhydride in tetrahydrofuran proceeds instantaneously at room temperature with a half-life ($t_{1/2}$) of less than one minute. Additionally, the conjugate addition of *p*-tolSH to maleic anhydride reaction does not occur

until a catalytic quantity of triethylamine is added, at which point the reaction proceeds at room temperature ($t_{1/2}$ =55 min). Finally, it was found that the reaction of **33** with *p*-tolSH proceeds with a more complex kinetic profile than the previous reactions but results in 50% conversion to amide-acids **6a** and **6b** after 10 minutes at room temperature. These React IR experiments support that **6a** and **6b** are intermediates of the reaction and lead to the final formation of the lactam 4CR product in the presence of benzaldehyde.

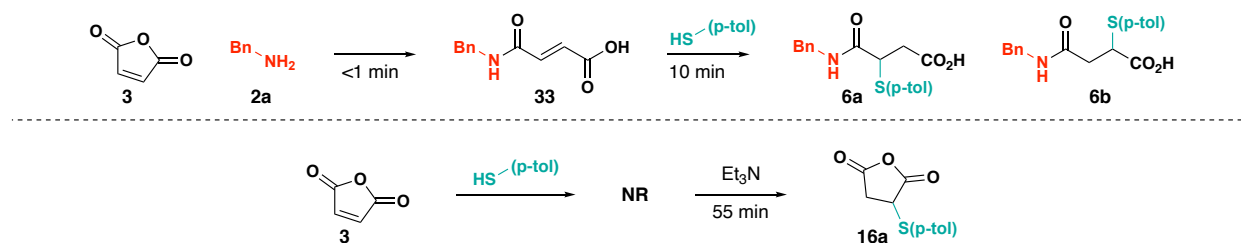


Figure 5.9 Relative rates examined by React IR technology in the Hein group.

5.2.1.3 Revised Mechanism of the 4-Component Reaction

Based on the results of the crossover experiments as well as the ReactIR data, we propose a mechanism for the 4CR that explains both the regio- and diastereoselectivity observed in the initial reaction. We can conclude that the mechanism of the 4CR proceeds through the rapid acylation of **2**, followed by conjugate addition of the thiol **4** to afford amide-acids **6a** and **6b** (Figure 5.10). These amide-acids can then cyclize under refluxing conditions to form thioaryl-substituted succinic anhydride **16** and amine **2**. The reaction of a carboxylic acid breaking an amide bond to form anhydride has been observed previously^{14, 15} and is consistent with the exchange reactions described. Although this process is unfavorable, it is driven forward by the rapid formation of the imine. Once the imine is formed, it can react with the anhydride through a Mannich-like mechanism in a

Zimmerman-Traxler Transition State **34** to form the γ -lactam **5** as a single regioisomer and diastereomer.

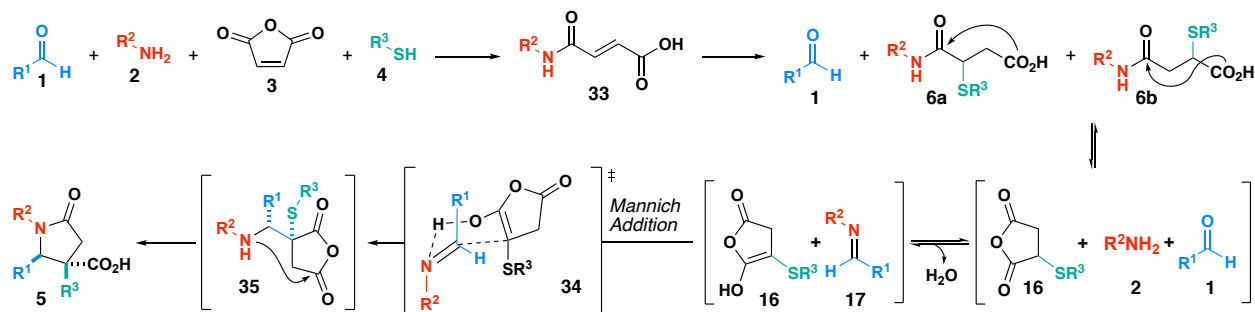


Figure 5.10 Proposed mechanism for the formation of lactams **5** through the 4CR.

5.2.2 Mechanistic Investigation of the 3-Component Reaction

The information gained from the study of the 4-component reaction prompted an investigation into the mechanism of the 3CR. Krasavin had previously proposed that the formation of amide-acid regioisomer **36a** would prevent reaction progress to dihydroisoquinolone products.¹³ However, based on the results of the mechanistic investigation into the 4CR, we hypothesized that the 3CR would proceed with an analogous mechanism to the 4CR wherein amide acid **36a** is in equilibrium with homophthalic anhydride **7** and amine **2**, which ultimately leads to products **8** (Figure 5.11).

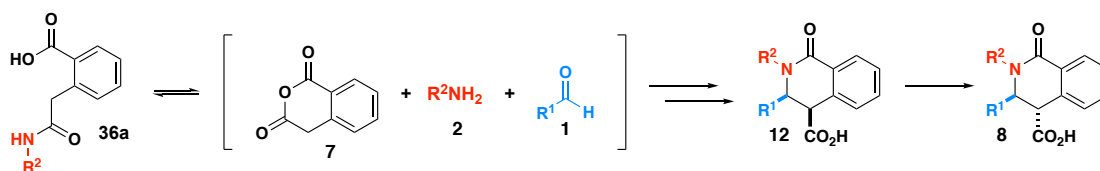


Figure 5.11 Proposed mechanism based on the mechanism elucidated in the studies of the 4CR

5.2.2.1 Synthesis of Amide-Acids of Homophthalic Anhydride

A series of experiments were conducted to understand the structure and reactivity of the amide-acid intermediate formed in the 3CR. First, when homophthalic anhydride was

heated in the presence of benzylamine for one hour, a single amide-acid intermediate **36a** was observed, the structure of which was determined by X-ray crystallography (Figure 5.12). The same product was observed when the reaction was performed at room temperature for 24 h. This product was consistent with the regioisomer (**36b**) isolated and observed by Krasavin in the development of the 3CR of homophthalic diacid, aldehydes, and amines. In order to obtain standards for the proposed reaction outcomes from crossover experiments, amide-acid **36b** was also synthesized with *p*-chlorobenzylamine **2c** to afford **36b**.

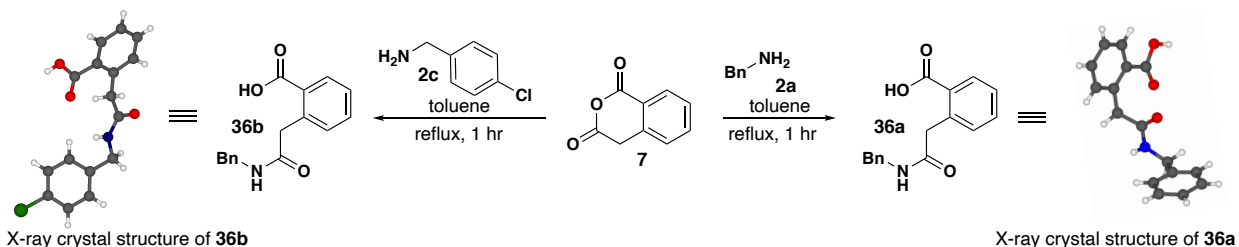


Figure 5.12 Synthesis of amide acids **36a** and **36b**.

5.2.2.2 Crossover Experiments of the 3-Component Reaction

Having confirmed that the amide-acid was consistent with the product observed by Krasavin, a crossover experiment was performed to understand the role of amide-acid **36** in the 3CR. First, amide-acid **36a** was isolated and treated with *p*-chlorobenzylamine in refluxing toluene for 6 hours (Figure 5.13). When the unpurified reaction mixture was analyzed by LCMS, both amide-acids **36a** and **36b** were observed, indicating that amide exchange had occurred. Next, we were interested in determining if amide-acid **36a** could be converted to dihydroisoquinolones **8a**. To do this, amide-acid **36a** was isolated and combined with benzaldehyde in refluxing toluene which resulted in product **8a** in >95:5 dr

and 84% yield! Additionally, it was found that mixing homophthalic anhydride, benzylamine, and benzaldehyde in refluxing toluene yielded lactam *trans*-**8a** in 82% yield.

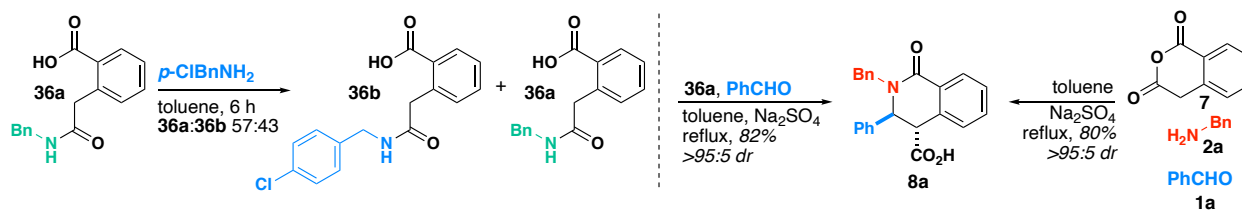


Figure 5.13 Crossover experiments leading to the development of the novel 3CR.

5.2.2.3 Revised Mechanism of the 3-Component Reaction

Based on the results of the crossover experiments, we hypothesize that the mechanism of the 3CR proceeds through a similar mechanism as the 4CR. The first step of the 3CR involves the initial attack of the amine on the phenylacetyl carbonyl of homophthalic anhydride to provide amide-acid **36a**, which is in equilibrium with homophthalic anhydride **7** and amine **2** (Figure 5.14). In the presence of aldehyde, the amine can condense to form imine, which can then proceed through Mannich addition to provide the *cis* product **10**. Under refluxing conditions, the *cis* lactam epimerizes to the *trans* isomer **27** over the course of 24 hours.

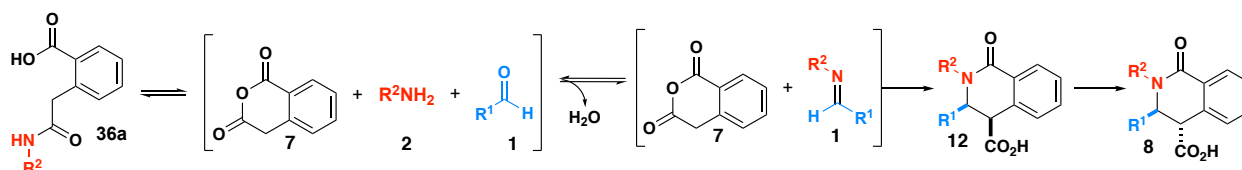


Figure 5.14 Proposed mechanism for the 3CR of amines, aldehydes, and homophthalic anhydride to yield dihydroisoquinolones **8**.

5.2.3 Development of Novel Reaction Conditions for the 3-Component Reaction

5.2.3.1 Reaction Optimization

Having found that the reaction of homophthalic anhydride, benzylamine, and benzaldehyde leads to dihydroisoquinolone **8a**, I hoped to expand the scope of this modified 3CR. Dehydrating agents were screened, including sodium sulfate and 4 Å mol sieves (Figure 5.15). The 3CR was found to proceed with similar reaction outcomes regardless of the dehydrating agent used and can proceed in the absence of dehydrating agent as well. Notably, the diastereomer ratio was highly dependent on the method of heating, the reaction vessel used, and the reaction length. Small scale reactions heated at reflux using a reflux condenser consistently dried out over the course of the reaction, including when reactions were attempted with a Vigreux column and Dean-Stark trap. To alleviate this issue, the reactions were instead performed in sealed microwave vials, which resulted in excellent yields and isolation of a single *trans* diastereomer of product. Reaction diastereoselectivity suffered when using baths containing aluminum beads, whereas reactions heated with silicone oil baths proceeded with consistently excellent diastereoselectivity. Finally, when the reaction was run for a shorter length of 6 hours, a mixture of *cis* and *trans* diastereomers was observed. Presumably, the kinetic *cis* diastereomer is formed first, and under reaction conditions it can epimerize to the *trans* diastereomer over time. Optimized reaction conditions consisted of equimolar quantities of amine, aldehyde, anhydride, and sodium sulfate heated in toluene at reflux for 24 hours.

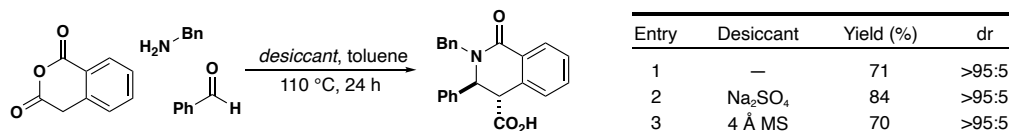


Figure 5.15 Desiccant screen for the 3CR methodology.

Following screening, a series of substrates were synthesized using this 3CR method in good yields and excellent diastereoselectivity for the *trans* diastereomer (Figure 5.16). Reactions proceeded favorably with both benzyl and aryl amines. The electronics of the aldehyde portion of the molecule did not have significant impact on reaction outcomes.

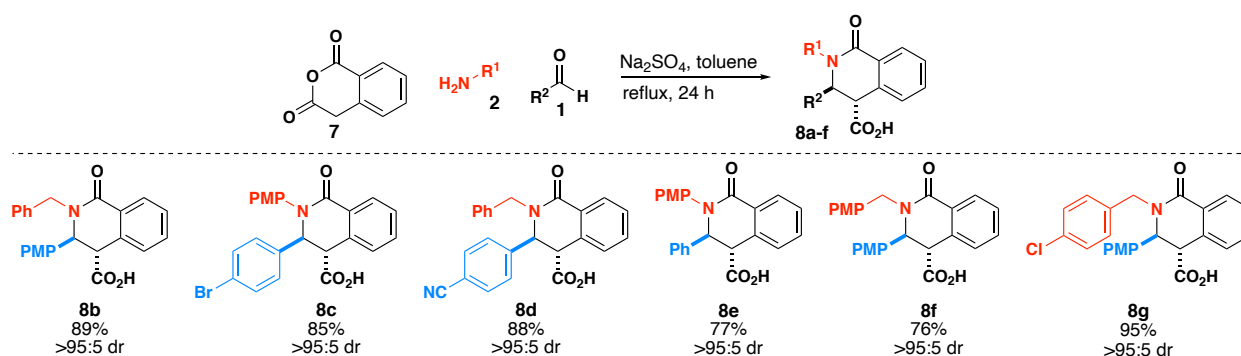


Figure 5.16 Substrate scope for the synthesis of dihydroisoquinolone products **8**.

5.3 Conclusion

In summary, we have provided experimental evidence for the proposed mechanism of the 3- and 4- component variants of the CCR. These reactions proceed through analogous amide-acid intermediates which are formed through initial nucleophilic attack of the amine on the anhydride. This amide-acid is in equilibrium with the anhydride and amine and in the presence of aldehyde, the amine can condense to form imine and

proceed through the classic CCR. This mechanistic investigation led to the development of a new variant of the 3CR and allowed for the synthesis of a series of δ -lactams.

5.4 Experimental Section

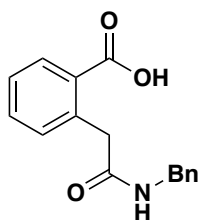
Materials and Instrumentation

Unless otherwise specified, all commercially available reagents were used as received. All reactions using dried solvents were carried out under an atmosphere of argon in oven-dried glassware with magnetic stirring. Dry solvent was dispensed from a solvent purification system that passes solvent through two columns of dry neutral alumina. ^1H NMR spectra and proton-decoupled ^{13}C NMR spectra were obtained on a 400 MHz or 800 MHz Bruker or 600 MHz Varian NMR spectrometer. ^1H Chemical shifts (δ) are reported in parts per million (ppm) relative to TMS (s, δ 0). Multiplicities are given as: s (singlet), d (doublet), t (triplet), q (quartet), p (pentet), h (hextet), and m (multiplet). Complex splitting will be described by a combination of these abbreviations, i.e. dd (doublet of doublets). ^{13}C NMR chemical shifts are reported relative to CDCl_3 (t, δ 77.4) unless otherwise noted. High-resolution mass spectra were recorded on either positive or negative ESI mode. Melting points were taken on an EZ-melting apparatus and were uncorrected. Infrared spectra were taken on a Mettler Toldedo ReactIR 700 (serial number B929971514) with a liquid N_2 MCT detector fitted with a DiComp probe (serial number B939349478). The system was filled with liquid N_2 and allowed to cool for 1 h before use. Chromatographic purifications were performed by flash chromatography with

silica gel (Fisher, 40–63 μm) packed in glass columns or by use of a Teledyne Isco Combi-Flash. The eluting solvent for the purification of each compound was determined by thin-layer chromatography (TLC) on glass plates coated with silica gel 60 F254 and visualized by ultraviolet light.

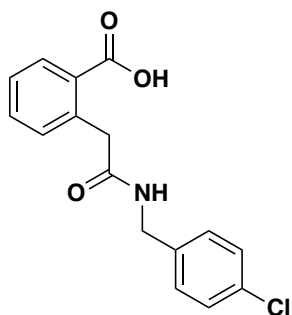
Note: for the three-component reaction, the reaction mixture must be heated to at least 110 °C in order to fully epimerize from the cis to trans diastereomer. Use of aluminium beads resulted in poor diastereoselectivity, whereas silicone oil baths led to excellent diastereoselectivity.

Synthesis of Amide-Acids for Crossover Experiments



2-(2-(benzylamino)-2-oxoethyl)benzoic acid (36a) To a flame dried round bottom flask was added homophthalic anhydride (0.81 g, 5.0 mmol) and dissolved in CH_2Cl_2 (10.0 mL, 0.5 M). Benzylamine (0.54 mL, 5.0 mmol) was added, and the reaction was stirred at rt for 24 h. The reaction was concentrated in vacuo and characterized without further purification to provide **36a** (1.3 g, 96%), a single regioisomer, as an off-white crystalline solid: mp range 135.3-140.3 °C; ^1H NMR (400 MHz, DMSO- d_6) δ 12.87 (s, 1H), 8.38 (t, $J = 6.0$ Hz, 1H), 7.83 (dd, $J = 7.7, 1.5$ Hz, 1H), 7.48 (td, $J = 7.5, 1.5$ Hz, 1H), 7.38 – 7.17 (m, 7H), 4.27 (d, $J = 5.9$ Hz, 2H), 3.92 (s, 2H).; ^{13}C NMR (101 MHz, DMSO- d_6) δ 170.1, 168.6, 139.6, 137.0, 131.9, 131.5, 131.2, 130.2, 128.2, 127.1, 126.7 (2 carbons), 42.2,

40.5.; IR: 2961.0 (broad), 2153.4, 1716.5, 1619.0, 1552.3 cm^{-1} ; AMM (ESI-TOF) m/z calcd for $\text{C}_{16}\text{H}_{14}\text{NO}_3^-$ $[\text{M}-\text{H}]^-$ 268.0979, found 268.0981.

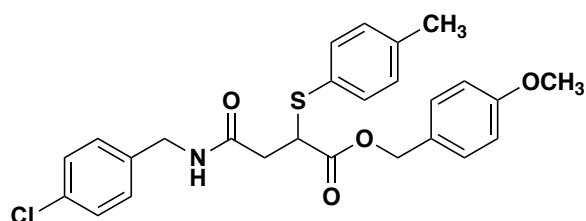


2-(2-((4-chlorobenzyl)amino)-2-oxoethyl)benzoic acid (**36b**)

To a flame dried round bottom flask was added homophthalic anhydride (0.081 g, 0.5 mmol) and dissolved in toluene (1.0 mL, 0.5 M). *p*-chlorobenzylamine (0.060 mL, 0.5 mmol) was added, and the reaction was stirred for 30 minutes. The reaction was concentrated in vacuo and characterized without further purification to afford **36b**, a single regioisomer, as a white crystalline solid (0.134 g, 96%): mp range 172.7-173.9 $^{\circ}\text{C}$; ^1H NMR (400 MHz, DMSO- d_6) δ 8.40 (t, J = 6.1 Hz, 1H), 7.84 (d, J = 7.6 Hz, 1H), 7.48 (t, J = 7.5 Hz, 1H), 7.42 – 7.23 (m, 6H), 4.25 (d, J = 6.0 Hz, 2H), 3.92 (s, 2H).; ^{13}C NMR (101 MHz, DMSO- d_6) δ 170.4, 168.7, 138.8, 137.0, 132.1, 131.7, 131.3, 131.2, 130.3, 129.1, 128.2, 126.9, 41.7, 40.7.; AMM (ESI-TOF) m/z calcd for $\text{C}_{16}\text{H}_{13}\text{ClNO}_3^-$ $[\text{M}-\text{H}]^-$ 302.0589, found 302.0594.

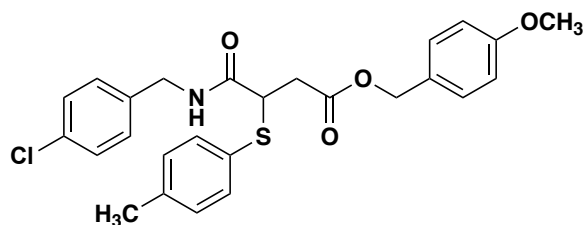
Synthesis of 27a and 27b: To a flame dried round bottom flask was added (1.55 g, 7 mmol) and *p*-chlorobenzylamine (0.851 mL, 7 mmol) and dissolved in acetone (70 mL, 0.1 M). After 10 minutes, K_2CO_3 (0.967 mg, 7 mmol), KI (1.162 g, 7 mmol), and *p*-

methoxybenzylchloride (1.03 mL, 7 mmol) were added, and the reaction was stirred overnight. The crude reaction mixture was concentrated in vacuo, then dissolved in EtOAc and H₂O, extracted with EtOAc (3x 20 mL), and dried over Na₂SO₄. Purification by gradient flash column chromatography (20-100% EtOAc:Hexanes) afforded regioisomer **27b** as an off white amorphous solid (0.393 g, 12%) and **27a** (0.080 g, 3%) as an off white amorphous solid.



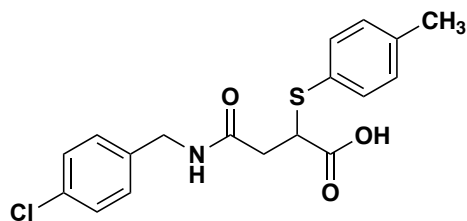
4-methoxybenzyl 4-((4-chlorobenzyl)amino)-4-oxo-2-(p-tolylthio)butanoate (**27a**)

The structure of **27a** was assigned based on the comparison of *J* coupling values.¹ ¹H NMR (400 MHz, CDCl₃) δ 7.30 – 7.09 (m, 8H), 7.02 (d, *J* = 7.9 Hz, 2H), 6.90 – 6.80 (m, 2H), 6.12 (t, *J* = 5.8 Hz, 1H), 5.07 (d, *J* = 12.0 Hz, 1H), 4.95 (d, *J* = 11.9 Hz, 1H), 4.39 – 4.23 (m, 2H), 4.07 (dd, *J* = 9.3, 5.8 Hz, 1H), 3.79 (s, 3H), 2.73 (dd, *J* = 15.1, 9.3 Hz, 1H), 2.58 (dd, *J* = 15.2, 5.8 Hz, 1H), 2.30 (s, 3H).; ¹³C NMR (101 MHz, CDCl₃) δ 171.5, 169.5, 159.6, 139.0, 136.6, 134.5, 133.2, 130.1, 129.8, 129.0, 128.7, 127.9, 127.5, 113.8, 66.9, 55.3, 46.3, 42.8, 38.2, 21.2.; AMM (ESI-TOF) *m/z* calcd for C₂₆H₂₆ClNO₄SNa⁺ [M+Na]⁺ 506.1163, found 506.1173.



4-methoxybenzyl 4-((4-chlorobenzyl)amino)-4-oxo-3-(*p*-tolylthio)butanoate (**27b**) 4-

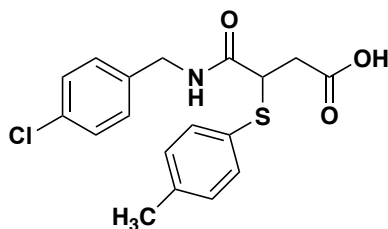
The structure of **27b** was assigned based on the comparison of J coupling values.¹ ¹H NMR (400 MHz, CDCl₃) δ 7.27 (dd, *J* = 8.4, 6.4 Hz, 4H), 7.23 – 7.18 (m, 2H), 7.14 – 7.02 (m, 4H), 6.94 – 6.82 (m, 2H), 6.66 (s, 1H), 5.15 – 4.94 (m, 2H), 4.46 – 4.28 (m, 2H), 3.95 (dd, *J* = 7.5, 6.3 Hz, 1H), 3.80 (s, 3H), 3.12 (dd, *J* = 16.9, 7.5 Hz, 1H), 2.78 (dd, *J* = 16.9, 6.3 Hz, 1H), 2.32 (s, 3H).; ¹³C NMR (101 MHz, CDCl₃) δ 170.9, 169.9, 159.7, 138.8, 136.4, 133.3, 133.1, 130.2, 130.1, 129.1, 128.8, 128.5, 127.7, 114.0, 66.7, 55.3, 48.3, 43.3, 36.7, 21.1.; AMM (ESI-TOF) *m/z* calcd for C₂₆H₂₆ClNO₄SNa⁺ [M+Na]⁺ 506.1163, found 506.1182.



4-((4-chlorobenzyl)amino)-4-oxo-2-(*p*-tolylthio)butanoic acid (**28a**)

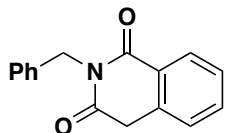
To a flame dried round bottom flask was added **27a** (0.050 g, 0.103 mmol) and dissolved in dichloromethane (5.15 mL, 0.02 M). TFA (0.052 mL, 0.2M) was added and the reaction was stirred overnight. The reaction was concentrated in vacuo. Hexanes (10 mL) was added, followed by diethyl ether (10 mL) and a white solid precipitated out. The solid was filtered and used without further purification (0.023 g, 62%): mp range 130.1-131.9 °C; ¹H NMR (400 MHz, MeOD) δ 7.41 – 7.36 (m, 2H), 7.32 – 7.23 (m, 4H), 7.15 (d, *J* = 7.9 Hz,

2H), 4.32 (d, $J = 3.2$ Hz, 2H), 3.99 (dd, $J = 8.8, 6.6$ Hz, 1H), 2.79 (dd, $J = 15.4, 8.8$ Hz, 1H), 2.63 (dd, $J = 15.4, 6.6$ Hz, 1H), 2.33 (s, 3H).; ^{13}C NMR (101 MHz, CD_3OD) δ 174.7, 172.4, 140.1, 138.8, 135.3, 133.9, 130.8, 130.1, 130.1, 129.5, 47.9, 43.3, 39.0, 21.2.; AMM (ESI-TOF) m/z calcd for $\text{C}_{18}\text{H}_{17}\text{ClNO}_3\text{S}^-$ $[\text{M}-\text{H}]^-$ 362.0623, found 362.0626.



4-((4-chlorobenzyl)amino)-4-oxo-3-(*p*-tolylthio)butanoic acid (**28b**)

To a flame dried round bottom flask was added **27b** (0.384 g, 0.8 mmol) and dissolved in dichloromethane (40.0 mL, 0.02 M). TFA (4.0 mL, 0.2M) was added and the reaction was stirred overnight. The reaction was concentrated in vacuo. Hexanes (15 mL) was added, followed by diethyl ether (15 mL) and a white solid precipitated out. The solid was filtered and used without further purification (0.243 g, 83%): mp 123.9-126.6 °C; ^1H NMR (600 MHz, $\text{DMSO}-d_6$) δ 8.69 (t, $J = 6.1$ Hz, 1H), 7.34 (d, $J = 8.1$ Hz, 2H), 7.30 (d, $J = 7.7$ Hz, 2H), 7.23 (d, $J = 8.1$ Hz, 2H), 7.14 (d, $J = 7.8$ Hz, 2H), 4.24 (qd, $J = 15.5, 6.0$ Hz, 2H), 3.97 (dd, $J = 9.5, 5.3$ Hz, 1H), 2.76 (dd, $J = 16.7, 9.5$ Hz, 1H), 2.29 (s, 3H), 1.09 (t, $J = 7.0$ Hz, 2H).; ^{13}C NMR (101 MHz, $\text{DMSO}-d_6$) δ 172.3, 170.3, 138.7, 138.3, 133.8, 131.7, 130.1, 129.4, 129.1, 128.5, 46.5, 42.0, 37.0, 21.1.; AMM (ESI-TOF) m/z calcd for $\text{C}_{18}\text{H}_{17}\text{ClNO}_3\text{S}^-$ $[\text{M}-\text{H}]^-$ 362.0623, found 362.0628.

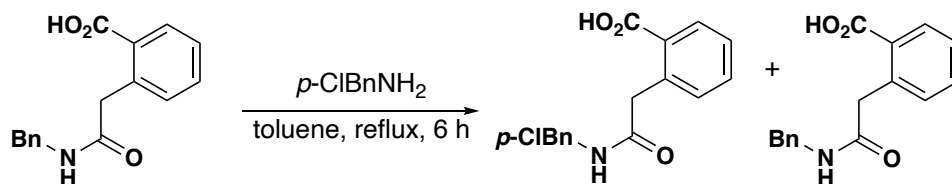


2-benzylisoquinoline-1,3(2*H*,4*H*)-dione (**30**)

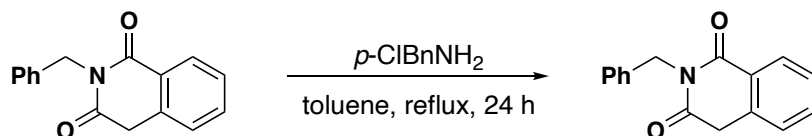
To a flame dried round bottom flask was added homophthalic anhydride (0.81 mg, 0.5 mmol) and dissolved in toluene (1.0 mL). Benzylamine (0.054 mL, 5.0 mmol) was added, and the reaction was stirred at reflux for 24 h. The reaction was then cooled and concentrated in vacuo. Purification by gradient flash column chromatography (20-100% EtOAc:Hexanes) **S3** (69.8 mg, 56%), as an off-white amorphous solid: ¹H NMR (400 MHz, CDCl₃) δ 8.22 (dd, *J* = 8.0, 1.4 Hz, 1H), 7.58 (td, *J* = 7.5, 1.4 Hz, 1H), 7.48 – 7.41 (m, 3H), 7.32 – 7.26 (m, 3H), 7.26 – 7.22 (m, 1H), 5.19 (s, 2H), 4.07 (s, 2H).; ¹³C NMR (101 MHz, CDCl₃) δ 169.9, 164.9, 137.1, 134.1, 133.7, 129.3, 129.0, 128.4, 127.8, 127.5, 127.1, 125.4, 43.3, 36.5.; AMM (ESI-TOF) *m/z* calcd for C₁₆H₁₄NO₂⁺ [M+H]⁺ 252.1019, found 252.1024.

Crossover Experimental Procedures

Liquid Chromatography–Mass Spectrometry Experiments

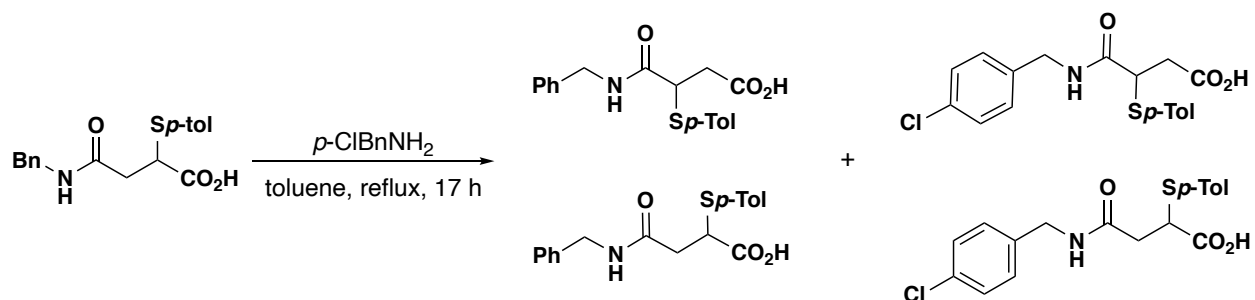


Three-component amide-exchange experiment: To a flame dried microwave vial was added **36a** (0.135 g, 0.5 mmol), *p*-chlorobenzylamine (0.036 mL, 0.5 mmol), and dissolved in toluene (4.5 mL, 0.5 M) and heated to reflux. After 6 h the reaction was cooled to room temperature and concentrated in vacuo. The mixture was analyzed using Liquid Chromatography–Mass Spectrometry which contained masses corresponding to amides **36a**, and **36b**.

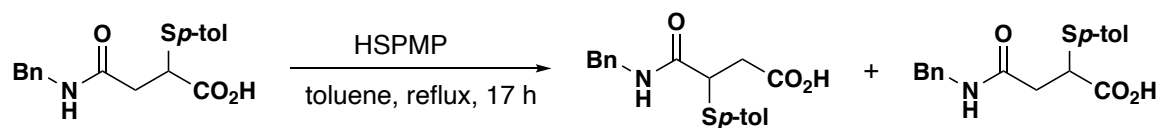


Imide exchange experiment:

To a flame dried microwave vial was added **30** (0.055 g, 0.22 mmol). **30** was dissolved in toluene, (1.0 mL, 0.22 M), then *p*-chlorobenzylamine (0.027 mL, 0.22 mmol) was added and the reaction was heated to reflux. After 24 h, the reaction was cooled to room temperature and concentrated in vacuo. The mixture was analyzed using Liquid Chromatography–Mass Spectrometry which contained masses corresponding only to **30** and *p*-chlorobenzylamine.



Four-component amide-exchange experiment: To a flame dried microwave vial was added **6b** (0.100 g, 0.30 mmol), *p*-chlorobenzylamine (0.036 mL, 0.30 mmol), and dissolved in toluene (4.5 mL, 0.066 M) and heated to reflux. After 17 h the reaction was cooled to room temperature and concentrated in vacuo. The reaction was cooled to room temperature and concentrated in vacuo. The mixture was analyzed using Liquid Chromatography–Mass Spectrometry which contained masses corresponding to amides **6a**, **6b**, **28a**, and **28b**.



Four-component thiol-exchange experiment: To a flame dried microwave vial was added **6b** (0.100 g, 0.30 mmol), *p*-methoxythiophenol (0.036 mL, 0.30 mmol), and dissolved in toluene (4.5 mL, 0.066M) and heated to reflux. After 17 h the reaction was cooled to room temperature and concentrated in vacuo. The mixture was analyzed using Liquid Chromatography–Mass Spectrometry, which contained masses corresponding to **6a**, **6b**, and negligible quantities of **28a** and **28b**.

General Procedure for the Three-Component Synthesis of 8a-g

Desiccant Screen for the synthesis of dihydroisoquinolones

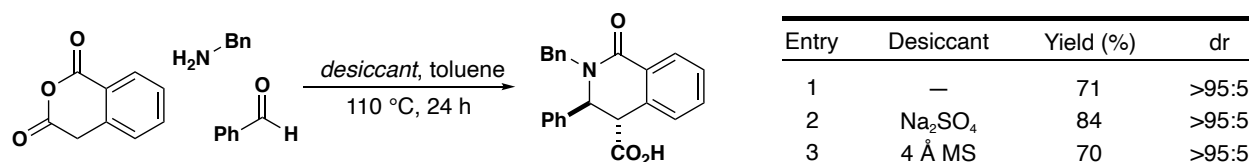
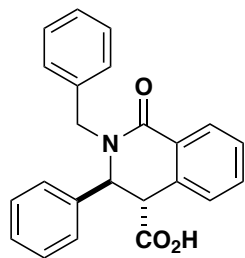


Figure S1. Desiccant screen for the 3CR

General procedure for the synthesis of dihydroisoquinolones (8): Homophthalic anhydride (81.0 mg, 0.5 mmol) and Na₂SO₄ (1 equiv) were added to a flame dried microwave vial under argon and dissolved in toluene (1.0 mL, 0.5 M). Aldehyde (0.5 mmol, 1 equiv) and amine (0.5 mmol, 1 equiv) were added sequentially, and the vial was sealed shut. The vial was then placed in a silicone oil bath and heated to 110 °C. After 24 h, the reaction was concentrated in vacuo. The crude reaction mixture was purified using gradient flash column chromatography (EtOAc:Hexanes).

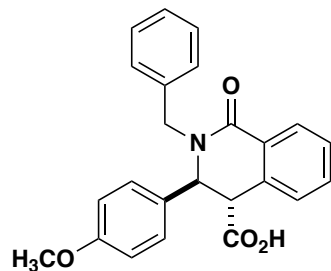


***trans*-2-benzyl-1-oxo-3-phenyl-1,2,3,4-tetrahydroisoquinoline-4-carboxylic acid (8a)**

Prepared according to the general three component reaction procedure. The crude reaction mixture was purified by gradient flash column chromatography (40-100% EtOAc:Hexanes) to afford **8a** (0.150 g, 84%), a single diastereomer, as a white solid.

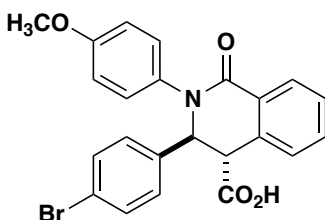
8a was also prepared on a 1 mmol scale. In this experiment, **8a** was purified by sequential trituration from hexanes then ether to afford (0.285 g, 80%), a single diastereomer, as a white solid.

Finally, **8a** was also prepared in two-steps from **36a**. **36a** (0.134 g, 0.5 mmol) and Na₂SO₄ (0.071 g, 0.5 mmol) was added to a flame dried microwave vial under argon and dissolved in toluene. Benzaldehyde (0.051 mL, 0.5 mmol) was added to the reaction mixture and the vial was sealed shut. The vial was then placed in a silicone oil bath and heated to 110 °C. The vial was then placed in a silicone oil bath and heated to 110 °C. After 24 h, the reaction was concentrated in vacuo. The crude reaction mixture was purified using gradient flash column chromatography (EtOAc:Hexanes) to afford **8a** (0.146 g, 82%), a single diastereomer, as a white solid: mp 220.2-224.3 °C; ¹H NMR (600 MHz, CDCl₃) δ 8.29 (dd, *J* = 7.6, 1.6 Hz, 1H), 7.46 (dtd, *J* = 25.4, 7.5, 1.4 Hz, 2H), 7.26 – 7.21 (m, 5H), 7.18 – 7.12 (m, 3H), 7.11 – 7.06 (m, 1H), 7.06 – 7.02 (m, 2H), 5.66 (d, *J* = 14.5 Hz, 1H), 5.11 (s, 1H), 3.87 (s, 1H), 3.70 (d, *J* = 14.6 Hz, 1H).; ¹³C NMR (101 MHz, CDCl₃) δ 175.1, 163.8, 138.2, 136.5, 132.3, 131.3, 129.3, 129.1, 128.9 (2 carbons), 128.8, 128.4, 128.3, 128.1, 127.6, 126.3, 60.1, 50.9, 49.0.; AMM (ESI-TOF) *m/z* calcd for C₂₃H₁₈NO₃⁻ [M-H]⁻ 356.1292, found 356.1293.



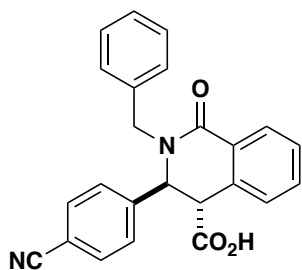
***trans*-2-benzyl-3-(4-methoxyphenyl)-1-oxo-1,2,3,4-tetrahydroisoquinoline-4-carboxylic acid (8b)**

Prepared according to the general three component reaction procedure. The crude reaction mixture was purified by gradient flash column chromatography (20-100% EtOAc:Hexanes) to afford **8b** (0.142 g, 89%), a single diastereomer, as a yellow solid: mp 102.4-105.3 °C; ¹H NMR (600 MHz, CDCl₃) δ 8.28 (dd, *J* = 7.5, 1.6 Hz, 1H), 7.46 (dtd, *J* = 20.9, 7.5, 1.4 Hz, 2H), 7.23 (dd, *J* = 6.9, 2.7 Hz, 2H), 7.13 (dd, *J* = 5.3, 1.9 Hz, 3H), 7.09 (d, *J* = 7.3 Hz, 1H), 6.95 (d, *J* = 8.6 Hz, 2H), 6.76 – 6.74 (m, 2H), 5.64 (d, *J* = 14.7 Hz, 1H), 5.04 (s, 1H), 3.83 (s, 1H), 3.74 (s, 3H), 3.68 (d, *J* = 14.6 Hz, 1H).; ¹³C NMR (101 MHz, CDCl₃) δ 175.3, 163.8, 159.5, 136.7, 132.4, 131.6, 130.3, 129.5, 129.3, 129.0, 128.9, 128.5, 128.5, 127.7, 127.7, 114.4, 59.8, 55.4, 51.2, 49.0.; AMM (ESI-TOF) *m/z* calcd for C₂₄H₂₀NO₄⁻ [M-H]⁻ 386.1398, found 386.1400.



***trans*-3-(4-bromophenyl)-2-(4-methoxyphenyl)-1-oxo-1,2,3,4-tetrahydroisoquinoline-4-carboxylic acid (8c)**

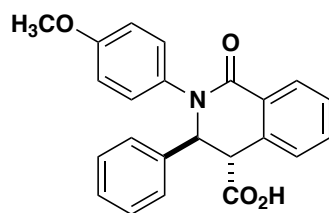
Prepared according to the general three component reaction procedure. The crude reaction mixture was purified first by trituration with hexanes, followed by gradient flash column chromatography (20-100% EtOAc:Hexanes) to afford **8c** (0.192, 85%) a single diastereomer, as an off-white solid: ^1H NMR matches reported literature spectrum¹³: ^1H NMR (400 MHz, DMSO- d_6) δ 7.98 (d, J = 7.5 Hz, 1H), 7.44 (d, J = 7.8 Hz, 4H), 7.25 (d, J = 8.7 Hz, 3H), 7.16 (d, J = 8.3 Hz, 2H), 6.94 (d, J = 8.8 Hz, 2H), 5.62 (s, 1H), 4.19 (s, 1H), 3.74 (s, 3H).



***trans*-2-benzyl-3-(4-cyanophenyl)-1-oxo-1,2,3,4-tetrahydroisoquinoline-4-carboxylic acid (**8d**)**

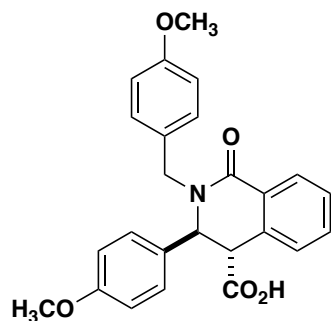
Prepared according to the general three component reaction procedure. The crude reaction mixture was purified by gradient flash column chromatography (20-100% EtOAc:Hexanes) to afford **8d** (0.167 g, 88%), a single diastereomer, as an off-white amorphous solid: ^1H NMR (400 MHz, CDCl_3) δ 8.27 (dd, J = 7.4, 1.8 Hz, 1H), 7.54 – 7.37 (m, 4H), 7.23 – 7.16 (m, 2H), 7.16 – 7.02 (m, 6H), 5.43 (d, J = 14.5 Hz, 1H), 5.18 (s, 1H), 3.96 (d, J = 14.5 Hz, 1H), 3.81 (d, J = 1.5 Hz, 1H).; ^{13}C NMR (101 MHz, CDCl_3) δ 174.3, 163.6, 143.7, 135.9, 132.7, 132.7, 130.7, 129.2, 129.2, 129.1, 128.9, 128.6, 128.4, 127.9,

127.1, 118.1, 112.2, 60.1, 50.7, 49.6.; AMM (ESI-TOF) m/z calcd for $C_{24}H_{17}N_2O_3^-$ [M-H]⁻ 381.1245, found 381.1246.



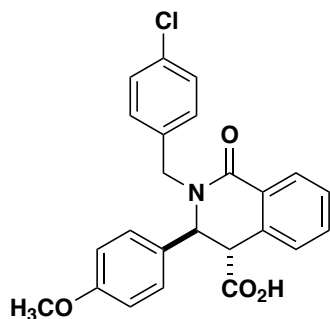
***trans*-2-(4-methoxyphenyl)-1-oxo-3-phenyl-1,2,3,4-tetrahydroisoquinoline-4-carboxylic acid (**8e**)**

Prepared according to the general three component reaction procedure. The crude reaction mixture was purified by gradient flash column chromatography (20-100% EtOAc:Hexanes) to afford **8e** (0.144 g, 77%), a single diastereomer, as a brown amorphous solid: ¹H NMR (400 MHz, CDCl₃) δ 8.55 (s, 1H), 8.20 (dd, *J* = 5.8, 3.4 Hz, 1H), 7.41 (dd, *J* = 5.7, 3.3 Hz, 2H), 7.21 – 7.14 (m, 6H), 7.13 – 7.08 (m, 2H), 6.78 – 6.71 (m, 2H), 5.52 (d, *J* = 1.4 Hz, 1H), 3.96 (d, *J* = 1.5 Hz, 1H), 3.70 (s, 3H).; ¹³C NMR (101 MHz, CDCl₃) δ 174.3, 164.3, 158.5, 139.0, 134.9, 132.7, 132.6, 129.6, 129.3, 128.9, 128.7, 128.5, 128.2, 128.1, 126.6, 114.4, 65.3, 55.4, 51.7.; AMM (ESI-TOF) m/z calcd for $C_{23}H_{18}NO_4^-$ [M-H]⁻ 372.1241, found 372.1241.



***trans*-2-(4-methoxybenzyl)-3-(4-methoxyphenyl)-1-oxo-1,2,3,4-tetrahydroisoquinoline-4-carboxylic acid (**8f**)**

Prepared according to the general three component reaction procedure. The crude reaction mixture was purified by gradient flash column chromatography (EtOAc:Hexanes) to afford **8f** (0.158 g, 76%), a single diastereomer as a yellow amorphous solid: ^1H NMR (400 MHz, CDCl_3) δ 8.27 – 8.21 (m, 1H), 7.43 (qt, $J = 7.4, 3.6$ Hz, 2H), 7.22 – 7.13 (m, 2H), 7.08 (dd, $J = 6.9, 1.8$ Hz, 1H), 6.99 – 6.91 (m, 2H), 6.79 – 6.66 (m, 4H), 5.57 (d, $J = 14.4$ Hz, 1H), 5.10 – 5.01 (m, 1H), 3.82 (d, $J = 1.5$ Hz, 1H), 3.73 (s, 3H), 3.68 (s, 3H), 3.63 (d, $J = 14.5$ Hz, 1H).; ^{13}C NMR (101 MHz, CDCl_3) δ 175.5, 163.7, 159.3, 159.0, 132.2, 131.6, 130.3, 130.2, 129.3, 129.1, 128.8, 128.7, 128.3, 127.5, 114.2, 113.7, 59.5, 55.3, 55.2, 51.2, 48.3.; AMM (ESI-TOF) m/z calcd for $\text{C}_{25}\text{H}_{22}\text{NO}_5^-$ $[\text{M}-\text{H}]^-$ 416.1503, found 416.1506.



***trans*-2-(4-chlorobenzyl)-3-(4-methoxyphenyl)-1-oxo-1,2,3,4-tetrahydroisoquinoline-4-carboxylic acid (**8g**)**

Prepared according to the general three component reaction procedure. The crude reaction mixture was purified by gradient flash column chromatography (EtOAc:Hexanes) to afford **8g** (0.200 g, 95%), a single diastereomer, as a white solid: mp range 247.3-249.3 °C; ¹H NMR (400 MHz, DMSO-d₆) δ 7.98 (dd, *J* = 7.2, 2.0 Hz, 1H), 7.49 – 7.37 (m, 2H), 7.30 (d, *J* = 2.3 Hz, 4H), 7.23 – 7.17 (m, 1H), 6.94 (d, *J* = 8.7 Hz, 2H), 6.79 (d, *J* = 8.7 Hz, 2H), 5.22 (d, *J* = 15.1 Hz, 1H), 5.18 (s, 1H), 4.03 (s, 1H), 3.84 (d, *J* = 15.0 Hz, 1H), 3.66 (s, 3H).; ¹³C NMR (101 MHz, DMSO-d₆) δ 172.1, 163.5, 158.7, 136.5, 133.9, 132.1, 131.8, 130.8, 130.0, 129.7, 128.9, 128.2, 128.0, 127.3, 127.0, 114.1, 60.8, 55.1, 51.0, 48.6.; IR: 2949.0, 2831.6, 1697.8, 1641.5 cm⁻¹; AMM (ESI-TOF) *m/z* calcd for C₂₄H₁₉ClNO₄⁻ [M-H]⁻ 420.1008, found 420.1011.

5.5 References

1. Wei, J.; Shaw, J. T., *Org. Lett.* **2007**, *9* (20), 4077-4080.
2. Yadav, J. S.; Reddy, B. V. S.; Saritha Raj, K.; Prasad, A. R., *Tetrahedron* **2003**, *59* (10), 1805-1809.
3. Azizian, J.; Mohammadi, A. A.; Karimi, A. R.; Mohammadizadeh, M. R.; Koohshari, M., *Heterocycles* **2004**, *63* (9), 2013-2017.
4. Azizian, J.; Mohammadi, A. A.; Karimi, A. R.; Mohammadizadeh, M. R., *J. Org. Chem.* **2005**, *70* (1), 350-352.
5. Wang, L.; Liu, J.; Tian, H.; Qian, C.; Sun, J., *Adv. Synth. Catal.* **2005**, *347* (5), 689-694.
6. Azizian, J.; Mohammadi, A. A.; Soleimani, E.; Karimi, A. R.; Mohammadizadeh, M. R., *J. Heterocycl. Chem.* **2006**, *43* (1), 187-190.
7. Ng, P. Y.; Masse, C. E.; Shaw, J. T., *Org. Lett.* **2006**, *8* (18), 3999-4002.
8. Yadav, J. S.; Reddy, B. V. S.; Reddy, A. R.; Narsaiah, A. V., *Synthesis* **2007**, (20), 3191-3194.
9. Karimi, A. R.; Pashazadeh, R., *Synthesis* **2010**, (3), 437-442.
10. Mohammadi, M. H.; Mohammadi, A. A., *Synth. Commun.* **2011**, *41* (4), 523-527.
11. Karimi, A. R.; Momeni, H. R.; Pashazadeh, R., *Tetrahedron Lett.* **2012**, *53* (27), 3440-3443.
12. Ghorbani-Choghamarani, A.; Hajjami, M.; Norouzi, M.; Abbasityula, Y.; Eigner, V.; Dušek, M., *Tetrahedron* **2013**, *69* (32), 6541-6544.
13. Chupakhin, E.; Dar'in, D.; Krasavin, M., *Tetrahedron Lett.* **2018**, *59* (26), 2595-2599.

14. Balasubramaniyan, V.; Argade, N. P., *Synth. Commun.* **1989**, *19* (18), 3103-3111.
15. Kshirsagar, U. A.; Argade, N. P., *Tetrahedron* **2009**, *65* (27), 5244-5250.

Appendix A: Relative Rates of the Castagnoli-Cushman Reaction

A.1 Introduction

A.1.1 Introduction to pK_E Calculations

The enol form of carboxylic acid derivatives has been suggested as an intermediate in a variety of organic transformations including the CCR.¹⁻³ The proposed enol intermediates have prompted studies to further the understanding of their formation and equilibrium concentration in reactions.⁴⁻⁶ The measurement of the $-\log$ of the equilibrium concentration of a carbonyl versus its enol form is called the pK_E value.⁷ These values can be calculated using the equation $\Delta G = -RT \ln(K_E)$ where the K_E corresponds to the equilibrium constant of keto-enol tautomerization. The ΔG values of keto-enol tautomerization have previously been calculated using density functional theory (DFT) for a range of carboxylic acid derivatives including anhydrides, esters, amides, and acyl halides.⁴ It has been suggested that the equilibrium of carboxylic acid derivatives do not lie towards the enol form in comparison to other carbonyl systems, due to stabilization of the keto-tautomer **2** by resonance structure **3** (Figure A.1).^{4, 7} Notably, the presence of substituents attached to the enol carbon (**R**) can influence the propensity for enolization, leading to lower pK_E values.^{4, 7-10} Specifically, the presence of electron withdrawing groups (EWGs) provide resonance stabilization of the negative charge and may form hydrogen bonding interactions with the enol, causing stabilization of the enol resonance form.^{4, 11} We initiated a study of the pK_E values of anhydrides commonly used in the CCR to enable a facile method to predict anhydride reactivity based on α -substituents.

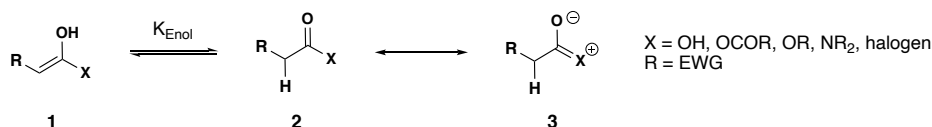


Figure A.17 Resonance stabilization of the keto form of carboxylic acid derivatives.

A.1.2 Effect of Electron Withdrawing Anhydride Substituents on Reaction Time in the Castagnoli Cushman Reaction

The reactivity of cyclic anhydrides can be generally correlated to the ability of the α -substituent to stabilize the enol form of the anhydride. This trend is particularly evident when comparing the temperature required for the CCR of anhydrides **4-11** (Figure A.2). Reactions of succinic and glutaric anhydrides (**10, 11**), some of the least enolizable anhydrides, require refluxing xylenes and increased reaction times. On the other hand, reactions of homophthalic anhydride (**4**), the most readily enolizable anhydride, occur at room temperature over a period of 30 minutes. The reactivity of other anhydrides commonly used in the CCR (**5-9**) typically fall in between these two extremes, ostensibly dependent on the stabilizing ability of the substituent at the α -position.

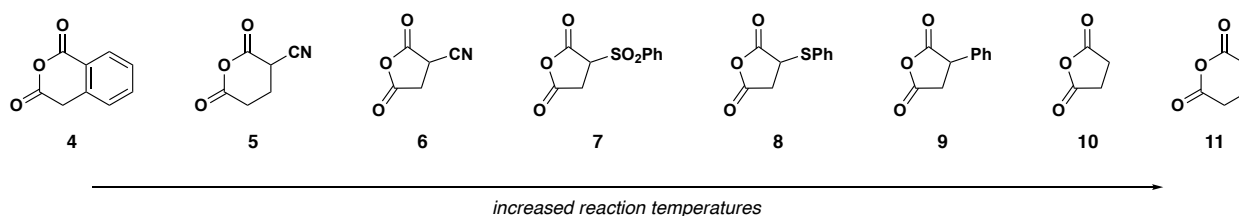


Figure A.18 Anhydrides commonly used in the CCR are performed with ranging reaction temperatures, from room temperature to 150 °C.

The computational evidence for the Mannich-like mechanism for the CCR showed that the rate determining step for the major diastereomer of the reaction is Mannich addition. The formation of a hydrogen-bonding enol complex **13-14** is found to be an

intermediate on the reaction coordinate prior to Mannich addition with cyano-succinic anhydride (Figure A.3).^{2, 3} An important consideration for the CCR mechanism is the difference in the transition state structures of CCRs with more enolizable anhydrides like cyanosuccinic anhydride compared to less enolizable anhydrides such as thiosuccinic anhydrides. Specifically, reactions with more readily enolizable anhydrides such as homophthalic anhydride and cyanosuccinic anhydride are thought to proceed through a closed transition states, and reactions of thioarylsuccinic anhydrides and arylsuccinic anhydrides are thought to proceed through open transition states such as **18**. These hypotheses have been supported by the stereochemical outcomes of the CCR with varying anhydrides.^{3, 12} In both of these cases, it is hypothesized that the reaction proceeds through similar hydrogen-bonding enol complexes. Although enol formation is not the rate determining step of the reaction, it is possible that the rate of the CCR is dependent on the ability of an anhydride to enolize.

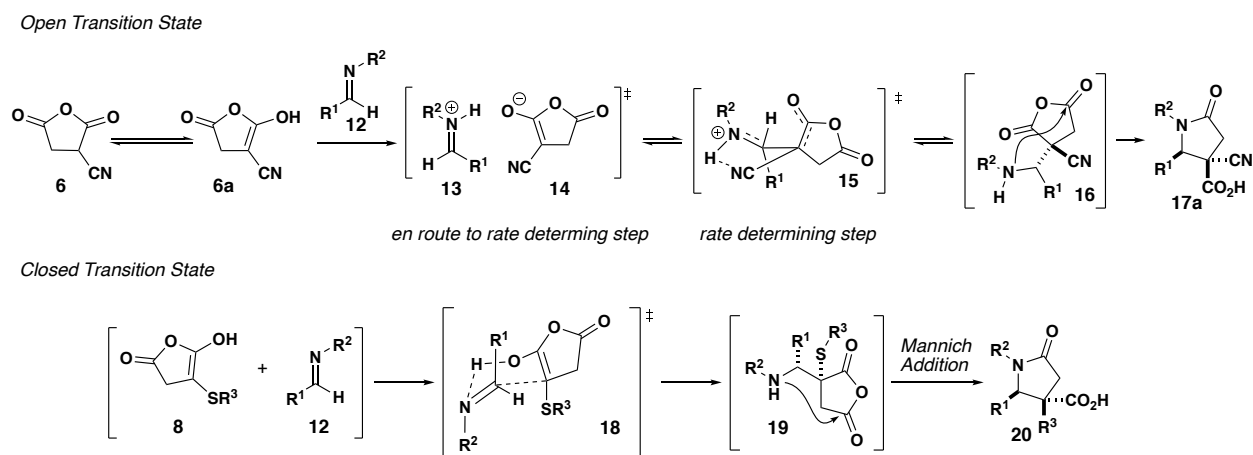


Figure A.19 Computational evidence has shown that the CCR of cyano-succinic anhydride proceeds through a Mannich-like mechanism wherein Mannich addition is the rate-determining step, as well as the comparison between the two possible reaction pathways.

Due to the COVID-19 pandemic, lab-based research was halted for several months. While in quarantine I was interested in both expanding my knowledge of computational chemistry and further studying the proposed Mannich-like mechanism. To do this, the relative enolizability of anhydrides commonly used in the CCR were calculated and compared to the rate of the CCR. We hypothesized that the calculated pK_E values should be directly correlated to the rate of the CCR, which would allow for a simple, efficient way to delineate the reactivity of anhydrides in the CCR based on the α -substituent.

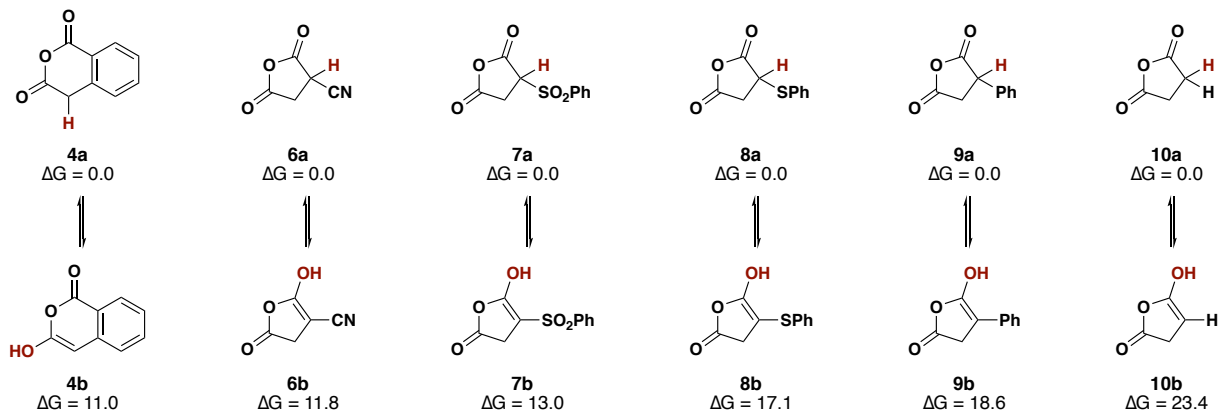
A.2 Results and Discussion

A.1.3 pK_E Value Calculations of Anhydrides Commonly used in the Castagnoli Cushman Reaction

Initial investigation involved calculating pK_E values of anhydrides **4** and **6–10** (Figure A.2). Using the program Avogadro, a conformer search was performed on both the anhydride and enol form of the substrates containing rotatable bonds. Next, the geometries of the anhydrides (**4**, **6–10**) and their enol tautomers were optimized using Gaussian 16 using DFT, specifically B3LYP/631-G** in dichloromethane. To obtain the pK_E value of the anhydrides, first the ΔG values were extracted and plugged into the equation $\Delta G = -RT \ln K_E$ to afford K_E values (Table 1). Next, pK_E values were calculated by taking the $-\text{Log}(K_E)$. As a measure of the validity of these calculations, pK_E values were correlated to the pK_a values of acetophenone derivatives with the same substituents at the alpha position. As expected, a linear relationship between pK_a and calculated pK_E

was observed, indicating that the acidity of the anhydride was directly related to its enolizability

Calculated ΔG Values of Enolization



Known pK_a values of acetophenone derivatives

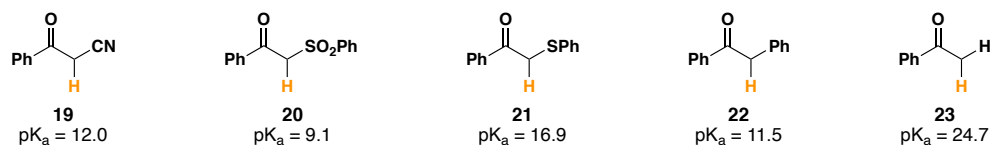


Figure A.20 (Top) Calculated ΔG values of anhydrides commonly used in the CCR. (Bottom) Known pK_a values of acetophenone derivatives with the same substituents.

Table 3: Calculated pKE values of anhydrides **4**, and **6-10**

	Energy in HF	Energy in kcal/mol	$\Delta G = -RT\ln(K_E)$	pK_E
CH₂Cl₂	B3LYP/631G**			
10a	-380.488706	-238760.0874		
10b	-380.450056	-238735.8342		
ΔG	0.03865	24.25322285	1.62326E-18	17.8
8b	-1009.655544	-633567.9408		
8a	-1009.627588	-633550.3981		
ΔG	0.027956	17.5426416	1.35695E-13	12.9
9a	-611.472063	-383704.2228		
9b	-611.441922	-383685.309		
ΔG	0.030141	18.91374877	1.33926E-14	13.9
6a	-472.721981	-296637.2976		
6b	-472.70215	-296624.8534		
ΔG	0.019831	12.44413098	7.45237E-10	9.1
7a	-1160.035386	-727932.645		
7b	-1160.013842	-727919.126		
ΔG	0.021544	13.5190539	1.21295E-10	9.9
4a	-572.187803	-359052.9961		
4b	-572.1705	-359042.1383		
ΔG	0.017303	10.85778823	1.0861E-08	8.0

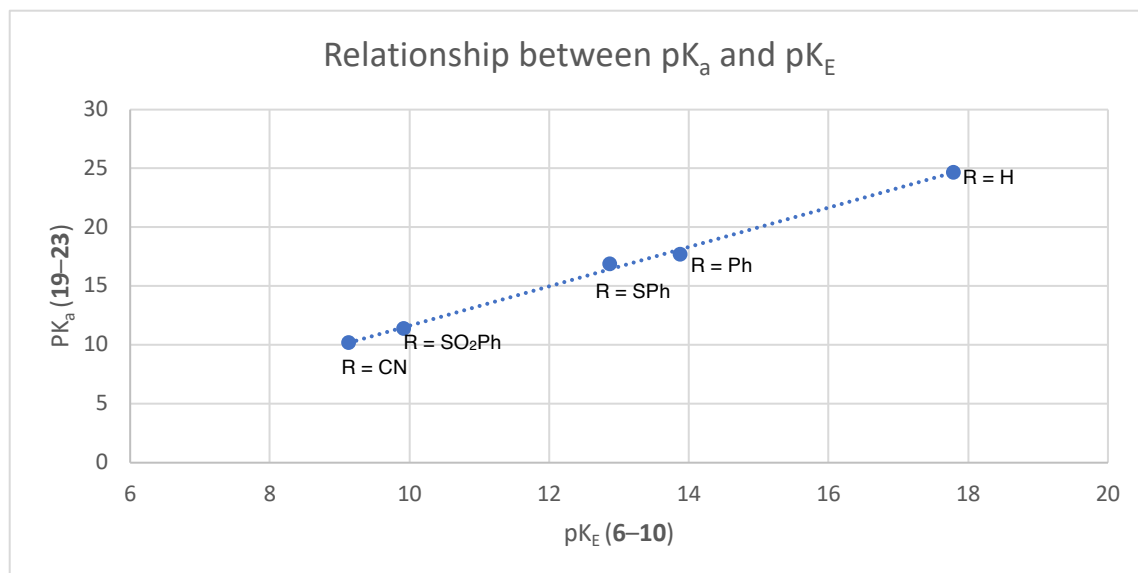


Figure A.21 Comparison of calculated pK_E values of compounds **6-10**, compared to Known pK_a values of acetophenone derivatives (**21-25**).

Next, the rates of the reactions of these anhydrides were to be determined using ReactIR. Several ReactIR experiments were run with varying results. First, it was found that the reaction of homophthalic anhydride (**4**) and *N*-benzylidene methylamine (**26**) occurred so rapidly at room temperature that it was unable to be analyzed using the ReactIR (Figure A.6). Additionally, the reaction of *N*-benzylidene methylamine (**26**) with phenyl-succinic anhydride (**9**) provided an interesting result, wherein the imine and anhydride were being consumed at different rates (Figure A.7). Due to my inexperience with ReactIR technology, it is possible that this is explained by overlapping frequencies leading to inconsistent, unclear outcomes. As a result, we initiated a collaboration with the Hein group at University of British Columbia due to their expertise in reaction monitoring and analysis.

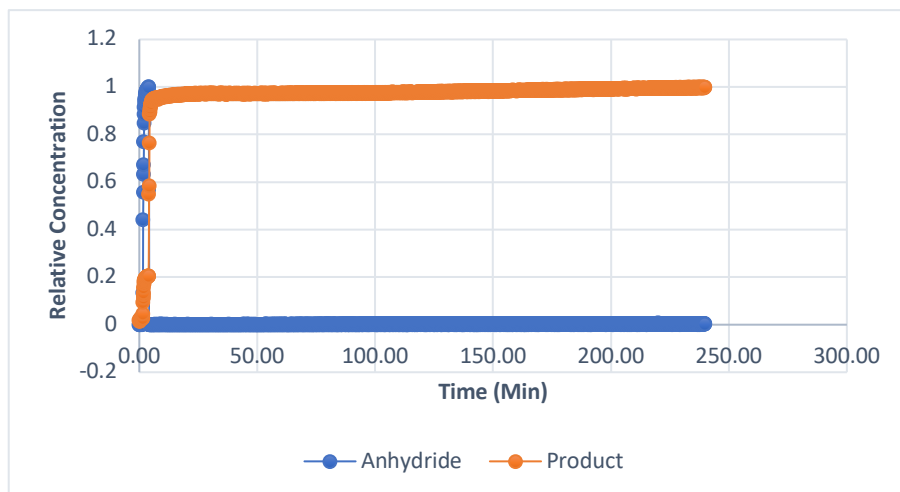
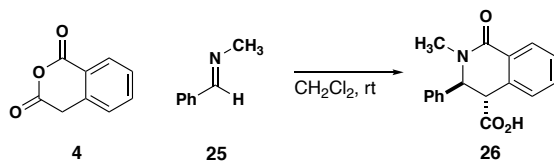


Figure A.22 React IR experiment of homophthalic anhydride with *N*-benzylidene methylamine

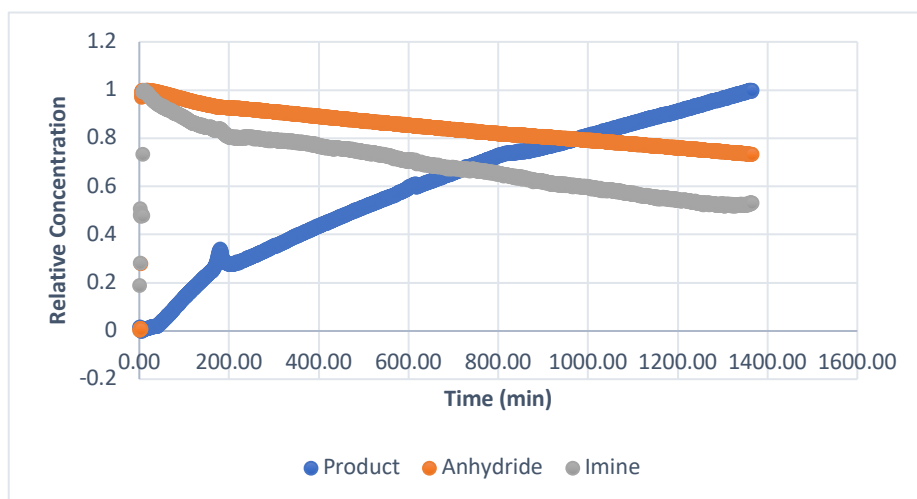
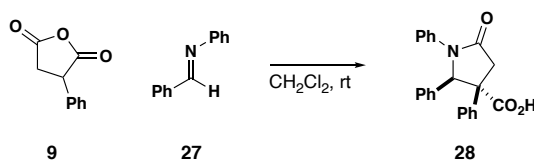


Figure A.23 React IR experiment of phenylsuccinic anhydride and *N*-benzylidene aniline

Finally, several anhydrides that were to be tested by the Hein group using ReactIR were synthesized, as well as three uncharacterized CCR products. First, cyanosuccinic anhydride was synthesized. Several attempts at the formation of cyanosuccinic anhydride (**6**) from ethylcyanoacetate (**29**) and ethylbromoacetate (**30**) proved futile and led exclusively to the dialkylated product **32**. This synthesis is known to be challenging, and instead cyanosuccinic anhydride was synthesized from commercially available diester **33**. Thiophenyl succinic anhydride (**8**) was synthesized by conjugate addition reaction of thiophenol and maleic anhydride in modest yield. Notably, the bottle of maleic anhydride used in the reaction had hydrolyzed to the diacid, leading to inconsistent results in previous attempts. Purification of maleic anhydride led to better reaction outcomes. Ultimately, γ -lactams **35**, **36a**, and **36b** were synthesized using known methods in good yields as mixtures of diastereomers.

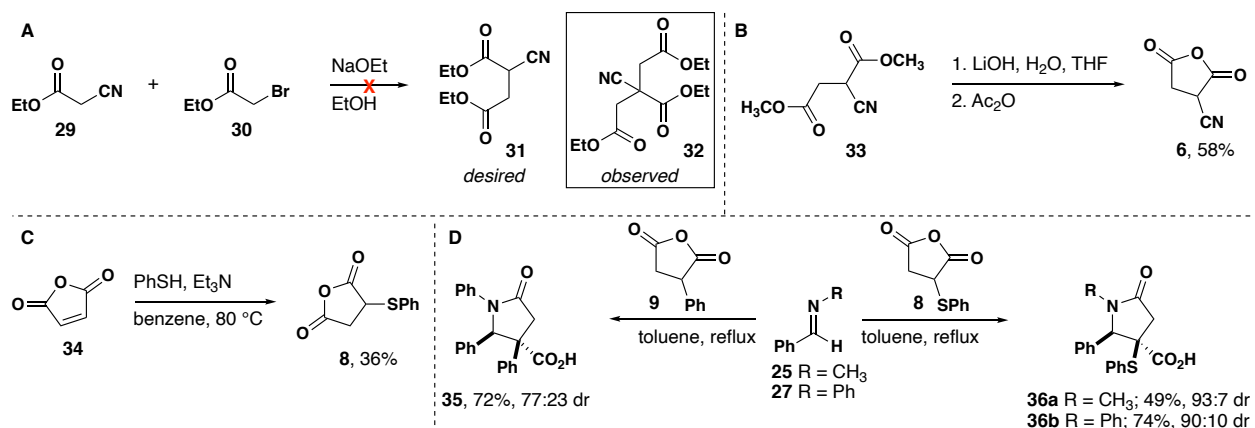


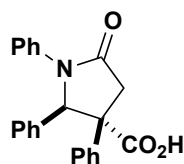
Figure A.24 **A**. Failed synthesis of cyanosuccinic anhydride. **B**. Successful synthesis of cyanosuccinic anhydride. **C**. Synthesis of thiophenylsuccinic anhydride **D**. Synthesis of uncharacterized lactams **35**–**36**.

A.3 Conclusion

In conclusion, the pK_E values of a variety of anhydrides have been computed using DFT in Gaussian16. As expected, anhydrides containing stabilizing groups in the alpha position had lower pK_E values, and those with less stabilizing substituents had higher pK_E values. These results suggest that the relative enolizability of an anhydride can be determined using DFT calculations. With this knowledge, the pK_E values of anhydrides less commonly used can be easily computed to determine the reaction conditions necessary to successfully perform CCR experiments. Future work will involve collaboration with the Hein group to determine the rates of the reactions of anhydrides **4** and **6-11** with *N*-benzylidene aniline and *N*-benzylidene methylamine using infrared spectroscopy in situ (React-IRTM).

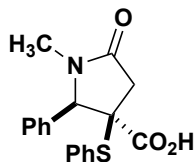
A.4 Experimental Section

General Procedure: To a flame dried microwave vial was added anhydride (0.5 mmol) and dissolved in toluene (2.0 M). Imine (1 equiv) was added to the reaction mixture and the microwave vial was sealed. The reaction was then heated to reflux in a silicone oil bath overnight. The unpurified reaction mixture was cooled to room temperature and concentrated in vacuo and purified by flash column chromatography.



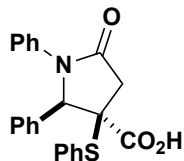
***trans*-5-oxo-1,2,3-triphenylpyrrolidine-3-carboxylic acid (35):**

Following the general procedure with phenyl succinic anhydride (0.088 g, 0.5 mmol) *N*-benzylidene aniline (0.090 g, 0.5 mmol) in toluene (2.5 mL, 2.0 M), product **35** was isolated as an off white amorphous solid (0.128 g, 72%) as a mixture of diastereomers (77:23 dr). Major diastereomer: ¹H NMR (400 MHz, CDCl₃) δ 8.05 (s, 1H), 7.42 (d, *J* = 7.9 Hz, 2H), 7.26 – 6.89 (m, 13H), 6.09 (s, 1H), 3.59 (d, *J* = 16.9 Hz, 1H), 3.42 (d, *J* = 16.9 Hz, 1H).; ¹³C NMR (101 MHz, CDCl₃) δ 177.4, 172.0, 137.7, 135.3, 134.7, 128.9, 128.4, 128.2, 128.0, 128.0, 127.7, 127.1, 125.8, 122.9, 70.3, 58.1, 38.1. AMM (ESI-TOF) *m/z* calcd for C₂₃H₂₀NO₃⁺ [M+H]⁺ 358.1438, found 358.1436.



***trans*-1-methyl-5-oxo-2-phenyl-3-(phenylthio)pyrrolidine-3-carboxylic acid (36a):**

Following the general procedure with thiophenyl succinic anhydride (0.104 g, 0.5 mmol) *N*-benzylidene methylamine (0.064 mL, 0.5 mmol) in toluene (2.5 mL, 2.0 M), product **36a** was isolated as an off-white amorphous solid (0.083 g, 49%) as a mixture of diastereomers (93:7 dr). Major diastereomer: ¹H NMR (600 MHz, CDCl₃) δ 7.45 (d, *J* = 5.7 Hz, 3H), 7.33 – 7.25 (m, 5H), 7.21 (t, *J* = 7.4 Hz, 2H), 5.24 (s, 1H), 3.19 (d, *J* = 17.4 Hz, 1H), 2.88 (d, *J* = 17.4 Hz, 1H), 2.75 (s, 3H).; ¹³C NMR (151 MHz, CDCl₃) δ 175.2, 173.0, 136.2, 133.8, 129.9, 129.9, 129.5, 129.5, 129.2, 128.8, 70.3, 58.2, 40.6, 29.1.; AMM (ESI-TOF) *m/z* calcd for C₁₈H₁₈NO₃S⁺ [M+H]⁺ 328.1002, found 328.0997.

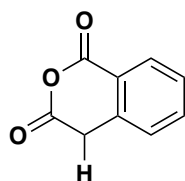


***trans*-5-oxo-1,2-diphenyl-3-(phenylthio)pyrrolidine-3-carboxylic acid (36b):**

Following the general procedure with thiophenyl succinic anhydride (0.104 g, 0.5 mmol) *N*-benzylidene aniline (0.090 g, 0.5 mmol) in toluene (2.5 mL, 2.0 M), product **36b** was isolated as an off white amorphous solid (0.144 g, 74%) as a mixture of diastereomers (90:10 dr). Major diastereomer: ¹H NMR (400 MHz, CDCl₃) δ 7.40 (d, *J* = 4.4 Hz, 8H), 7.29 (d, *J* = 8.8 Hz, 2H), 7.21 (td, *J* = 7.9, 2.9 Hz, 4H), 7.08 (t, *J* = 7.4 Hz, 1H), 5.82 (s, 1H), 3.27 (d, *J* = 17.1 Hz, 1H), 3.03 (d, *J* = 17.1 Hz, 1H).; ¹³C NMR (101 MHz, CDCl₃) δ 175.3, 171.1, 137.5, 136.2, 134.5, 130.0, 129.3, 129.3, 129.1, 128.9, 128.8, 128.1, 125.7, 122.2, 69.7, 58.5, 41.2.; AMM (ESI-TOF) *m/z* calcd for C₂₃H₂₀NO₃S⁺ [M+H]⁺ 390.1158, found 390.1156.

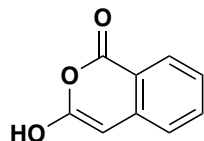
Energies and Coordinates

General Procedure: Conformer searches were performed on both the anhydride and enol form of the substrates containing rotatable bonds using Avogadro. Next, the geometries were optimized using Gaussian 16 at B3LYP/631-G** level of theory in dichloromethane.



Calculated Energy: HF=-572.2798264 Hartrees (-359105.59 kcal/mol)

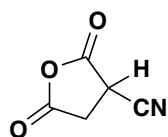
Center Number	Atomic Number	Atomic Type	Coordinates (Angstroms)		
			X	Y	Z
1	6	0	-1.596436	-1.616425	0.050462
2	6	0	-2.834541	-0.988679	-0.075839
3	6	0	-2.919631	0.406661	-0.147082
4	6	0	-1.760472	1.170088	-0.093653
5	6	0	-0.513544	0.537897	0.028373
6	6	0	-0.423723	-0.858299	0.104594
7	1	0	-1.538661	-2.699538	0.107141
8	1	0	-3.737953	-1.589202	-0.120512
9	1	0	-3.885975	0.890129	-0.245686
10	1	0	-1.792785	2.252407	-0.149012
11	6	0	0.922167	-1.506978	0.283499
12	1	0	1.061166	-1.797183	1.335548
13	1	0	1.014388	-2.428646	-0.296457
14	6	0	2.106697	-0.636325	-0.064570
15	6	0	0.699843	1.378485	0.071034
16	8	0	1.933315	0.732495	-0.003126
17	8	0	3.200635	-1.057862	-0.328892
18	8	0	0.715758	2.582053	0.135526



Calculated Energy: HF=-572.2632254 Hartrees (-359095.17 kcal/mol)

Center Number	Atomic Number	Atomic Type	Coordinates (Angstroms)		
			X	Y	Z
1	6	0	-1.581500	-1.658670	0.000236
2	6	0	-2.832206	-1.058624	0.000067
3	6	0	-2.961895	0.341559	-0.000148
4	6	0	-1.823943	1.132773	-0.000161
5	6	0	-0.551134	0.536839	0.000023
6	6	0	-0.410442	-0.872972	0.000190
7	1	0	-1.493269	-2.741740	0.000379
8	1	0	-3.723236	-1.680851	0.000085
9	1	0	-3.946779	0.798301	-0.000288
10	1	0	-1.888101	2.215921	-0.000281
11	6	0	0.631028	1.396203	0.000094
12	6	0	1.977281	-0.607683	0.000025
13	6	0	0.911067	-1.441955	0.000277
14	1	0	1.051678	-2.517347	0.000554
15	8	0	3.278784	-0.937687	-0.000032

16	1	0	3.360711	-1.905584	0.000004
17	8	0	1.871213	0.736171	-0.000231
18	8	0	0.661186	2.604826	-0.000246

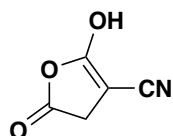


Calculated Energy: HF=-472.7606923 Hartrees (-296657.33 kcal/mol)

Center Number	Atomic Number	Atomic Type	Coordinates (Angstroms)		
			X	Y	Z

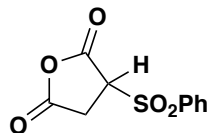
1	6	0	0.444450	-1.277727	0.169466
2	6	0	-0.687553	-0.306360	0.552170
3	6	0	-0.159217	1.068249	0.091025
4	6	0	1.633249	-0.366770	-0.075508
5	1	0	0.679190	-2.013061	0.940782
6	1	0	0.227746	-1.818021	-0.758176
7	1	0	-0.785232	-0.242645	1.644465
8	8	0	2.785626	-0.644755	-0.214619
9	8	0	-0.756158	2.096196	-0.015790
10	6	0	-2.002216	-0.615661	-0.004786
11	7	0	-3.038095	-0.887185	-0.450052

12 8 0 1.192117 0.957764 -0.153456



Calculated Energy: HF=-472.7421825 Hartrees (-296645.72 kcal/mol)

Center Number	Atomic Number	Atomic Type	Coordinates (Angstroms)		
			X	Y	Z
1	6	0	-0.505557	-1.322475	0.000041
2	6	0	0.664269	-0.368732	-0.000138
3	6	0	0.158722	0.891980	-0.000064
4	6	0	-1.693123	-0.371814	-0.000141
5	1	0	-0.559360	-1.969297	-0.882874
6	1	0	-0.559312	-1.969056	0.883136
7	8	0	-1.199452	0.948873	-0.000200
8	8	0	-2.867039	-0.586399	0.000297
9	8	0	0.719808	2.088269	-0.000090
10	1	0	1.686804	2.001633	0.000160
11	6	0	2.036284	-0.686342	-0.000183
12	7	0	3.177395	-0.932132	0.000348

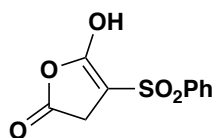


Calculated Energy: HF=-1160.1564453 Hartrees (-727998.17 kcal/mol)

Center Number	Atomic Number	Atomic Type	Coordinates (Angstroms)		
			X	Y	Z

1	6	0	2.487592	0.846499	-0.748480
2	6	0	1.100889	0.204856	-0.809930
3	6	0	3.373504	-0.229822	-0.151634
4	1	0	2.541415	1.757796	-0.148462
5	1	0	2.862220	1.094022	-1.745982
6	6	0	1.346123	-1.261001	-0.472704
7	8	0	2.651505	-1.422258	-0.061729
8	8	0	4.516836	-0.171117	0.187912
9	8	0	0.574747	-2.176160	-0.524676
10	6	0	-1.640057	0.298177	0.165493
11	6	0	-2.040551	-0.825130	0.892398
12	6	0	-2.477240	0.916255	-0.767326
13	6	0	-3.746943	0.382540	-0.981494
14	6	0	-3.314849	-1.344173	0.667556
15	6	0	-4.161758	-0.744822	-0.267582

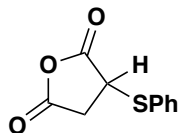
16	1	0	-4.413618	0.851479	-1.697847
17	1	0	-3.645228	-2.214768	1.224472
18	1	0	-1.372956	-1.271007	1.619858
19	1	0	-5.152604	-1.154640	-0.437162
20	1	0	-2.146776	1.804396	-1.294124
21	16	0	-0.015303	0.989018	0.454444
22	1	0	0.590420	0.300557	-1.769172
23	8	0	0.477021	0.543836	1.768611
24	8	0	-0.042394	2.419146	0.107323



Calculated Energy: HF=-1160.1369419 Hartrees (-727985.93 kcal/mol)

Center Number	Atomic Number	Atomic Type	Coordinates (Angstroms)		
			X	Y	Z
1	6	0	1.615070	1.251135	0.745335
2	6	0	1.161585	-0.095309	0.261257
3	6	0	2.914046	1.431629	-0.032622
4	1	0	1.828495	1.296895	1.819504

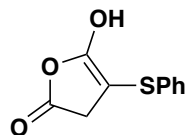
5	1	0	0.938379	2.080173	0.507565
6	6	0	2.088275	-0.573455	-0.610777
7	8	0	3.126799	0.284999	-0.821046
8	8	0	3.690432	2.338711	-0.049127
9	8	0	2.173940	-1.699092	-1.275741
10	16	0	-0.226939	-1.024725	0.738436
11	8	0	-0.105054	-2.297008	-0.036723
12	8	0	-0.333890	-1.069353	2.204605
13	1	0	1.387102	-2.235675	-0.997076
14	6	0	-1.670375	-0.155730	0.119303
15	6	0	-2.036488	-0.306459	-1.221206
16	6	0	-2.392841	0.662549	0.989968
17	6	0	-3.148734	0.385947	-1.695909
18	1	0	-1.470755	-0.964339	-1.871692
19	6	0	-3.503279	1.351245	0.499861
20	1	0	-2.097693	0.739385	2.030295
21	6	0	-3.877618	1.215043	-0.838241
22	1	0	-3.449353	0.274298	-2.732701
23	1	0	-4.077375	1.987754	1.165512
24	1	0	-4.743420	1.751490	-1.213937



Calculated Energy: HF=-1009.7714488 Hartrees (-633631.58 kcal/mol)

Center Number	Atomic Number	Atomic Type	Coordinates (Angstroms)		
			X	Y	Z
1	6	0	-2.284544	-1.209541	-0.391914
2	6	0	-1.070746	-0.288744	-0.221994
3	6	0	-3.475338	-0.272745	-0.404745
4	1	0	-2.408432	-1.893509	0.455292
5	1	0	-2.264429	-1.814522	-1.299629
6	6	0	-1.690044	1.050775	0.183192
7	8	0	-3.062227	0.997118	-0.006023
8	8	0	-4.619222	-0.495734	-0.673656
9	8	0	-1.157928	2.048557	0.578927
10	16	0	0.168584	-0.943332	0.973474
11	6	0	1.729353	-0.358444	0.301805
12	6	0	2.725156	-1.308011	0.038076
13	6	0	1.986934	1.004650	0.101701
14	6	0	3.231380	1.405232	-0.386392
15	6	0	3.975490	-0.893414	-0.423290

16	6	0	4.228340	0.461450	-0.643510
17	1	0	1.219459	1.737328	0.326559
18	1	0	3.425477	2.461058	-0.550403
19	1	0	4.745334	-1.632637	-0.623385
20	1	0	5.198251	0.780944	-1.012454
21	1	0	2.518897	-2.362723	0.189125
22	1	0	-0.552764	-0.129417	-1.172248

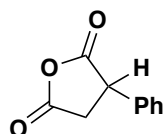


Calculated Energy: HF=-1009.7411141 Hartrees (-633612.55 kcal/mol)

Center Number	Atomic Number	Atomic Type	Coordinates (Angstroms)		
			X	Y	Z

1	6	0	1.603855	0.751676	-1.100521
2	6	0	1.100749	-0.458369	-0.350458
3	6	0	2.017126	-0.743471	0.594541
4	6	0	2.914960	1.066785	-0.400103
5	1	0	1.795413	0.566474	-2.164363
6	1	0	0.942961	1.624931	-1.042164
7	8	0	3.103709	0.110990	0.609731
8	8	0	3.718400	1.935175	-0.581271
9	8	0	2.054863	-1.720375	1.495358
10	1	0	2.868509	-1.643190	2.016547
11	16	0	-0.315325	-1.418714	-0.736590
12	6	0	-1.693657	-0.386637	-0.204457
13	6	0	-1.581008	0.572847	0.806832
14	6	0	-2.931405	-0.603806	-0.823808
15	6	0	-2.699824	1.315898	1.186875

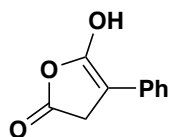
16	1	0	-0.625216	0.734100	1.295096
17	6	0	-4.047830	0.131025	-0.424902
18	1	0	-3.019196	-1.340249	-1.617503
19	6	0	-3.936509	1.097130	0.577288
20	1	0	-2.602998	2.062789	1.969748
21	1	0	-5.004019	-0.045076	-0.909077
22	1	0	-4.804753	1.674850	0.878884



Calculated Energy: HF=-611.5895603 Hartrees (-383772.45 kcal/mol)

Center Number	Atomic Number	Atomic Type	Coordinates (Angstroms)		
			X	Y	Z
1	6	0	-1.403461	2.010342	0.138738
2	6	0	-0.537946	3.106473	-0.510359
3	6	0	-2.449432	1.680542	-0.905756
4	1	0	-1.882561	2.303902	1.074247
5	1	0	-0.824183	1.101805	0.336447
6	6	0	-0.920284	3.011901	-1.989848
7	8	0	-2.073750	2.244958	-2.120847

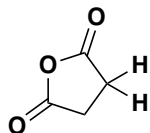
8	8	0	-3.451124	1.031777	-0.806472
9	8	0	-0.395465	3.508811	-2.943615
10	6	0	0.953595	3.039136	-0.252874
11	6	0	1.718932	1.966646	-0.732071
12	6	0	1.583926	4.038696	0.495106
13	6	0	2.951799	3.969141	0.765792
14	6	0	3.085107	1.896879	-0.465102
15	6	0	3.705245	2.897602	0.286914
16	1	0	3.425886	4.753218	1.348415
17	1	0	3.666043	1.063072	-0.847445
18	1	0	1.251084	1.185155	-1.325903
19	1	0	-0.904465	4.089813	-0.189636
20	1	0	4.769620	2.842742	0.494131
21	1	0	1.002394	4.877579	0.868158



Calculated Energy: HF=-611.5608487 Hartrees (-383754.43 kcal/mol)

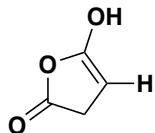
Center	Atomic	Atomic	Coordinates (Angstroms)		
Number	Number	Type	X	Y	Z

1	6	0	-1.435552	-1.263306	0.187789
2	6	0	-0.504975	-0.085136	0.026142
3	6	0	-2.815080	-0.628073	0.116842
4	1	0	-1.327413	-1.794214	1.141100
5	1	0	-1.358128	-2.017860	-0.605521
6	6	0	-1.297705	0.991178	-0.160070
7	8	0	-2.651395	0.735273	-0.106562
8	8	0	-3.905121	-1.118014	0.214757
9	8	0	-1.057876	2.281322	-0.417870
10	6	0	0.957809	-0.132563	0.039149
11	6	0	1.638559	-1.311271	-0.322545
12	6	0	1.733590	0.983280	0.418221
13	6	0	3.126396	0.932123	0.396550
14	6	0	3.030709	-1.362136	-0.332332
15	6	0	3.783998	-0.239095	0.017301
16	1	0	3.697756	1.805700	0.696669
17	1	0	3.529735	-2.283531	-0.618362
18	1	0	1.071540	-2.192177	-0.607820
19	1	0	-0.121023	2.382153	-0.646848
20	1	0	1.247510	1.881812	0.789543
21	1	0	4.868663	-0.280545	0.006364



Calculated Energy: HF=-380.5344606 Hartrees (-238785.37 kcal/mol)

Center Number	Atomic Number	Atomic Type	Coordinates (Angstroms)		
			X	Y	Z
1	6	0	-0.000000	1.149973	0.214893
2	6	0	-0.000548	0.764989	-1.253895
3	6	0	0.000548	-0.764989	-1.253895
4	6	0	-0.000000	-1.149973	0.214893
5	1	0	0.878298	1.207209	-1.729993
6	1	0	-0.880834	1.205748	-1.728732
7	1	0	-0.878298	-1.207209	-1.729993
8	1	0	0.880834	-1.205748	-1.728732
9	8	0	-0.000000	-0.000000	0.996783
10	8	0	0.000506	2.238950	0.713201
11	8	0	-0.000506	-2.238950	0.713201



Calculated Energy: HF=-380.4947587 Hartrees (-238760.46 kcal/mol)

Center Number	Atomic Number	Atomic Type	Coordinates (Angstroms)		
			X	Y	Z
1	6	0	0.852262	1.256156	0.000036
2	6	0	-0.650293	1.280539	-0.000058
3	6	0	-1.065627	0.011734	-0.000059
4	6	0	1.168334	-0.234094	-0.000034
5	1	0	1.320076	1.717162	-0.879348
6	1	0	1.319961	1.717075	0.879528
7	1	0	-1.281395	2.155086	-0.000087
8	8	0	-0.040539	-0.929280	0.000003
9	8	0	-2.297968	-0.508449	-0.000082
10	8	0	2.219051	-0.812360	0.000171
11	1	0	-2.231061	-1.474622	-0.000137

Full G16 Citation

Gaussian 16, Revision A.03, M. J. Frisch, G. W. Trucks, H. B. Schlegel, G. E. Scuseria, M. A. Robb, J. R. Cheeseman, G. Scalmani, V. Barone, G. A. Petersson, H. Nakatsuji, X. Li, M. Caricato, A. V. Marenich, J. Bloino, B. G. Janesko, R. Gomperts, B. Mennucci, H. P. Hratchian, J. V. Ortiz, A. F. Izmaylov, J. L. Sonnenberg, D. Williams-Young, F. Ding, F. Lipparini, F. Egidi, J. Goings, B. Peng, A. Petrone, T. Henderson, D. Ranasinghe, V. G. Zakrzewski, J. Gao, N. Rega, G. Zheng, W. Liang, M. Hada, M. Ehara, K. Toyota, R. Fukuda, J. Hasegawa, M. Ishida, T. Nakajima, Y. Honda, O. Kitao, H. Nakai, T. Vreven, K. Throssell, J. A. Montgomery, Jr., J. E. Peralta, F. Ogliaro, M. J. Bearpark, J. J. Heyd, E. N. Brothers, K. N. Kudin, V. N. Staroverov, T. A. Keith, R. Kobayashi, J. Normand, K. Raghavachari, A. P. Rendell, J. C. Burant, S. S. Iyengar, J. Tomasi, M. Cossi, J. M. Millam, M. Klene, C. Adamo, R. Cammi, J. W. Ochterski, R. L. Martin, K. Morokuma, O. Farkas, J. B. Foresman, and D. J. Fox, Gaussian, Inc., Wallingford CT, 2016.

A.5 References

1. Dalby, K. N., *Annu. Rep. Prog. Chem., Sect. B: Org. Chem.* **2002**, *98*, 253-291.
2. Pattawong, O.; Tan, D. Q.; Fettinger, J. C.; Shaw, J. T.; Cheong, P. H.-Y., *Org. Lett.* **2013**, *15* (19), 5130-5133.
3. Tan, D. Q.; Younai, A.; Pattawong, O.; Fettinger, J. C.; Cheong, P. H.-Y.; Shaw, J. T., *Org. Lett.* **2013**, *15* (19), 5126-5129.
4. Rappoport, Z.; Lei, Y. X.; Yamataka, H., *Helv. Chim. Acta* **2001**, *84* (6), 1405-1431.
5. Lei, Y. X.; Casarini, D.; Cerioni, G.; Rappoport, Z., *J. Org. Chem.* **2003**, *68* (3), 947-959.
6. Song, J.; Lei, Y. X.; Rappoport, Z., *J. Org. Chem.* **2007**, *72* (24), 9152-9162.
7. Kresge, A. J.; Meng, Q., *Can. J. Chem.* **1999**, *77* (9), 1528-1536.
8. Basheer, A.; Rappoport, Z., *Org. Biomol. Chem.* **2008**, *6* (6), 1071-1082.
9. Basheer, A.; Rappoport, Z., *J. Phys. Org. Chem.* **2008**, *21* (6), 483-491.
10. Basheer, A.; Mishima, M.; Rappoport, Z., *ARKIVOC* **2015**, (3), 18.
11. Lei, Y. X.; Cerioni, G.; Rappoport, Z., *J. Org. Chem.* **2000**, *65* (13), 4028-4038.
12. Ng, P. Y.; Masse, C. E.; Shaw, J. T., *Org. Lett.* **2006**, *8* (18), 3999-4002.